# UNIVERSITY OF SOUTHAMPTON

## Faculty of Engineering and the Environment

Engineering Sciences


# Repetitive Current Control of Two-Level and Interleaved Three-Phase PWM Utility Connected Converters


By

**Mohsin Jamil**


A Thesis Submitted for the Degree of

**DOCTOR OF PHILOSOPHY**

February 2012

UNIVERSITY OF SOUTHAMPTON

ABSTRACT

FACULTY OF ENGINEERING AND THE ENVIRONMENT

**Doctor of Philosophy**

# REPETITIVE CURRENT CONTROL OF TWO-LEVEL AND INTERLEAVED THREE-PHASE PWM UTILITY CONNECTED CONVERTERS

**By Mohsin Jamil**

This thesis is mainly concerned with investigations into digital repetitive current control of two-level and interleaved utility connected PWM converters. The research is motivated by the relatively poor performance of classical (PI) controllers when the utility voltage harmonic distortion is high. This is due to the low gain, and poor disturbance rejection of the PI controller at the utility harmonic frequencies. Repetitive feedback controllers have the ability to track or reject periodic disturbances, such as utility harmonics, as they naturally have high gains at the utility voltage harmonic frequencies, assuming that these frequencies do not change.

Repetitive controllers (RC) are known for being sensitive to variations in system parameters and disturbance frequency, which in practice renders them either ineffective or unstable. Another challenge arises from the memory requirements of RC in case of the absence of even harmonics, which can make its practical implementation difficult and expensive. In addition, another problem that has not been investigated extensively in the literature is that the effectiveness of RC is severely limited by the limited bandwidth of the plant (the utility connected converter and its filter). Theoretical analysis and simulation results presented in this thesis show that RC could not effectively reject disturbances at frequencies above the closed loop system bandwidth. The design of the converter's output filter bandwidth and the values of its components need to be selected carefully, to enable RC to be used effectively.

The research in this thesis focuses on investigating the practical implementation and performance limits of two types of repetitive controllers (conventional and odd-harmonics), used for current control of two-level utility connected converter with LCL output filter. The odd-harmonic repetitive controller halves the memory requirement and offers higher gains only at odd harmonic frequencies of interest. The overall control scheme consists of the traditional classical tracking controller with a dual loop feedback system and RC. The results indicate that the repetitive controller improves the steady state error and the total harmonic distortion of the output current, provided that the plant's bandwidth is sufficiently large.

Finally, a repetitive controller for an interleaved utility connected converter has been designed and investigated in this study. The interleaved converter system has higher bandwidth than the two-level converter, which improves the effectiveness of RC. It provides good disturbance rejection compared to classical controllers which results in low output current THD. The RC was demonstrated to be robust despite uncertainty in utility impedance, while achieving a fast almost zero error convergence. The proposed RC has been experimentally implemented using a DSP and the results indicate that the quality of output current complies with international standards on harmonic limits and matches simulation results obtained from the Matlab/Simulink model of the system.

# LIST OF CONTENTS

## CHAPTER 4: REPETITIVE FEEDBACK CONTROL OF TWO-LEVEL THREE-PHASE UTILITY CONNECTED CONVERTER



## CHAPTER 5: REPETITIVE FEEDBACK CONTROL OF AN INTERLEAVED THREE-PHASE UTILITY CONNECTED CONVERTER AND ITS EXPERIMENTAL IMPLEMENTATION

# LIST OF ABBREVIATIONS

| | |
|---|---|
| ANSI | American National Standards Institute |
| BPS | Bowman Power System Ltd. |
| CB-PWM | Carrier Based Pulse Width Modulation |
| CHP | Combined Heat and Power |
| DSP | Digital Signal Processor |
| DG | Distributed Generator |
| DN | Distribution Network |
| ESR | Equivalent Series Resistance |
| FIR | Finite Impulse Response Filter |
| FACTS | Flexible AC Transmission System |
| IEEE | Institute of Electrical and Electronic Engineers |
| IGBT | Insulated Gate Bipolar Transistor |
| ILC | Iterative Learning Control |
| LQG | Linear Quadratic Gaussian Control |
| LCL | Inductor-Capacitor-Inductor |
| MIMO | Multi Input-Multi Output System |
| PWM | Pulse width Modulation |
| PID | Proportional-Integral-Derivative |
| PQR | Power Quality & Reliability |
| PZ- Map | Pole-Zero Map |
| RC | Repetitive Controller |
| RMS | Root Mean Square |
| SISO | Single Input-Single Output System |
| SMC | Sliding Mode Controller |
| SVM | Space-Vector Modulation |
| THD | Total Harmonic Distortion |
| VSC | Voltage-Source Converter |
| VS-PWM | Voltage-Source Pulse Width Modulation |

# LIST OF FIGURES

Page No.

# LIST OF TABLES

Page No.

# DECLARATION OF AUTHORSHIP

I, **Mr. Mohsin Jamil** declares that the thesis entitled **Repetitive Current Control of Two-Level and Interleaved Three-Phase PWM Utility Connected Converters** and the work presented in the thesis are both my own, and have been generated by me as the result of my own original research. I confirm that:

- this work was done wholly or mainly while in candidature for a research degree at this University;
- where any part of this thesis has previously been submitted for a degree or any other qualification at this University or any other institution, this has been clearly stated;
- where I have consulted the published work of others, this is always clearly attributed;
- where I have quoted from the work of others, the source is always given. With the exception of such quotations, this thesis is entirely my own work;
- I have acknowledged all main sources of help;
- where the thesis is based on work done by myself jointly with others, I have made clear exactly what was done by others and what I have contributed myself;
- parts of this work have been published as: [ See Appendix]

**Signed:** ……..

**Date:**……

# ACKNOWLEDGEMENTS

I would like to thank all the members of staff in the Electro-Mechanical research group at the University of Southampton who provided me with assistance during the period of this research, especially my main supervisor, Dr. Sharkh, for his advice, guidance and encouragement. I owe thanks to Dr. R. Boltryk for her guidance during the initial stage of my PhD.

I would also like to thank Dr. Abusara from University of Exeter for his help and advice throughout my PhD and for conducting the experimental work to implement the repetitive controller on an interleaved converter in his laboratory. I am thankful to Mr. Rusllim, Mr. Babar and other colleagues for valuable discussions and moral support.

I am very grateful to my parents and younger brother for their support throughout my PhD. I am also thankful to my wife and lovely daughter for facing hardships with me.

I am also highly thankful to the National University of Science and Technology (NUST), Higher Education Commission (HEC) and the Government of Pakistan, for awarding me a scholarship for my PhD studies.

**To my Family and lovely daughter Wardah with love**

# Chapter 1

## INTRODUCTION

### 1.1 Motivation and System Description

Fossil fuels are running out and current centralised power generation plants are inefficient, producing harmful emissions and greenhouse gases, and a significant amount of energy being lost as heat to the environment. Furthermore, current power systems, especially in developing countries, suffer from several limitations such as high cost of expansion and efficiency improvement limits within the existing utility infrastructure. Renewable energy sources can help address these issues, but it can be a challenge to get stable power from these sources, as they are variable in nature. Distributed generators (DGs), including renewable sources, within microgrids can help overcome power system limitations, improve efficiency, reduce emissions and manage the variability of renewable sources. A microgrid is a zone within the main utility where a cluster of electrical loads and small micro generation systems, such as solar cell, fuel cell, wind turbine and small combined heat and power (CHP) systems, exist together under an embedded management and control system with the need of storage devices (Sharkh et al., 2006). A schematic diagram of microgrid is shown in Fig. 1.1.

Power electronic converters used in microgrids are widely employed as the interface and power flow management of DGs to the utility (Jamil et al., 2009; Picardi and Sgro, 2009). They manage the energy exchanges with the utility and in general control the power flow between DGs and the utility. They are normally used to connect renewable energy sources such as solar, wind, or marine, to the utility to convert DC or variable frequency AC into 50/60 Hz fixed frequency AC to inject into the utility or to supply local loads. They are also used to interface high power density micro turbines, flywheel energy storage systems, batteries, and fuel cells. These converters play a vital role in the control of power flow and improvement of power quality by providing a low total harmonic distortion (THD) output current as laid down by guidelines and standards (Engineering Recommendation G59/1,

1991; IEEE Standard 519, 1993; Energy Networks Association, 1995; IEEE Standard 929, 2000; Basso and DeBlasio, 2004; Dugan et al., 2005). The current harmonic limits standard being followed by the system described in this thesis is the ANSI/IEEE Standard 519-1992 (IEEE Standard 519, 1993) as shown in Table 1.1.

| Odd harmonic order n | $n \leq 11$ | $11 \leq n \leq 17$ | $17 \leq n \leq 23$ | $23 \leq n \leq 35$ | $35 \leq n$ | THD |
|---|---|---|---|---|---|---|
| Percentage of fundamental. (%) | 4.0 | 2.0 | 1.5 | 0.6 | 0.3 | 5.0 |

*Table 1.1: Harmonic currents limits according to ANSI/IEEE Standard 519-1992 (IEEE Standard 519, 1993)*

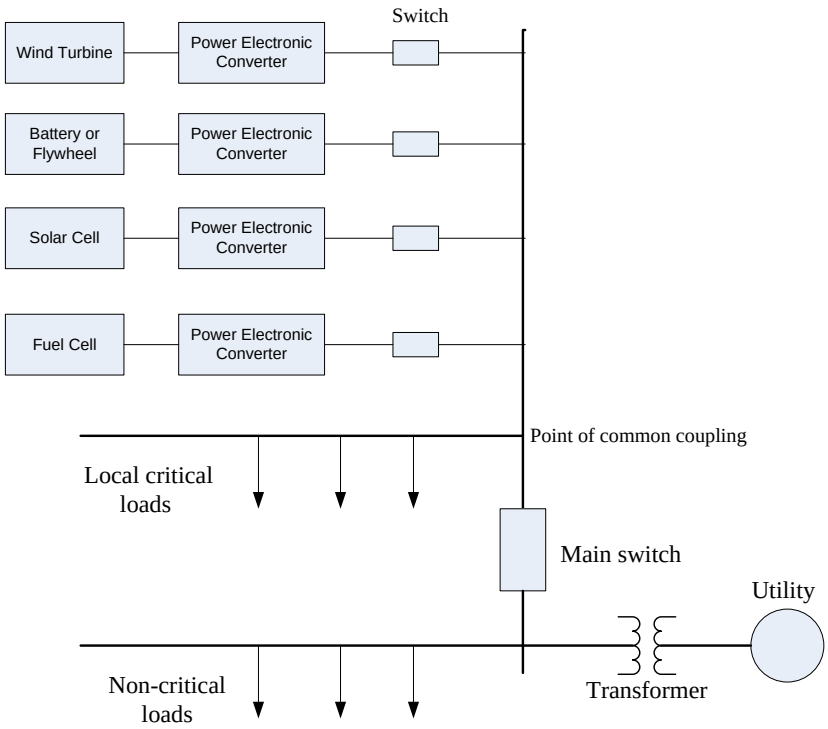


*Fig. 1.1: A schematic diagram of a microgrid*

There exist different types of power electronic converters for interfacing with the utility. The most common is the two-level bridge converter. However, the need to improve efficiency and to reduce the size and cost of both the converter and the output filter, has encouraged more research into using different topologies. Many multilevel converters have been proposed, including neutral point diode clamped (Bouhali et al., 2006) and cascaded

converters (Selvaraj and Rahim, 2009). Moreover, the novel structures of these converters e.g. multiphase modular converters ($M^2LC$) have been further developed and are used by industry. Modular architecture can provide high reliability and easy maintenance in addition to bidirectional power flow at all ports with active and reactive control (Bifaretti et al., 2011). These converters have the advantage of reducing the voltage step changes at the expense of increased complexity and cost of the power electronics and control components. An alternative to the multilevel converter is to use an interleaved converter topology, which in effect comprises several low power, high frequency, multilevel bridge converters connected in parallel (Abusara and Sharkh, 2010). Other possible converter topologies worth investigating for this application, include current source converters (Lee et al., 2008) and matrix converters (Garces and Molinas, 2012). The matrix converter is particularly appealing when the power source is AC, e.g. high frequency turbine generator or variable frequency wind turbine generator. Using a matrix converter, the cost of the AC/DC conversation stage and the requirement for a DC link capacitor or inductor, could be saved. This thesis focuses on the control of two-level bridge and an interleaved converter.

A circuit diagram of the two-level three-phase pulse-width modulated (PWM) voltage source converter for utility interface investigated in this thesis is shown in Fig. 1.2. The parameters and component values of the available two systems are shown in Table 1.2 and Table 1.3. In this circuit, the three-phase outputs of the converter are connected to the three-phase utility system via an LCL filter. Filter capacitors are connected to the DC link. In this filter configuration, the middle of the DC-link has almost zero voltage with respect to the neutral point, which means that the voltage produced in one phase does not depend upon the voltages produced in the other phases. The function of the output LCL filter is to 'block' the PWM switching frequency components from entering the utility supply. The order of the transfer function of the system, becomes third order when an LCL filter is used in the two-level bridge converter. This increases the complexity of the control strategy to manage filter resonance. Additionally, the impedance of $L_2C$ in Fig.1.2 tends to be relatively low, and provides an easy path for current harmonics to flow from the utility, which can cause the THD to go beyond permitted limits in cases where the utility voltage THD is relatively high. Ideally, this drawback could be overcome by increasing the feedback controller gain in a current controlled utility connected converter. But this can

prove to be difficult to achieve in practice while maintaining good stability and having almost zero steady state error. For example, the use of a linear conventional PI controller in the stationary frame results in an unstable system if the loop gain is increased further from a specific limit. There also exists steady state error. This will be discussed further in the next chapter. Alternatively, PI regulators in synchronous (d-q) form could be used to achieve almost zero steady state error. However, a synchronous frame regulator is more complex as it involves transformation, which can introduce errors if the synchronous frame identification is not accurate (Zmood and Holmes, 2003). The synchronous frame identification is normally based on a phase locked loop (PLL) system, which may not be able to provide accurate phase information when the utility is non-ideal. An attractive approach to eliminate errors could be Proportional Resonant (PR) controllers, also known as generalised integrators. The PR controller works on the internal model principle, which introduces the mathematical model of sinusoidal reference along the open loop path to ensure almost zero steady state error. However, the PR can act only on limited harmonics (Teodorescu et al., 2006). This will be discussed in detail in chapter 2. The repetitive controller (RC) which also works on the internal model principle has potential to achieve almost zero steady state error while maintaining stability in the utility connected converter application by acting on all harmonics at the same time.

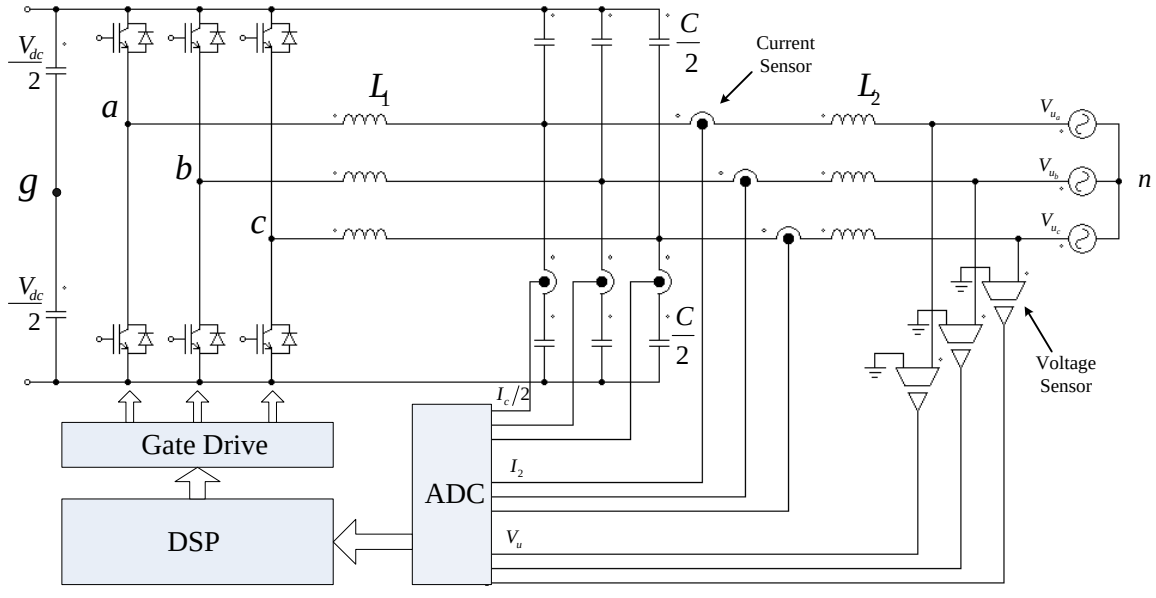


*Fig. 1.2: Two-level power electronic converter interface with LCL filter*

| Components | Description | Rating values |
|---|---|---|
| $P_{inv}$ | Rated power | 80 KVA |
| $V_u$ | Utility phase voltage | 230 V (rms) |
| $V_{DC}$ | DC link voltage | 750 V DC |
| $L_1$ | 1st Inductor of filter | 350 µH |
| $L_2$ | 2nd Inductor of filter | 50 µH |
| $C$ | Filter capacitance | 160 µF |
| $f_{sw}$ | Switching frequency | 8 KHz |
| $f_s$ | Sampling frequency | 16 KHz |
| $f$ | Utility frequency | 50 Hz |
| $N$ | No. of samples per period | 320 |

*Table 1.2: First system parameters and component values for the two-level utility connected converter with LCL filter*

| Components | Description | Rating values |
|---|---|---|
| $P_{inv}$ | Rated power | 80 KVA |
| $V_u$ | Utility phase voltage | 230 V (rms) |
| $V_{DC}$ | DC link voltage | 800 V DC |
| $L_1$ | 1st Inductor of filter | 350 µH |
| $L_2$ | 2nd Inductor of filter | 50 µH |
| $C$ | Filter capacitance | 22.5 µF |
| $f_{sw}$ | Switching frequency | 10 KHz |
| $f_s$ | Sampling frequency | 20 KHz |
| $f$ | Utility frequency | 50 Hz |
| $N$ | No. of samples per period | 400 |

*Table 1.3: Second system parameters and component values for the two-level utility connected converter with LCL filter*

The other converter analysed in this research is an interleaved two-level three-phase PWM converter as shown in Fig. 1.3. Table 1.4 shows the parameters and component values for an interleaved utility connected converter. Here each phase consists of six half bridge channels connected in parallel which gives a low capacitor ripple current due to a ripple cancellation feature and as a result, the overall filter size is smaller (Abusara and Sharkh, 2010). Relatively small filter capacitors could be used to filter out the switching frequency ripples. This also eliminates the need for a second output filter inductor (i.e. using an LCL filter instead of an LC filter) that is normally used in the two-level utility connected converters to block the switching ripple in cases where the utility impedance is too low. Furthermore, the resonance frequency and the bandwidth of the interleaved system will be high due to the much smaller output filter capacitors and inductors (Abusara and Sharkh, 2010). This provides more flexibility by having a larger system bandwidth compared to the two-level converter for controller design. Another advantage of having an interleaved converter is the presence of small devices such as power switches, capacitors and inductors, which help in fast switching and reduce the filter size further. Practical realisation of this converter will be further discussed in detail in chapter 5 (section 5.4.1) by providing its hardware description.

In real system, THD could be any value (depending upon the utility harmonics) and the output current will be more distorted, when THD is high and vice versa. It is desired to have pure sinusoidal current (clean current without harmonics) as much as possible without any distortions. An example of distorted current and pure current can be seen in Fig. 2.6. The required low THD output current from converters can be achieved by implementing an effective control strategy. Conventional classical controllers have been widely used for utility connected converters (Abusara, 2004; Hussein, 2000; Kazmierkowski et al., 2002; Selvaraj et al., 2008; Twining and Holmes, 2003). Simulation studies of the classical PI controller applied to the two-level system, have been carried out by the author to analyse performance and robustness of the overall two-level utility bridge system against different utility THD values. The classical PI controller was found not to provide output current as per the required standards when the utility voltage harmonic distortion is high. This is due to the low gain, higher steady state error and poor disturbance rejection of the PI controller at the utility harmonic frequencies. This will be further discussed in chapter 2.

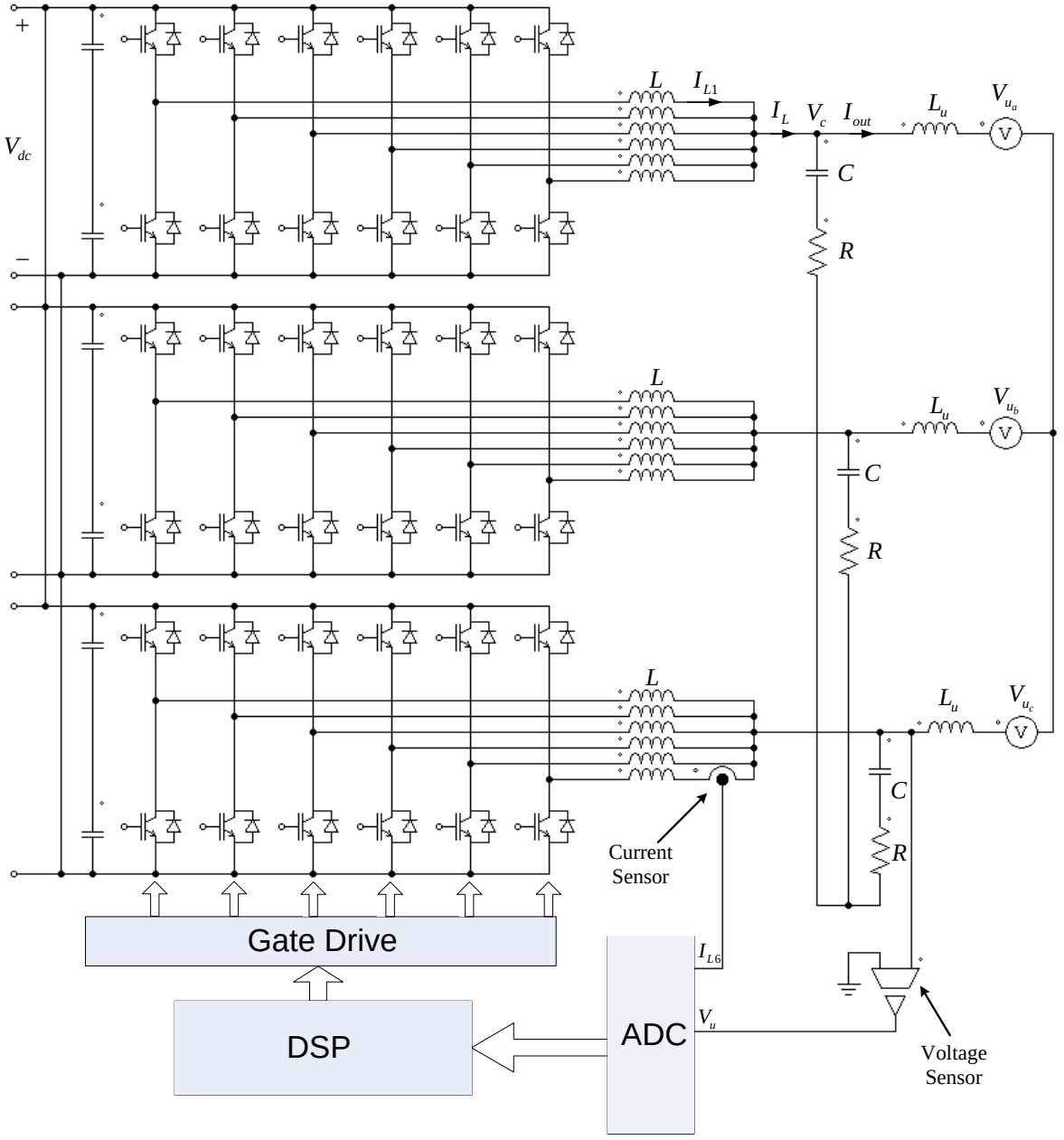


*Fig. 1.3: Three-phase utility connected interleaved converter-showing block diagram of a control system for one channel of one phase*

| Components | Description | Rating values |
|---|---|---|
| $P_{inv}$ | Rated power | 60 KVA |
| $V_u$ | Utility phase voltage | 230 V (rms) |
| $V_{DC}$ | DC link voltage | 750 V DC |
| $R$ | Passive damping resistance | 0.5 Ω |
| $N_o$ | Number of channels | 6 |
| $L$ | Channel inductor | 150 µH |
| $L_u$ | Utility inductance | 5-50 µH |
| $C$ | Filter capacitance | 10.8 µF |
| $f_{sw}$ | Switching frequency | 35 KHz |
| $f_s$ | Sampling frequency | 35 KHz |
| $f$ | Utility frequency | 50 Hz |
| $T_d$ | Time delay | 15µs |
| $N$ | No. of samples per period | 700 |

*Table 1.4: System parameters and component values for interleaved utility connected converter*

A better controller is required with a high gain at the fundamental and all harmonic frequencies of interest. Alternative controllers have been proposed, such as deadbeat control (Moreno et al., 2009; Qu et al., 2009), optimal control strategies (Lee et al., 2007), state-feedback approach (Gabe et al., 2007), sliding mode controllers (Kim, 2006) and resonant controllers (Timbus et al., 2006). The objective of these controllers is to increase the outer loop gain, and, hence improve disturbance rejection. Each controller has some advantages and disadvantages. It is common to use the d-q transformation as well to translate the measured AC signals of voltage and current to DC, which simplifies controller design and implementation using a microprocessor based controller. But, such an approach assumes that the measured signals are pure sinusoids and that the utility is balanced, which in practice is often not the case. A slight imbalance in addition to harmonic distortions are often present, which act as disturbances that cause a deterioration of the output current THD (Twining and Holmes, 2003).

In a utility connected converter, the utility voltage disturbance is periodic or repetitive, which has motivated many researchers to investigate the use of repetitive controllers (RC) based on the internal model principle. According to this principle, the controlled outputs track a set of reference inputs without steady state error provided that the model generating these references is included in the stable closed loop system (Ying-Yu et al., 1997). Repetitive feedback based control techniques with advanced algorithms (Chen et al., 2008, Pengfei et al., 2006; Qing-Chang et al., 2002; Sharkh et al., 2001;Wang et al., 2005; Weiss et al., 2004) have been used to control utility connected converters. They have the potential to improve the output current THD and provide higher gains at 50Hz and its harmonic frequencies of interest. They have the ability to track or reject periodic errors as well.

Although there are many publications on RC based techniques, there remains a need to explore the limits of performance and practical implementation for current control of utility connected converters. RC is known for being sensitive to variations in system parameters and disturbance frequency, which in practice renders them either ineffective or unstable. For example, the gain of the conventional RC drops very rapidly at frequencies slightly lower or higher than the nominal frequency for which it is designed, which means that a small change in the frequency of the disturbance away from its nominal value would result in a significant deterioration of the disturbance rejection performance of the RC. Another challenge arises from the data memory requirements of RC in case of the absence of even harmonics in the system. For example, the required number of samples per period (N) for the system mentioned in Table 1.2 would be 320 if it contains both even and odd harmonics. However, only odd harmonics are dominant in this case, so the required number of samples per period (N) would be only 160. This could offer faster convergence of error as it involves only half the memory cells compared to the earlier case (Zhou et al., 2006). Another problem that has not been investigated extensively in the literature is that the effectiveness of RC is severely limited by the limited bandwidth of the plant (the utility connected converter and its filter) and this issue will be discussed in this thesis.

This study investigates the practical implementation and limits of performance of two types of RC controllers (conventional and odd-harmonics) used for current control of two utility connected converters. The odd-harmonic repetitive controller (ORC) has lower memory requirement (half of RC) and only offers higher gains at odd harmonic frequencies of

interest. This thesis considers design constraints, the trade-off between steady state error and system transient response and utility impedance variations, limited filter bandwidth and memory requirement issues based on theoretical analysis and detailed simulations. The results of the detailed simulations were further used to provide parameters and develop algorithm for experimental implementation of RC controllers.

## 1.2 Aims and Objectives of the Research

This thesis is mainly concerned with investigations into digital current control of utility connected two-level with LCL filter and interleaved PWM converters using RC. The main aim of the study was to investigate RC strategy for these converters to improve the system's performance in terms of steady state error and output current THD.

The objectives of the research were:

- Develop appropriate computer simulation models (PWM switching model and linear transfer function model) for two-level and interleaved utility connected converters using Matlab/Simulink.
- Investigate the two-level converter with LCL filter and access the performance of the classical PI controller in terms of steady state error and output current THD requirement with different utility THD levels.
- Design and analyse digital RC for the two-level utility connected converter with LCL filter. Investigate the limits of performance of RC for this converter, particularly concerning system bandwidth by changing capacitance values of the LCL filter.
- Design and analyse digital RC for an interleaved utility connected converter using nonlinear PWM switching mode and linear transfer function model in presence of utility harmonics. Investigate the effect of variations in utility impedance and time delay on the performance of RC.
- Investigate stability constraints, the trade-off between steady state error and system transient response with respect to different parameters of RC such as RC gain and Q-filter.

- Develop an RC algorithm with due consideration to implementation methods and conduct simulations to provide parameters for experimental implementation of RC using DSP for the interleaved utility connected converter.

## 1.3 Contributions of the Thesis

The main novel contributions of this study are:

- To provide practical realisation of RC system for an innovative interleaved utility connected PWM converter. This application has not been previously discussed in the literature. The design of the RC takes into account practical constraints of the DSP hardware and system bandwidth limitations. The interleaved converter offers higher bandwidth compared to the two-level converter with LCL output filter, which improves effectiveness of RC. It provides good disturbance rejection compared to the classical controllers which results in low output current THD. The RC was demonstrated to be robust despite uncertainty in utility impedance, while achieving a fast almost zero error convergence. The proposed RC has been experimentally implemented using a DSP and the results indicate that the quality of output current complies with international standards on harmonic limits and matches with simulation results obtained from a Matlab/Simulink model of the system.

- To have fundamental investigations into the effect of system bandwidth on the performance of a RC system. The research has shown that the plants bandwidth needs to be higher than the harmonics that the RC is attempting to eliminate. This issue has not been investigated in depth in the literature. The system bandwidth is varied by changing the capacitance values of LCL filter in the presence of different low-pass Q-filters such as constant, causal and non-causal filters. The effectiveness of the proposed current controller has been tested in the presence of different utility voltage harmonics and uncertainty in utility impedance.

The following papers have been published as a result of this research and are a contribution. Copies of these papers are included in the appendix.

- M. Jamil, B. Hussain, S. M. Sharkh, M. A. Abusara, R. J. Boltryk, "Microgrid power electronic converters: state of the art and future challenges", *44th International Universities Power Engineering Conference (UPEC)*, 1-4 September 2009, Glasgow, United Kingdom.

- M. Jamil, S. M. Sharkh, M. A. Abusara, R. J. Boltryk, "Robust repetitive feedback control of a three-phase grid connected inverter", *5th IET International Conference on Power Electronics and Drives (PEMD)*, 19-21 April 2010, United Kingdom.

- M. Jamil, S. M. Sharkh and M. A. Abusara, "Current regulation of three-phase grid connected voltage source inverter using robust digital repetitive control", *International Review of Automatic Control*, vol. 4, pp.211-219, 2011.

## 1.4 Organisation of the Thesis

Chapter 2 presents a review of different structures and current control methods such as PID, deadbeat, PR and others used for utility connected converters. The RC is adopted because it can deal a large number of harmonics simultaneously and can address the limitations of other control techniques. Different structures of RC are critically reviewed in order to select the most suitable structure for the application. A special type of RC known as ORC is also discussed. The output and error transfer functions of both types of RC are derived and form the basis for analysis in the proceeding chapters.

Chapter 3 describes the Matlab/Simulink simulation model used to aid the design and evaluation of current controllers for the utility interface. The block diagram of the converter based upon a single-phase equivalent circuit is derived. The block diagram and transfer function form the basis for analysis and design of the control system for the voltage source utility connected converter. Criteria for direct comparison and evaluation of different current controller performance are defined.

Chapter 4 discusses the design and analysis of a linear digital repetitive feedback controller for a two-level utility-connected voltage-source converter, connected between a DC source and the utility through an LCL filter. Stability constraints and trade-offs between the steady state error and system transient response are analysed by considering different parameters.

A special type of RC, known as ORC, is also designed and analysed. Simulation results are presented to show the effectiveness of the applied control technique.

Chapter 5 discusses the design and analysis of a linear digital repetitive controller for an interleaved utility connected converter. The effect of variations in utility impedance and other parameters are discussed. The experimental results obtained with the help of Dr. Abusara are presented to validate the simulation and theoretical results. The significance of direct form I and direct form II have been discussed for the practical implementation of RC using TMS320LF2808 digital signal processor (DSP). The direct form I requires more delay elements and is the straightforward implementation of the difference equation. The direct form II implementation requires fewer numbers of delays, adders and multipliers, yielding in the same transfer function as the direct form I implementation.

The final chapter presents the conclusions of the research and recommendations for further work.

# Chapter 2

## UTILITY CONNECTED CONVERTER CONTROL TECHNIQUES AND REPETITIVE CONTROL

## 2.1 Introduction

Alternative control strategies and structures for utility connected converters are the subject of active research to improve the performance of systems. Conventional classical controllers (P/PI/PID) have been widely used. However, these controllers tend to suffer from low loop gain at the fundamental frequency and its harmonics and hence tend to have poor disturbance rejection which results in poor output current total harmonic distortion (THD) if the utility voltage THD is relatively high. The limitations of classical controllers are being overcome by alternative control techniques such as proportional resonant (PR), deadbeat, repetitive control (RC) and many others (see section 2.2.2). Moreover, modifications in existing control structures can also help to address these limitations.

This chapter discusses different current control techniques and structures used for utility connected converters and focuses mainly on RC. The discrete form of the RC is discussed. The working principle, structure and transfer function of the RC is derived and will be used in subsequent chapters.

## 2.2 Current Controllers for Utility Connected Converters

The performance of the utility connected converter system depends mainly on the quality of the applied current control strategy and the structure of the system. There exist different structures (e.g. Fig. 2.1, Fig. 2.2, Fig. 2.3 and Fig. 2.4) of the two-level converter with output LCL filters. In this section, the common structures of the two-level converter based upon single and double feedback loops with output LCL filter are reviewed. The structure of the interleaved converter is relatively new on its own (Fig. 1.3) and will be further investigated in chapter 5.

The choice of the LCL filter for a two-level converter is due to its superior performance when compared to LC and L filters (Twining and Holmes, 2003). In systems where LC filter is used, the utility impedance determines the resonance frequency of the filter, which is uncertain. This makes life difficult and the filter resonance cannot be dampened. Whereas in systems where only coupling inductors are used, large size inductors are required to limit the $\frac{dI}{dt}$ and, hence, the ripple current. In case of high rating devices, the losses in the inductors cannot be ignored. Moreover, larger inductors are more expensive than the smaller ones. The LCL filter topology allows the use of smaller inductors, thus ensuring low losses, reduced cost and size of the overall system. For the two-level converters (Fig. 1.2), the selection of the value of the inductor $L_1$ is based on switching frequency, DC link voltage and maximum current ripple. The capacitance value is selected such that its impedance at the switching frequency is much lower than that of inductor $L_2$. The inductor $L_2$ represents an actual inductance in the filter and it is not utility impedance. The importance of the inductor $L_2$ is due to three reasons: (1) it ensures filtration of current harmonics, (2) it makes the controller performance less sensitive to utility impedance variations and (3) it facilitates wireless paralleling of multiple systems.

This LCL filter based configuration, requires a suitable control technique to handle the filter resonance problem. The purpose of the controller is to achieve low output current THD with zero steady state error. In other words, a better disturbance rejection and good tracking is desirable.

### 2.2.1 Structures of Two-Level Converters with LCL Filter

Hussein (2000) and others (Kazmierkowski and Malesani, 1998) proposed a single feedback loop structure for a voltage source PWM utility connected converter as shown in Fig. 2.1, where the $L_1$ inductor current $I_1$ is used as the only feedback control signal. This results in a stable and simple system, which requires only one measurement of each phase current ($I_1$). For this structure, the plant transfer function $G_1(s)$ and disturbance transfer function $D_1(s)$ are as follows:

$$G_1(s) = \frac{1}{(L_1L_2C)s^3 + (K(s)L_2C)s^2 + (L_1 + L_2)s} \tag{2.1}$$

$$D_1(s) = (L_1Cs^2 + K(s)Cs + 1) \tag{2.2}$$

The input-output relation of this structure is given by,

$$I_2 = \frac{K(s)G_1(s)}{1 + K(s)G_1(s)} I_{ref} - \frac{G_1(s)}{1 + K(s)G_1(s)} D_1(s)V_u(s) \tag{2.3}$$

The disadvantage of this structure is that the plant (two-level converter and output LCL filter) transfer function $G_1(s)$ and the disturbance transfer function $D_1(s)$ are functions of controller $K(s)$. If the controller $K(s)$ has to be designed to improve reference tracking and disturbance rejection, this will result in a change in $G_1(s)$ and $D_1(s)$, which complicates the controller design. Also, it does not control the output current directly, which makes it difficult to achieve performance in terms of reference tracking and disturbance rejection.

The utility voltage $V_u$ forms a source of disturbance to the system. Ideally, this disturbance can be rejected by implementing a feedforward loop of exactly the same shape as the utility disturbance transfer function $D_1(s)$. In reality, however, it may be difficult to apply the first and second derivatives of the utility voltage $V_u$, due to noise amplification problem. Alternatively, the fundamental component of the utility voltage and its derivatives can be used. The derivatives are obtained by an offline calculation using a well-known nominal value (230 Vrms) of the utility voltage (Hussain, 2000; Abusara, 2004).

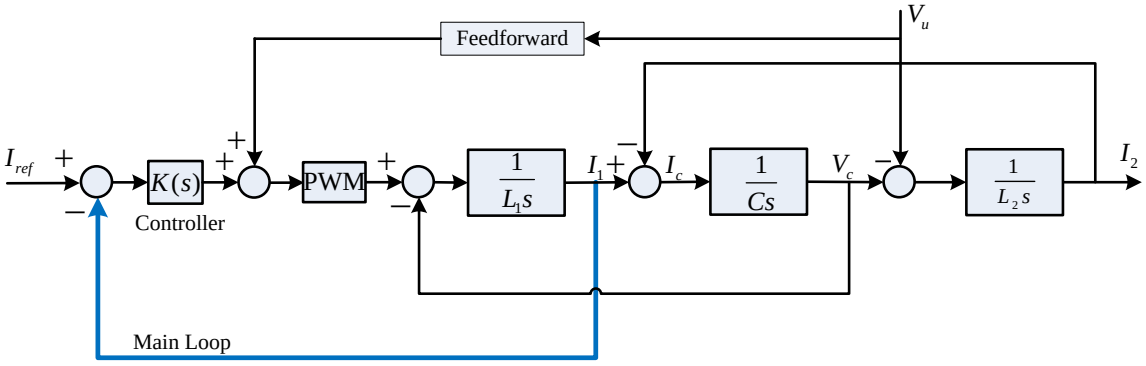


*Fig. 2.1: Single loop feedback structure of* $I_1$ (Hussain, 2000)

Abusara (2004) used a two loops feedback system with the output current as the outer loop and the capacitor current as the inner loop (Fig. 2.2). The direct feedback of the output utility current of an LCL filter on its own, is inherently unstable and it is necessary to have another feedback loop of the capacitor current $I_c$, or the current in the main inductor $L_1$ (Sharkh and Abusara, 2004; Sharkh et al., 2001; Twining and Holmes, 2002). Using output current $I_2$ and capacitor current $I_c$, the plant transfer function $G(s)$ and disturbance transfer function $D(s)$ are as follows (the derivation is detailed in section 3.4):

$$G(s) = \frac{1}{(L_1 L_2 C)s^3 + K_c L_2 C s^2 + (L_1 + L_2)s} \tag{2.4}$$

$$D(s) = L_1 C s^2 + K_c C s + 1 \tag{2.5}$$

The input-output relation of this structure is given by,

$$I_2 = \frac{K(s)G(s)}{1 + K(s)G(s)} I_{ref} - \frac{G(s)}{1 + K(s)G(s)} D(s)V_u(s) \tag{2.6}$$

In this structure, the plant transfer function $G(s)$ and the disturbance transfer function $D(s)$ are functions of the inner loop gain $K_c$ and are independent of the controller $K(s)$. This adds an extra degree of freedom, which makes the design of a controller easier. The voltage feedforward is implemented by having fundamental voltage and its derivatives.

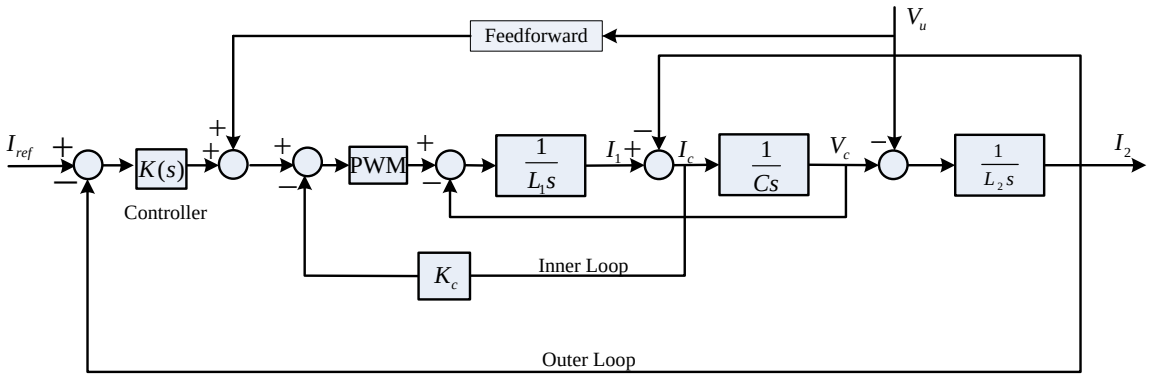


*Fig. 2.2: Double feedback loop structure of* $I_2$ and $I_c$ (Abusara, 2004)

Another interesting structure is proposed by Guoqiao et al. (2008). The main idea is to split the LCL filter capacitor into two capacitors in parallel by having an LCCL filter (Fig. 2.3), and adding a minor feedback loop of the current measured after the first capacitor. The authors used the sum of the utility current and a part of the capacitor current as feedback. By carefully selecting the capacitor values, the transfer function of the system can be reduced to first order, which helps to mitigate the resonance problem and enables the outer loop gain to be increased, thus improving disturbance rejection. In practice, it may be difficult to find capacitors with the right values and the uncertainty in the filter values, will make the condition for resonance elimination difficult to achieve.

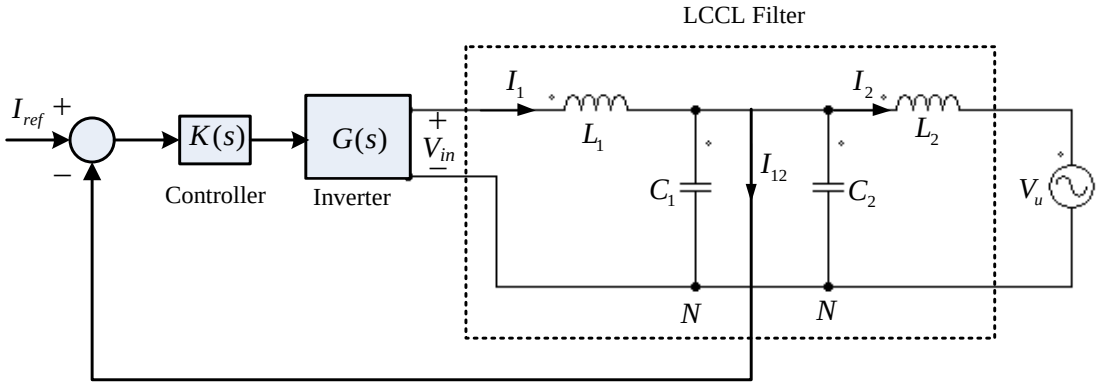


*Fig. 2.3: Block diagram of LCCL based control structure proposed by (Guoqiao et al., 2008)*

Another structure proposed by the same authors (Guoqiao et al., 2010) suggested the use of both feedback currents i.e. $I_1$ through the first inductor of the LCL filter and the output current $I_2$. The weighted average of both currents is used as current feedback to control the converter. This way, the third transfer function can be reduced to first order, similar to the L-type filter due to pole-zero cancellation. However, the switching ripple current injected into the utility is still attenuated by a third order LCL filter. This method involves an extra current sensor, compared to Hussain (2000) and Guoqiao et al. (2008). Moreover, it also requires a passive damping resistor attached in series to the capacitor as shown in Fig. 2.4. However, in high power applications, a damping resistor will be subject to losses and efficiency of the system would be affected (Zhao and Chen, 2009). Alternatively, active damping could be used, which requires the same number of sensors as used by Abusara (2004) and discussed earlier. Active damping is obtained through the product of the

capacitor current ($I_c = I_1 - I_2$) and gain $K_c$. This structure can handle larger utility harmonics very well compared to the earlier schemes.

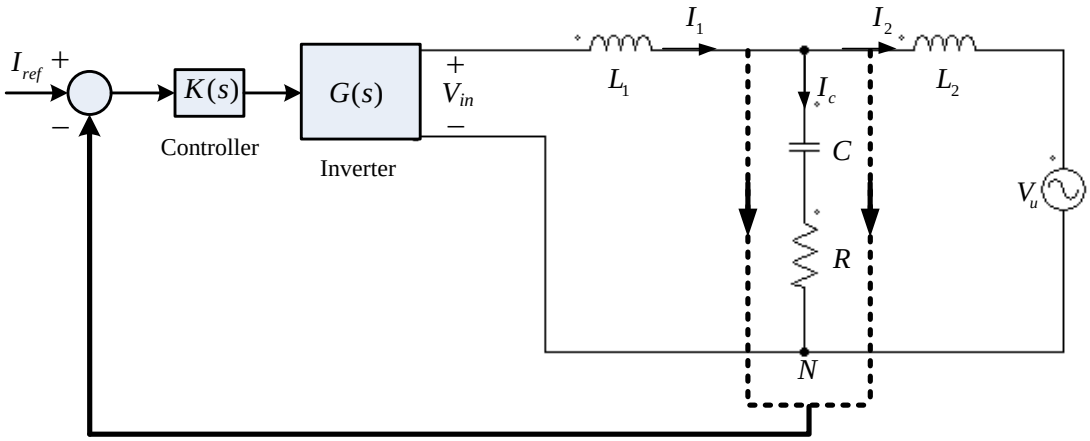


*Fig. 2.4: Block diagram of two loops feedback structure with passive damping proposed by (Guoqiao et al., 2010)*

The main aim of this thesis is not to investigate alternative structures of converters. The structure used by Abusara (2004), as shown in Fig. 2.2., is selected for further investigation. The two-level converter based on this structure is available in the laboratory. This structure involves the use of the output current and inner loop capacitor current as discussed earlier. One of the challenging aspects of this structure is that it is not possible to have a high outer loop gain using a simple compensation, which suggests looking at different control methods.

### 2.2.2 Current Control Methods

Different feedback control techniques have been used to achieve satisfactory performance in terms of disturbance rejection and steady state error requirements for utility connected converters. The most relevant used for this purpose are considered first and then other control methods are briefly considered.

#### I. Classical PID Control

Classical PID control is the most common technique employed for different applications for many decades. Its theory is essentially based on the complex-domain approach, which is applicable to linear time-invariant, single-input single-output (SISO) systems. The

advantage of this approach is its simplicity. The simple algebraic and graphical technique provides the designer with intuitive design criteria. The system performance is assessed from the system's input-output relationship in terms of its stability, steady state error (accuracy), rejection of disturbances and dynamic response. The main issue with PID control is the selection of suitable proportional ($K_p$), integral ($K_i$) and derivative gains ($K_d$). The desired closed loop performance can be achieved by adjusting these gains iteratively by tuning (Silva et al., 2002) or through other control methods, such as root locus or frequency response.

PI control has been used for utility connected voltage source converters (VSC) in a natural (abc) reference frame (Shuitao et al., 2011, Selvaraj and Rahim, 2009) due to easy implementation. Its design is briefly discussed here, to evaluate its performance in terms of disturbance rejection and steady state error requirement for the two-level converter against different utility harmonics. In Fig. 2.2, the controller $K(s)$ is the PI controller having proportional gain $K_p$ and integral gain $K_i$. The plant transfer function $G(s)$ is given by equation (2.4). The three parameters, proportional gain $K_p$, integral gain $K_i$ and inner loop capacitor gain $K_c$, are designed using the Bode plot and root locus. Table 2.1 summarises the results. To increase utility THD, different levels of harmonics have been added to the utility voltage to evaluate the performance of the controller. Utility voltage is modelled to have only dominant odd harmonics up to the $13^{th}$ harmonic. Three cases, on the basis of low (3.8%), medium (5.8%) and high (10.44%) utility THD levels, have been selected to test the performance of the PI controller. The reason for selecting these high values of THD level, is to test the effectiveness of the controller. In practice, the utility THD is normally lower. The Matlab SISO Toolbox has been used for the tuning of proportional, integral and inner loop gains where the graphical approach gives a clear insight. The values of the system parameters are given in Table 1.2. The controller gains need to be carefully selected to ensure stability. If the inner loop gain $K_c$=3.2 is fixed and outer loop gain is varied such that proportional gain $K_p$ from 1→2.4 and integral gain $K_i$ from 1→3, then it is observed that suitable values of proportional gain and integral gain are 1.8 and 2 respectively. Fig. 2.5 shows the Bode diagram of output current transfer function $G_{I2}(s)$ with different gains.

When the proportional gain $K_p$ is selected to be 1 and integral gain $K_i$ to be 2, the gain and phase margins are higher but the gains are low at the fundamental frequency and its harmonics. The low gains result in poor disturbance rejection. However, when the proportional gain $K_p$ is increased, the system becomes unstable. As an example, Fig. 2.6 shows the distorted output current when utility THD is 5.8%. This does not meet the required standards of the disturbance rejection.

In addition, there exists steady state error as well: the reference current peak value is 100A. The maximum current could be 116A as per the parameters given in Table 1.2. The simulation results reveal that when the utility THD is more than 5%, the classical PI controller is unable to produce an output current as per required standards. With the use of voltage feedforward, steady state error could be reduced considerably but attenuation of current harmonics is still not possible. The most common reason is that PI control regulators are not suitable for AC current regulation and suffer from stability limits and steady state error because of low loop gains. Moreover, it is interesting to mention here that almost the same performance can be achieved with a simple proportional (P) controller with only proportional controller gain $K_p$. Therefore, there is not much difference between P or PI control in this application.

| **No.** | **Controller Gains** | | **Utility THD** (%) | **Output Current THD (%)** |
|---|---|---|---|---|
| | $K_p$ | $K_i$ | | |
| Case 1 | 1.8 | 1 | 3.8 | 4.8 |
| | 2 | 2 | | 4.7 |
| | 2.3 | 3 | | 5.0 |
| Case 2 | 1.8 | 2 | 5.8 | 6.3 |
| | 2 | 1 | | 6.2 |
| | 2.3 | 3 | | 6.5 |
| Case 3 | 1.8 | 1 | *10.44* | 9.5 |
| | 2 | 1 | | 9.3 |
| | 2.3 | 3 | | 9.4 |

*Table 2.1: Percentage THD of output current with PI controller*

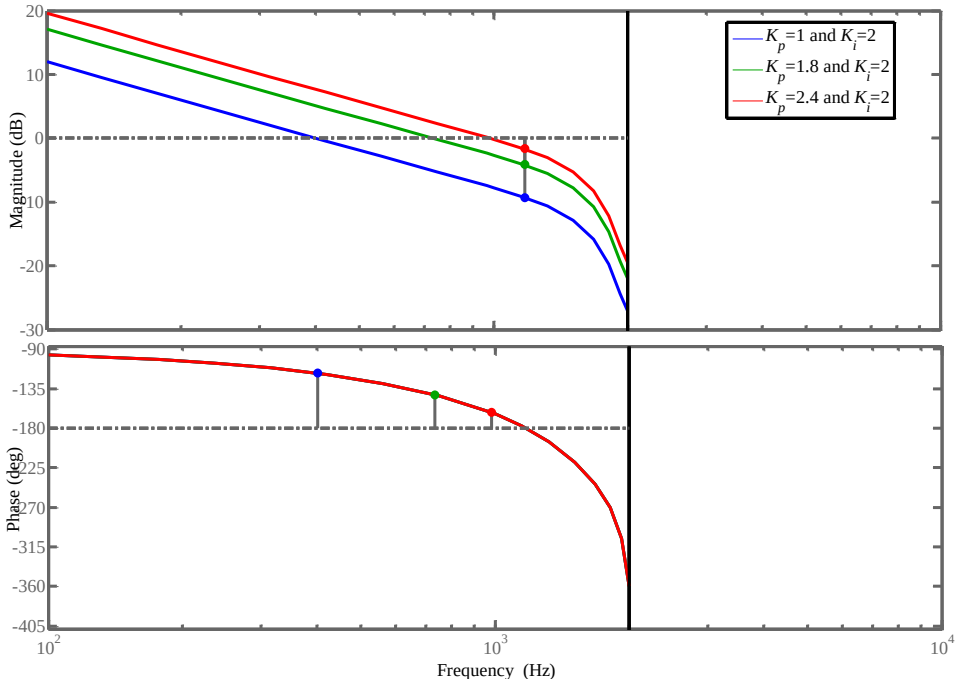


*Fig. 2.5: Bode diagram of output current transfer function with classical (PI) controller*

[Transfer function: $G_{I2}(s) = \dfrac{K_p K_i G(s)}{1 + K_p K_i G(s)} I_{ref}$ and $G(s) = \dfrac{1}{(L_1 L_2 C)s^3 + K_c L_2 C s^2 + (L_1 + L_2)s}$]

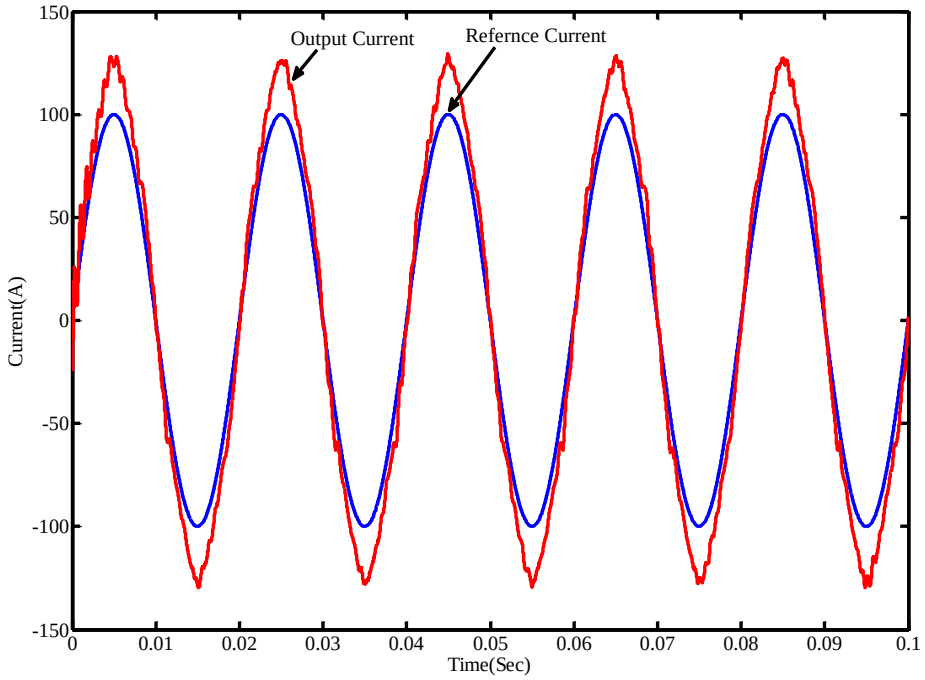


*Fig. 2.6: Output current of two-level converter with PI controller when utility THD is 5.8%*

*,Output current THD is 6.2 % and* $I_{ref}(peak) = 100A$

The synchronous (d-q) PI regulators can address the limitations of the reference frame PI regulators (Zmood and Holmes, 2003). The synchronous (d-q) transformation (see Fig. 2.7) translates the measured AC signals of voltage and current to DC, which simplifies controller design and conventional DC regulators can be used (Twining and Holmes, 2003). However, this approach assumes that the converter is synchronised with the utility voltage, which in practice is often not the case. This could be due to incorrect information of the amplitude, phase angle and frequency of the utility voltages, which are normally provided by phase locked loop algorithms (Picardi and Sgro, 2009). Another reason might be the presence of strong harmonic distortions, which act as disturbances that cause deterioration of the output current THD (Weiss et al., 2004). Moreover, it will involve an extra computational burden because it requires transforming the stationary frame AC currents to rotating frame DC quantities, and transforming the obtained quantities back to a stationary frame for generation of PWM signals.

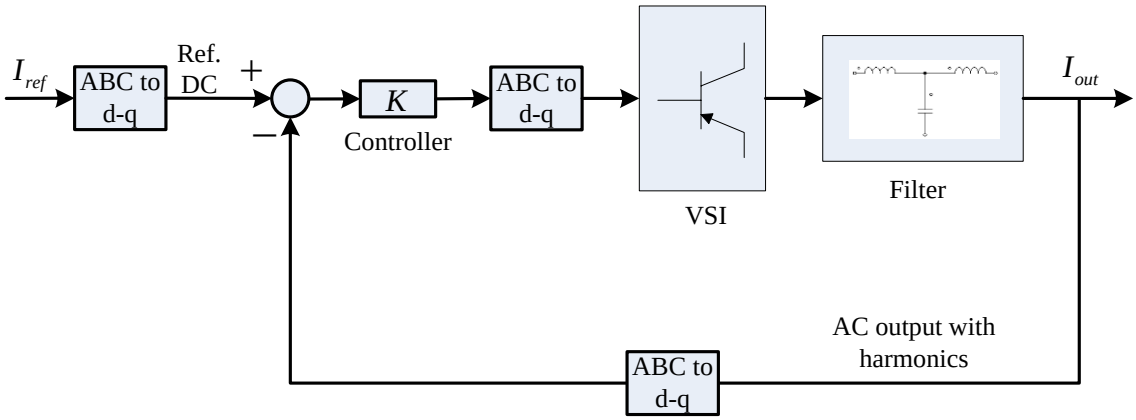


*Fig. 2.7: The basic idea of synchronous d-q approach for VSC*

The possible solution to avoid complexity, obtain zero steady state error and better disturbance rejection is the use of proportional resonant (PR) controllers, which achieve the same transient and steady state performance as a synchronous (d-q) PI regulators (Guoqiao et al., 2010; Sung-Yeul et al., 2008) and is discussed shortly.

## II. Predictive and Deadbeat Control

Deadbeat controllers have been widely used for voltage-source PWM converters (Mohamed and El-Saadany, 2007; Svensson and Lindgren, 1999; Timbus et al., 2009). They belong to the predictive control family in which utility current is predicted at the beginning of each sample and the current error is found. Then the control action is developed to minimize the forecast error so that the reference current can be tracked properly without any error. It can be easily implemented on digital processors. When the poles of the characteristic equation are placed at the origin, the predictive controller is often called a deadbeat controller (Kazmierkowski and Malesani, 1998; Kojabadi et al., 2005; Qingrong and Liuchen, 2005).

Deadbeat control has a fast transient response and is widely employed for active power filters too. Odavic et al. (2011) have recently used a one-sample-period-ahead predictive current control for active power filter applications (Odavic et al., 2011). The same ideas have been used for current control of utility connected converters as well (Hornik and Zhong, 2011; Gao et al., 2011; Espi et al., 2011). Espi et al. (2011) designed adaptive robust predictive control for utility connected converters and performance is independent of the output filter type (L or LCL). The resistive part of the filter is estimated by the resulting control. The error correction is achieved by means of an adaptive strategy that works in parallel with the deadbeat control algorithm. A fast response can be achieved, however, deadbeat control signals largely depend on a precise model of the PWM utility connected converter. Prediction could be a difficult task when utility voltage has high harmonic content and under varying system parameters, such as utility impedance.

In order to overcome the shortcomings of deadbeat control, other control techniques could be combined to enhance the performance. For example, Gao et al. (2011) used RC with deadbeat current controller for PWM rectifiers.

## III. Proportional Resonant (PR) Control

Proportional resonant (PR) controllers have been widely used for utility connected converters due to their ability to get rid of the steady state error and attenuation of individual harmonics (Hwang et al., 2010; Guoqiao et al., 2010; Teodorescu et al., 2006;

Liserre et al., 2006; Zmood and Holmes, 2003). It theoretically introduces an infinite gain at a selected resonance frequency. It can be regarded as an AC regulator/integrator and is similar to an integrator whose infinite DC gain, forces the error to be zero (Teodorescu et al., 2006). By having PR control in a stationary frame, there is not much computational effort of transformation involved in synchronous (d-q) regulators and there is the same performance as synchronous (d-q) PI regulators (Hwang et al., 2010).

The basic PR controller derived by Zmood and Holmes (2001), can be represented by the transfer function given in equation (2.7). Where, $K_p$ is the proportional gain, $K_r$ is the gain of resonant term and $\omega_o$ is the resonant frequency. This basic PR cannot be implemented in practice due to the demand of infinite gain at resonant frequencies from either an analog or digital system. Normally, it is modified by introducing a new term, quality factor $Q$, as shown in equation (2.8). Additional selective compensators can be added to equation (2.8) to reject selective harmonics such as third, fifth and seventh order as represented by equation (2.9). The block diagram can be represented by Fig. 2.8, where input current error is fed into the PR controller.

The quality factor $Q$ is a ratio between the central resonant frequency ( $f_o$ ) and the difference of upper ( $f_H$ ) and lower ( $f_L$ ) frequencies i.e. $Q = f_o/(f_H - f_L)$ (Lenwari et al., 2009). At upper and lower frequencies, the gain of the system drops to 0.707 (-3dB) of the gain at central resonant frequency. The higher value of quality factor $Q$ will provide a higher gain and narrow bandpass region around the resonant frequency. Whereas, a lower value of $Q$ will provide low gain that could result in a higher steady state error and low disturbance rejection. So, a higher value of $Q$ is desirable without affecting stability to have a better reference tracking and higher disturbance rejection (Lenwari et al., 2009). Fig. 2.9 shows the Bode plot of the resonant controller without adding the proportional term given in equation (2.8) against variations in $Q$.

$$G_{PR1}(s) = K_P + \frac{K_r \omega_o s}{s^2 + \omega_o^2} \tag{2.7}$$

$$G_{PR2}(s) = K_P + \frac{K_r \omega_o s}{s^2 + (\omega_o/Q)s + \omega_o^2} \tag{2.8}$$

$$G_{PR3}(s) = K_P + \frac{K_r \omega_o s}{s^2 + (\omega_o/Q)s + \omega_o^2} + \sum_{h=3,5,7} \frac{K_{rh}(h\omega_o)s}{s^2 + (h\omega_o/Q)s + (h\omega_o)^2} \tag{2.9}$$

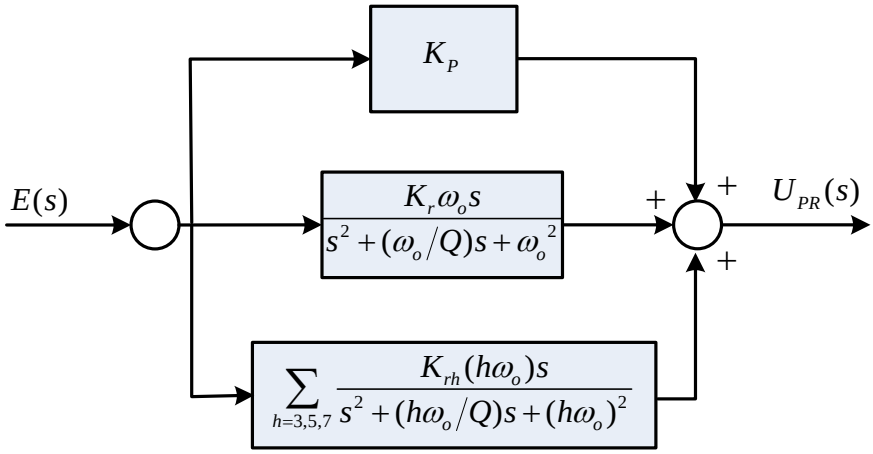


*Fig. 2.8: Structure of proportional resonant (PR) control*

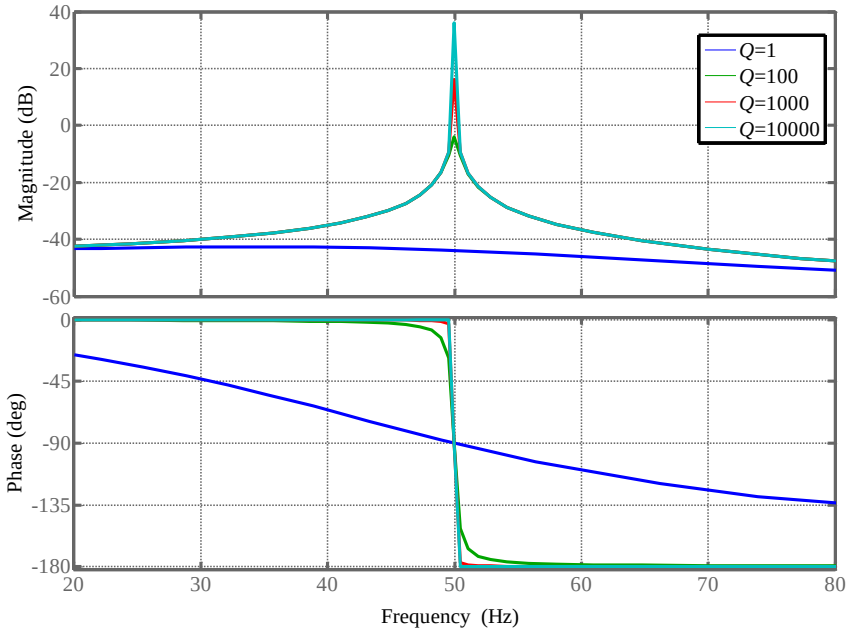


*Fig. 2.9: Bode plot of resonant controller when quality factor Q is varied*

The Bode diagram of PR control (equation 2.9) for the two-level utility connected converter (Table 1.2) is shown in Fig. 2.10 to provide an insight into its working. The suitable values

of the resonant controller gain $K_r = 2$, the quality factor $Q = 1000$ and the proportional controller gain $K_p = 1.8$ have been selected by looking at the Bode plot. It can be seen that PR can provide higher gains at the fundamental frequency (50 Hz) and its third, fifth and seventh order harmonic frequencies. The system open loop system gain margin is 2.9dB and phase margin is $17.5^o$. In case of classical (PI) controller (designed earlier in same section), the suitable value of $K_p = 1.8$ and $K_i = 2$ gives a gain margin of 4.17dB and phase margin of $37.9^o$ as shown in Fig. 2.10. In terms of stability margins/reference tracking, there is not much difference between the classical (P or PI) controller and PR controllers. However, in terms of disturbance rejection/steady state error, the resonant controller provides better performance due to higher gains at fundamental frequency and its harmonics.

By having multiple PR controllers we can control higher order harmonics. However, a bank of resonant controllers will increase the complexity of the system and complicate the digital hardware implementation. Moreover, the harmonic compensators present in PR are limited to low order harmonic frequencies due to stability limits. The difficulty arises due to bandwidth constraints while compensating higher order harmonic frequencies (Teodorescu et al., 2006, Zmood and Holmes, 2003). Passive damping is normally used to avoid instability at the cost of losses and degradation in filter performance. The use of active damping methods by having an extra loop for the current through the first inductor has been proposed (Guoqiao et al., 2010). However, this requires extra current sensor and increases computational burden on microprocessors (Sung-Yeul et al., 2008) as discussed earlier.

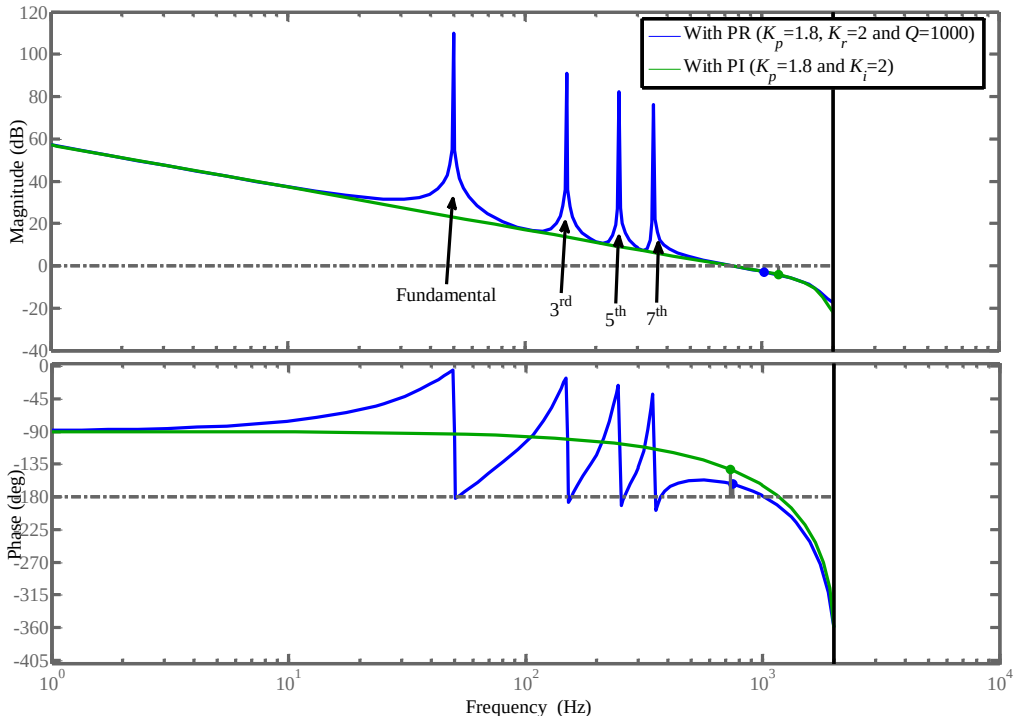


*Fig. 2.10: Bode plot of a PR controller for the two-level converter*

## IV. Other Controllers

In addition to the above controllers, many other controllers such as state feedback using pole placement, optimal (LQG/LQR), nonlinear (e.g. sliding mode, hysteresis, intelligent) and $H_\infty$ controllers have been used for control of utility connected converters. The purpose of all the different controllers is to enhance the loop gain effectively and improve the disturbance rejection by rejecting utility voltage harmonics. These controllers are briefly discussed here.

One of the attractive solutions for the control of converters could be a state-feedback approach using pole placement technique (Dannehl et al., 2010). The resonant poles due to the presence of LC or LCL filters in the converters can be dampened using state feedback. However, this is quite effective especially when all states are possible to measure. With the state feedback, it is possible to use optimal methods to find the coefficients or gains of control law. The idea about optimal methods is based on the criteria function (or performance index) describing the behaviour of the system where the minimum (or maximum) of the criteria function gives the control signal. When the system to be

controlled is linear, all states are possible to measure and the criterion is a quadratic function of the states and control signal, the control system will be a linear quadratic (LQ) control system. When all states are not possible to measure and disturbances considerably affect the system, a Kalman Filter (observer) can be applied for state estimation and the control system would be known as a linear quadratic Gaussian (LQG) control system (Peltoniemi et al., 2009). Alepuz et al. (2006) used a multivariable state-space LQ controller for current control of a three-level utility connected inverter and found some promising results. However, multivariable state feedback approaches are complex in nature and require extra computational efforts for implementation especially when observers estimate the state.

The nonlinear controllers such as sliding mode, hysteresis and intelligent controllers have also been used for PWM converters. Sliding control is a special version of on-off control and is a variable structure controller. The key idea is to apply strong control action when a system deviates from the desired behaviour. The sliding mode controller can provide good performance against parameter variations. However, these controllers tend to make difficulty in debugging and testing when combined with modulation circuits (Camargo and Pinherio, 2005). Additionally, their performance is degraded when a limited sampling is used. Other nonlinear controllers such as the hysteresis controller can also be used to control the output current using the hysteresis band. It is simple and fast in nature but results is high and variable sampling frequencies that can cause high current ripples and poor current THD (Hornick and Zhong, 2011). Other type of nonlinear controllers such as intelligent controllers based on neural network and fuzzy is not a strong candidate in this application since the PWM converter models are well known and its nonlinearity is not severe. Instead, the linear controllers are used, as they are easy to implement and are well known (Camargo and Pinherio, 2005).

An alternative robust controller such as $H_\infty$ can be a good candidate for current control of utility connected converters (Hornick and Zhong, 2011). It can address the plant uncertainties (such as variations in utility impedance) while rejecting utility harmonics (disturbances) in the output current. $H_\infty$ controller can provide higher gains similar to PR if weighting functions of $H_\infty$ controller are carefully selected (Shuitao et al., 2011). The

desired loop shapes can be obtained using standard $H_\infty$ synthesis using a robust control toolbox in Matlab.

Each controller has some advantages and disadvantages as discussed earlier. Other than the above-mentioned controllers, the repetitive controller (RC) is good candidate due to the presence of periodic errors in this application of utility connected converters. Moreover, RC can naturally offer higher gains at the fundamental and its harmonics, which can provide lout output current THD. This control technique is discussed in the next section.

## 2.3 A Brief Overview of Repetitive Control (RC)

Repetitive feedback control has been derived from the concept of iterative learning control (ILC). The RC works based on the ILC algorithm. Error between the reference value and feedback utility connected current on a cycle-by-cycle basis is the input to the RC. The RC is perhaps most similar to the ILC except that the RC is intended for continuous operation, whereas the ILC is intended for discontinuous operations. For example, an ILC application might be to control a robot that performs a task, returns to its home position, and comes to rest before repeating the task (Owens and Liu, 2011; Ratcliffe et al., 2006). In contrast, an RC based application might be to control some hard disk drive's application, in which each iteration is a full rotation of the disk, and the next iteration immediately follows the current iteration (Moore et al., 1992). In terms of implementation, there is no difference between ILC and RC in our application. As the utility connected converter system is required to follow the same position profile for each cycle, it is ideally suited to have an RC. The RC slowly removes the position error as the number of completed iterations increases. A memory is used to store the cumulative effect of some proportion of the tracking error over the previous iterations, which is then used to update the demand for current iteration. The RC tracks all periodic signals for one cycle and then generates compensating signals for correction to ensure perfect tracking or servo control. So a delay of one cycle in the output is observed at the advantage of more design freedom.

RC has been widely used for many practical industrial systems in manufacturing (Chen and Hsieh, 2007), robotics (Tinone and Aoshima, 1996) and chemical processes (Won et al., 2010), where mass production on an assembly line leads to repetition. However, the

application of an RC in current control of a utility connected system is still an active area of research. There are very few publications (Gao J. et al., 2011; Hornik and Zhong, 2011) related to current control which describe the effect of different parameter variations present in RC and their effect on the system's overall stability and transient response. Moreover, limits of performance of RC with reference to system bandwidth need to be investigated, especially for two-level utility connected converters due to the resonance and higher capacitance values of the output LCL filter.

RC is also related to the internal model principle (IMP). According to this principle (Francis and Wonham, 1976), the output of a closed-loop system tracks an input reference signal without steady state error if the model that generates this reference is included in the stable feedback system. Based on the IMP, a periodic signal generator could be included in the RC feedback loop as the internal model. The transfer function of a periodic signal generator can be represented by equation (2.10), where $T_p$ is the period of input signal.

$$G_g(s) = \frac{e^{-sT_p}}{1-e^{-sT_p}} = \frac{1}{e^{sT_p}-1} \tag{2.10}$$

A typical conventional basic RC includes a gain $K_R$ multiplied by the transfer function of the periodic signal generator as shown below.

$$G'_{RC}(s) = K_R \frac{e^{-sT_p}}{1-e^{-sT_p}} = \frac{K_R}{e^{sT_p}-1} \tag{2.11}$$

For further insight of this transfer function, we can rewrite it as follows:

$$G_g(s) = K_R \left[ -\frac{1}{2} + \frac{1}{2}\left( \frac{1+e^{-sT_p}}{1-e^{-sT_p}} \right) \right] \tag{2.12}$$

From the properties of the exponential function, we know that

$$\pi \frac{e^{\pi x}+e^{-\pi x}}{e^{\pi x}-e^{-\pi x}} = x \sum_{k=-\infty}^{\infty} \frac{1}{x^2+k^2} = \frac{1}{x} + \sum_{k=1}^{\infty} \frac{2x}{x^2+k^2} \tag{2.13}$$

Thus equation (2.12) can be transformed as follows by substituting $x = \frac{s}{\omega_o}$ in equation (2.13),

$$G_{rc}(s) = K_R \left\{ -\frac{1}{2} + \frac{1}{T_p}\left[ \frac{1}{s} + \frac{2s}{s^2 + \omega_p{}^2} + \frac{2s}{s^2 + (2\omega_p)^2} + \frac{2s}{s^2 + (3\omega_p)^2} + .... \right] \right\} \tag{2.14}$$

According to above equation, the RC is mathematically equivalent to a parallel combination of an integral controller, many resonant controllers and a proportional controller (Lu et al., 2010).

RC is normally implemented in the discrete domain. In a discrete time domain, periodic signals with a known period $T_p$ can be generated by a time delay block $z^{-N}$ with a positive feedback loop as shown in Fig. 2.11. *N* is given by following equation.

$$N = \frac{T_p}{T_s} \tag{2.15}$$

Where, $T_p$ is the time period of any periodic input and $T_s$ corresponds to sampling time.

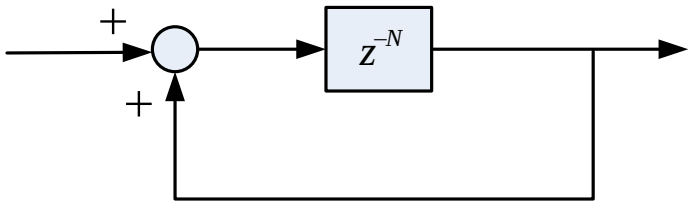


*Fig. 2.11: Periodic signal generator*

The transfer function of the discrete time periodic signal generator can be written as follows:

$$G_g(z) = \frac{z^{-N}}{1 - z^{-N}} = \frac{1}{z^{-N} - 1} \tag{2.16}$$

The above transfer function has *N* number of poles equally distributed around the unit circle [ $z = e^{j2k\pi/N}$ and $k = 0,1,2,.....$], therefore, it is possible to track a periodic reference or

reject periodic disturbances with the same fundamental frequency or its harmonics (Rech and Pinheiro, 2004). The magnitude frequency response of a periodic signal generator can be seen in Fig. 2.12, which also shows that different gains (like resonant controller) can be applied to fundamental frequency and its harmonics.

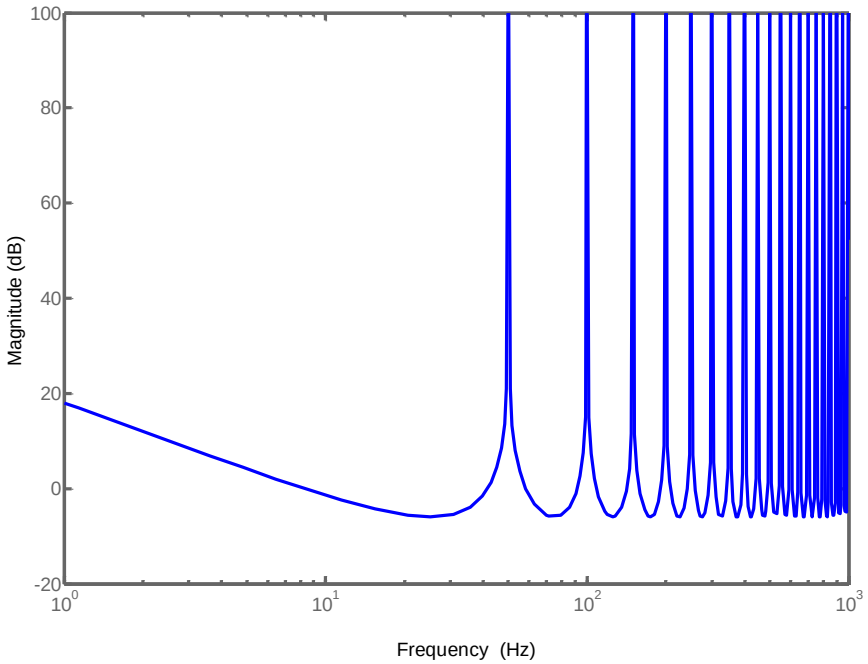


*Fig.2.12: Magnitude frequency response of a periodic signal generator*

There are different notations and different versions of RCs. A typical conventional basic RC includes RC gain $K_R$ multiplied by the transfer function of the periodic signal generator,

$$G_{RB} = \frac{Y(z)}{I_e(z)} = K_R \frac{z^{-N}}{1 - z^{-N}} = \frac{K_R}{z^N - 1} \tag{2.17}$$

The term $z^{-N}$ in the above transfer function refers to delay, which postpones the control effort so that the error detected in the current cycle could be corrected in the next cycle. Normally *N* is a very large number and requires large memory buffers, which is a drawback (Pipeleers et al., 2009) of RC. Moreover, it is noticeable that the selection of *N* is related to proper sampling time, which is crucial for the discrete periodic signal generator. If the

sampling time is too low (i.e. corresponding sampling frequency is high), the time delay would be of a higher order, which makes it difficult to stabilise the controller.

The control objective is to find an appropriate optimal value of the RC gain $K_R$ such that the tracking error converges to zero as the number of iterations approaches to infinity.

$$\lim_{k\to\infty} \|E(K_R)\| = 0 \tag{2.18}$$

This basic RC is most suitable for those applications where (i) we know precisely about the input and its period $T$ (ii) period $T$ is constant or accurately measureable (Pipeleers et al., 2009). This RC structure produces a significant rise in error, similar to other controllers designed in the literature (Sharkh et al., 2001) needs resetting after a few cycles. Modifications are needed to avoid instability and the requirement of resetting after a few cycles. This can be achieved by incorporating more parameters (e.g. a low-pass filter) as discussed in the following section.

### 2.3.1 Modified Repetitive Control (RC)

It is a nontrivial problem to stabilize the system due to the time delay elements of the positive feedback loop present in RC. Moreover, the open loop poles of the repetitive controller are on the stability boundary, where the stability of the overall system is sensitive to non-modelled dynamics. To overcome this limitation and to enhance robustness of the system, a low-pass filter is introduced to filter out the high frequency components of the frequency response (Keliang and Danwei, 2001, Chen et al., 2008). Robustness is achieved at the expense of performance at high frequency. The design of the low-pass filter is very important and it reflects the trade-off between closed loop system performance and stability robustness. Due to using a low-pass filter, the actual location of poles of the internal model move inside the unit circle. Thus, the basic ideal RC is modified by adding low-pass filter $Q(z)$ to make it practical as shown in Fig. 2.13 or Fig. 2.14. By the introduction of $Q(z)$, the overall RC structure changes from pure integral to quasi-integral form, avoiding $N$ open loop poles located on the boundary of the unit circle caused by pure integration which makes the system critically stable. This significantly improves the stability and robustness of RC.

An alternative to using a low-pass filter $Q(z)$, a constant smaller than 1 has also been used (Jamil et al., 2010) but in practice it is not sufficient and RC cannot attenuate the unwanted components around the cut-off frequency effectively. This could result in an unstable system if parameters of RC are changed. In (Yingjie et al., 2009), $Q(z)$ has been selected as a low-pass filter. It increases the stability margin at the cost of reduced bandwidth. Another similar approach is described in (Keliang and Danwei, 2001; Pipeleers et al., 2009) where a finite impulse response (FIR) low-pass filter has been selected as $Q(z)$. Keliang and Danwei (2001) used RC for sinusoidal voltage control and they combined RC with a stable one-sample ahead controller. They applied RC in a plug-in fashion and found that the controller can handle variations in parameters very well (Keliang and Danwei, 2001). Zhang et al. (2008) proposed a phase-lead compensator option within the RC structure to control the output voltage under different loads as well as assuming balanced supply conditions. However, in reality, the supply conditions are distorted and unbalanced. There are various configurations of the modified repetitive control as well. For example , the authors in Wu et al., (2010) used the so-called plug-in repetitive controller as shown in Fig. 2.13. They placed the low-pass filter outside the loop. Here, $Q(z)$ still attenuates the high frequency gain but it will face difficulties in tracking high frequency elements. The number of samples is $N = N_1 + N_2$, where $N_1$ is used to compensate the phase lag caused by the low- pass filter and signal transmission and $N_2$ is regarded as a phase angle compensator. The current error $E(z)$ is input to RC and $U_{RC}(z)$ is the output of RC. The transfer function of this RC is given by,

$$G_{RC1}(z) = \frac{U_{RC}(z)}{E(z)} = Q(z)\frac{K_{RC}z^{-N1}}{1-z^{-N}} \tag{2.19}$$

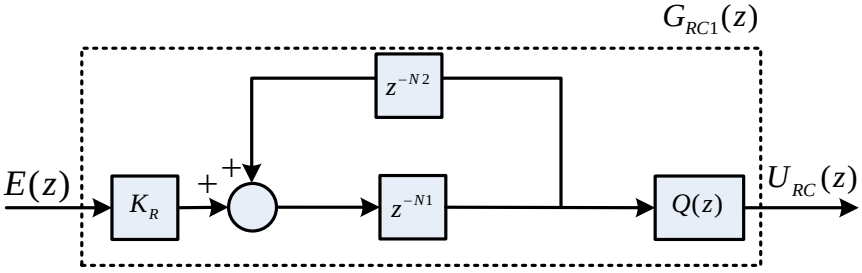


*Fig.2.13: Structure of RC by* (Wu et al., 2010)

Another interesting structure of RC has been used by (Rohouma et al., 2010) for the matrix power supply converter's control as shown in Fig. 2.14. Here, $Q(z)$ has been selected as constant (0.9), but a second order low-pass filter $G_f(z)$ has been placed outside the signal generator loop to reject high frequency components. The rest of the design is almost similar to Wu et al., (2010) where $N = N_1 + M$ . The transfer function of this RC is given by,

$$G_{RC2}(z) = \frac{U_{RC}(z)}{E(z)} = \frac{Q(z)z^{-M}}{1 - Q(z)z^{-N}} K_{RC} G_f(z) \tag{2.20}$$

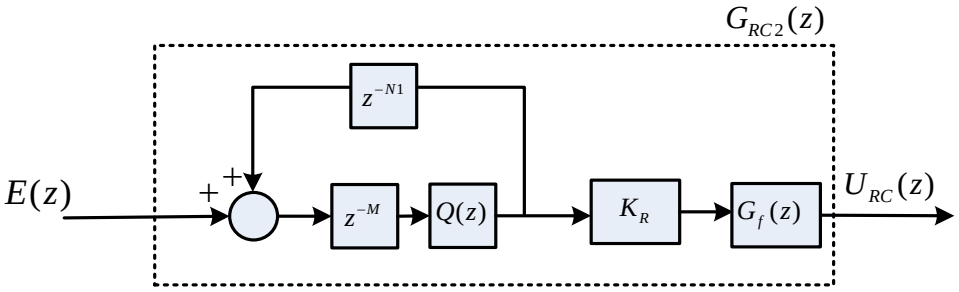


*Fig.2.14: Structure of RC by (Rohouma et al., 2010)*

The above-mentioned approaches are quite similar in the sense of rejecting unwanted components around a cut-off frequency, which causes instability. These mentioned approaches can be used for current control of utility connected converters as well. In general, the value of *N* as a delay block in the forward path can be used with $Q(z)$ as shown in Fig. 2.15 for the work carried out in this thesis and the phase compensator is used later on. This can achieve fast error convergence and better control of individual harmonics. Selection of the compensator $G_f(z)$ in Fig. 2.15 depends upon the characteristics of the original feedback closed loop system. The selection relies on the effect that the original feedback system is stable enough. For minimum phase plants (no zero outside unit circle), it is desirable to choose $G_f(z)$ to be the inverse of the system model to achieve zero-phase error tracking. However in practice the utility impedance varies significantly and the transfer function is therefore not known (Zhang et al., 2008, Yongqiang et al., 2006). Moreover, this results in a complex compensator, which is computationally costly to implement. A reasonable approximation is achieved by selecting a phase-lead compensation scheme given by,

$$G_f(z) = z^m \tag{2.21}$$

The time advance $z^m$ compensates for the phase lag of the converter to improve stability. Basically this phase leading is responsible for overall phase lag of the plant in the low and intermediate frequencies (Liang et al., 2006).

The RC gain, $K_R$, determines the amount of repetitive control action. The speed of error convergence is directly related to the gain $K_R$ .

The structure of RC used in this thesis is shown in Fig. 2.15 and Fig. 2.16. Fig. 2.15 represents the structure of RC and Fig. 2.16 represents the overall control system including RC. It is worth mentioning here that the RC is added to the existing feedback control system, which must be stable as per the requirement of stability conditions. These conditions will be discussed in the next chapter. Although, the RC mathematically ensures that the tracking errors will converge to zero when repetition goes to infinity, however, poor tracking accuracy and transients can be observed if the filter $Q(z)$ is not properly designed (Longman, 2000). The conventional controller is normally required due to the tracking accuracy and it must be stable for overall stability. The simplest tracking controller could be a proportional controller, which has been selected in this application. However, combination of other controllers with RC would be subject of the future work.

Here the conventional controller is $G_c(z)$, plant including filter is $G_p(z)$ and the RC is $G_{RC}(z)$. The output current is $Y(z)$, reference current is $R(z)$, error $E(z) = R(z) - Y(z)$ and the disturbance $D(z)$ is related to utility harmonics.

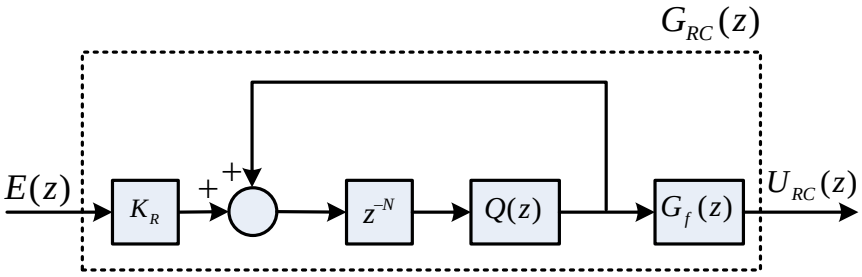


*Fig. 2.15: Structure of RC used in this thesis*

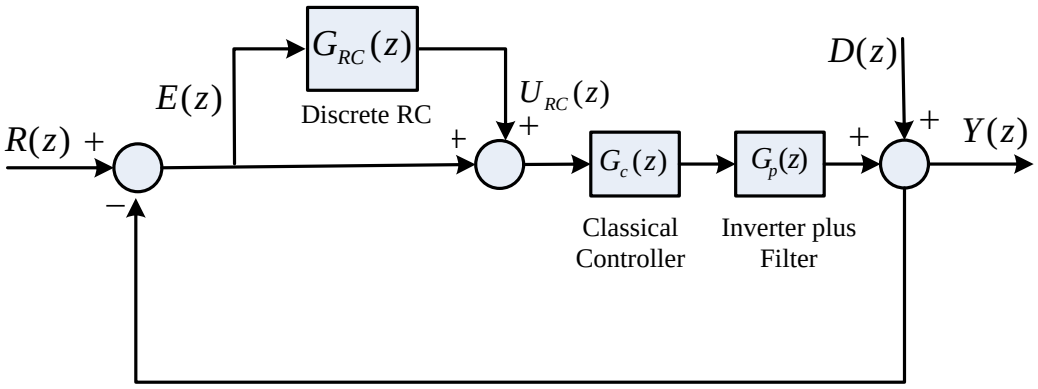


*Fig. 2.16: Overall block diagram of the system with RC*

As concluding remarks, it is worth mentioning that splitting the value of *N* in two parts as shown in Fig. 2.14 and using the compensator of type ($G_f(z) = z^m$) is similar to the other structure shown in Fig. 2.15.

The RC transfer function is given by $G_{RC}(z)$

$$G_{RC}(z) = \frac{E(z)}{U_{RC}(z)} = \frac{K_R Q(z) z^{-N}}{1 - Q(z) z^{-N}} G_f(z) \tag{2.22}$$

The transfer function of the RC given by the above equation (2.22) differs from equation (2.19) and equation (2.20) in a sense that the number of samples *N* is not divided into two parts.

The conventional controller PI has been selected to have enough gain and phase margins in our case. Other controllers can also be used instead of PI for tracking purposes and the RC can be added to improve steady error and disturbance rejection. For example, authors in Weiss et al. (2004) used the $H_\infty$ controller instead of the PI as a conventional controller with RC and found good results in voltage control of DC-AC converters at different loads. Other control techniques mentioned earlier, could also be used with RC. The transfer function of the feedback control system without RC (Fig. 2.16) is given by,

$$G_o(z) = \frac{G_c(z)G_p(z)}{1+G_c(z)G_p(z)} \tag{2.23}$$

Now the overall transfer function of the system with respect to the reference using Fig. 2.16 is derived and is given by,

$$\frac{Y(z)}{R(z)} = \frac{\left(1+G_{RC}(z)\right)G_c(z)G_P(z)}{1+\left(1+G_{RC}(z)\right)G_c(z)G_P(z)} \tag{2.24}$$

Using equation (2.22) and (2.23), the following equation is obtained,

$$G_R(z) = \frac{Y(z)}{R(z)} = \frac{\left(1-Q(z)z^{-N}+K_RQ(z)z^{-N}G_f(z)\right)G_o(z)}{1-Q(z)z^{-N}\left(1-K_RG_f(z)G_o(z)\right)} \tag{2.25}$$

Similarly, the overall transfer function with respect to disturbance in Fig. 2.16 is derived and is given by,

$$\frac{Y(z)}{D(z)} = \frac{1}{1+(1+G_{RC}(z))G_c(z)G_P(z)} \tag{2.26}$$

Using equation (2.22) and (2.23), the following equation is obtained,

$$G_D = \frac{Y(z)}{D(z)} = \frac{1-Q(z)z^{-N}}{\left(1+G_c(z)G_p(z)\right)\left(1-Q(z)z^{-N}(1-K_RG_f(z)G_o(z))\right)} \tag{2.27}$$

The overall error transfer function of the system is as follows,

$$G_E(z) = \frac{E(z)}{R(z)-D(z)} = \frac{1}{1+\left(1+G_{RC}(z)\right)G_c(z)G_P(z)} \tag{2.28}$$

$$G_E(z) = \left(\frac{1-Q(z)z^{-N}}{\left(1+G_c(z)G_p(z)\right)}\right)\left(\frac{1}{1-Q(z)z^{-N}\left(1-K_RG_f(z)G_o(z)\right)}\right) \tag{2.29}$$

The above equations will be used for analysis and deriving stability conditions in the following chapters.

### 2.3.2 Odd-Harmonic Repetitive Control (ORC)

The odd-harmonic repetitive control (ORC) is a special type of RC, which lowers the microprocessor's memory requirement and computational effort. In a typical RC, $N$ is a very large number (e.g. $N$=400 in Table 1.3) as mentioned earlier and requires a large memory buffer which is a drawback of RC. Normally we have only dominant odd harmonics in power systems (Costa-Castello et al., 2004), so instead of providing higher gains at even harmonics, only dominant odd harmonics can be considered. The usage of ORC for active power filters and DC-AC converters are described in the literature (Zhaou et al., 2006; Miret et al., 2009; Keliang et al., 2005; Grino et al., 2007; Grino and Costa-Castello, 2005; Ramos et al., 2010; Costa-Castello et al., 2004 and Costa-Castello et al., 2006). The working principle of ORC is similar to conventional RC but it updates all memory cells after every $N/2$ sample intervals whereas conventional RC updates its memory cells after $N$ sample intervals. So ideally error convergence is twice as fast for the ORC system compared to conventional RC system (Zhou et al., 2006). A periodic discrete time signal $w(n)$ with period $N$ can be written as:

$$w(n+N) = w(n) \qquad \forall\, n \in \mathbb{Z} \tag{2.30}$$

And its Fourier series is given by

$$w(n) = \sum_{k=0}^{N-1} a_k e^{j2\pi kn/N} \tag{2.31}$$

$$a_k = \frac{1}{N}\sum_{n=0}^{N-1} w(n) e^{-j2\pi kn/N} \tag{2.32}$$

If the signal has odd harmonics only, then

$$w(n+N/2) = -w(n) \tag{2.33}$$

The corresponding periodic discrete transfer function of a periodic signal generator can be represented by the following function:

$$G_{go}(z) = -\frac{z^{-N/2}}{1+z^{-N/2}} = -\frac{1}{z^{N/2}+1} \tag{2.34}$$

The above equation has poles at $z = e^{j(2k+1)2\pi/N}$ with $k = 0,1,2,.....,(N/2-1)$. It offers infinite gain only at all odd harmonic frequencies $W_k = e^{j(2k+1)2\pi/N}$. The structure of ORC is shown by Fig. 2.17 and Fig. 2.18 represents the overall system including ORC. The transfer function of ORC can be written as follows,

$$G_{ORC}(z) = -\frac{K_R Q(z) z^{-N/2}}{1+Q(z)z^{-N/2}} G_f(z) \tag{2.35}$$

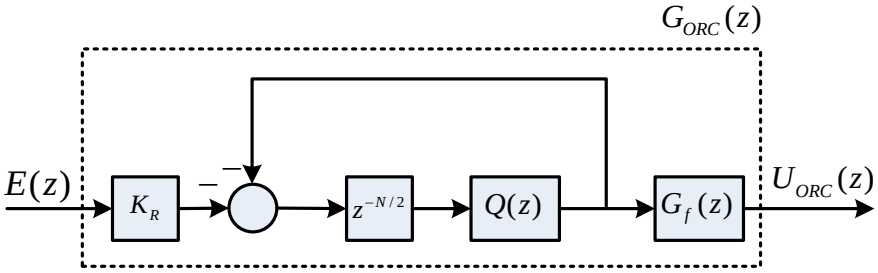


*Fig. 2.17: Structure of ORC used in this thesis*

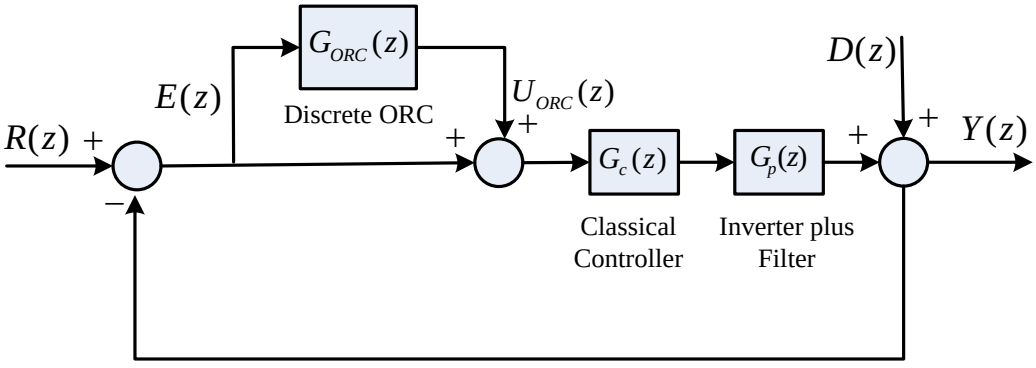


*Fig. 2.18: Overall block diagram of the system with ORC*

Now we can derive the overall transfer function of ORC with respect to the reference as follows.

$$\frac{Y(z)}{R(z)} = \frac{\left(1+G_{ORC}(z)\right)G_c(z)G_P(z)}{1+\left(1+G_{ORC}(z)\right)G_c(z)G_P(z)} \tag{2.36}$$

Using equations (2.23) and (2.35) we get the following,

$$G_{OR}(z) = \frac{Y(z)}{R(z)} = \frac{\left(1+Q(z)z^{-N/2}+K_R Q(z)z^{-N/2}G_f(z)\right)G_o(z)}{1+Q(z)z^{-N/2}\left(1-K_R G_f(z)G_o(z)\right)} \tag{2.37}$$

The disturbance transfer function is given by,

$$\frac{Y(z)}{D(z)} = \frac{1}{1+(1+G_{ORC}(z))G_c(z)G_P(z)} \tag{2.38}$$

Using equation (2.23) and (2.35), we get the following,

$$G_{OD}(z) = \frac{Y(z)}{D(z)} = \frac{1+Q(z)z^{-N/2}}{\left(1+G_c(z)G_p(z)\right)\left(1+Q(z)z^{-N/2}(1-K_R G_f(z)G_o(z))\right)} \tag{2.39}$$

Finally, the error transfer function is given by the following equation,

$$G_{OE}(z) = \frac{E(z)}{R(z)-D(z)} = \frac{1+Q(z)z^{-N/2}}{\left(1+G_c(z)G_p(z)\right)\left(1+Q(z)z^{-N/2}(1-K_R G_f(z)G_o(z))\right)} \tag{2.40}$$

The above equations will be used for analysis and deriving stability conditions in the following chapters.

## 2.4 Summary

In this chapter we looked at different current control techniques and structures used for utility connected converters. The different relevant current control methods such as PID, deadbeat, PR, RC and others have been discussed. Every method has some advantages and disadvantages. For example, in the case of the PID method, the limitations come due to low loop gains and high steady state error. The PI type of controllers are not suitable for sinusoidal reference tracking, but they are easy to implement. In the deadbeat current control method, one can achieve a very fast performance but they are sensitive to system parameters and prediction could be a difficult task when utility voltage has large harmonic contents and under varying system parameters such as utility impedance. In the next method, the importance of PR control is discussed which has been widely employed for current control of utility connected converters. This works based on the internal model principle and can be a good option for the limited number of harmonics. Finally, the RC is adopted because it can deal a very large number of harmonics simultaneously and can address the limitations of other control techniques. It also works based on the internal model principle. The continuous and discrete forms of the RC is analysed. The structure of the modified RC is described. A special type of RC known as ORC has also been discussed. The working principle, structure and transfer function of both types is derived which will be used in the coming chapters for analysis. Different control and system issues are also discussed in this chapter.

From the literature review, we can conclude the following:

- Utility connected converter technology is still in its infancy. The converter current control struggles to meet THD standards and other steady state error requirements especially when classical control techniques are used.
- Fundamentally, a variety of different control methods can be applied to current control of utility connected converters. RC is a suitable candidate due to its ability to track or reject periodic errors. It can offer higher gains at fundamental frequency and its harmonics.

- Although in the past decade, the theory and application of RC have been developing rapidly. In the field of power electronics, most of the publications are related to voltage control of the utility connected converters. There are few publications related to current control application of RC, which address all the issues of parameter variations, memory issues and establish its limits of performance with respect to system bandwidth.

# Chapter 3

## METHODOLOGY

## 3.1 Introduction

Computer simulations are widely used for analysing the behaviour of newly developed circuits in power electronics applications. This chapter deals with the computer simulation model and method of current control of utility connected converters. A switching simulation model and a linear transfer function model of the utility connected converters and controller are developed using Matlab. The Simpower Toolbox of Matlab is used for the development of the switching simulation model.

The reason for selecting Matlab/Simulink is presented in section 3.2. Section 3.3 describes the elements of the developed simulation model in detail. The linear models of the two-level and interleaved utility connected converters are derived and presented in sections 3.4 and 3.5. Section 3.6 briefly describes the performance criteria for evaluation and comparison of current control methods.

## 3.2 Background: General Selection of Software

In any simulation study, it is important that the nature of the simulation, its limitations and the assumptions made are discussed, so that the problems associated with the modelling and the simulation process can be well appreciated and the simulation results can be appropriate. One of the problems in the modelling of switching devices in power electronic circuits lies in the complexity of their actual characteristics. Accurate models of real switching devices are not always available. This is also true for magnetic components such as inductors. It is important that the objectives of the simulation are evaluated so that they can be achieved without the need to make the model any more complex than it needs to be, hence saving valuable modelling and computation times.

Passive and active switching circuits exhibit nonlinear behaviour during their transition from one switching state to the other. The nonlinearity introduced by the switching devices need to be considered when choosing a suitable computer simulation tool. The software has to be capable of performing this type of simulation. It needs to have the capability to run the simulations with the appropriate resolution to represent the smallest time constant in the simulation model with acceptable accuracy. The simulations of switching circuits generally take quite a long time to execute due to the large difference between the smallest and the largest time constants in the circuit, which can be several orders of magnitude. Therefore, it is important that the software is efficient in solving numerical problems. At the same time, the software also needs to be able to represent the controller with relative ease.

### 3.2.1 Reason for Selecting Matlab

Matlab is a well-known computer package for high-performance numerical computation and visualization with many available toolboxes for different applications. The convenient built-in features and various specialised toolboxes in Matlab make it easier to use. Matlab is developed to perform array and matrix manipulations easily; therefore it solves numerical problems in a fraction of the time compared to other software packages including SPICE (Baha, 1998). Simulink, an extension to Matlab, is a powerful graphical pre-processor developed especially for simulations of dynamic systems. Circuit models in Simulink are described as block diagrams. Block libraries containing various functions are supplied with the software. In addition, the users have the flexibility to create their own blocks with the use of the S-function written in C or Matlab M-files. Such a degree of flexibility cannot be found in circuit-oriented simulators. The various Matlab toolboxes, such as the Control System Toolbox and the Signal Processing Toolbox, provide the tool for control system design and manipulation of results from the simulation made readily available by Simulink. Due to these advantages, Matlab/Simulink has been chosen to carry out the computer simulation studies in this project.

Other than Matlab (Simpower Toolbox), different software packages such as Saber, OrCAD Capture, PSCAD etc. can also be used to design power electronic/electrical systems. However, Matlab is normally preferred due to the features already mentioned.

## 3.3 Description of the Two-Level Converter Simulink Model:

A model of the two-level converter was developed in Simulink to analyse the performance of the system. The model consists of the given electrical system (DC-link, converter, LCL filter, and utility) and the controller (current measurements, ADCs, PWM generator, reference currents, feed forward signals, summation operators and gains). During modelling and simulation, it is always required to represent the actual system as closely as possible. However, to simplify the modelling and reduce the simulation time, the following assumptions were made in some or all the simulation studies:

- Initially simulations assumed that the utility voltage has no harmonics, but in practice it is impossible to have zero harmonics. So in the latter stage of the work, harmonic content was introduced.
- Inductor saturation has been ignored as it could occur only in extreme cases of very high currents, which were not considered in this thesis.
- The equivalent series resistances (ESR) of the inductor has been ignored because these resistances improve the resonance damping of the system and the simulation condition has to take into account the worst scenario. However, a very small resistance (in the order of ten micro ohms) has been added in series with the capacitors in the DC connection configuration, because Simulink does not accept loops only containing capacitors. The value of 10 μΩ is added to the capacitor to have model convergence i.e. algebraic loops converge to a definite answer. It is known that without having a solution of algebraic loops can result in an error message and ending of the simulation.
- As the utility impedance is generally unknown and its variations can decrease controller performance, inductance $L_2$ represents the impedance from the filter capacitor to the point of common coupling (PCC) in the utility system.
- The DC link voltage is set to be constant. In practice, a DC voltage regulator/controller is used in the outer loop, which normally defines the amplitude of the reference current and the converter can support a seamless bidirectional power flow between converter and utility (Sivakumar et al., 2002). The reason for

having constant DC voltage is that it is assumed enough high, which can drive the current through the first inductor in the desired direction, e.g. in this case into the utility. This thesis focuses on the current control aspect of the utility connected converter only in one direction, but bidirectional power flow would be subject of the future work.

- Selection of the numerical solver depends upon the nature of the variables present in a model. The solver allows the selection of the numerical integration method and to set parameters for integration step size. It could be either a fixed-step or a variable-step solver. With a fixed-step solver, the step size remains the same throughout the simulation. In contrast, the variable-step solver can vary its step size to meet the error tolerance by considering the model dynamics. In general, variable-step solvers are more efficient and can reduce the simulation time. In our switching model, a continuous variable-step type of solver is selected. The simulation switching model works fine with ODE45 (default one) and other variable-step solvers. However, it is observed that the simulation can run slightly faster if a non-default solver such as ODE23 or ODE23t is selected due to the presence of slow and fast changing variables in the system.
- The simulation step size is normally selected in accordance with the converter's switching frequency. A rule of thumb is to choose a simulation step size 100 times smaller than the switching period. If the simulation step size is set too high, the simulation results can be erroneous. The universal converter block in Matlab allows the use of bigger simulation time steps, since it does not generate minor time constants (due to the RC snubbers) inherent to the detailed converter. For a controller sampling time of 50μs and 62.5μs (sampling frequency of 16 and 20KHz) for the two-level converter and 28μs (sampling frequency of 35KHz) for the interleaved converter, good simulation results have been obtained for a simulation time step of 0.1 μs. This time step can, of course, not be higher than the controller time step.

The complete Simulink model of the two-level utility connected three-phase converter is represented in Fig. 3.1. The two-level utility connected system with the addition of the RC

loop and supply harmonics, is shown in Fig. 3.2, whereas Fig. 3.3 shows the Simulink model of the interleaved utility connected converter system.

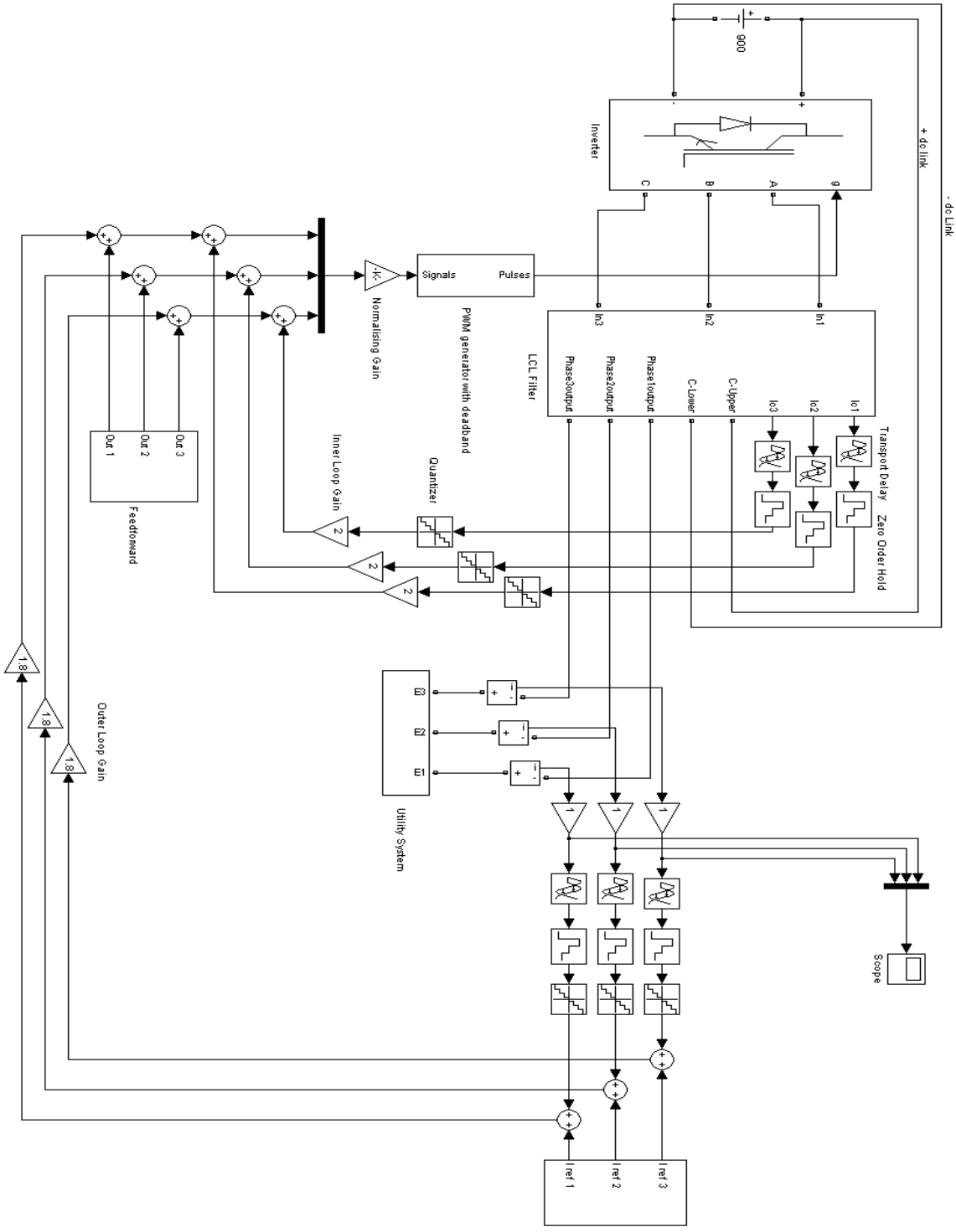


*Fig. 3.1: Three phase Simulink model of the utility connected converter without RC*

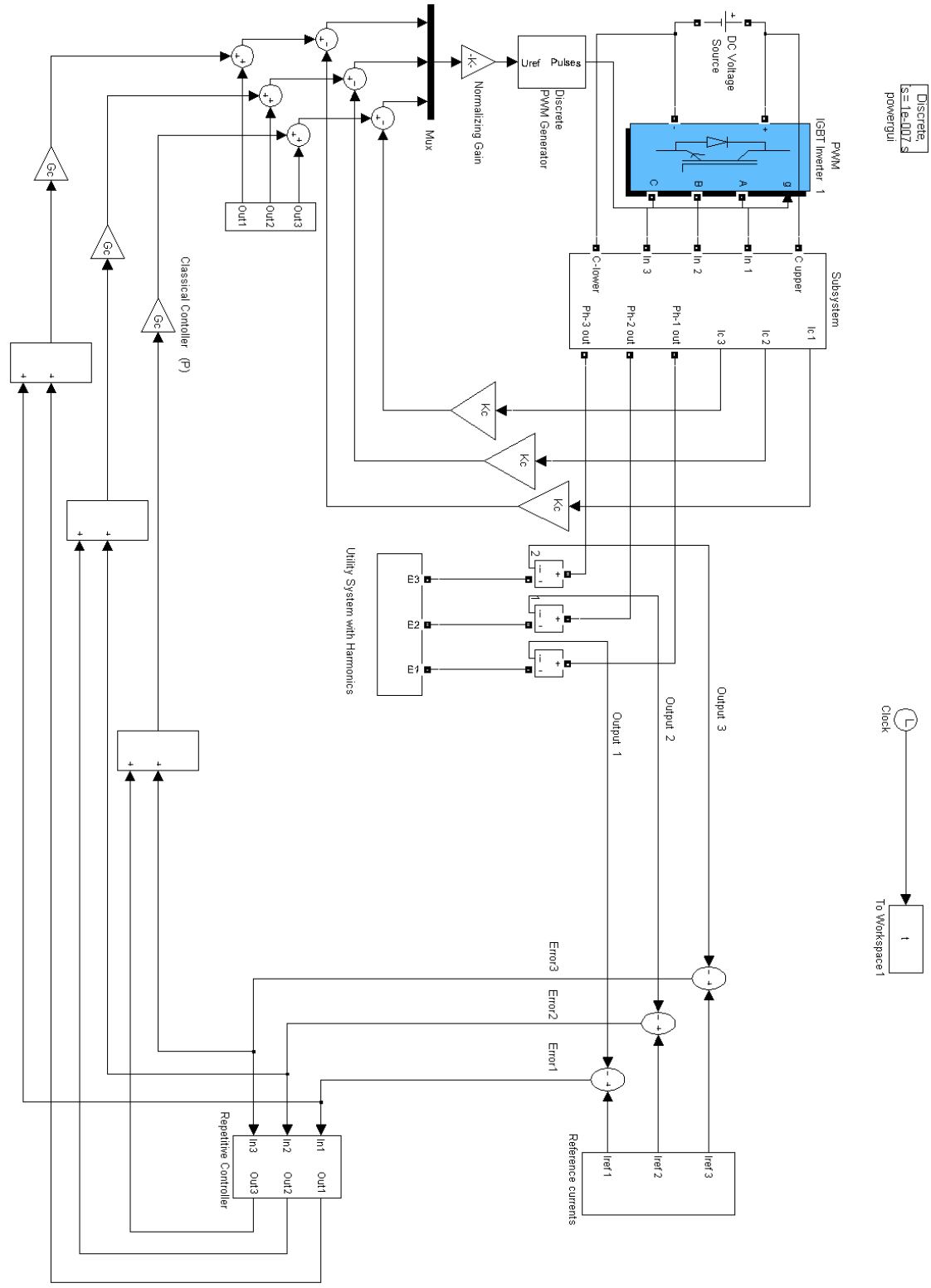


*Fig. 3.2: Three phase Simulink model of the two-level utility connected converter with RC*

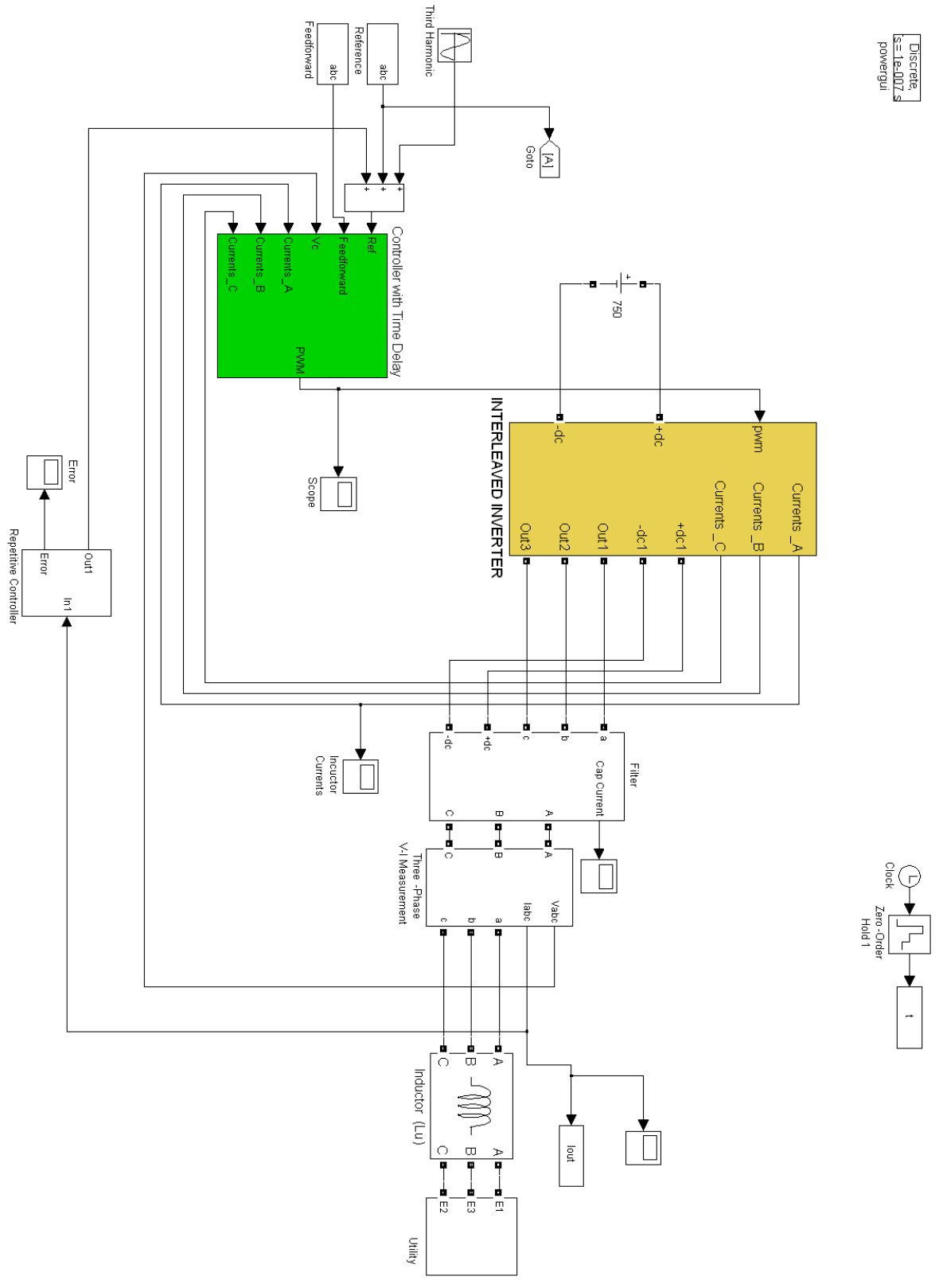


*Fig. 3.3: Three phase Simulink model of the interleaved utility connected converter with RC*

### 3.3.1 Elements of the Three Phase Simulink Model

## 1. Three-Phase Converter

The Universal Bridge block in the Simulink Simpower Toolbox is set up to be the three-phase converter. The switching devices are selected to be Insulated Gate Bipolar Transistors (IGBTs) with diodes across them. The switching time is set to the typical IGBT switching time (0.2μs). The on-state voltage drop across the IGBTs and the diodes is set to 0.7V. It is relatively large due to the power diodes. The snubber resistance in case of the two-level configuration has been selected and its value is 5KΩ because it is considered enough for the rapid rise in voltage across an IGBT/diode and can prevent the erroneous switching-off of the devices. In the case of the interleaved converter, the snubber resistance is set as 0.1μΩ and the on-state voltage drop across the diodes is ignored.

## 2. PWM Generator

A PWM generator block is available in Simulink. The modulating signal is compared with a triangular carrier signal to produce the switching commands: one for the upper switch and the other for the lower switch. The carrier frequency is set to 8 or 10 KHz for the two-level converter and 35 KHz for the interleaved converter.

## 3. LCL Filter

In the used configuration, the capacitors of the filter are connected to the DC-link. In this filter configuration, the middle of the DC-link has almost zero voltage with respect to the neutral point, which means that the voltage produced in one phase does not depend upon the voltages produced in the other phases. In contrast, when the filter capacitors are star-connected, the phases are interdependent and the phase interaction term (or disturbance) needs to be considered (Abusara, 2004).

The Simulink model of this configuration is shown in Fig. 3.4. For each phase in the case of the two-level converter, two capacitors of the value C/2 are connected to the DC-link

(one to the +DC-link and one to the –DC-link). The capacitor current measurements for each phase will be the summation of the currents flowing in the two capacitors.

## 4. Utility System

The utility is assumed to be a three-phase stiff voltage source, which is not affected by the current injected into it. It is modelled as a balanced three-phase voltage source with amplitude of 230 $V_{rms}$ line to neutral and frequency of 50Hz. When the voltage harmonics of the utility are considered, they are added as voltage sources in series as shown in Fig. 3.5.

## 5. Analog to Digital Converters (ADCs)

An Analog to digital converter (ADC) is modelled by a sample and hold circuit (zero order hold) followed by a quantizer as shown in feedback loops in Fig. 3.1. The sampling frequency is set to 20 KHz and the quantizer is set to model the ten-bit resolution of the ADC.

## 6. Computational Time Delay

The digital signal processor needs time to perform calculations and the associated time delay has a significant effect on the controller's performance, and therefore it needs to be included in the computer simulation model. Computational time delay is modelled by a transport delay block prior to the zero-order hold block as shown in Fig. 3.1, so that all the measurements are delayed by computational time. In case of the two-level converter, its value is equal to one sampling period time and in case of the interleaved converter, its value is half of the sampling period time. The sampling period time for the two-level converter is 62.5 µs or 50 µs (sampling frequency of 16 or 20 KHz), which is related to the configuration of the LCL filter used as shown in Table 1.2 and Table 1.3. In case of the interleaved converter, the value of the sampling period time is 28 µs (sampling frequency of 35 KHz).

## 7. Reference Current

This is simply a sinusoidal signal with amplitude of a desired magnitude. The frequency needs to be changed into hertz as by default the value is in rad/sec. This is shown in Fig. 3.6.

## 8. Repetitive Controller

The repetitive controller is a discrete transfer function block. The numerator and denominator are defined through an M-file. Error in the current is injected into the RC block and then its output is added to the conventional controller as shown in Fig. 3.2.

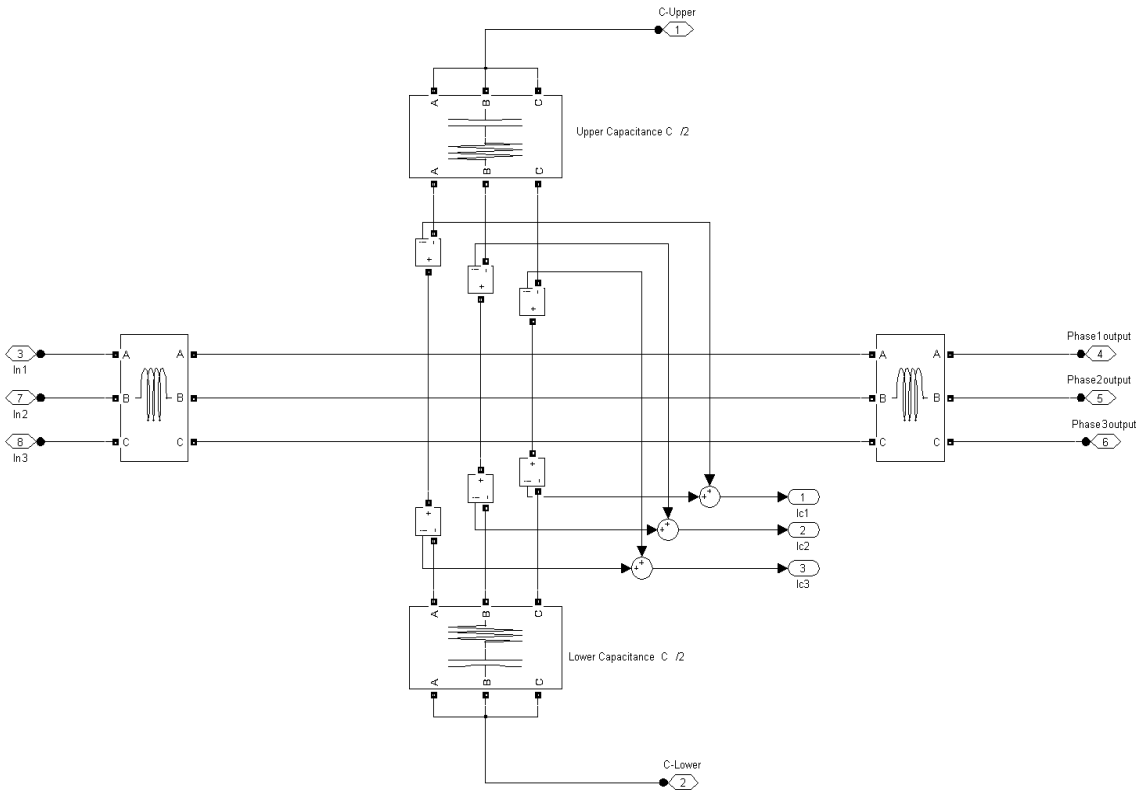


*Fig. 3.4: Simulink model of the LCL filter for two-level converter*

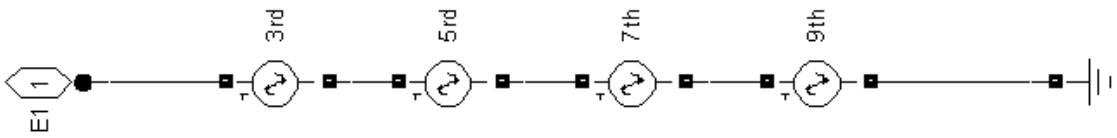


*Fig. 3.5: Simulink model of utility voltage harmonics*

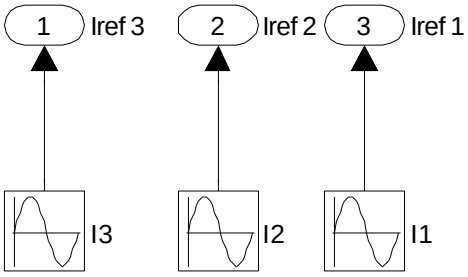


*Fig. 3.6: Simulink model of reference current*

## 3.4 Linear Model of the Two-Level Bridge Converter

The analysis and design of the current controller is based upon the single-phase equivalent circuit of the converter and filter. The circuit was derived initially for star (or delta) connected filter capacitors in the literature (Ito and Kawauchi, 1995). This is shown in Fig. 3.7:

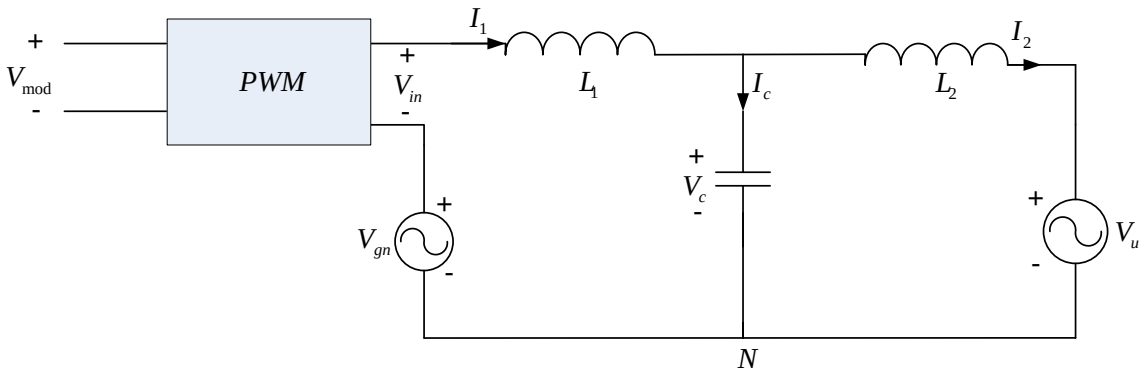


*Fig. 3.7: Single-phase equivalent circuit of the converter*

In Fig. 3.7, the voltage source $V_{gn}$ is the voltage difference between the neutral point and middle of the DC-link that is a source of disturbance caused by phase interaction in control terms. The disturbance $V_{gn}$ can be represented by the following equation:

$$V_{gn} = \frac{V_{ag} + V_{bg} + V_{cg}}{3} \tag{3.1}$$

where, $V_{ag}$, $V_{bg}$ and $V_{cg}$ are phase voltages of phase a, b and c with respect to ground. equation (3.1) shows that the phase coupling voltage $V_{gn}$ depends upon the switching states of all three phases. This is negligible when the capacitors are connected to the DC-link (Abusara, 2004) .

By considering the single-phase equivalent circuit for the utility connected voltage source converter without phase interaction term, the following equations can be developed:

$$V_{in} - V_c = L_1 \frac{dI_1}{dt} \tag{3.2}$$

$$I_c = I_1 - I_2 \tag{3.3}$$

$$I_c = C \frac{dV_c}{dt} \tag{3.4}$$

$$V_c - V_u = L_2 \frac{dI_2}{dt} \tag{3.5}$$

Based on the above equations, a block diagram of the single-phase equivalent circuit can be derived as shown in Fig. 3.8 and the expression of the output current in *s* domain is derived as shown below:

Substitute equation (3.4) in (3.3) and differentiating:

$$\frac{dI_1}{dt} = \frac{d}{dt}\left[ C \frac{dV_c}{dt} \right] + \frac{dI_2}{dt} \tag{3.6}$$

By putting (3.6) in (3.2) and after rearranging, we get:

$$V_{in} = L_1\left[C\frac{d^2V_c}{dt} + \frac{dI_2}{dt}\right] + V_c \tag{3.7}$$

Substitute the value of $v_c$ from equation (3.5) into the above equation.

$$V_{in} = L_1\left[C\frac{d^2}{dt}\left(V_u + L_2\frac{dI_2}{dt}\right) + \frac{dI_2}{dt}\right] + V_u + L_2\frac{dI_2}{dt} \tag{3.8}$$

Applying Laplace transform and rearranging, we get

$$I_2 = \frac{1}{(L_1L_2C)s^3 + (L_1 + L_2)s}V_{in} - \frac{L_1Cs^2 + 1}{(L_1L_2C)s^3 + (L_1 + L_2)s}V_u \tag{3.9}$$

Using equation (3.9), the two loops feedback structure can be developed. The output current $I_2$ can be used as the main feedback control signal as shown in Fig. 3.9. It is subtracted from the reference current and error is fed into the controller $K(s)$. The output current is now given by:

$$I_2 = \frac{K}{(L_1L_2C)s^3 + (L_1 + L_2)s + K}I_{ref} - \frac{L_1Cs^2 + 1}{(L_1L_2C)s^3 + (L_1 + L_2)s + K}V_u \tag{3.10}$$

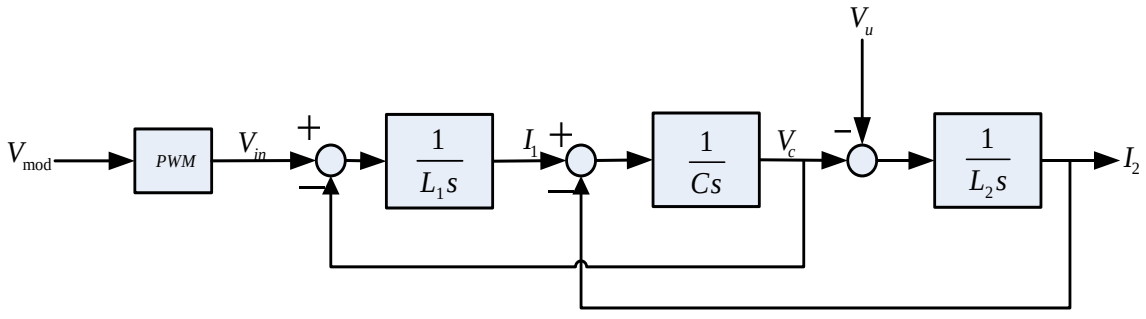


*Fig. 3.8: Block diagram of the single-phase equivalent circuit of two-level converter*

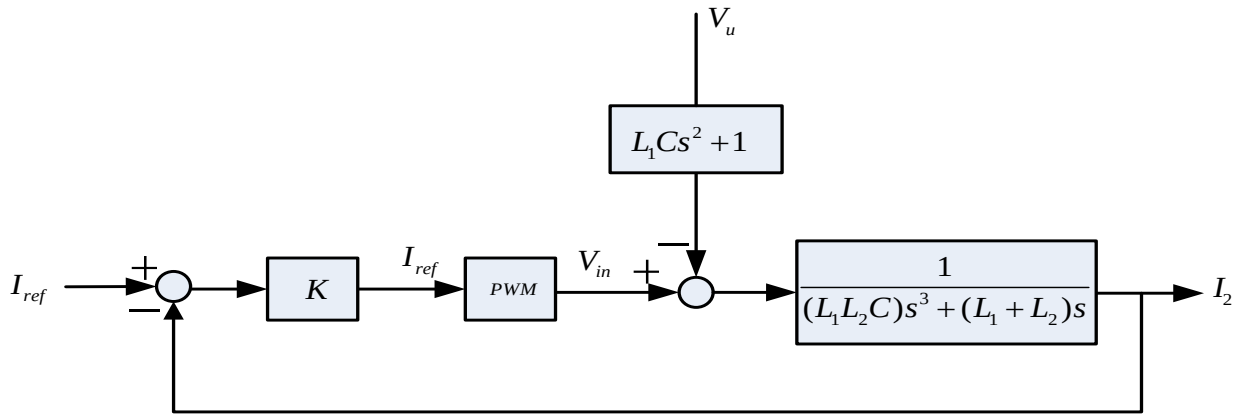


*Fig. 3.9: Single feedback loop structure of* $I_2$

**Modification of Transfer Function:**

The absence of *"$s^2$"* in the denominator of equation (3.10) indicates that the system is unstable according to stability criterion, such as pole-zero map or root locus. In order to ensure that the system is stable and the response is dampened, an *"$s^2$"* term has to be introduced into the characteristic equation. This can be achieved by applying a stabilizing loop with the transfer function of $B(s)$ such that $B(s) = bs^2$

The resulting system is illustrated in Fig. 3.10, and the output current is now given by:

$$I_2 = \frac{K}{(L_1L_2C)s^3 + bs^2 + (L_1+L_2)s + K} I_{ref} - \frac{1 + L_1Cs^2}{(L_1L_2C)s^3 + bs^2 + (L_1+L_2)s + K} V_u \qquad (3.11)$$

However, this method may not be desirable due to the involvement of a double derivative. But it is observed that expression of $I_c$ contains an $s^2$ term of $I_2$ such that

$$I_c = L_2Cs^2I_2 + sV_u \qquad (3.12)$$

Multiplying $I_c$ by gain $K_c$ and feeding it back would provide the required damping term for the system. The complete controller structure with minor feedback loop of the capacitor current is shown in Fig. 3.11. To derive the transfer functions, the implementation of minor

feedback loop of $K_cI_c$ is represented in a block diagram as shown in Fig. 3.12. Fig. 3.13 is a further simplified model. The open loop transfer function $G(s)$ can be defined as:

$$G(s) = \frac{1}{(L_1L_2C)s^3 + K_cL_2Cs^2 + (L_1 + L_2)s} \tag{3.13}$$

And let the utility disturbance be defined as $D(s)$

$$D(s) = L_1Cs^2 + K_cCs + 1 \tag{3.14}$$

The output current is now given by:

$$I_2 = \frac{KG(s)}{1 + KG(s)} I_{ref} - \frac{G(s)}{1 + KG(s)} D(s)V_u(s) \tag{3.15}$$

The main advantage of this controller structure over the one with single feedback of $I_1$ is that the transfer function of the controlled plant $G(s)$ and the disturbance transfer function $D(s)$, are functions of the inner loop gain $K_c$ and are independent of the outer loop gain $K$. However, this structure requires an extra current sensor.

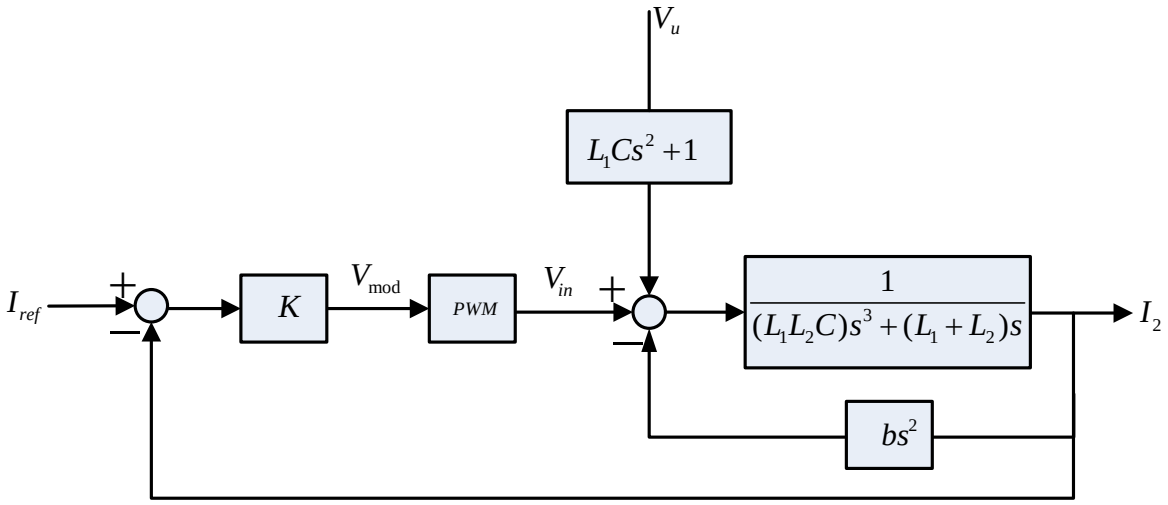


*Fig. 3.10: The control system with minor stabilizing feedback loop of* $bI_2s^2$

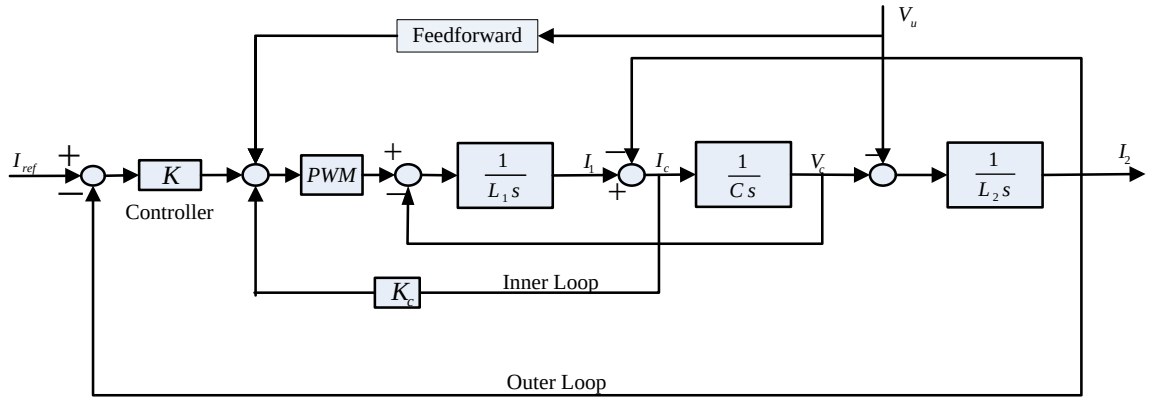


*Fig. 3.11: Controller structure with two loops feedback*

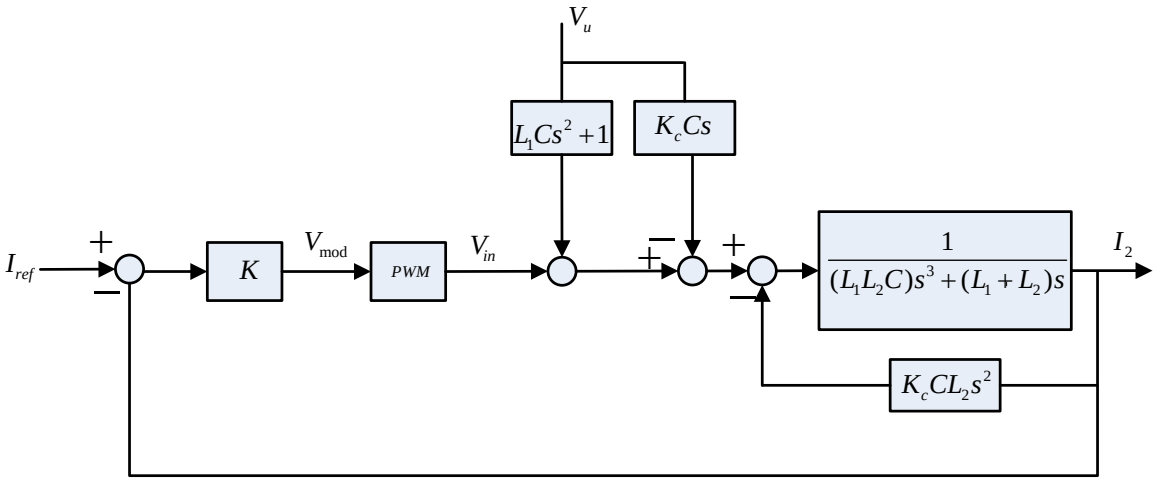


*Fig. 3.12: Simplified block diagram of the control system with minor feedback loop of $I_c$*

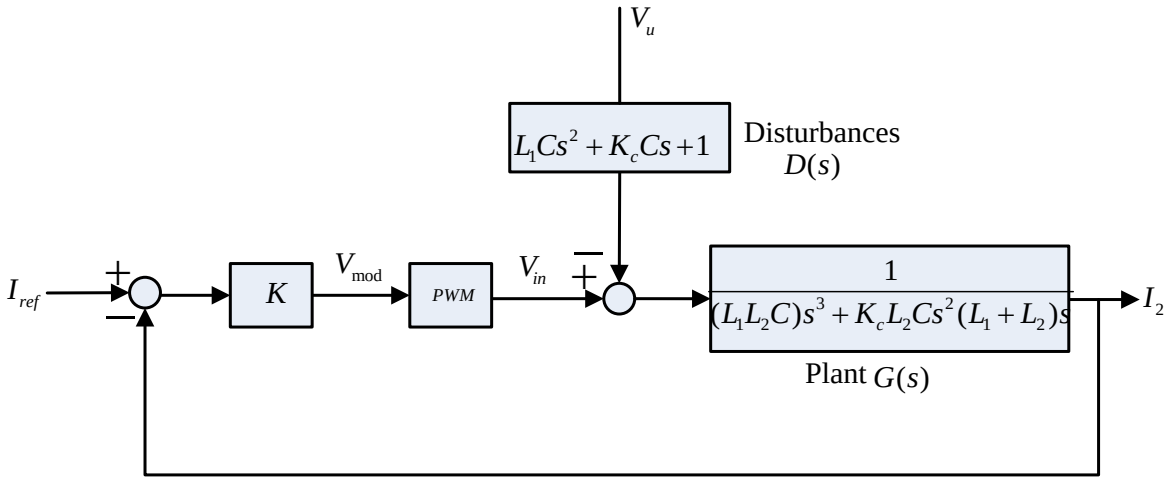


*Fig. 3.13: Further simplified control system with minor feedback loop of $I_c$*

As far as the design of the outer loop controller is concerned, it can be seen from the block diagram of Fig.3.13 that the utility voltage $V_u$ forms a source of disturbance to the system. Ideally, this disturbance can be rejected by implementing a feedforward loop (Abusara, 2004, Hussein, 2000) of exactly the same shape as the utility disturbance transfer function $D(s) = L_1 C s^2 + K_c C s + 1$. In reality, however, it may be difficult to apply the first and second derivatives of the utility voltage due to noise amplification problem. Alternatively, if the amplitude and the phase angle of the fundamental component and the dominant harmonic components of the utility voltage are known, then the first derivative of each component can be obtained by shifting the signal by $90^o$ and multiplying the amplitude by the frequency value. In this method for finding utility voltage harmonics, the dominant harmonic components are extracted from utility voltage signal by correlating one cycle of the measured voltage with stored sine and cosine waveforms of the component with the required harmonic frequency. The magnitude $A_n$ and phase $\theta_n$ of $n^{th}$ harmonic component can be obtained as follows:

$$A_n = \sqrt{x^2 + y^2} \tag{3.16}$$

$$\theta_n = \tan^{-1}(y/x) \tag{3.17}$$

Where

$$x = \int_0^{T_p} V_u(t).\sin(\omega_n t)dt \tag{3.18}$$

$$y = \int_0^{T_p} V_u(t).\cos(\omega_n t)dt \tag{3.19}$$

Where, $\omega_n$ is the angular frequency of a desired harmonic and $T_p$ is the cycle period of utility voltage $V_u$.

However, this method adds more complexity to the algorithm and it requires a faster processor to be able to extract the dominant harmonic components from the utility voltage signal within reasonable time. It is observed that a satisfactory performance of the controller can be obtained only if the fundamental component of the utility voltage and its derivatives are fed forward (Abusara, 2004). The inner loop controller gain $K_c$ and outer loop controller $K$ are then selected to attenuate the other utility voltage harmonics. It is interesting to mention here (as discussed in section 2.2.2), that the classical (P or PI) controllers are not able to attenuate utility harmonics when the utility voltage THD is high. Therefore, the additional loop of the RC can be used to reject utility harmonics efficiently. This will be discussed in more detail in chapter 4.

The derivatives of utility voltage are obtained by offline calculation using a well-known nominal value ($230 V_{rms}$) of utility voltage. This method has been selected for its simplicity and its ability to produce an output current quality as per required standards. It should be noted here that the voltage feedforward is based upon reconstructing clean 50Hz signal from RMS measurement. . It is also interesting to mention here that the voltage feedforward loop could be eliminated when RC is used. However, small amount of transient current would be observed in the output before steady state current without voltage feedforward. This can be seen in section 4.4 (Fig. 4.20).

## 3.5 Linear Model of the Interleaved Utility Connected Converter

To derive the linear model for an interleaved utility connected converter, we can start with the single-phase equivalent circuit (Abusara and Sharkh, 2010) as shown in Fig. 3.14. Since there are six channels, the output of each channel is connected to the common point of coupling of the utility through the inductance $L$, carrying a share $I_{Lx}$ of the total current such that,

$$I_L = N_o I_{Lx} \tag{3.20}$$

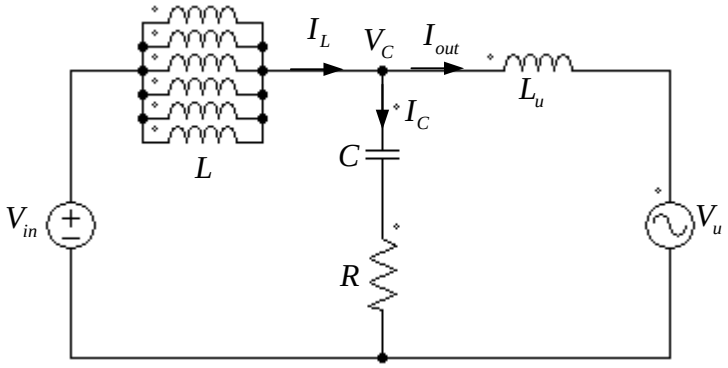


*Fig. 3.14: Single-phase equivalent circuit of the interleaved utility connected converter system*

The following equations can be developed:

$$I_{out} = \frac{1}{L_u s}(V_C - V_u) \tag{3.21}$$

$$V_C = \frac{RC+1}{Cs}(I_L - I_{out}) \tag{3.22}$$

$$I_L = \frac{N_o}{Ls}(V_{in} - V_C) \tag{3.23}$$

Using the above equations we can make the block diagram of the system as shown in Fig. 3.15. This could be used to derive the transfer function of the inductor current in any channel $I_{Lx}$ with respect to input voltage $V_{in_x}$ and utility disturbance $V_u$.

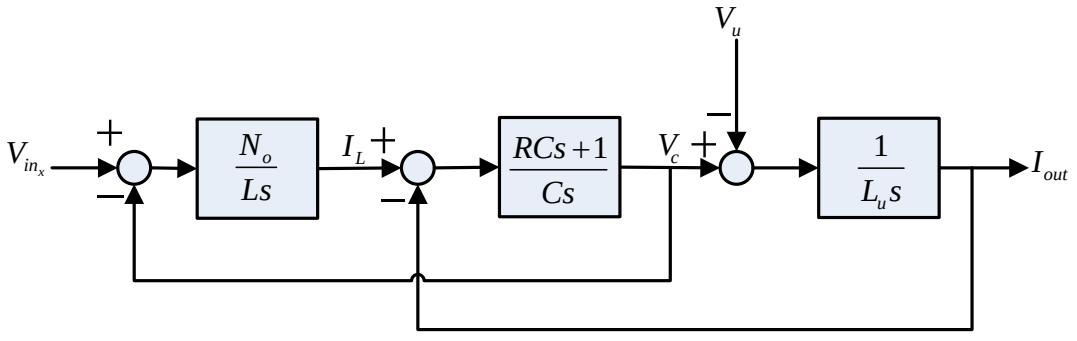


*Fig. 3.15: Block diagram of the single-phase equivalent circuit for the interleaved converter*

The open loop transfer function of the inductor current in any channel $I_{Lx}$ with respect to input voltage $V_{in_x}$ is given by,

$$G_p(s) = \frac{I_{Lx}}{V_{in_x}} = \frac{L_u Cs^2 + RCs + 1}{LL_u Cs^3 + Rc(L + N_o L_u)s^2 + (L + N_o L_u)s} \tag{3.24}$$

The utility disturbance transfer function of the inductor current with respect to utility disturbance is given by,

$$G_d(s) = \frac{I_{Lx}}{V_u} = \frac{RCs + 1}{LCs^2 + RCs + 1} \tag{3.25}$$

Thus the overall inductor current in any channel is

$$I_{Lx} = (V_{in} - G_d(s)V_u)G_p(s) \tag{3.26}$$

The detailed block diagram of one phase and its controller will be discussed in chapter 5. Fig. 3.16 represents the overall structure of the controller and system without RC and Fig. 3.17 gives the overall system with RC.

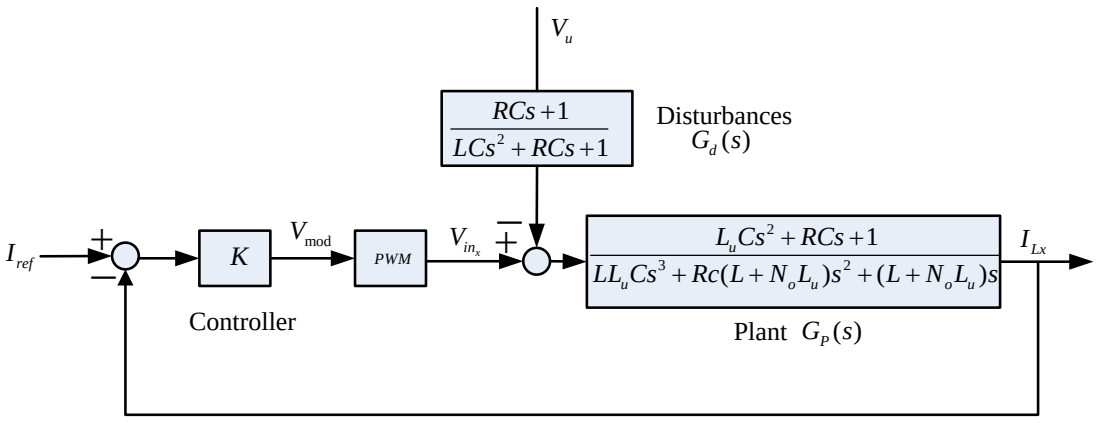


*Fig. 3.16: Overall structure of the interleaved utility connected converter without RC*

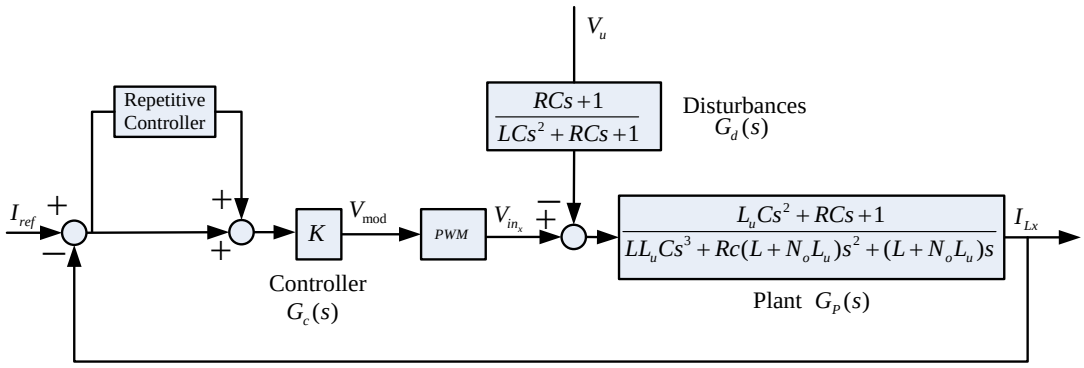


*Fig. 3.17: Overall structure of the interleaved utility connected converter with RC*

A feedforward loop of the utility voltage at the point of common coupling $V_c$ can also be included to cancel the voltage disturbances at the fundamental frequency and its harmonics, as discussed in the case of the two-level converter. However, in contrast to the two-level converter, satisfactory performance (see section 5.3.1) can be achieved with only the fundamental component of the utility voltage as feedforward. The derivatives of the utility voltage can be avoided, as these derivatives can cause either noise amplification problems or increase the computational effort through the offline method discussed earlier.

Additionally, the inner loop of the capacitor current is not implemented in the case of interleaved converter, which was used to provide active damping in the case of two-level converter. Instead, a resistor in the series with the filter capacitor is used to provide passive damping as sampling frequency (35 KHz) is only 1.47 to 3.2 times the natural resonance frequency, which depends upon the value of utility inductance as shown in Table 3.1. This natural resonance frequency $f_n$ can be found either by using Matlab or the following equation,

$$f_n = \frac{1}{2\Pi}\sqrt{\frac{L_1 + N_o L_u}{L_1 L_u C}} \tag{3.27}$$

As a rule of thumb, in order to control the system resonance frequency, the sampling rate needs to be at least 8 to 10 times faster than the natural resonance frequency. This resonance appears due to the presence of the LC filter in the output of the interleaved

converter (Fig.1.3). By considering the utility side inductor, this resonance is like the LCL filter, which needs to be handled by a suitable controller. Fortunately, due to the ripple cancellation feature of the interleaving topology, the capacitor current is quite small and hence the power dissipation in the resistor is small and losses are acceptable (Abusara and Sharkh, 2010).

| **Utility Side Inductor** $L_u$ (μH) | **Natural Resonance Frequency** $f_n$ (kHz) |
|---|---|
| 5 | 23.7 |
| 10 | 18.1 |
| 50 | 11.9 |
| 75 | 11.2 |
| 100 | 10.8 |

*Table 3.1: Natural dampened frequency and utility side inductance*

## 3.6 Performance Criteria for Evaluation and Comparison of Current Control Methods

In the simulation and experimental studies, the performance criterion for the current controllers is the quality of the current waveforms they produced. In order to permit a direct comparison in the performance of different current control methods, a criteria by which the controllers are evaluated needs to be defined. The quality of current waveforms produced by the control methods under study can be expressed in terms of the distortion in the waveform. The lowest distortion index indicates the highest quality waveform. Two complement indices are defined as total harmonic distortion and percentage RMS current error based on the steady state performance requirement. Additionally, transient performance requirement is also important which is briefly discussed here. Other than steady state and transient performance requirements, losses also become important for utility connected converters especially while performing power flow control. This will be discussed in future work.

### 3.6.1 Total Harmonic Distortion (THD)

The amount of distortion in the line current waveform is quantified by means of an index called the total harmonic distortion (Mohan Ned et al., 2006). It is the sum of the Fourier (harmonic) components of the fundamental frequency current as a percentage of the fundamental component. By obtaining the THD in the current waveforms generated by different current controllers, the performance of the current controllers can be compared with each other and with the current harmonic limit standards such as ANSI/IEEE Standard 519-1992 mentioned in chapter 1.

The input current in steady state is the sum of its Fourier (harmonic) components,

$$i_s(t) = i_{s1}(t) \sum_{h \neq 1} i_{sh}(t) \tag{3.28}$$

Where, $i_{s1}$ is the fundamental component (line-frequency $f_1$) and $i_{sh}$ is the component at the '$h$' harmonic frequency.

The distortion in the current waveform,

$$I_{dis}(t) = i_s(t) - i_{s1}(t) = \sum_{h \neq 1} i_{sh}(t) \tag{3.29}$$

In terms of the root mean square (rms) values,

$$I_{dis(t)} = \sqrt{[I^2{}_s - I^2{}_{s1}]} = \sqrt{(\sum_{h \neq 1} I^2{}_{sh})} \tag{3.30}$$

The THD in the line current is defined as,

$$\text{THD} = 100 \times \frac{I_{dis}}{I_{s1}}$$

$$= 100 \times \frac{\sqrt{I_s^{\,2} - I_{s1}^{\,2}}}{I_{s1}}$$

$$\text{THD} = 100 \times \sqrt{\sum_{h \neq 1} \left( \frac{I_{sh}}{I_{s1}} \right)^2} \qquad (3.31)$$

### 3.6.2 Percentage RMS Current Error

While the THD provides a direct comparison for the performance of the different controllers in terms of the percentage harmonic contents in the current waveform with respect to the fundamental component, it does not however take into account other distortions such as offsets, scaling and phase shifts, which are errors with respect to the reference current. Another index which can be used to complement THD is the 'percentage rms value of current error' (Mohan Ned et al., 2006). As the name implies, the rms value of the current error is expressed as a percentage of the reference current. The index compares the actual current to the demanded current reference to obtain an index indicating how well the controller performs to produce an actual current as close as possible to the reference current.

Percentage rms current error is defined as,

$$\text{Percentage RMS Current Error} = \frac{\sqrt{\frac{1}{T}\int_T (I_{actual} - I_{ref})^2 dt}}{I_{ref}} \text{ x } 100 \qquad (3.32)$$

### 3.6.3 Transient Performance Requirements

In addition to steady state performance requirements, in terms of better disturbance rejection and low steady state error, it is essential to have an accurate and fast transient response as well. It is desired to have a reduced overshoot and settling time without any oscillations in any controller design. It becomes more important in converter control when

operating into a distorted supply. Overcurrents and overshoots are most likely to happen in presence of unbalance supply. Normally suitable protection schemes are employed for this purpose. For example, current limiting resistors will be used in the experimental set-up.

It is known from classical control theory that transient response i.e. oscillatory frequency depends upon the imaginary parts of dominant complex-conjugate poles. If these poles are moved further away from the imaginary axis, the transient response would be faster. Guo and Wu (2009) have addressed the slow exponentially decaying transient in the stratup of the PR controller by moving the poles away from the imaginary axis. In the case of the classical (P or PI) controller, an importance of transient system response is discussed now. The design of the PI controller is similar as discussed in section 2.2.2. By having proportional gain $K_p = 1$ and integral gain $K_i = 1$, the suitable transient response can be achieved without oscillations when step change is introduced at t=0.0455 seconds as shown in Fig. 3.18. However, when proportional gain is further increased, such that $K_p = 2$ and $K_i = 1$, the oscillations can be observed in Fig. 3.19. The reference current was 50A initially and then changed to 80A when step change is introduced. By having RC, the transient response can also be improved in addition to steady state error and disturbance rejection as compared to classical (P or PI) controllers. In the case of RC, the RC gain is carefully selected to improve the transient response. However, its selection is always a tradeoff between harmonic rejection performance and transient response. This will be further discussed in section 4.4.2.

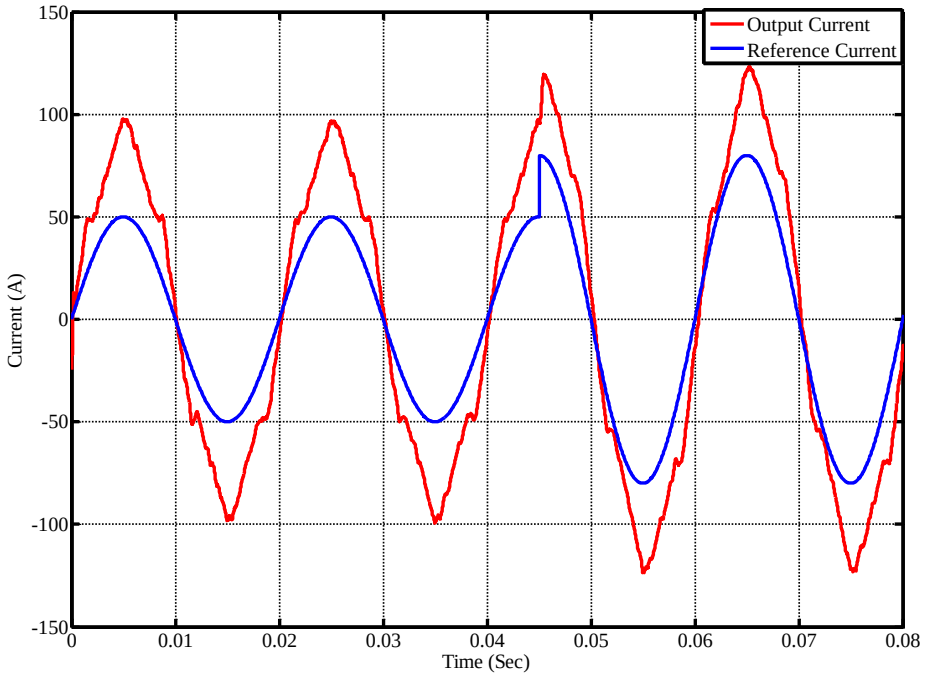


*Fig. 3.18: Transient response of the two-level converter with PI control when* $K_p = 1$ and $K_i = 1$

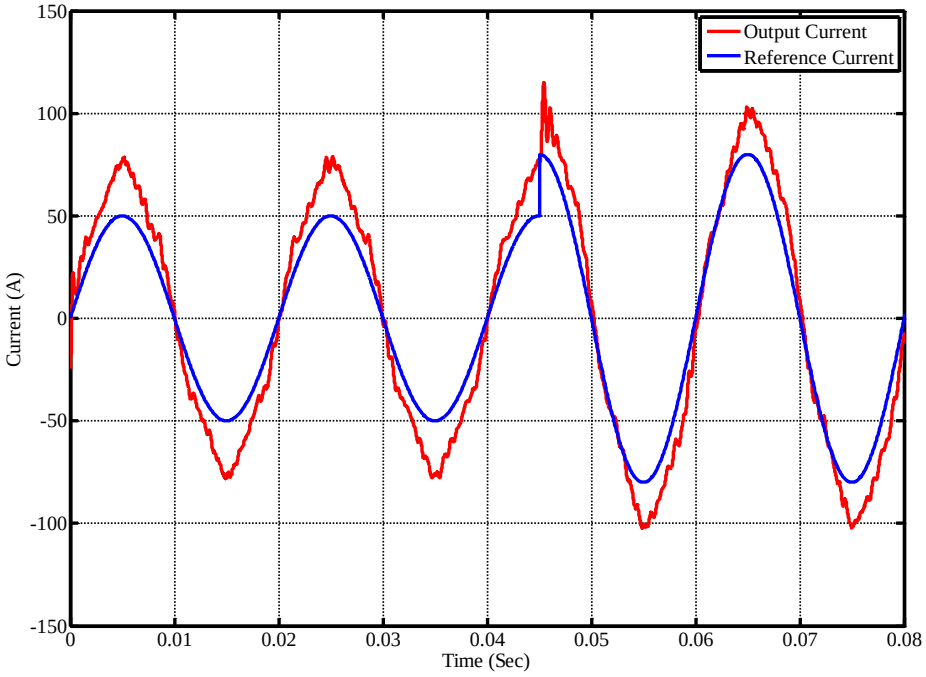


*Fig. 3.19: Transient response of the two-level converter with PI control when* $K_p = 2$ and $K_i = 1$

## 3.7 Summary

The general-purpose dynamic system software, Matlab/Simulink has been selected as the tool for the simulation studies. A nonlinear switching simulation model of the utility connected converter and controller has been developed using Matlab Simpower Toolbox. The nature of the simulation studies has been discussed. The elements of the simulation model have also been described. The linear transfer function model of the two-level and the interleaved utility connected converter have been derived and will be used for analysis in the following chapters. The performance criteria for the evaluation and comparison of current control methods have also been described.

# Chapter 4

## REPETITIVE FEEDBACK CONTROL OF A TWO-LEVEL THREE-PHASE UTILITY CONNECTED CONVERTER

## 4.1 Introduction

This chapter discusses the design of a repetitive feedback controller (RC) for a two-level three-phase utility connected voltage-source converter as shown in Fig. 4.1. The overall control scheme consists of a traditional tracking controller with a dual loop feedback system, and an RC. The dual loop feedback system includes the feedback of the output current and the capacitor current. Initially a conventional tracking proportional controller was designed and then the RC added to improve the performance of the converter. The stability conditions of the RC were analysed and the effectiveness of the RC with respect to the bandwidth of the plant and utility impedance variations are investigated. This chapter also discusses the design of an odd-harmonic repetitive control (ORC) which lowers the memory requirement and offers higher gains at odd harmonic frequencies of interest.

A criterion for selection of a low-pass Q-filter, within the RC structure, with respect to the capacitance values of LCL filter is also discussed in detail. Different designs of RC low-pass Q-filters such as constant, casual and non-casual are compared in terms of stability and attenuation of individual harmonics. After having a suitable low-pass filter in terms of disturbance rejection and stability, the results show that the proposed RC improves steady state error and the total harmonic distortion (THD) of the output current of the converter, in the presence of utility harmonics. The impact on the proposed controller of low system bandwidth if the capacitance value of LCL filter is not appropriate, is also discussed.

## 4.2 Design and Analysis of the Repetitive Controller (RC)

The general structure of the RC has already been derived and discussed in section 2.3. The Fig. 2.15 makes the basis for implementation of RC. The overall block diagram of the system having RC with conventional two loops feedback system is shown in Fig. 4.1. The

conventional controller $G_c(z)$ is simply a proportional controller with a gain $K_P$. The other control methods discussed in chapter 2 can also be used but this gives us a stable and simple implementable system. This system includes a voltage feedforward in addition to the capacitor current feedback loop. The voltage feedforward loop is added to reduce the transient duration and compensate for the utility voltage harmonic disturbance. The design of an RC involves the following major steps:

1. To ensure stability, the RC requires the system to be stable. In addition, for it to be effective, the stable system needs to have high bandwidth. Therefore, the first step is to design a stable tracking feedback controller for the utility connected converter. direct feedback of the output utility current of an LCL filter on its own is inherently unstable, and it is necessary to have another feedback loop of the capacitor current or the current in the main inductor $L_1$ (Sharkh and Abusara, 2004), which has already been discussed in section 2.2.1. This two loops feedback system with proportional controller is referred to as a conventional closed loop system.

2. Next, the RC loop is introduced around the closed loop feedback system designed in step 1. The system presented in Table 1.3 will be used to investigate the performance of RC in terms of stability and system bandwidth. The system bandwidth, which is directly related to the resonance frequency, can be varied by varying capacitance values of the LCL filter. For this purpose, different capacitors such as ($C = 160\,\mu\text{F}, C = 80\,\mu\text{F}$ and $C = 22.5\,\mu\text{F}$) will be used. These capacitor values are selected based on stability, bandwidth, resonance frequency and availability of LCL filter configurations.

3. Finally, the parameters of the RC need to be carefully selected as a slight change in the parameters could lead to instability. For example, a higher value of RC gain or constant Q-filter could make the system unstable, as it may not fulfil the stability conditions. These stability conditions are discussed shortly. The robustness of the system is tested against different utility harmonics and variations in the utility impedance, which are most crucial for this application.

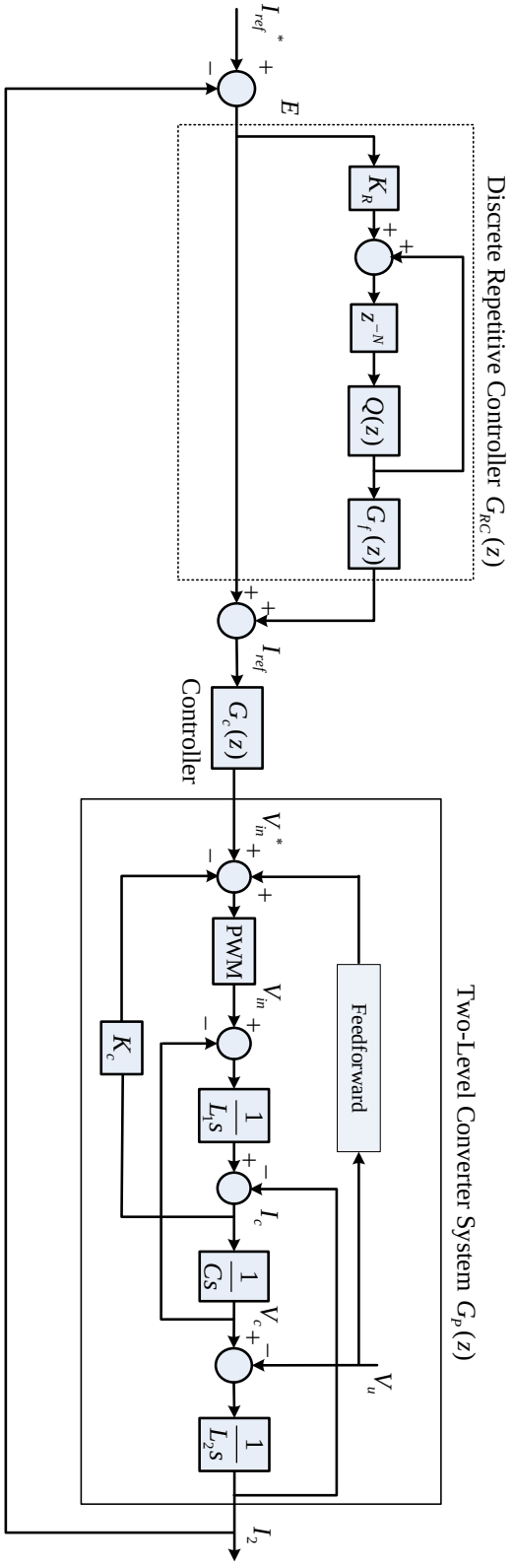


*Fig. 4.1: Overall block diagram of an RC system of the two-level converter incorporated in the basic classical (P) controller*

### 4.2.1 Conventional Closed Loop Feedback Controller

Using the system parameters in Table 1.3, a closed loop feedback system based on a proportional controller was simulated. This system which has a low capacitance value ($C = 22.5\,\mu\text{F}$) of the LCL filter as used by Hussein (2000), was investigated. The simulation method and linear analysis of the classical controller were described in chapter 3. Using that analysis, the transfer function of the output current $I_2$ and converter phase voltage $V_{in}$ when $K_c = 0$, can be written as follows,

$$G(s) = \frac{1}{(L_1 L_2 C)s^3 + (L_1 + L_2)s} \tag{4.1}$$

The above equation can be expressed in the general form as follows:

$$G(s) = \frac{K}{s}\left[\frac{\omega_n{}^2}{s^2 + 2\xi\omega_n s + \omega_n{}^2}\right] \tag{4.2}$$

where,

$K = \frac{1}{L_1 + L_2}$, and damping ratio $\xi$ =0

In addition, an undamped natural frequency can be found using, $f_n = \frac{1}{2\Pi}\sqrt{\frac{L_1 + L_2}{L_1 L_2 C}}$

The undamped natural frequency $f_n$ is 31873rad/s (5073 Hz). The system is unstable as there is no damping. Moreover, it is well known that the feedback of only the output current $I_2$ results in an inherently unstable system. In order to ensure that the system is stable and the resonance is dampened, an $s^2$ term is required to be introduced and this can be achieved by using feedback compensation. A minor feedback loop of the capacitor current (as shown in Fig. 4.1) ensures that the system is stable and the response is dampened. The resulting open loop transfer function of the output current $I_2$ with respect to voltage $V_{in}$* is as follows:

$$G_{ol}(s) = G_P(z) = \frac{I_2}{V_{in}*} = \frac{1}{(L_1L_2C)s^3 + (K_cL_2C)s^2 + (L_1 + L_2)s} \tag{4.3}$$

The value of gain $K_c$ and outer loop classical controller $G_c(z)$ (in our case $G_c(z) = K_p$) (Fig.4.1) have to be carefully selected to set the poles for each loop to obtain the desired value for the overall damping ratio. Based on a general design rule of a gain margin of 8-15dB and phase margin of 25°-60°, $K_c$ is selected to be 13 that gives enough damping and $K_p$ to be 3.2 that gives a gain margin of 13.3dB and phase margin of 72.3°. The Bode plot of the new system open loop transfer function is shown in Fig. 4.2. After obtaining a suitable value of $K_c$, tuning of the proportional gain $K_p$ is carried out using Matlab SISO Toolbox. The loop gain can be easily adjusted to have enough stability as shown in Fig. 4.3. From tuning, it is observed that if the gain is further increased, the system could become either less stable or unstable.

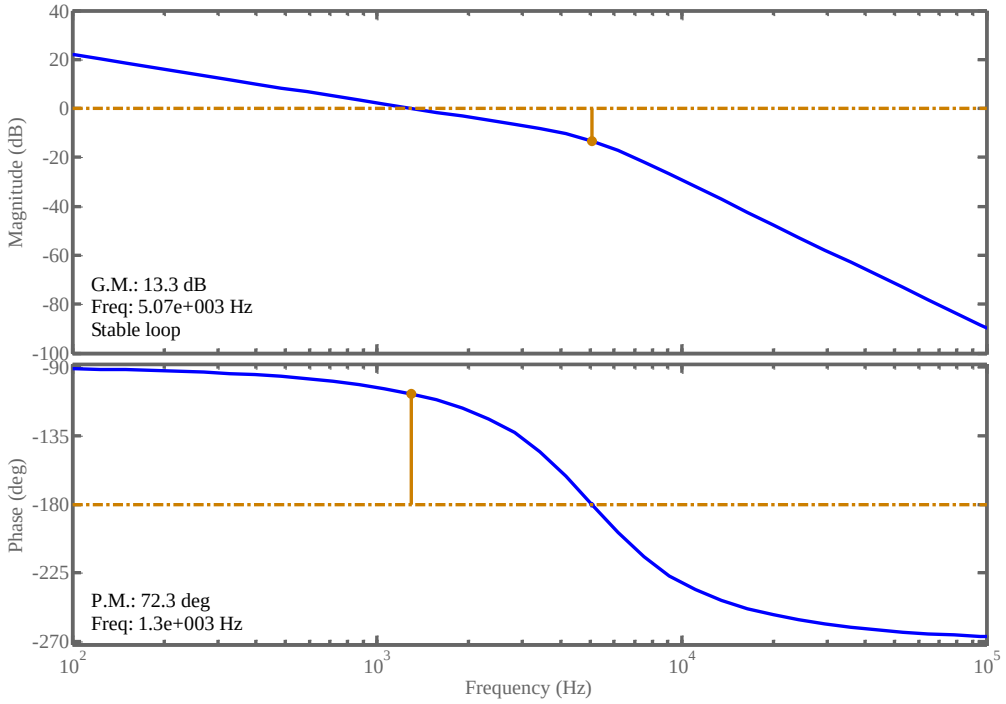


*Fig. 4.2: Bode diagram of output current transfer function with classical controller in Fig. 4.1 when* $K_c = 13$ and $K_P = 3.2$

[Transfer function: $G_{I2}(s) = \frac{K_P G_{ol}(s)}{1 + K_P G_{ol}(s)} I_{ref}$ and $G_{ol} = \frac{1}{(L_1L_2C)s^3 + K_cL_2Cs^2 + (L_1 + L_2)s}$]

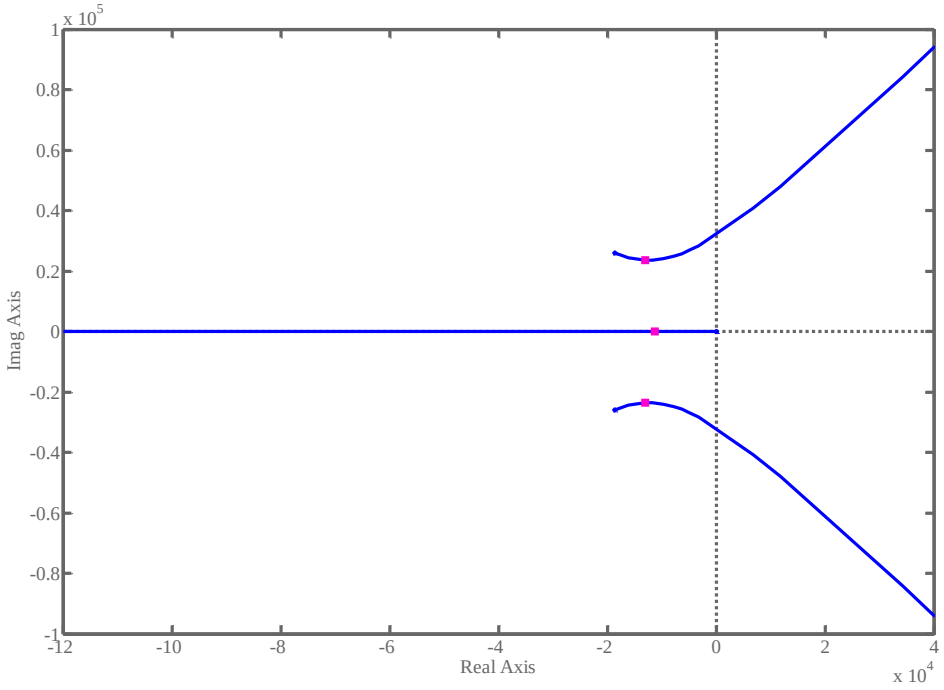


*Fig. 4.3: Root locus plot of the output current transfer function with classical controller in Fig. 4.1 when* $K_c = 13$ and $K_P = 3.2$

[Transfer function: $G_{I2} = \dfrac{K_P G_{ol}(s)}{1 + K_P G_{ol}(s)} I_{ref}$ and $G_{ol} = \dfrac{1}{(L_1 L_2 C)s^3 + K_c L_2 C s^2 + (L_1 + L_2)s}$ ]

## 4.2.2 Repetitive Controller Incorporated In the Conventional Two loops Feedback System

In the second step, an RC is added to the conventional closed loop system (Fig. 4.1). To derive the necessary stability conditions in the presence of an RC, the general terms $R$, $Y$ and $D$ can be used to represent reference current $I_{ref}$, output current $I_2$ and utility disturbance $V_u$ for analysis purposes. The error transfer function for the block diagram in Fig.4.1 derived in section 2.3.1 can be written as follows:

$$G_E(z) = \frac{E(z)}{R(z) - D(z)} = \frac{1}{1 + \left(1 + G_{RC}(z)\right) G_c(z) G_P(z)} \tag{4.4}$$

$$G_E(z) = \left( \frac{1 - Q(z)z^{-N}}{\left(1 + G_c(z)G_p(z)\right)} \right) \left( \frac{1}{1 - Q(z)z^{-N}\left(1 - K_R G_f(z) G_o(z)\right)} \right) \tag{4.5}$$

In Fig. 4.1, the RC transfer function is $G_{RC}(z)$, the two loops feedback system's transfer function is $G_p(z)$ and the closed loop transfer function of the classical controller $G_c(z) = K_p$ with the converter system $G_p(z)$ is equal to $G_o(z)$. The necessary stability conditions could be obtained using the following theorem (Costa-Castello et al., 2005).

*Theorem*: Assume two systems $G_1$ and $G_2$ are connected in a feedback loop, then the closed loop system is stable if $\|G_1\| . \|G_2\| < 1$

According to the above gain theorem, the conditions for stability are:

Condition 1: The roots of the characteristic equation $1 + G_c(z)G_p(z) = 0$ of the conventional two loops feedback system without RC should be inside the unit circle.

Condition 2: From equation (4.5)

$$\left\| Q(z)(1 - K_R G_f(z) G_o(z) \right\| < 1 \tag{4.6}$$

For all $z = e^{j\omega}$, $0 < \omega < \frac{\Pi}{T_p}$ and $G_o(z) = \frac{G_c(z)G_p(z)}{1 + G_c(z)G_p(z)}$ (4.7)

Thus using equation (4.6), it can be seen that the RC gain $K_R$, the low-pass filter $Q(z)$, compensator $G_f(z)$ and closed loop product $G_o(z)$ of classical controller $G_c(z)$ and two loops feedback plant $G_p(z)$ should be designed properly such that poles of the system are within the unit circle.

### 4.2.3 Selection and Design of the RC Parameters

The most important parameters are the low-pass filter $Q(z)$ and RC gain $K_R$. The compensator $G_f(z)$ is less crucial as it only compensates the phase lag of the system. It can be incorporated by selecting the appropriate classical feedback controller $G_c(z)$.

### A. Low-pass Filter $Q(z)$

A low-pass filter $Q(z)$ is necessary to filter out the peaks of individual gains at higher frequencies (near the crossover frequency) that lead to instability. A proper design of the low-pass filter will provide enough stability margins, tracking performance and disturbance rejection capability of the RC. Robustness is achieved at the expense of performance at a high frequency. However, the frequencies of interest in this application are mainly the low order harmonics. The design reflects the trade-off between THD, speed of response and robustness to the utility harmonics.

The filter $Q(z)$ can be a constant or a zero-phase low-pass filter. It is worth comparing both cases. There could be further choices of low-pass filters including causal or non-causal low-pass filters. A causal filter is designed using Matlab's 'fir1' function. The causal filter can be regarded as a finite impulse response (FIR) filter. The order of the filter needs to be decided. This method is normally known as frequency sampling method. It is also required to decide the cutoff frequency and sampling frequency. The following two cases of causal low- pass filters $Q_1(z)$ and $Q_2(z)$ are considered.

$$Q_1(z) = 0.0689 + 0.8623z^{-1} + 0.0689z^{-2} \tag{4.8}$$

$$Q_2(z) = 0.0471 + 0.04529z^{-1} + 0.4529z^{-2} \tag{4.9}$$

The low pass filter $Q_1(z)$ is found using Matlab by selecting order as $n = 2$ and a cutoff frequency of 100Hz and a sampling frequency of 20KHz. The other low pass filter $Q_2(z)$ is similar to $Q_1(z)$ except its coefficients are further tuned (reduced) by looking at the frequency response of the system. The frequency response of these filters is shown in Fig.

4.4. The specifications of these filters are selected after looking at the Bode diagram of the system and the required disturbance rejection in such a way that the peaks of the gains at higher order harmonics do not disturb the stability margins.

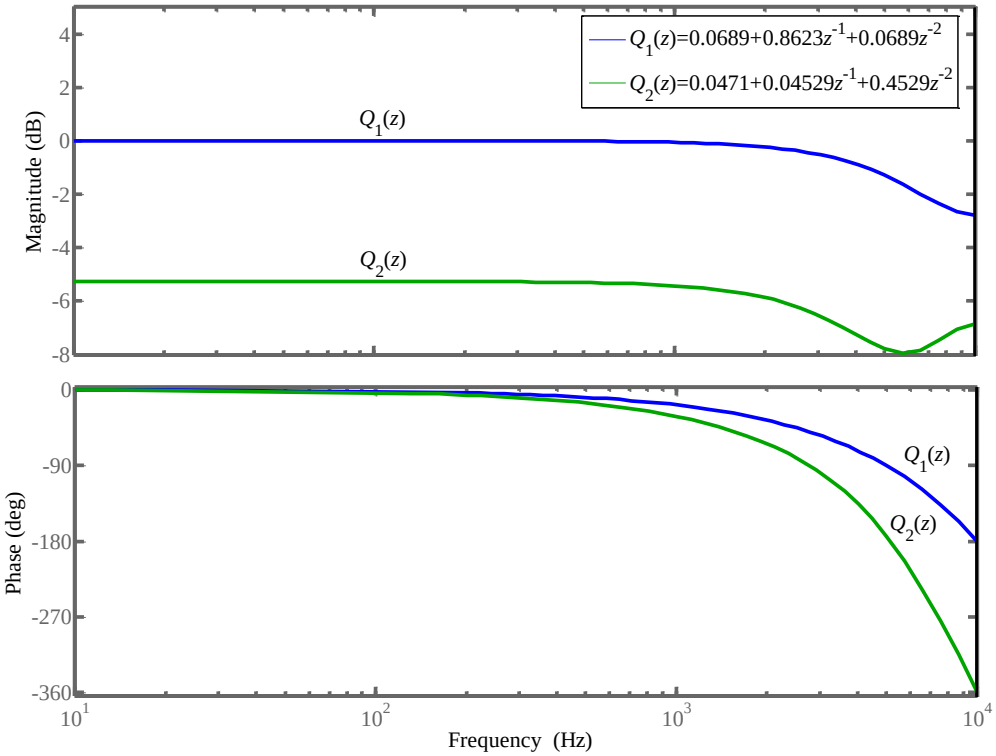


*Fig.4.4: Bode diagram of the low-pass filter $Q_1(z)$ and $Q_2(z)$*

In Fig. 4.4, it can be observed that both low-pass filters affect the phase of the system which is not required as we only want higher gains without disturbing the phase margin too much. A more effective solution would be a zero-phase low-pass filter which is a non-causal filter. No causality problem exists because the filter is cascaded with the transfer function of the RC having *N* number of samples per period as shown in Fig.4.1. The general form of non-causal filter is as follows (Michels et al., 2004).

$$Q(z)=\frac{\alpha_1 z+\alpha_o+\alpha_1 z^{-1}}{\alpha_o+2\alpha_1};\ \alpha_o,\alpha_1>1 \tag{4.10}$$

The normalized frequency response ($T_s=1$) of equation (4.10) is $Q(e^{j\omega})=\alpha_o+2\alpha_1\cos(\omega)$ and $\omega\in(0,\pi)$. By considering $\alpha_o+2\alpha_1=1$ for a unit gain response, we can write the magnitude of $Q(j\omega)$ as:

$$|Q(j\omega)| = \begin{cases} \alpha_o + 2\alpha_1 = 1 & \omega = 0 \\ \alpha_o + 2\alpha_1 \cos(\omega) & \omega \in (0, \pi) \\ \alpha_o - 2\alpha_1 & \omega = \pi \end{cases} \tag{4.11}$$

By selecting $\alpha_o = 0.5$ and $\alpha_1 = 0.25$, then

$$|Q(j\omega)| = \begin{cases} 1 & \omega = 0 \\ 0 < 0.5(1 + \cos\omega) < 1 & \omega \in (0, \pi) \\ 0 & \omega = \pi \end{cases} \tag{4.12}$$

Equation (4.12) concludes that $|Q(j\omega)|$ is unity at low frequencies and zero at high frequencies. Different low-pass filters can be achieved by using different $\alpha_o$ and $\alpha_1$. A first order filter is sufficient and is given by equation (4.13) and its frequency response is shown in Fig. 4.5. It can be seen in Fig. 4.5 that this filter does not introduce any phase change.

$$Q_3(z) = 0.25z + 0.5 + 0.5z^{-1} \tag{4.13}$$

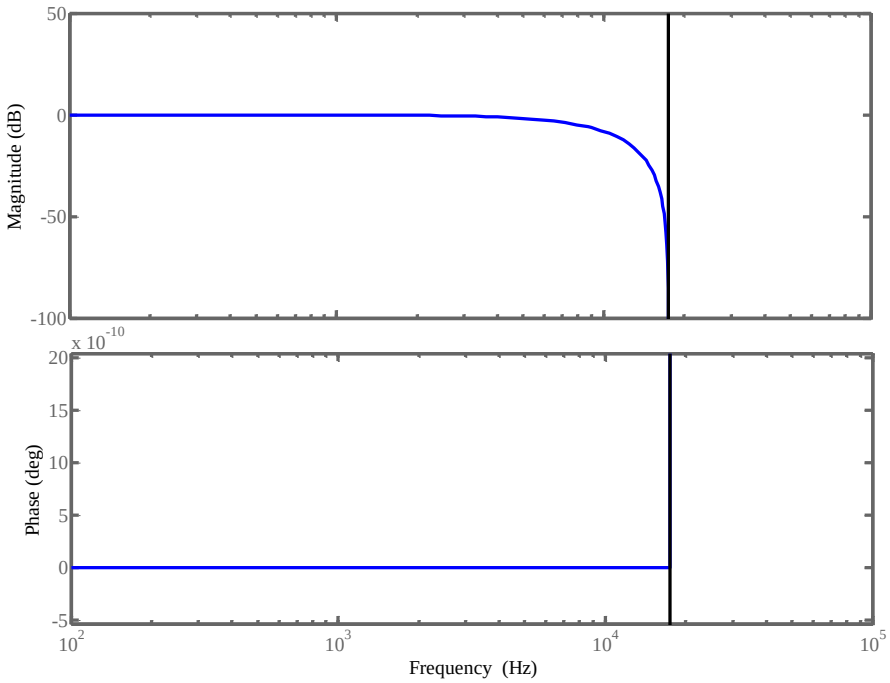


*Fig.4.5: Frequency response of the filter* $Q_3(z) = 0.25z + 0.5 + 0.25z^{-1}$

Now the performance of different filters is presented to select the most suitable filter for RC design.

## Case 1: Constant $Q(z)$

Normally $Q(z)$ is selected slightly less than unity. The system could be simple and easy to implement. But at the same time, the peaks of the gains at high frequency (near the crossover frequency) are not fully rejected which cause instability. Moreover, the magnitude of the gains at individual harmonics is not high enough.

Fig. 4.6 shows the Bode plot of the system when the value of $Q(z)$ is unity and the gain $K_R$ is 0.1. It can be observed that the system has higher gains at the fundamental frequency and its harmonics. In this case the gain margin is 0.13dB and phase margin is -2.28, which is not stable. To stabilize the system, $Q(z)$ needs to be slightly less than unity as shown in Fig. 4.7. The RC gain $K_R$ is selected to be 0.01, which means effectively the decrement in the RC action. It can be observed that the magnitude of individual gains around corner frequency is attenuated but at the same time we have a reduction in the amplitude of the individual gain at fundamental and low order harmonics as well. The system is stable by having a gain margin of 1.43dB and phase margin of $14.3^{o}$. But it can be easily observed that the effect of the RC gains at fundamental and its harmonics is very small which in practice cannot provide good disturbance rejection. So for effective RC action, normally a low-pass filter is necessary and is discussed in next section.

## Case 2: Causal Low-pass Filters $Q(z)$

The advantage of using a causal low-pass filter is that we can implement it in Matlab/Simulink without the need of combining it with the transfer function of RC. This is also known as a finite impulse response (FIR) low-pass filter as discussed earlier.

If the filter $Q_1(z)$ is selected ($K_R = 0.1$) as given by equation (4.8), the gain margin is 0.003dB and the phase margin is $0.0567^{o}$. It can be seen in Fig. 4.8 that the RC offers a higher gain at low order harmonics but the system has much lower margins which does not

provide good performance. Moreover, the strange behaviour of corner frequency is due to the filter that rejects higher frequency components. An alternative filter could be selected as $Q_2(z)$ given by equation (4.7), which gives stable margins such as gain margin of 8.25dB and a phase margin of $55.1^o$. The coefficients are selected by using Matlab and looking at the performance when used with the RC. The Bode diagram is shown in Fig. 4.9. It can be easily observed that the magnitude is much smaller at each harmonic frequency. When it is tested against the performance criteria of disturbance rejection, it fails. The obvious reason is not having enough gains at the fundamental and its harmonics.

Comparison of the two filters $Q_1(z)$ and $Q_2(z)$, shows that there is a need for enough higher gains to reject low order harmonics. If the magnitude of individual gains at a higher frequency (around corner frequency) is attenuated by selecting $Q_2(z)$, the system would be stable but it cannot reject low order harmonics due to the low gains at fundamental frequency and its harmonics. In another case when we had $Q_1(z)$, the RC system could offer higher gains at low order harmonics. But at the same time the system did not have enough stability margins. It can also be observed that unwanted peaks of the gains around corner frequency can disturb the stability when a low-pass filter $Q_1(z)$ is selected. It could easily become unstable with a slight change in parameters. So, in our concluding remarks, it is worth mentioning that the RC system is made stable with $Q_2(z)$ by effectively reducing the amplitude of peak gains at the fundamental and its harmonics. The other way around could be decreasing the RC gain which means reduction in RC action. In short, the filter $Q_1(z)$ is not suitable as stability margins are very small and on the other hand the filter $Q_2(z)$ is also not ideal to be used with the RC because it does not offer sufficient gains at fundamental frequency and its harmonics.

It can be concluded that the filters $Q_1(z)$ and $Q_2(z)$ are not suitable but have been used for the purpose of comparison and explanation with other low-pass filters.

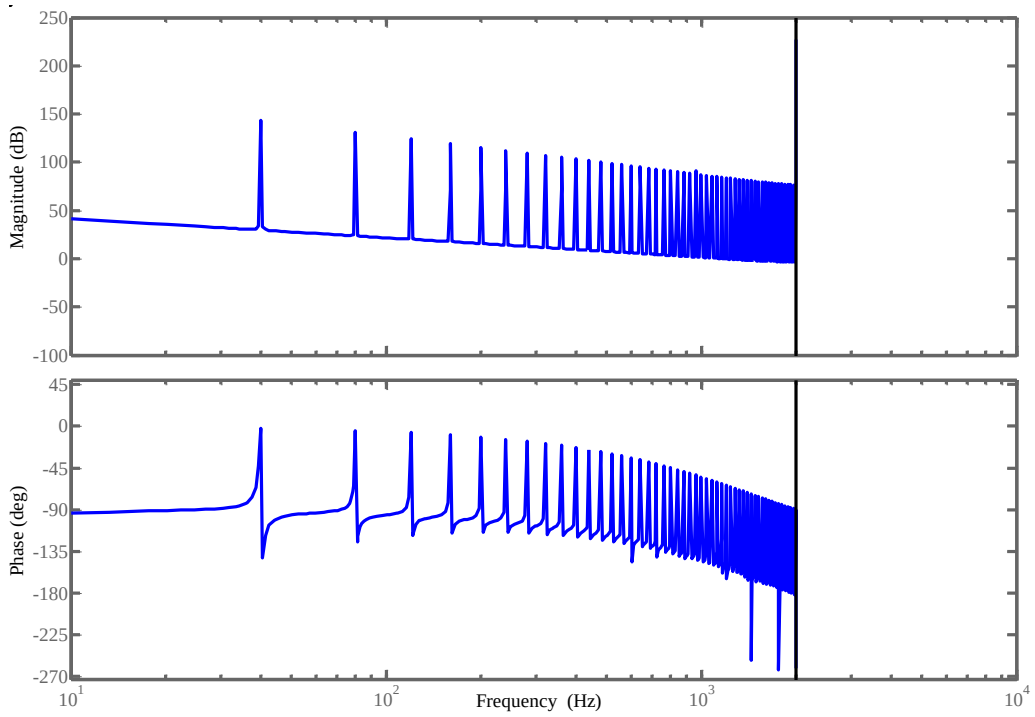


*Fig.4.6: Bode diagram of the open loop system when* $Q(z)$ *=1,* $K_R = 0.1$

System: $G_{ol}(z) = \left(1 + G_{RC}(z)\right) G_c(z) G_P(z)$ and $G_{RC}(z) = \dfrac{K_R Q(z) z^{-N}}{1 - Q(z) z^{-N}}$

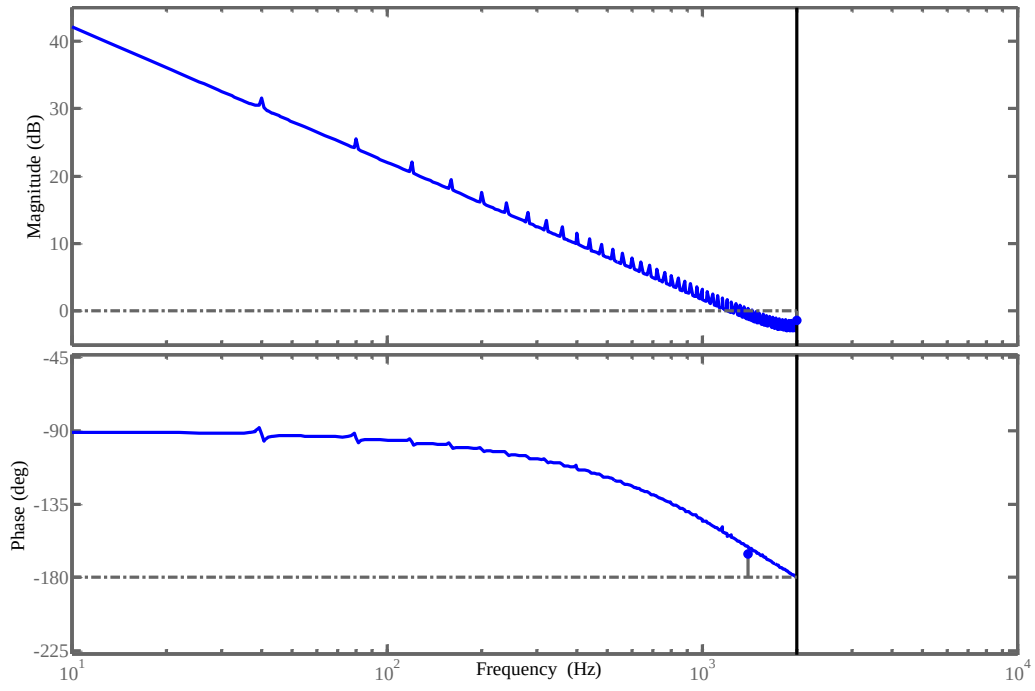


*Fig.4.7: Bode diagram of the open loop system when* $Q(z)$ *=0.95 and* $K_R = 0.01$

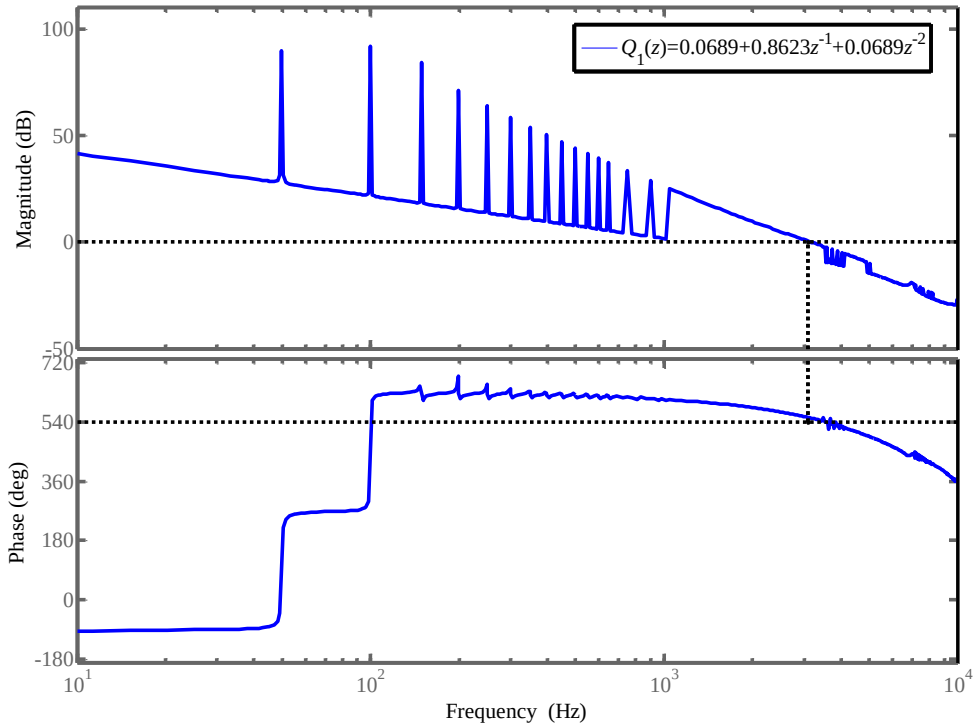


*Fig.4.8: Bode diagram of the system with* $Q_1(z)$

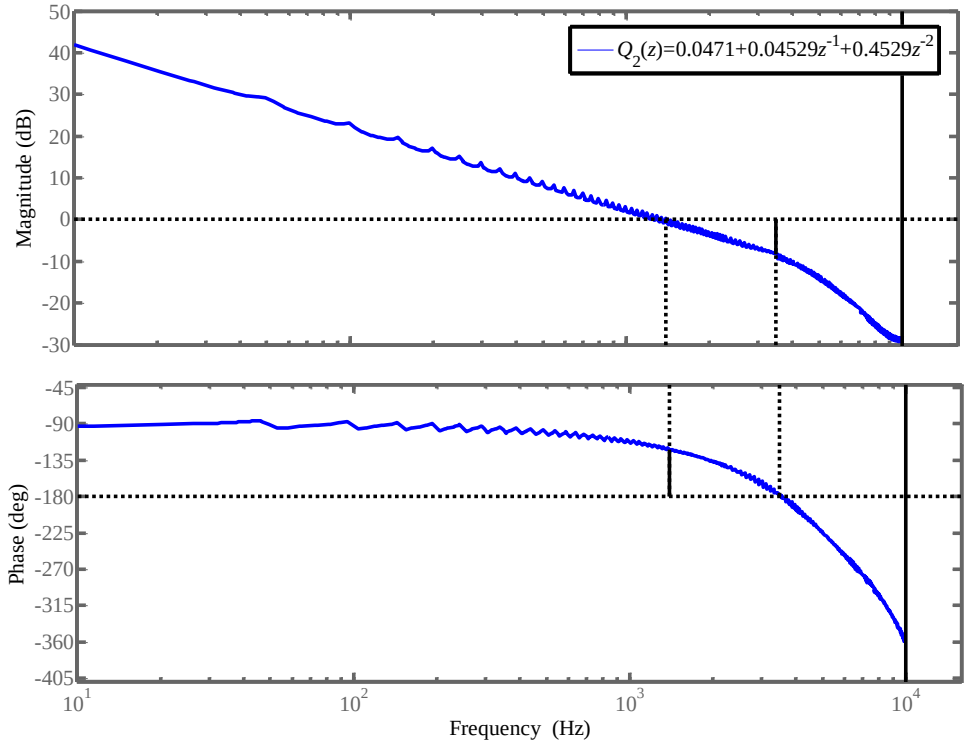


*Fig.4.9: Bode diagram of the system with* $Q_2(z)$

## Case 3: Non-Causal Low-pass Filter $Q(z)$

If the filter $Q_3(z)$ is selected as given by equation (4.13), the system has a gain margin of 6.53 dB and a phase margin of $24.4^o$. The magnitude of gain is high enough to reject low order harmonics. The Bode diagram of the system including this filter within RC is shown in Fig. 4.10, and the frequency response of the filter itself is already shown in Fig. 4.5. Now the function of the Q-filter could be better understood by comparing Fig. 4.10 (with filter) and Fig. 4.6 ( without filter i.e. $Q(z)=1$). In Fig. 4.6, there were unwanted peaks around the corner frequency when a constant unit Q-filter was selected. It can be observed that $Q_3(z)$ is responsible for attenuating the unwanted peaks of individual gains at a high frequency around corner frequency which causes instability. It is concluded that the filter $Q_3(z)$ gives better attenuation at higher frequencies and improves stability. This filter will be used as part of the final design of the RC.

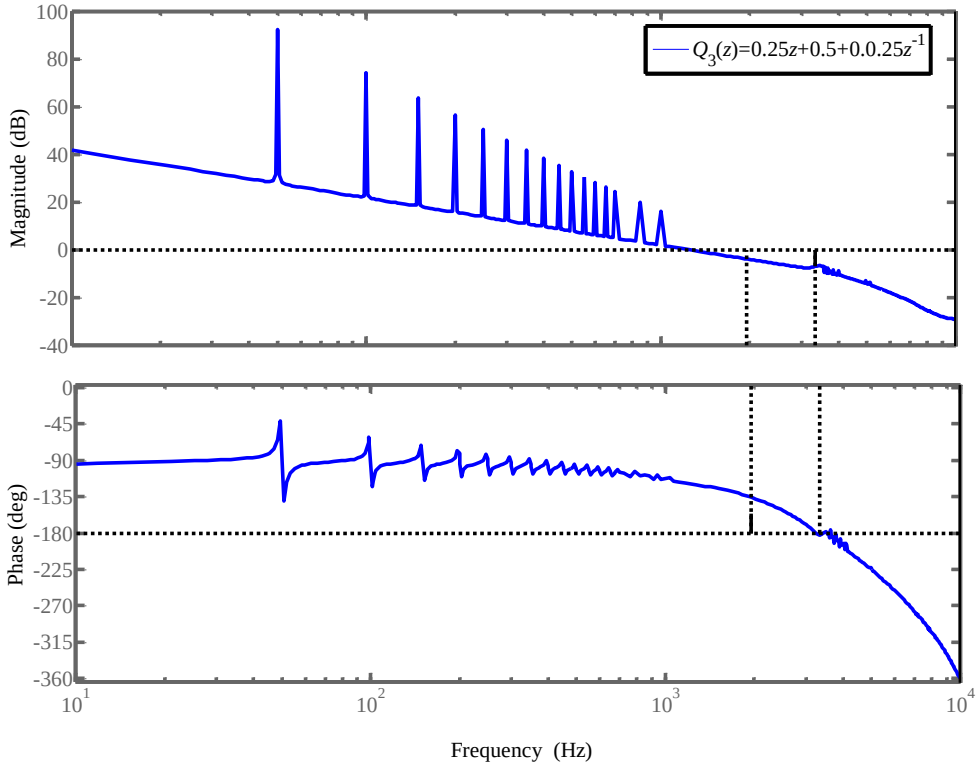


*Fig.4.10: Bode diagram of the system when $Q_3(z)$*

## B. Repetitive Controller Gain $K_R$

The RC gain $K_R$ determines the amount of repetitive control action. The value of gain $K_R$ needs to be carefully selected, as it is a key parameter for error convergence and stability of the system. It must fulfil the stability condition given by equation (4.6). At low values of RC gain $K_R$, more number of cycles are required to reach a steady state and vice versa. Higher RC gain $K_R$ results in fast convergence but the feedback system becomes less stable. It has been observed and can be seen in the simulation results (Fig. 4.19) that by selecting $K_R = 0.1$ for our application, we get a fast response (2 cycles to reach steady state) while maintaining stability.

## C. The Compensator $G_f(z)$

Since $G_0(z)$ is a minimum phase function (no zero outside unit circle), it is desirable to choose $G_f(z)$ to be the inverse of the system transfer function to achieve zero-phase error tracking. However in practice the utility impedance can vary significantly and the transfer function is therefore not known (Zhang et al., 2008). Instead a phase-lead compensation scheme is used such that,

$$G_f(z) = z^m \tag{4.14}$$

This phase-lead compensator compensates the phase lag introduced by the transfer function of the converter and hence improves the stability of the system. In addition, it can also compensate the unknown time delay, which is not modelled. By looking at the response of the system, a suitable value of $m = 3$ is selected in equation (4.14) in such a way that the system has higher stability margins. In our case, the gain margin improves from 6.53dB to 8.31dB and the phase margin improves from $24.4^o$ to $52.1^o$. This is obvious in Fig. 4.11. It would be interesting to mention here that an RC based system could be designed even without a compensator as it only improves stability in our case. It becomes necessary in those cases where unmodelled dynamics of the system exist, which is not very many in our case. In other words, the compensator is required when the basic system does not have higher stability margins, as it increases the stability margins to some extent.

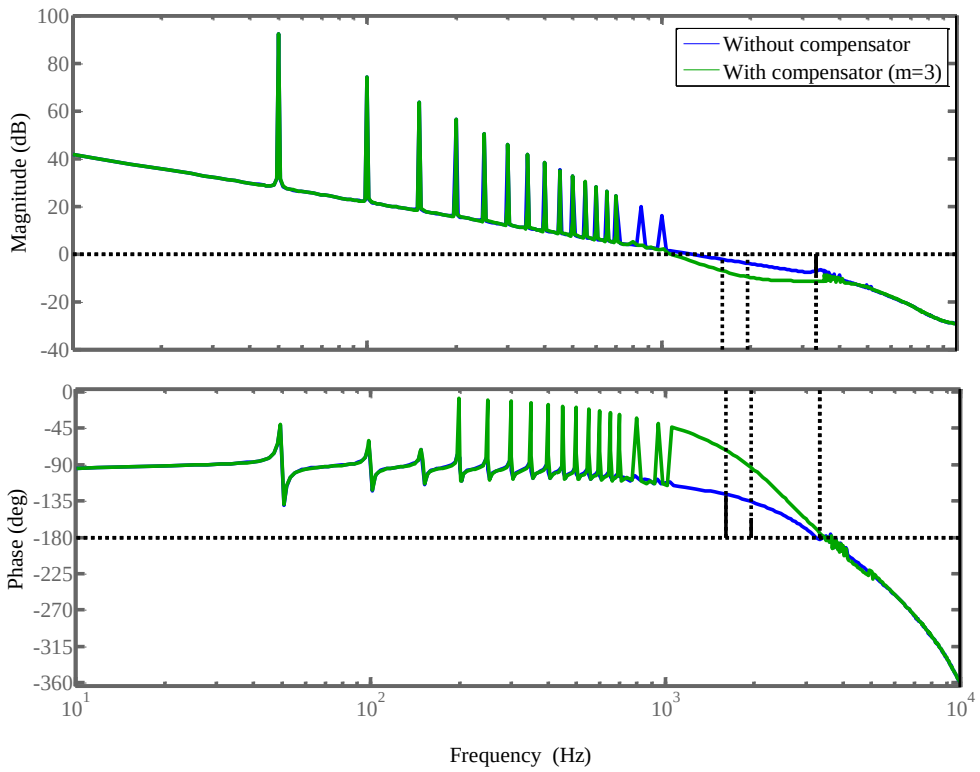


*Fig 4.11: Bode plot of the system with and without a compensator*

## 4.3 RC and Plant Bandwidth

The plant bandwidth plays a vital role in the design of any feedback controller. Its importance is more for RC based systems because it is required to provide higher gains at desired frequencies as discussed in section 4.2. One of the stability conditions for an RC based system is that the plant with a basic feedback controller without an RC should be stable. In this section , the design of the RC is discussed with respect to the LCL filter based plant and its bandwidth. The bandwidth of the system is related to the resonant frequency of the system and switching frequency. The resonant frequency of LCL filter based system can be varied, by changing the capacitance values of the LCL filter. In this way, the designer could have an idea about achievable harmonic compensation by the RC and required component values. The bandwidth of the system cannot exceed or even come close to the resonant frequency (Tang et al., 2012). As a rule of thumb, the switching frequency should be at least two times the resonant frequency for effective harmonic compensation around the switching frequencies.

Now the design of RC with different capacitance values of the LCL filter is discussed. These capacitor values can be selected as per the required resonance frequency and closed loop system bandwidth. Table 4.1 shows the resonant frequencies attached with different capacitor values. It can be easily observed that the low capacitor values result in high resonant frequencies and vice versa. The RC can be used to address the issues of higher resonance but the designer must select an appropriate bandwidth for the RC to be effective. For this purpose, design of the RC is investigated with respect to different low pass filters and capacitance values when we have RC gain $K_R = 0.1$. Table 4.2 summarises all these results in terms of gain margins (GM) and phase margins (PM). Table 4.2 and Fig. 4.12 show that the system has either very small stability margins ($C = 22.5\,\mu\text{F}$) or unstable margins ($C = 80\,\mu\text{F}$ and $C = 160\,\mu\text{F}$) when filter $Q_1(z)$ is used. The strange behaviour after the cut-off frequency can be observed which is mainly due to the behaviour of the low pass filter in a high frequency range. This is acceptable, as it does not affect the stability of the system.

For a stable system, the filter $Q_2(z)$ is used with different capacitor values. Fig. 4.13 shows the Bode diagram of a system when the filter $Q_2(z)$ is used. The coefficients of the filter $Q_2(z)$ can be selected in such a way that initial gains at different harmonics are not disturbed and curve is much steeper after the cut-off frequency (by having higher order filter like a phase lag). By this way, specific low order harmonics can be rejected. For example, it can reject up to the seventh harmonic in our case but not effective on higher order harmonics. It can be concluded that the filter $Q_2(z)$ gives higher stability margins for all three capacitor values but at the same time, the system would be subject to poor disturbance rejection due to low gains at the fundamental and its harmonics as discussed earlier. It can be effective in those situations where the utility harmonics are not strong enough. The other alternative solution would be use of the low pass filter $Q_3(z)$, which gives us higher stability margins when the resonant frequency is high in case of a low capacitor value ($C = 22.5\,\mu\text{F}$) of the LCL filter. However, a system is unstable when capacitor values of the LCL filter are higher such as $C = 80\,\mu\text{F}$ and $C = 160\,\mu\text{F}$.

The reason for instability in case of higher capacitor values ($C = 80\,\mu F$ and $C = 160\,\mu F$) of the LCL filters need to be investigated. For this purpose, the bandwidth of the system need to looked at. Table 4.3 shows the closed loop bandwidth for different capacitor values. Fig. 4.15 and Fig. 4.16 show the frequency response of an open loop and closed loop system respectively without RC at different capacitor values. Fig. 4.17 shows the frequency response of the closed loop system with RC. It can be observed from these figures that the system has a higher bandwidth when $C = 22.5\,\mu F$ when compared to the other capacitor values. By looking at the Fig. 4.14, it can be further observed that the higher order harmonics around cut-off frequency affect the stability margins due to the low bandwidth for higher capacitors values ($C = 80\,\mu F$ and $C = 160\,\mu F$).

We can summarise this as:

- When the value of capacitor is low ($C = 22.5\,\mu F$), the corner frequency is high and the controller design is easier to stabilize with enough gain and phase margin. The system has a high bandwidth and the performance is better. The system could have better attenuation of different harmonics as well.

- When we have higher values of capacitors ($C = 80\,\mu F$ and $C = 160\,\mu F$), the corner frequency is low and the system has a low bandwidth. A better filter such that $Q_2(z)$ can achieve stability, but it is found that the performance of the system is poor in terms of disturbance rejection due to lower gains at harmonic frequencies.

Thus, it is concluded that the effectiveness of RC is severely limited by the limited bandwidth of the system (the utility connected converter and its LCL filter). The design of the LCL filter of the converter and the selection of its bandwidth and the values of its components need to be selected, such that RC could be used effectively. In our case, the suitable capacitor value of the LCL filter is to be $C = 22.5\,\mu F$, which can provide a higher bandwidth. It has been further demonstrated that the RC is effective in handling the higher resonance for low capacitor values of the LCL filter.

| No. | Value of Capacitor (C) in LCL Filter | Natural Resonant Frequency $f_n = \frac{1}{2\Pi}\sqrt{\frac{L_1 + L_2}{L_1 L_2 C}}$ |
|---|---|---|
| 1. | $C = 160\,\mu F$ | 1.90 KHz |
| 2. | $C = 80\,\mu F$ | 2.69 KHz |
| 3. | $C = 22.5\,\mu F$ | 5.073 KHz |

*Table 4.1: Relationship between LCL filter capacitor values and resonant frequency*

| Low Pass Filter | Stability Margins | | | | | |
|---|---|---|---|---|---|---|
| | $C = 22.5\,\mu F$ | | $C = 80\,\mu F$ | | $C = 160\,\mu F$ | |
| | GM (dB) | PM (deg) | GM (dB) | PM (deg) | GM (dB) | PM (deg) |
| $Q_1(z)$ | 0.003 | 0.056 | -0.089 | 0.85 | -0.23 | 2.9 |
| $Q_2(z)$ | 8.03 | 52.7 | 6.16 | 26.4 | 5.36 | 16.6 |
| $Q_3(z)$ | 6.53 | 24.4 | -0.17 | 0.87 | 0.16 | -1.65 |

*Table 4.2: Stability margins of the RC based system with different low pass filters and capacitor values*

| No. | Capacitance (C) in LCL Filter | Closed Loop System Bandwidth |
|---|---|---|
| 1. | $C = 160\,\mu F$ | 1.30 KHz |
| 2. | $C = 80\,\mu F$ | 1.81 KHz |
| 3. | $C = 22.5\,\mu F$ | 3.06 KHz |

*Table 4.3: Relationship between LCL filter capacitor values and closed loop system bandwidth with RC having* $Q_3(z)$ and $K_R = 0.1$

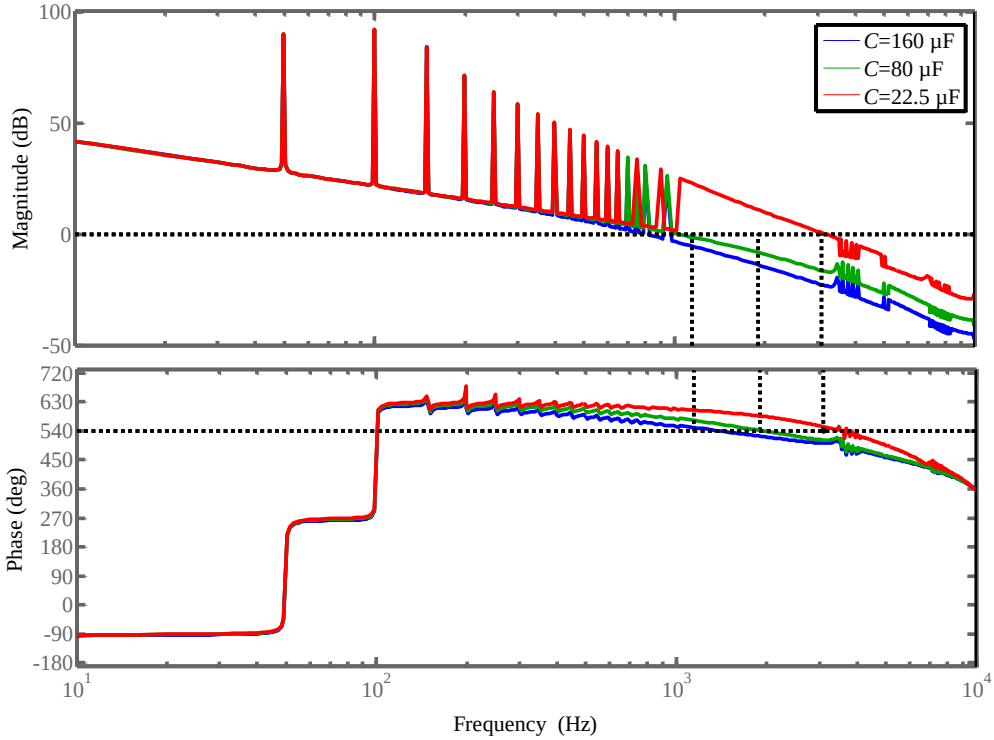


*Fig. 4.12: Frequency response of the open loop system with $Q_1(z)$ for different capacitor values of the LCL filter*

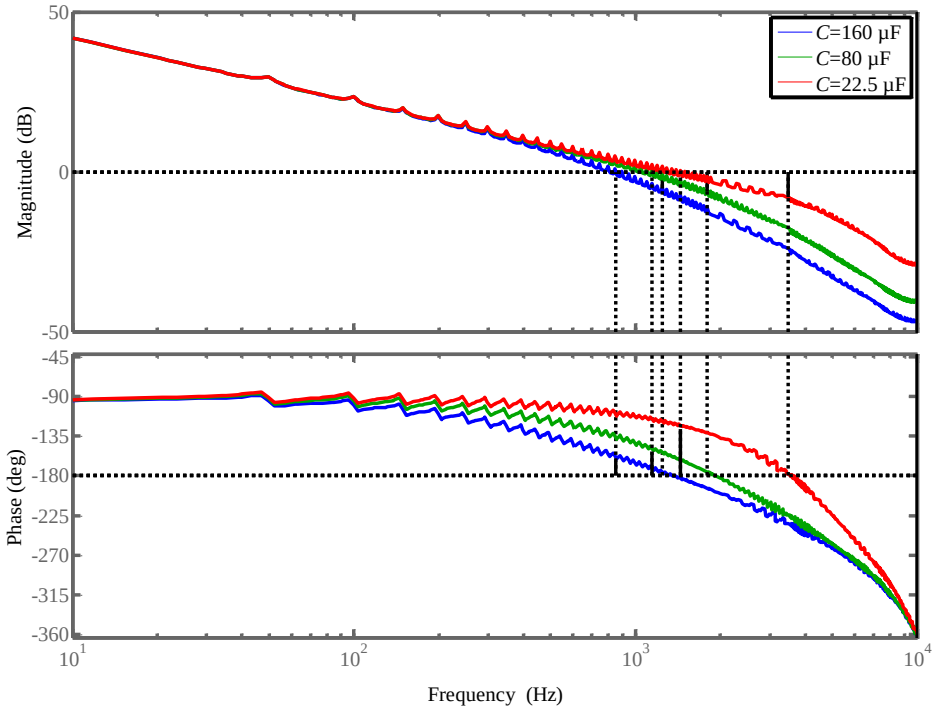


*Fig. 4.13: Frequency response of the open loop system with $Q_2(z)$ for different capacitor values of the LCL filter*

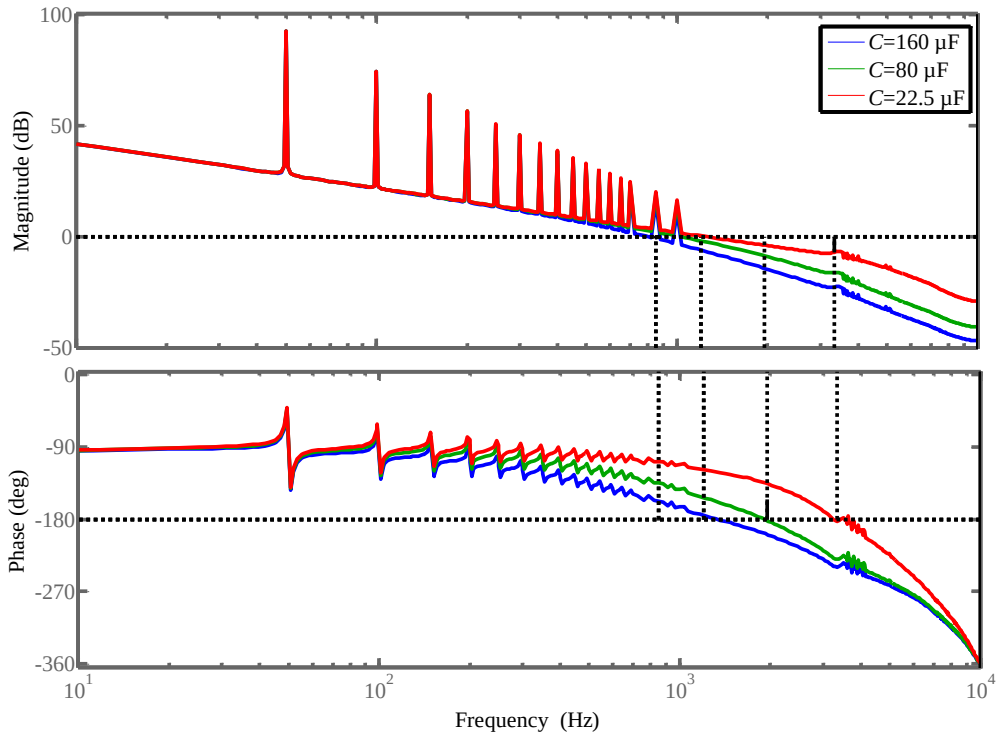


*Fig. 4.14: Frequency response of the open loop system with $Q_3(z)$ for different capacitor values of the LCL filter*

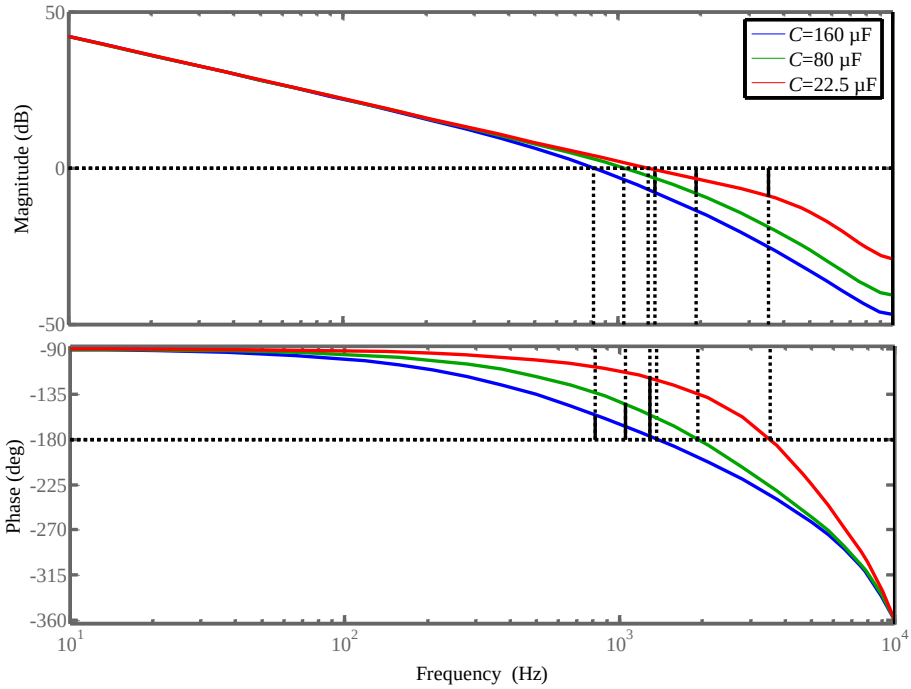


*Fig. 4.15: Frequency response of the open loop system without RC for different capacitor values of the LCL filter*

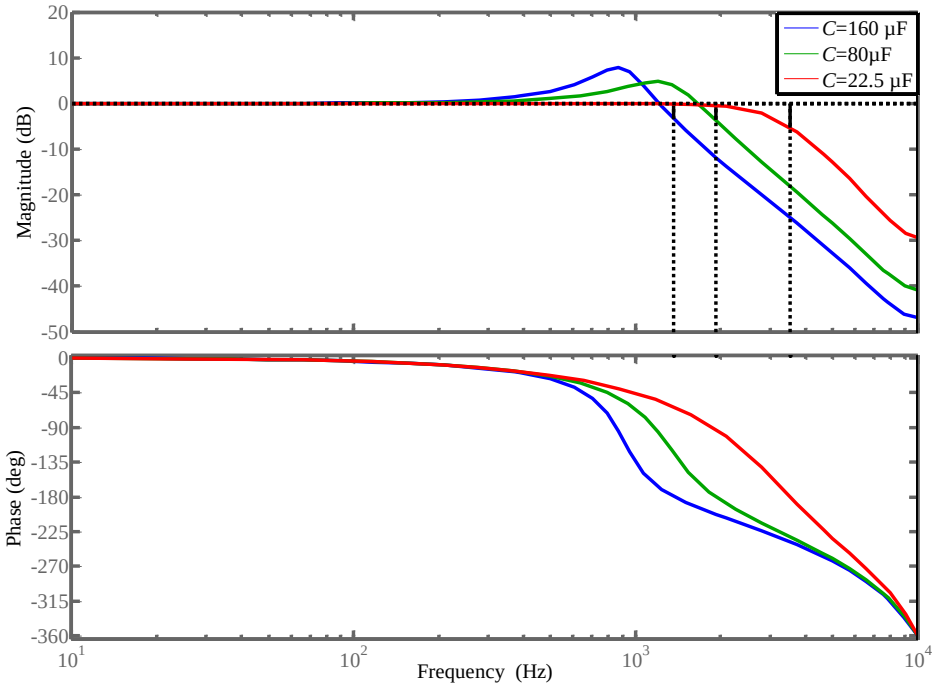


*Fig. 4.16: Frequency response of the closed loop system without RC for different capacitor values of the LCL filter*

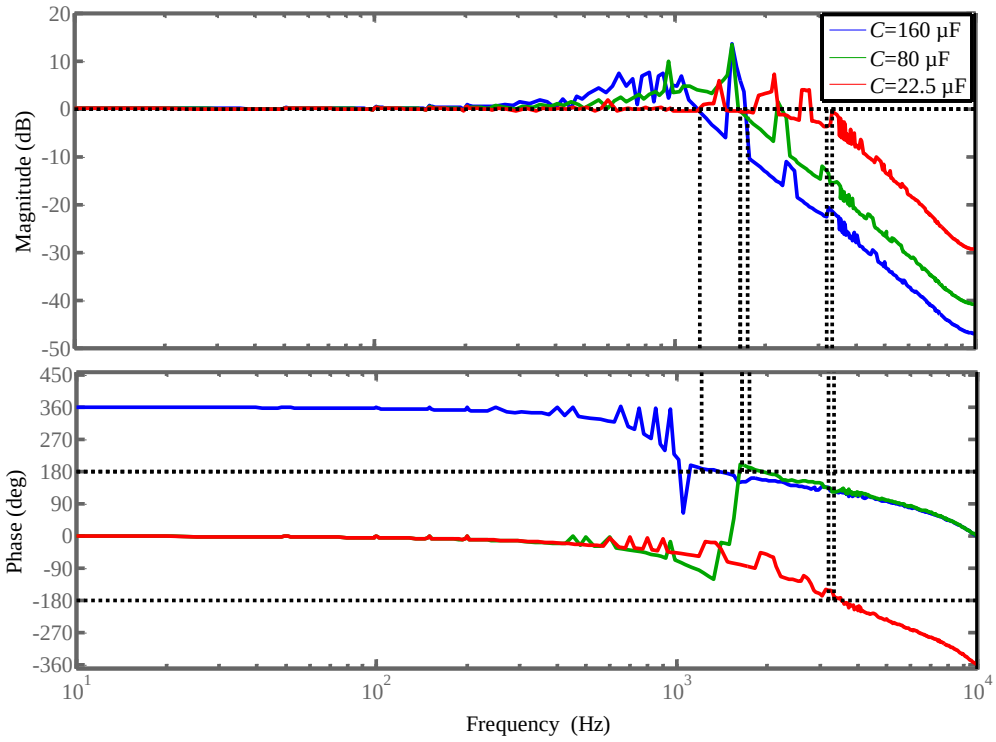


*Fig. 4.17: Frequency response of the closed loop system with RC having filter $Q_3(z)$ against different capacitor values of the LCL filter*

## 4.4 Performance of the RC System

The performance of the RC system in terms of disturbance rejection and under variations in utility impedance is investigated using the switching simulation model given in Fig. 3.2. The RC gain of 0.1 i.e. $K_R = 0.1$ and the RC filter $Q_3(z)$ is used. The classical proportional controller gain ($K_p$) and inner loop capacitor gain ($K_c$) are 13 and 3.2 respectively, (see section 4.2.1) for the LCL filter configuration given in Table 1.3. For other LCL filter configurations (section 2.2.1 and Table 1.2) or to see specific behaviour, these parameters may be varied and will then be mentioned separately.

### 4.4.1 Simulation Results

The performance of the controller is tested under different utility THD levels. Utility voltage is modelled to have only low order odd harmonics. The different values of the THD levels can be obtained by considering different utility voltage harmonics. The three cases that have been selected to test the performance of the controller are shown in Table 4.4 and Table 4.5. The first case shows the magnitude of all odd harmonics measured at the test site of the laboratory of Exeter University. The total utility THD was 2.74%. The other two cases are arbitrarily selected to test the effectiveness of the controller for worst-case situations. In the context of a real system, the other two systems could be considered as examples of complex power systems having severe utility voltage harmonics. In the second case, the utility THD is roughly assumed to be double compared to the actual measurement. In the third case, a more severe case of utility voltage harmonics (worst-case scenario) is assumed by considering higher (two times) THD compared to the second case. For this purpose, the different strong harmonics are added to the utility voltage as a percentage of the fundamental component (230Vrms) as shown in Table 4.4 and 4.5.

A demand of 100A (peak) is assumed as the system power ratings (80KVA) can support this current. The results for the third case (worst-case scenario) are presented here. Fig. 4.18 shows the output current without RC. It can be easily observed that the quality of output current is poor and current THD is quite high at 9.5%, which is not acceptable as per required standards. By having RC, the quality of the output current improves significantly

as shown in Fig. 4.19. The quality of the output current is high with almost zero steady state error and the current THD is just 2.5%. This demonstrates the effectiveness of the RC. Fig. 4.20 shows the output current without voltage feedforward. It can be observed that there exists a long initial transient when the voltage feedforward is not used. The error convergence is quite fast as shown in Fig. 4.21.

| **Harmonic number** (n) | **Case 1: Fundamental Component of Utility Voltage** V(rms) | **Case 2: Fundamental Component of Utility Voltage** V(rms) | **Case 3: Fundamental Component of Utility Voltage** V(rms) |
|---|---|---|---|
| $3^{rd}$ | 2.4 | 9.2 | 18.4 |
| $5^{th}$ | 4.22 | 6.9 | 11.5 |
| $7^{th}$ | 1.95 | 4.6 | 9.2 |
| $9^{th}$ | 2.37 | 3.45 | 4.6 |
| $11^{th}$ | 1.46 | 1.38 | 0.115 |
| $13^{th}$ | 1.95 | 0.69 | 0.057 |
| $15^{th}$ | 0.455 | 0.23 | 0.23 |
| $17^{th}$ | 0.65 | 0.23 | 0.23 |
| $19^{th}$ | 0.585 | 0.23 | 0.23 |
| **Utility Voltage THD** | **2.74%** | **5.8%** | **10.44%** |
| **Output Current THD with RC** | **1.12%** | **1.8%** | **2.5%** |

*Table 4.4: Output current THD under different utility voltage harmonics using RC*

| **Harmonic Order ( n)** | **$3^{rd}$** | **$5^{th}$** | **$7^{th}$** | **$9^{th}$** | **$11^{th}$** | **$13^{th}$** | **$15^{th}$** | **$17^{th}$** | **$19^{th}$** |
|---|---|---|---|---|---|---|---|---|---|
| **Case 2:** Percentage of Fundamental Vrms (%) | 4 | 4 | 2 | 1.5 | 0.6 | 0.3 | 0.1 | 0.1 | 0.1 |
| **Case 3:** Percentage of Fundamental Vrms (%) | 8 | 5 | 4 | 2 | 0.05 | 0.025 | 0.1 | 0.1 | 0.1 |

*Table 4.5: Harmonics added to the utility voltage for case2 and case 3 in terms of percentage of fundamental component*

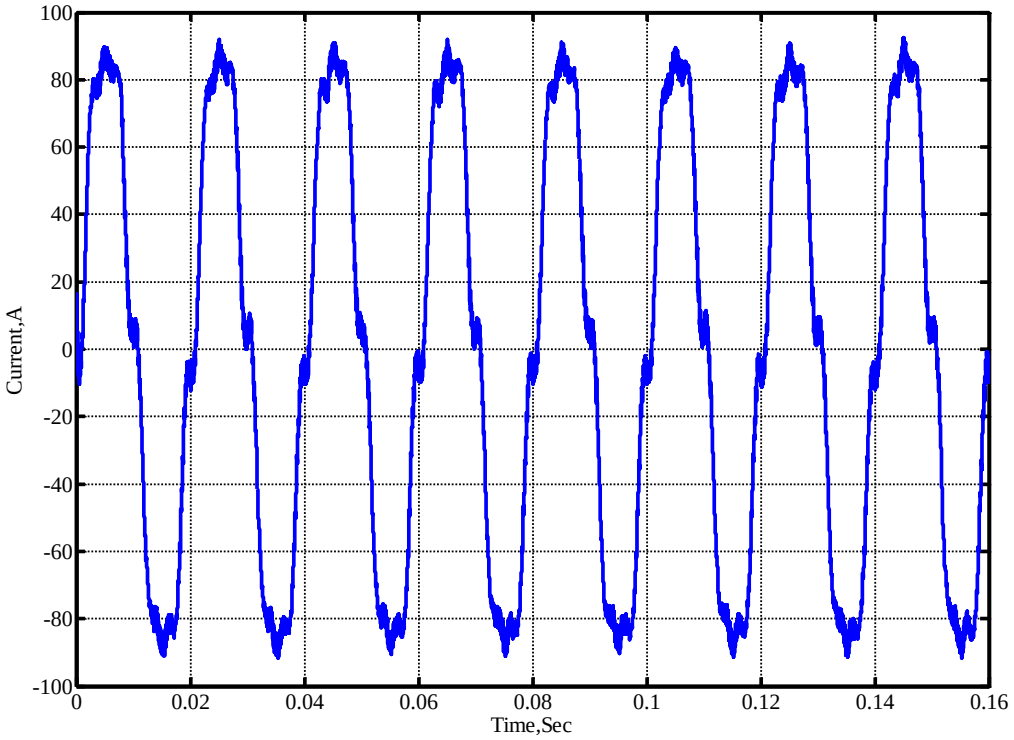


*Fig 4.18: Simulated output current without RC for case 3 (worst-case scenario) with voltage feedforward*

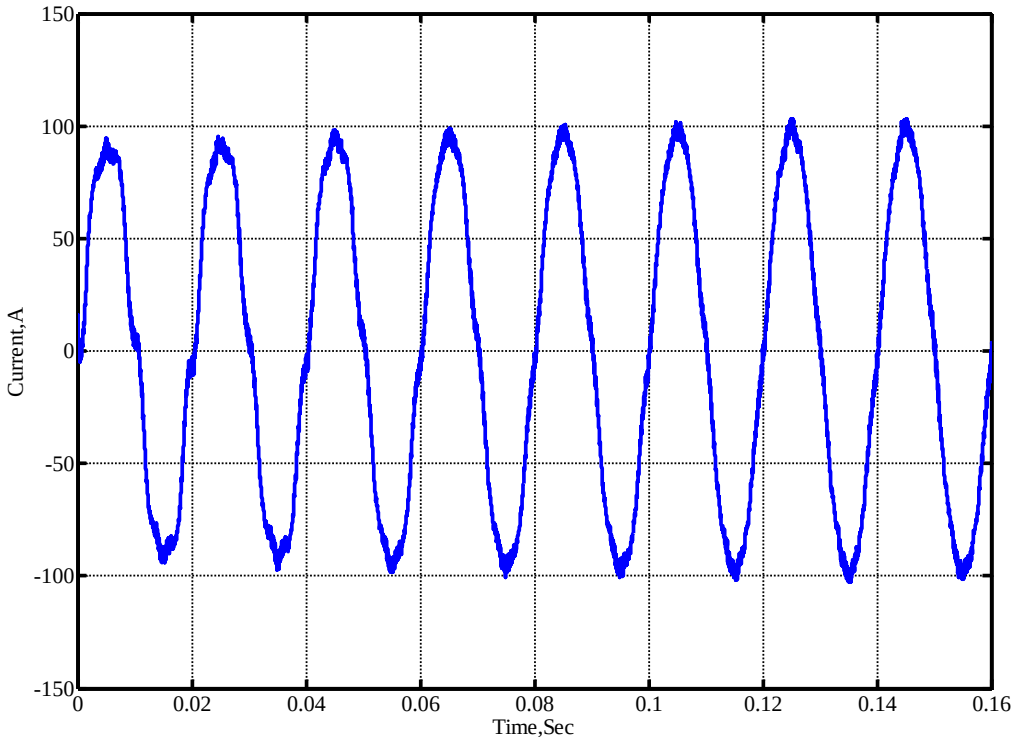


*Fig 4.19: Simulated output current with RC for case 3 (worst-case scenario) with voltage feedforward*

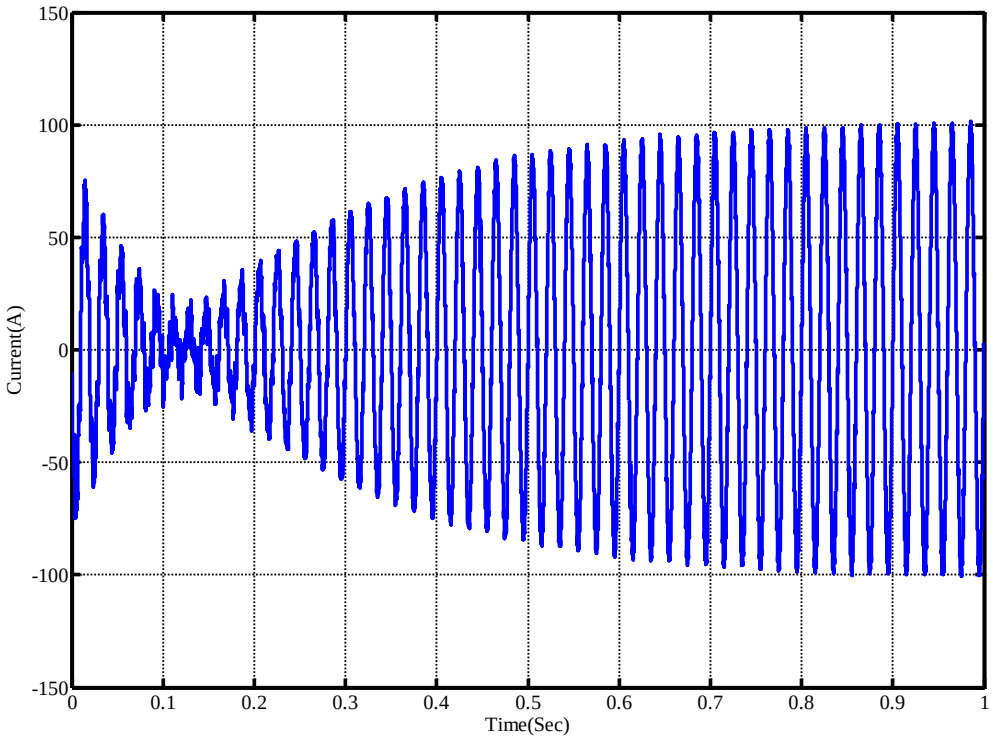


*Fig 4.20: Simulated output current with RC system for case 3 without voltage feedforward*

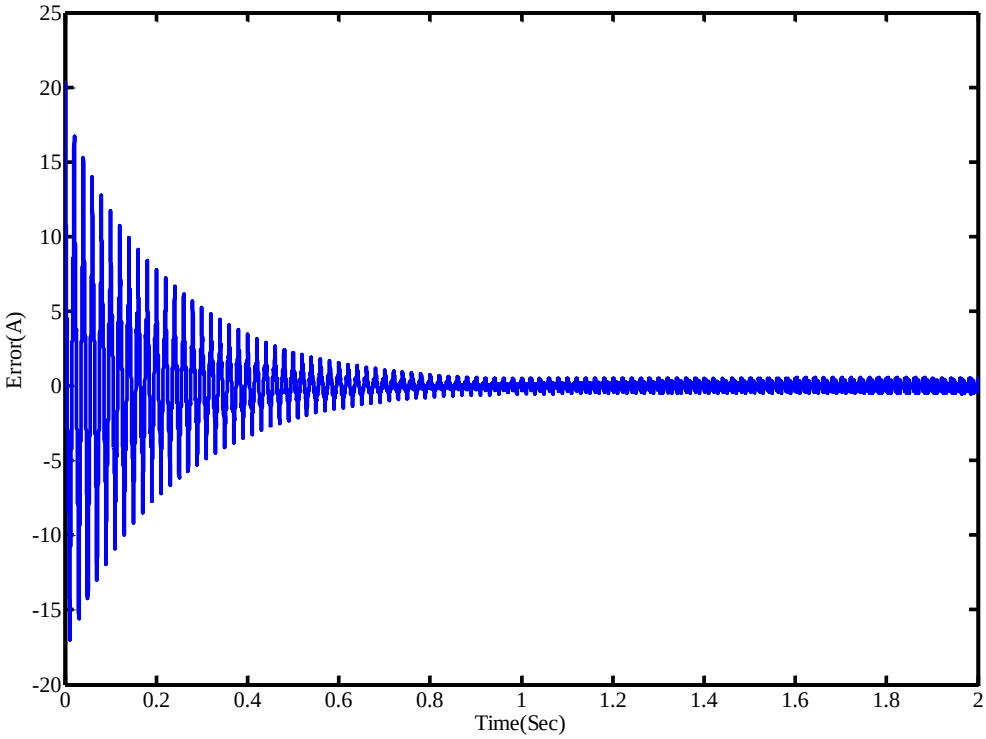


*Fig 4.21: Error convergence with RC for case 3 with voltage feedforward*

### 4.4.2 Transient Response

The transient response of the system with RC is analysed. For this purpose, two different values of the reference currents (50A and 100A) are used after steady state. Normally, a voltage regulator/controller is used in the outer loop, which defines the amplitude of the reference current. Instead of this, the two reference currents are manually changed using Matlab (signal builder block). The outer loop voltage control could be part of any future work. The value of the current is initially changed from 50A to 100A at t=0.405 sec and then it is changed from 100A to 50A at t=0.465 sec to see the transient response. Fig. 4.22 shows the transient response of the system with RC. It can be observed that the system is able to respond to the changes in the reference current without any noticeable transient.

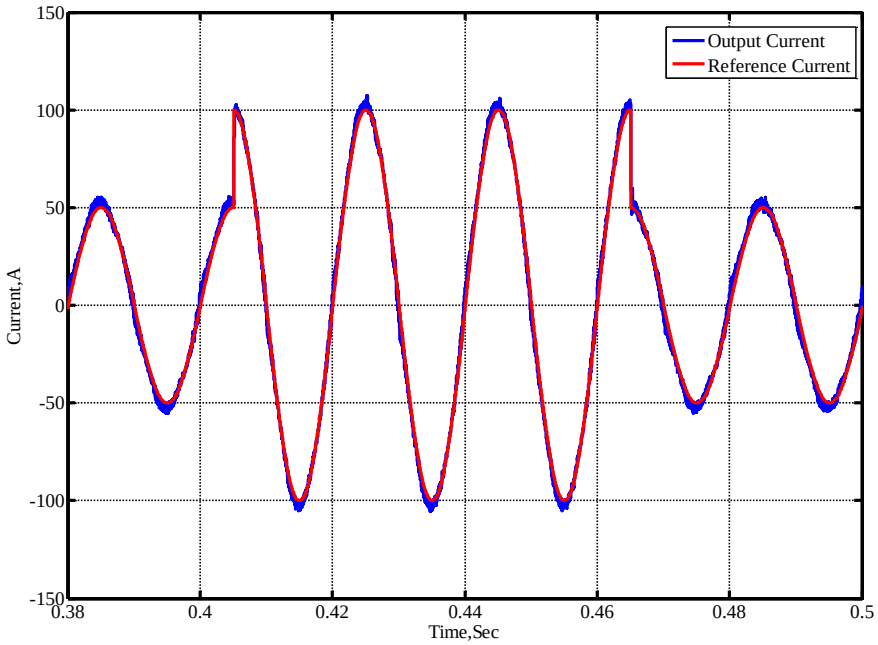


*Fig 4.22: Transient response of the system with RC with* $K_R = 0.1$ *and* $Q_3(z)$

The small amount of nonlinear behaviour can be observed when the reference current is varied, which is obvious due to the presence of nonlinear elements in the switching model. However, these are negligible and the system analysis is still valid using a linear average switching model approach (as discussed in section 3.4), which is common for this application. These nonlinearities can be reduced with appropriate gains at the cost of steady state error. For example, Fig. 4.23 shows the transient response of the system without RC and having proportional gain $K_p = 1$ and Fig. 24 shows the transient response with

proportional gain $K_p = 1.8$. It can be observed that when the gain is low (Fig. 4.23), the nonlinearities are not noticeable without any overshoot in the current, but steady state error is high. In contrast, when the gain is high (Fig. 4.24), overshoot and nonlinearities are noticeable but steady error is low. As concluding remarks, it can be said that the system transient response with RC is better than the classical proportional controller.

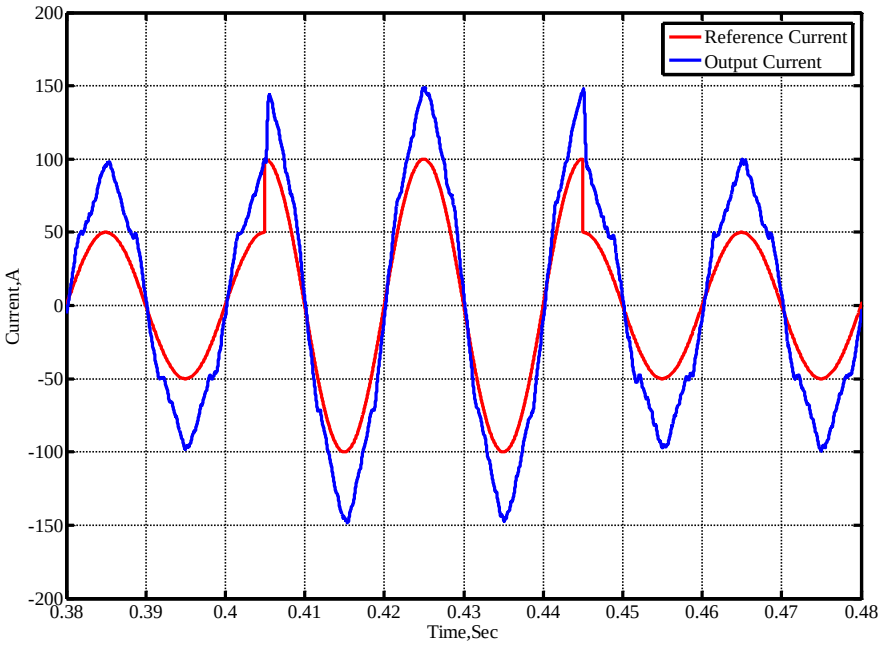


*Fig 4.23: Transient response of the system without RC and having* $K_p = 1$

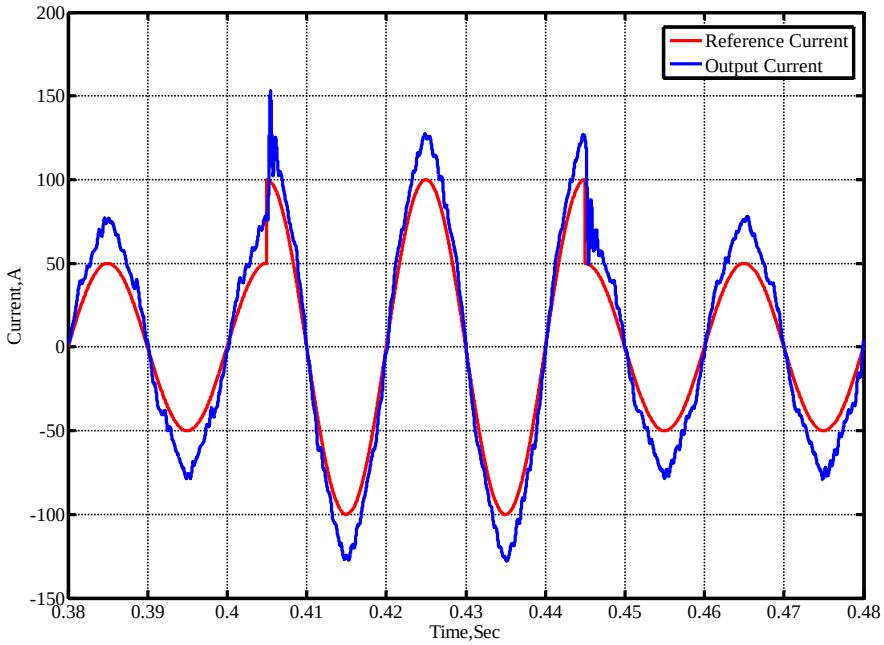


*Fig 4.24: Transient response of the system without RC and having* $K_p = 1.8$

### 4.4.3 Harmonic Rejection Capability

The disturbance transfer function of the system derived in chapter 2 can be written as follows:

$$G_D(z) = \frac{I_2}{V_u} = \frac{G_p(z)}{1+(1+G_{RC}(z))G_c(z)G_P(z)} \tag{4.15}$$

Where, $G_p(s)$, $G_{RC}(s)$ and $V_u(s)$ are transfer functions of plant, RC and disturbance. The disturbance is related to the utility voltage harmonics.

All cases of different LCL filter capacitor values with earlier designed low pass filters are presented to evaluate the effectiveness of the RC in terms of disturbance rejection. It is known from section 3.4 and earlier analysis that the low pass filter $Q_3(z)$ and the low capacitor value (C=22.5μF) can provide optimum performance in terms of stability, disturbance rejection and bandwidth. The stability and bandwidth have been investigated earlier with different test cases of the LCL filter capacitance values and low pass filters. However, performance of the RC in terms of disturbance rejection and ability to reject individual harmonics need to be investigated with different capacitance values ($C = 160\,\mu$F, $C = 80\,\mu$F and $C = 22.5\,\mu$F) and low pass filters such as $Q_1(z), Q_2(z)$ and $Q_3(z)$. For this purpose, the magnitude frequency response of the disturbance rejection for each case is plotted and the amount of attenuation in magnitude (dB) is observed for fundamental frequency and individual harmonics. The higher negative values of magnitude in dB will provide higher attenuation. The RC gain is selected to be $K_R = 0.1$ for all cases.

First, the magnitude frequency response of the disturbance transfer function without RC against different capacitor values is shown in Fig. 4.25. It can be observed that when $C = 160\,\mu$F, only frequencies (first and third) lower than 200Hz (F1 shown in Fig. 4.25) can be attenuated theoretically. After this, the magnitude becomes positive and not effective for frequencies greater than 200Hz (F2 shown in Fig. 4.25). When $C = 80\,\mu$F, the gain can be effective only for those frequencies, which are less than 400 Hz. For $C = 22.5\,\mu$F, all frequencies lower than 1.5 KHz (F3 shown in Fig. 4.25) can be attenuated due to higher

bandwidth as discussed earlier. In the next step, the magnitude frequency response of the disturbance transfer function with RC having low pass filter $Q_1(z)$ against different capacitor values is shown in Fig. 4.26. Since it is already known from the stability analysis that low pass filter $Q_1(z)$ results in stable system (though very low margins) for only capacitance value of $C = 22.5\,\mu\text{F}$. However, higher gains (e.g. first fundamental frequency is attenuated by -72dB) can be observed at all frequencies, which can provide better attenuation against fundamental frequency and its harmonics. In the next step, the magnitude frequency response of the disturbance transfer function with RC having low pass filter $Q_2(z)$ is investigated. It provides a stable system with different capacitance values ($C = 160\,\mu\text{F}$, $C = 80\,\mu\text{F}$ and $C = 22.5\,\mu\text{F}$) as discussed earlier. Here, the poor disturbance rejection capability of the RC against the fundamental frequency and its harmonics can be observed using Fig. 4.27. It can reject only low order frequencies (first, third and seventh) but is not effective at higher frequencies due to the lower amplitude of the gains at higher order harmonics. Finally, the magnitude frequency response of the disturbance transfer function with RC having low pass filter $Q_3(z)$ is investigated using Fig. 4.28. It can be observed that the RC can offer higher gains for the fundamental frequency and its harmonics without disturbing stability when the capacitance value of the LCL filter is $C = 22.5\,\mu\text{F}$.

It should be noted here that instead of giving only a stable and optimum case having $C = 22.5\,\mu\text{F}$ and $Q_3(z)$, all other cases are presented for the purpose of comparison and analysis. Table 4.6 shows the amount of attenuation in magnitude (dB) of fundamental frequency and dominant harmonics (third, fifth and seventh) with and without RC for all test cases. Now, the effectiveness of RC in terms of disturbance rejection is presented using Table 4.7, where simulation is carried out using a linear and switching model when utility THD is 2.74% (case 1). It can be observed that all harmonic frequencies are well attenuated in the output current that contribute towards low THD. It can be concluded that RC is quite effective in terms of disturbance rejection (harmonic attenuation) when compared to the classical controller even when utility harmonics are high. The RC is able to provide higher gains to reject individual harmonics, which makes it suitable in this application.

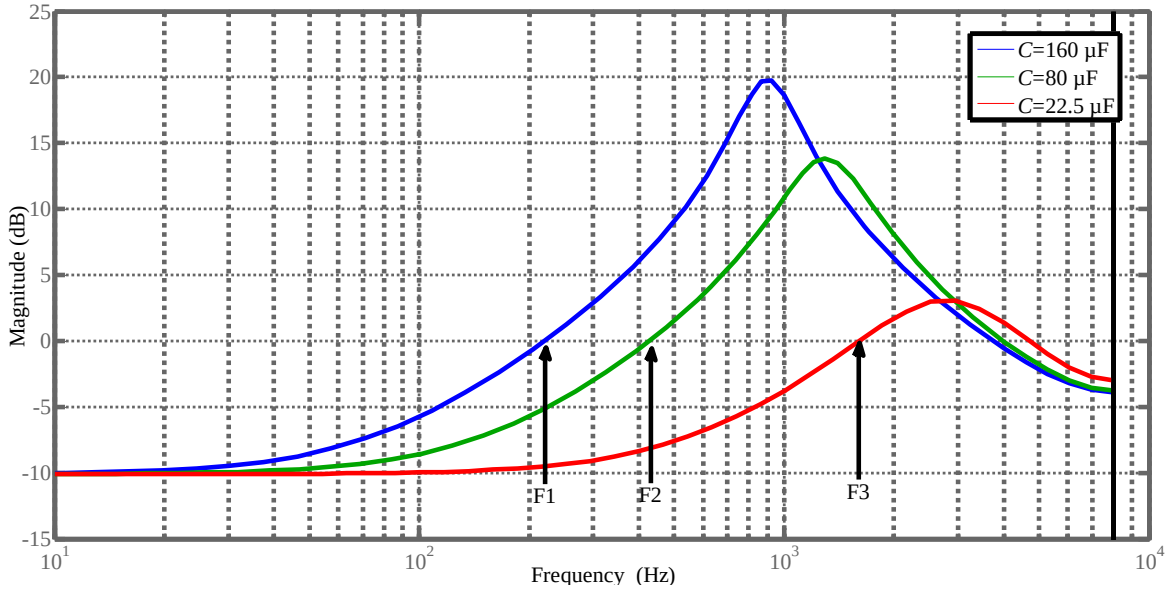


*Fig. 4.25: Magnitude frequency response of the disturbance transfer function $G_D(z)$ without RC for different capacitor values of LCL filter*

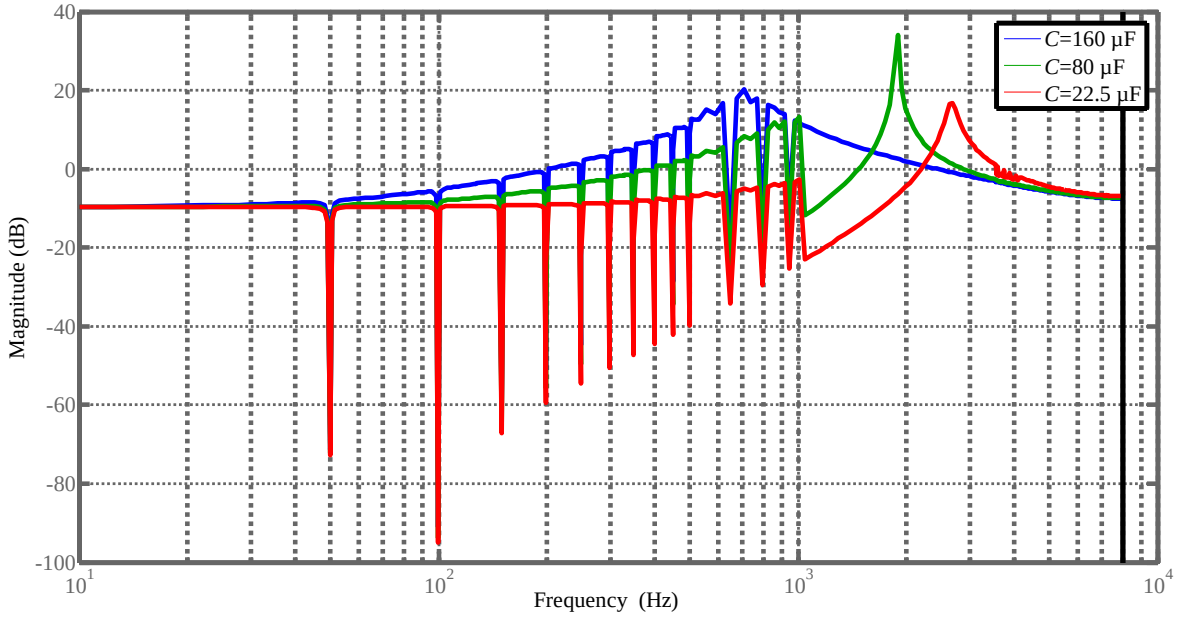


*Fig. 4.26: Magnitude frequency response of the disturbance transfer function $G_D(z)$ with $Q_1(z)$ for different capacitor values of LCL filter*

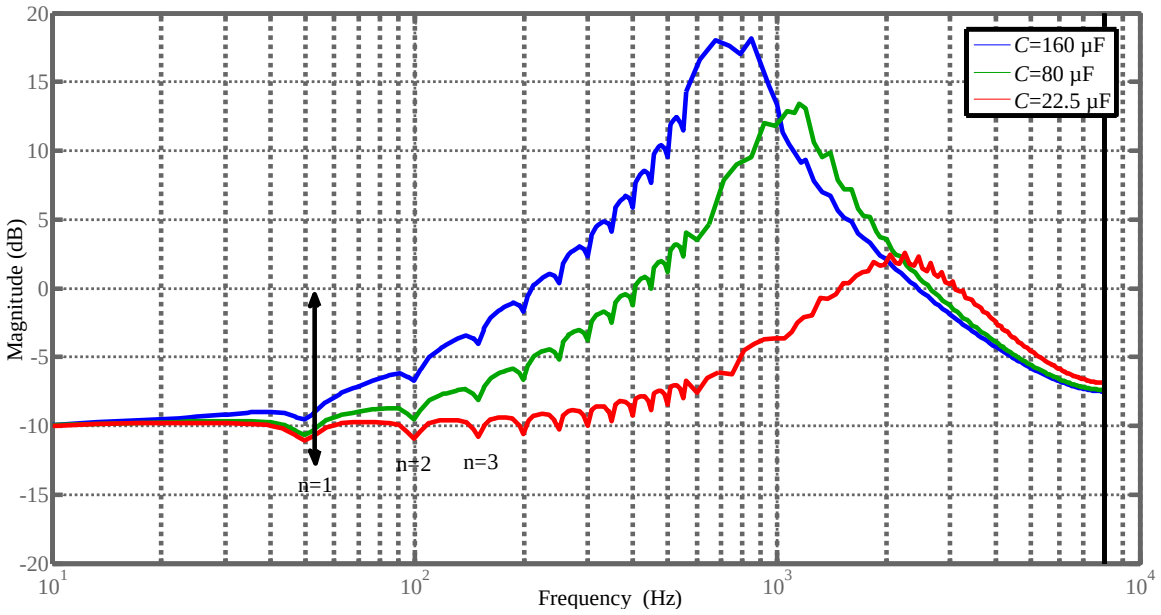


*Fig. 4.27: Magnitude frequency response of the disturbance transfer function $G_D(z)$ with $Q_2(z)$ for different capacitor values of LCL filter*

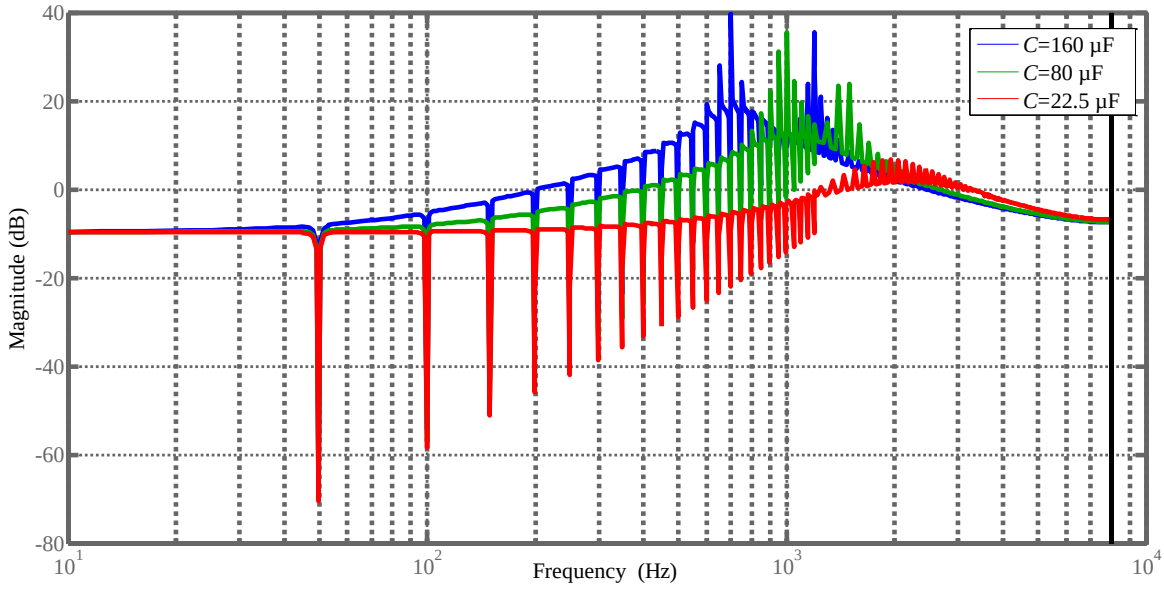


*Fig. 4.28: Magnitude frequency response of the disturbance transfer function $G_D(z)$ with $Q_3(z)$ for different capacitor values of LCL filter*

| Type of System | Amount of Attenuation in Magnitude ( dB) | | | | | | | | | | | |
|---|---|---|---|---|---|---|---|---|---|---|---|---|
| | $C = 22.5\,\mu F$ | | | | $C = 80\,\mu F$ | | | | $C = 160\,\mu F$ | | | |
| | $1^{st}$ | $3^{rd}$ | $5^{th}$ | $7^{th}$ | $1^{st}$ | $3^{rd}$ | $5^{th}$ | $7^{th}$ | $1^{st}$ | $3^{rd}$ | $5^{th}$ | $7^{th}$ |
| Without RC | -10 | -9.7 | -9.3 | -8.7 | -9.5 | -7.1 | -4 | -2.1 | -8 | -2.5 | 1.2 | 4 |
| With $Q_1(z)$ | -72 | -67 | -54 | -47 | -70 | -65 | -49 | -40 | -71 | -60 | -44 | -35 |
| With $Q_2(z)$ | -11 | -10.8 | -10.3 | -9.6 | -10.6 | -8.1 | -5.3 | -2.7 | -9.6 | -4.2 | 0.07 | 3.7 |
| With $Q_3(z)$ | -70 | -51 | -41 | -35 | -70 | -48 | -37 | -29 | -68 | -44 | -32 | -23 |

*Table 4.6: Amount of attenuation of fundamental frequency and individual ($3^{rd}$, $5^{th}$ and $7^{th}$) harmonics in dB with and without RC against different low pass filters and capacitor values*

| **Harmonic number** (n) | **Utility voltage** V(rms) | **Output current with switching model , A(rms)** | | **Output current with linear model , A (rms)** | |
|---|---|---|---|---|---|
| | | **Without RC** | **With RC** | **Without RC** | **With RC** |
| $3^{rd}$ | 2.4 | 0.32 | 0.12 | 0.78 | 0.02 |
| $5^{th}$ | 4.22 | 2.33 | 0.35 | 1.46 | 0.09 |
| $7^{th}$ | 1.95 | 0.84 | 0.41 | 0.73 | 0.52 |
| $9^{th}$ | 2.37 | 0.95 | 0.86 | 0.73 | 0.72 |
| $11^{th}$ | 1.46 | 0.58 | 0.28 | 0.67 | 0.13 |
| $13^{th}$ | 1.95 | 0.62 | 0.3 | 0.99 | 0.24 |
| $15^{th}$ | 0.455 | 0.14 | 0.1 | 0.25 | 0.08 |
| $17^{th}$ | 0.65 | 0.26 | 0.1 | 0.40 | 0.15 |
| $19^{th}$ | 0.585 | 0.38 | 0.12 | 0.40 | 0.18 |
| **THD (%)** | **2.74 %** | **2.84 %** | **1.12 %** | **2.37 %** | **0.96 %** |

*Table 4.7: Harmonic rejection with and without RC for case 1 when utility THD is 2.74%, the RC filter is $Q_3(z)$ and the RC gain is 0.1*

### 4.4.4 Effect of Variations in Utility Impedance

The effect of variations of the utility impedance on the performance of RC based system needs to be investigated. The value of the inductor $L_2$, which is determined by the utility impedance, can vary significantly depending on the site where the converter is installed. This uncertainty needs to be taken into account to ensure that the system can handle these uncertainties under the worst conditions. To assess the robustness of the system, the uncertainty in the value of $L_2$ is varied by ±50% and it is observed that the system is always stable having high enough gain and phase margins. It can be concluded that the RC system can handle variations in utility impedance very well as shown in Fig. 4.29. Thus, the system is robust against uncertainties in utility impedance variations.

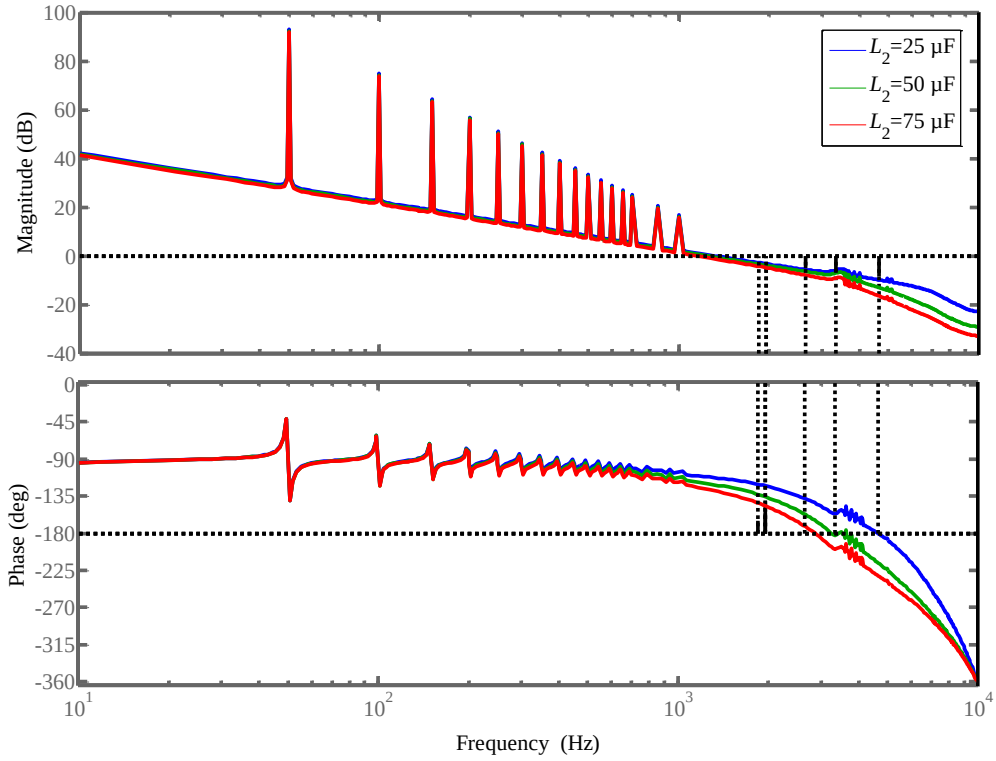


*Fig 4.29: Bode diagram showing the effect of variations in $L_2$ on overall RC system*

## 4.5 Design of Odd-Harmonic Repetitive Control (ORC)

The conventional RC with periodic signal generator described in the previous sections has high gains at both even and odd-harmonics. As mentioned in chapter 2, odd-harmonic repetitive control (ORC) offers high gain only at odd-harmonic frequencies of interest. The design and working principle is similar to the conventional RC except having a different periodic signal generator, which requires only $N/2$ elements. The design of an ORC for a two-level three-phase utility connected converter involves similar steps as discussed in the case of a conventional RC. The design of a two loops conventional closed loop system has been discussed earlier in the case of RC. The ORC assumes that a stable closed loop system (without RC) exists and it is properly designed such that it has enough high gains at low frequencies. The ORC is added to the closed loop system as shown in Fig. 4.30. The case with suitable low-pass filter $Q_3(z)$ will be presented.

The overall block diagram of the system having ORC with a conventional two loops feedback system is shown in Fig. 4.30. The general terms $R$, $Y$ and $D$ will be used to represent reference current $I_{ref}$, output current $I_2$ and utility disturbance $V_u$ for analysis purposes as discussed previously. The error transfer function derived in section 2.3.2 can be written as follows.

$$G_E(z) = \frac{E(z)}{R(z) - D(z)} = \frac{1}{1 + \left(1 + G_{ORC}(z)\right) G_c(z) G_P(z)} \tag{4.15}$$

$$G_{OE}(z) = \frac{1 + Q(z) z^{-N/2}}{\left(1 + G_c(z) G_p(z)\right)\left(1 + Q(z) z^{-N/2} (1 - K_R G_f(z) G_o(z))\right)} \tag{4.16}$$

The ORC transfer function is $G_{ORC}(z)$, plant transfer function is $G_P(z)$ and the closed loop (without ORC) of classical controller $G_C(z)$ with $G_P(z)$ is $G_o(z)$. The necessary stability conditions can be obtained using gain theorem. The stability conditions of the ORC are similar to the traditional RC.

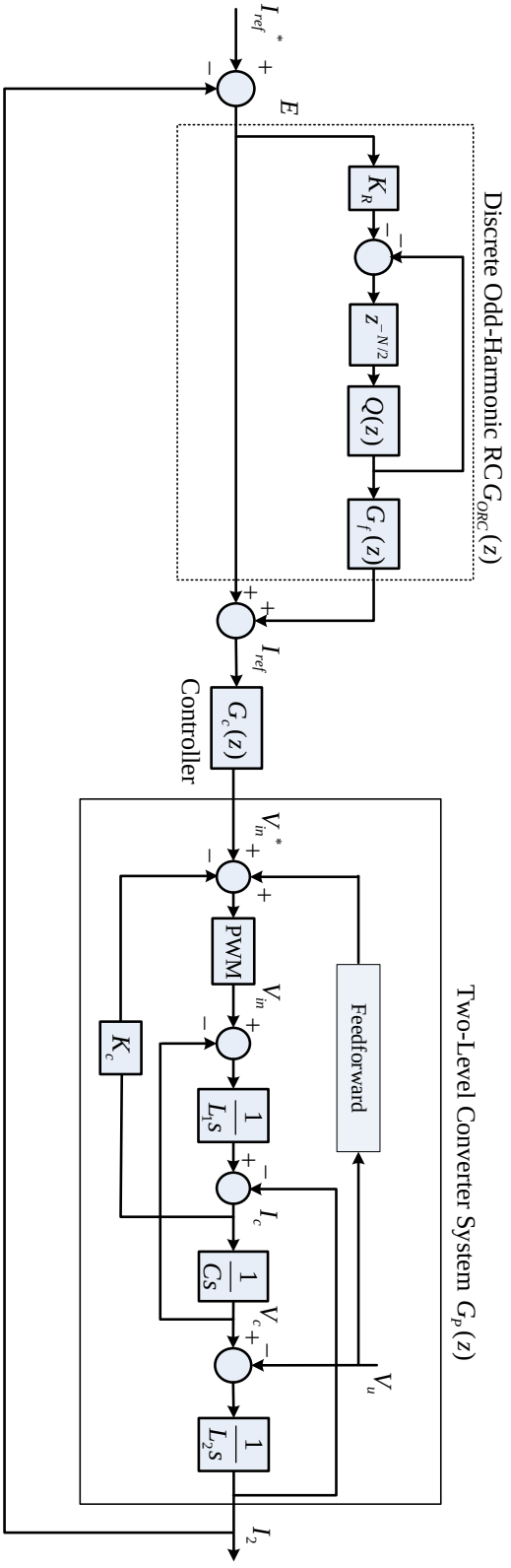


*Fig. 4.30: Overall block diagram of the ORC system of the two-level converter incorporated in the basic classical (P) controller*

From stability conditions, we know that the ORC gain $K_R$, the low-pass filter $Q(z)$, compensator $G_f(z)$ and closed loop control $G_o(z)$ of classical controller $G_c(z)$ and two loops feedback plant $G_P(z)$ should be designed properly such that poles of the system are within a unit circle. Since the two loops feedback system with conventional controller is already stable, the rest of the parameters need to be designed to ensure stability.

Similar to a conventional RC system, the ORC gain can be tuned for optimal performance. The dynamics of response can be controlled by varying this gain. Its selection is done by generating enough fast convergence and a stable system. The value of the ORC gain $K_R$ is selected to be 0.1. The low-pass filter $Q_3(z)$ provides good performance in this case as well.

### 4.5.1 Selection of Odd-Harmonic Repetitive Control (ORC) Parameters and Simulation Results

The parameters of the ORC are almost similar to the RC system except for the selection of the number of samples per period ($N$). Due to the presence of the term $z^{-N/2}$ in the transfer function of the ORC, just half the value of samples per period ($N$) is required. This means fewer samples in one period which could provide a fast response and less memory requirement compared to the conventional RC system. The most important parameters are low-pass filter $Q(z)$ and ORC gain $K_R$. The compensator $G_f(z)$ is less crucial as it only adjusts the system's phase lag. It can be incorporated by selecting an appropriate classical feedback controller $G_c(z)$. It is already known from section 4.3 that the low-pass filter $Q_3(z)$ and LCL filter capacitance $C = 22.5\,\mu\text{F}$ give optimum performance in terms of stability, bandwidth and disturbance rejection. These parameters will be used to design the ORC system. The design of the filter and other parameters is quite similar to the earlier case of RC. Fig. 4.31 shows the Bode diagram of the overall system with and without ORC. It can be observed here that higher gains are offered only at fundamental and its odd harmonics. This helps to provide a faster transient response. Moreover, it will save memory and time. The system has a gain margin of 12.8dB and a phase margin of $60.1^{\text{o}}$.

After having stabilized the system we tested the performance of the controller when utility impedance changes. The value of the inductor $L_2$ , which is determined by the utility impedance, can vary significantly depending on the site where the converter is installed. This uncertainty needs to be taken into account to ensure that the system can handle these uncertainties under the worst conditions. To assess the robustness of the system, the uncertainty in the value of $L_2$ is varied by ±50% and it is observed that the ORC system can handle these uncertainties very well, similar to the RC system. This can be seen in Fig. 4.32.

Now finally, simulation results for the ORC system are presented and are carried out using Matlab Simpower Systems Toolbox. The performance of the controller is tested against different utility THD levels. Here we present the worst-case scenario, when utility THD is 10.4% to test the effectiveness of the controller. It is interesting to mention here that in terms of THD reduction, the results are quite similar to RC but time to reject the harmonics is different, which is obvious as the ORC system has a fast response. Fig. 4.33 and Fig. 4.34 show the simulation results without and with the ORC respectively. Whereas, the transient response is provided by Fig. 4.35 by introducing a step change in the reference current at t=0.465 sec. The reference current is varied from 100A to 80A. It can be observed that the ORC system is able to adopt any change in the reference current quickly.

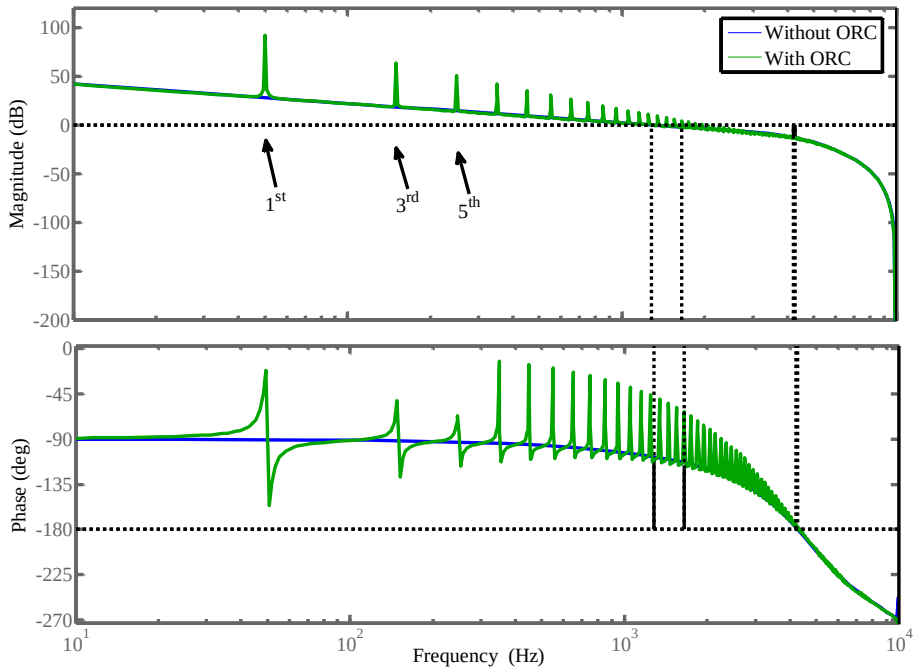


*Fig. 4.31: Bode diagram of the system with and without ORC*

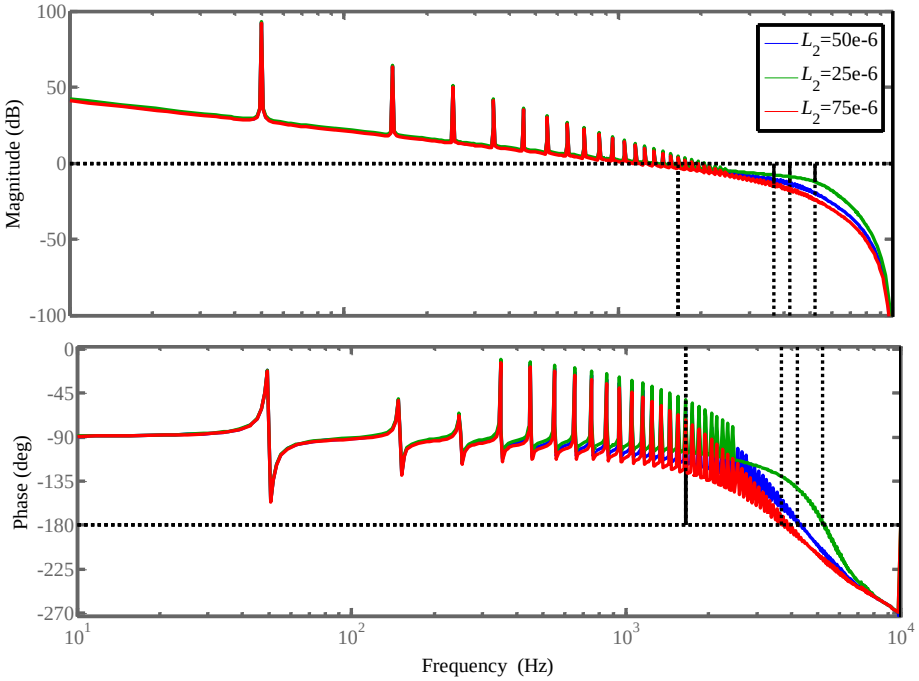


*Fig 4.32: Effect of variations in $L_2$ on the ORC system*

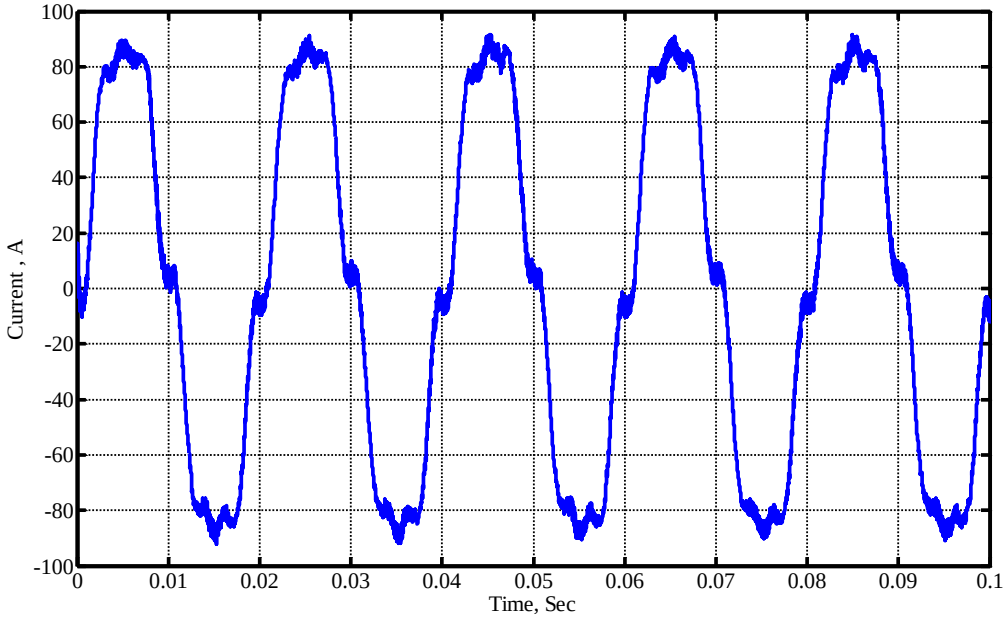


*Fig 4.33: Simulated output current without ORC- with voltage feedforward and utility voltage THD of 10.4% (worst-case scenario)*

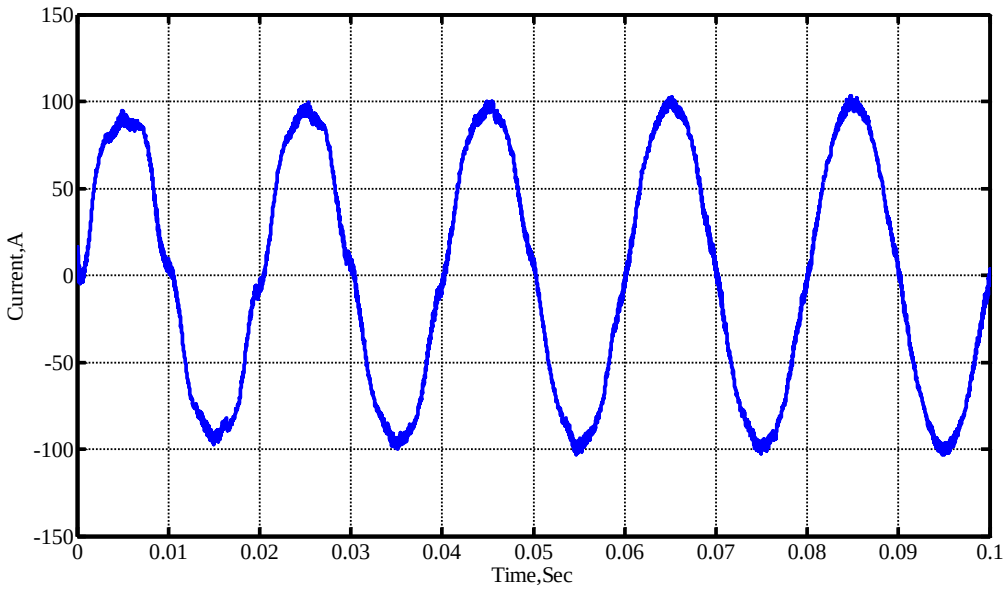


*Fig 4.34: Simulated output current with ORC- with voltage feedforward and utility voltage THD of 10.4% (worst-case scenario)*

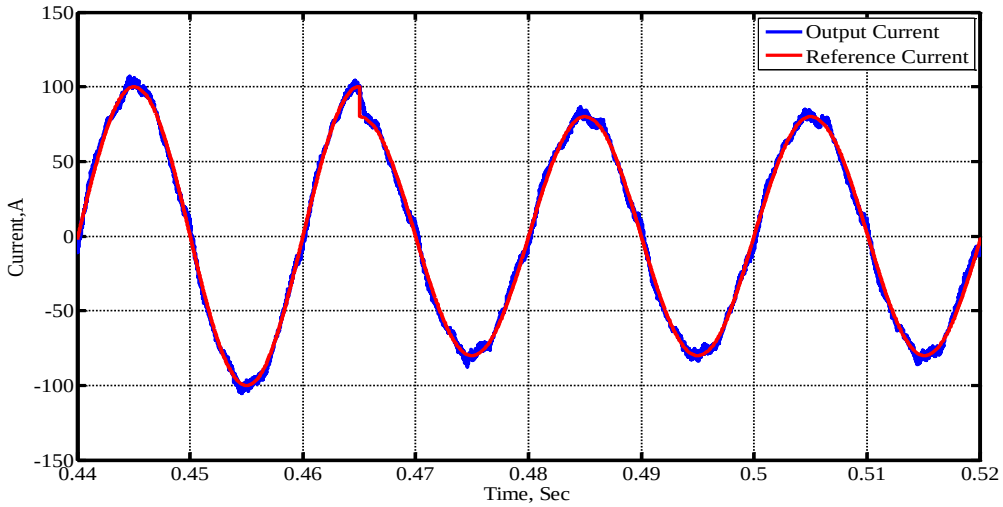


*Fig 4.35: Transient response of the system with ORC with* $K_R = 0.1$ *and* $Q_3(z)$

## 4.6 Summary

This chapter provides the procedure for designing the RC system of the two-level converter. First, a stable conventional two loops feedback system is designed and then the RC is augmented to improve performance and address the limitations of the conventional classical controller. Selection criteria of different parameters attached with the RC is defined through deriving stability conditions. The performance limitation of the RC system is investigated with respect to system bandwidth. The ORC system is also investigated and its performance is almost similar to the RC but it provides fast transient and error convergence. The ORC system is useful when there are limitations of memory and only odd harmonics are found which could not be true for some systems. We found that that the effectiveness of RC is severely limited by the limited bandwidth of the plant (the utility connected converter and its filter). Simulation results are presented to confirm that the introduction of the RC helps to improve the output current THD and steady state error which meets the requirement of different national and international standards even when utility THD is more than 5%. Theoretical analysis and simulation results presented in this chapter show that the RC could not effectively reject disturbances at frequencies above the plant's bandwidth. The design of the LCL filter and the values of its components need to be selected carefully to enable the RC to be used effectively. The effectiveness of RC with interleaved converter will be investigated in the next chapter, which can provide a higher bandwidth compared to the two-level converter.

# Chapter 5

## REPETITIVE FEEDBACK CONTROL OF AN INTERLEAVED THREE-PHASE UTILITY CONNECTED CONVERTER AND ITS EXPERIMENTAL IMPLEMENTATION

## 5.1 Introduction

This chapter discusses the design and practical implementation of a repetitive feedback current controller (RC) for a three-phase voltage source utility connected interleaved converter. Each phase consists of six half-bridge channels connected in parallel as shown in Fig. 1.3. Due to current ripple cancellation of the interleaving topology, only small capacitors are required which provide high impedance to the utility and a larger bandwidth for designing RC. This results in a better quality of current when compared to the two-level LCL topology discussed in previous chapters.

The proposed controller incorporates a conventional feedback current controller, feedforward loop of the utility voltage and phase lag compensator for system immunity against utility impedance variations, in addition to the RC loop. To control the high resonance frequency of the output filter, high sampling and switching frequencies are required. Alternatively, resistors in series with the filter capacitors are used to provide damping. This method becomes practically possible due to the low magnitude of the current in the filter capacitors and consequently low power dissipation in the damping resistors. The performance of the proposed method is investigated with variations in utility impedance and at different utility THD levels.

This chapter also discusses the experimental implementation of the proposed technique in the last section. The experimental implementation on the interleaved converter was carried out in the University of Exeter laboratory under the supervision of Dr. Abusara. The author investigated different ways of implementing RC and developed the algorithm for

implementing the RC. Dr. Abusara did the hardware setup/installation and digital signal processor (DSP) programming. Different simulation studies were conducted to provide the parameters for experimental implementation. This confirms the suitability and effectiveness of the RC for the interleaved converter and matches the simulation results in the presence of utility harmonics.

## 5.2 Design and Analysis of the Proposed Control Scheme Based on Repetitive Control

The overall proposed control scheme for the interleaved utility connected converter involves similar steps as discussed in case of the two-level converter. The block diagram of the one phase and its controller is shown in Fig. 5.1. First, a proportional controller with phase lag compensator is designed. A phase lag compensator is quite useful for utility impedance variations. Actually, a simple proportional controller can work alone for a certain amount of utility impedance variations but for higher variations, phase lag is quite useful (Abusara and Sharkh, 2010). Initially a linear model without a PWM converter as derived in chapter 4 is designed and investigated. Then a complete PWM converter model is simulated and its performance is predicted. At the next stage, a loop of RC is added to the conventional controller as shown in Fig.5.1. Finally, the parameters of the RC are tuned for optimal performance.

### 5.2.1 Conventional Closed Loop Feedback Controller

The placement of conventional feedback controller $K(z)$ is similar to the case of the two-level converter as shown in Fig. 5.1. This controller can also be regarded as a tracking controller and can be represented by $G_c(z)$ for general analysis later on. The linear model of the system has been discussed in section 3.5 already. The open loop transfer function is

$$G_{ol}(s) = \frac{I_L}{V_{in}} = \frac{L_u Cs^2 + RCs + 1}{LL_u Cs^3 + Rc(L + N_o L_u)s^2 + (L + N_o L_u)s} \tag{5.1}$$

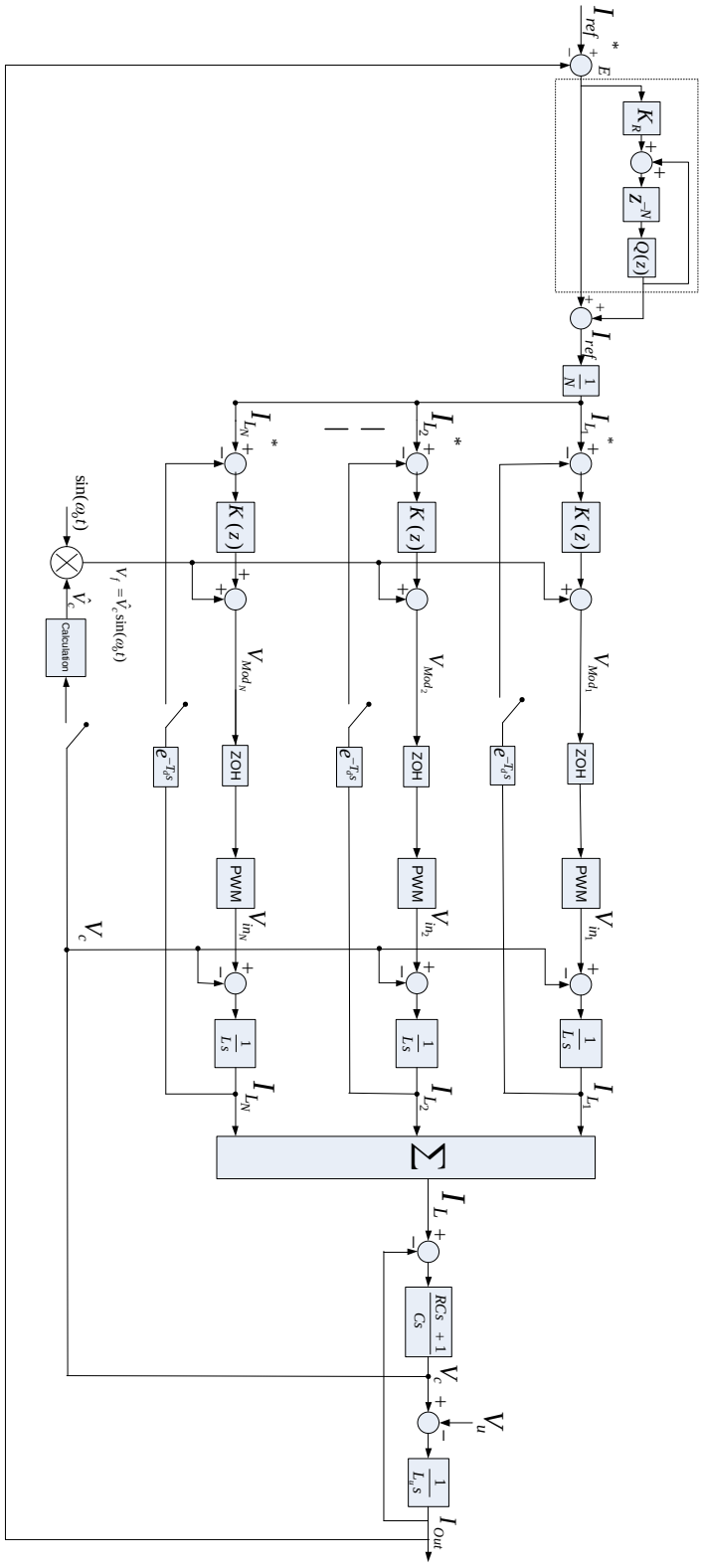


*Fig 5.1: Overall single-phase block diagram of the interleaved utility connected converter and its controller*

The time delay $T_d$ caused by the controlling processor computational time is modelled as $e^{-T_d s}$ shown in Fig.5.1. The analog to digital converters are modelled as Zero Order Hold (ZOH) blocks preceded by samplers. The continuous time open loop transfer function $G_{ol}(s)$ including time delay will therefore be given by,

$$G_p(s) = e^{-T_d s} G_{ol}(s) \tag{5.2}$$

Fig. 5.2 shows the sampling strategy for the proposed controller. The sample period is denoted by (n). The next sample is denoted by (n+1) and previous sample is denoted by (n-1). The inductor currents are sampled at the same rate as the switching frequency. Each inductor current is sampled when the PWM carrier reaches its trough. The processor then starts performing the controller calculations and updates the modulating voltage $V_{Mod}$ when the PWM carrier reaches its peak. In this case, the time delay equals half of the sampling period,

$$T_d = 0.5T_s \tag{5.3}$$

Where, $T_s$ is the sampling time. It should be noted here that equation (5.3) is realisable and has been tested experimentally. It has been reported in the literature as well (Deng et al., 2005, Abusara and Sharkh, 2011).

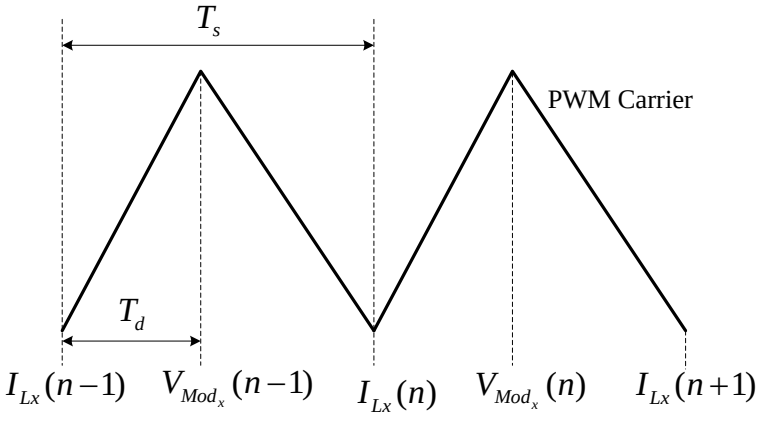


*Fig 5.2: Sampling strategy*

In the discrete domain, $G_P(z)$ can be obtained by performing the Z-transform of the $G_P(s)$ taking into account the zero order hold effect and can be computed using Matlab.

$$G_p(z) = z\left[\frac{1-e^{-T_s s}}{s} e^{-T_d s} G_{ol}(s)\right] \tag{5.4}$$

Now the analysis of the designed system is presented. Without any passive damping resistor, the close loop poles are on the stability boundary and system is unstable. This can be shown by the Bode diagram in Fig. 5.3. By having a passive damping resistor, the close loop poles could be brought inside the boundary but the system has not enough higher gains and could become unstable at high utility impedance. To handle this issue, a phase lag is introduced such that the conventional feedback controller $G_c(z)$ has good reference tracking, better disturbance rejection (due to higher gains) and higher stability margins compared to the earlier case. A suitable controller with phase lag is given by equation (5.5) and the Bode diagram is shown in Fig. 5.4 with different values of the utility impedance. The system always has good positive margins, which is the requirement for designing RC in next step. When the utility impedance $L_u$ =100μH, the system has a gain margin of 7.87dB and phase margin of $50.9^o$.

$$G_c(z) = K(z) = 10\frac{0.5z - 0.35}{z - 0.97} \tag{5.5}$$

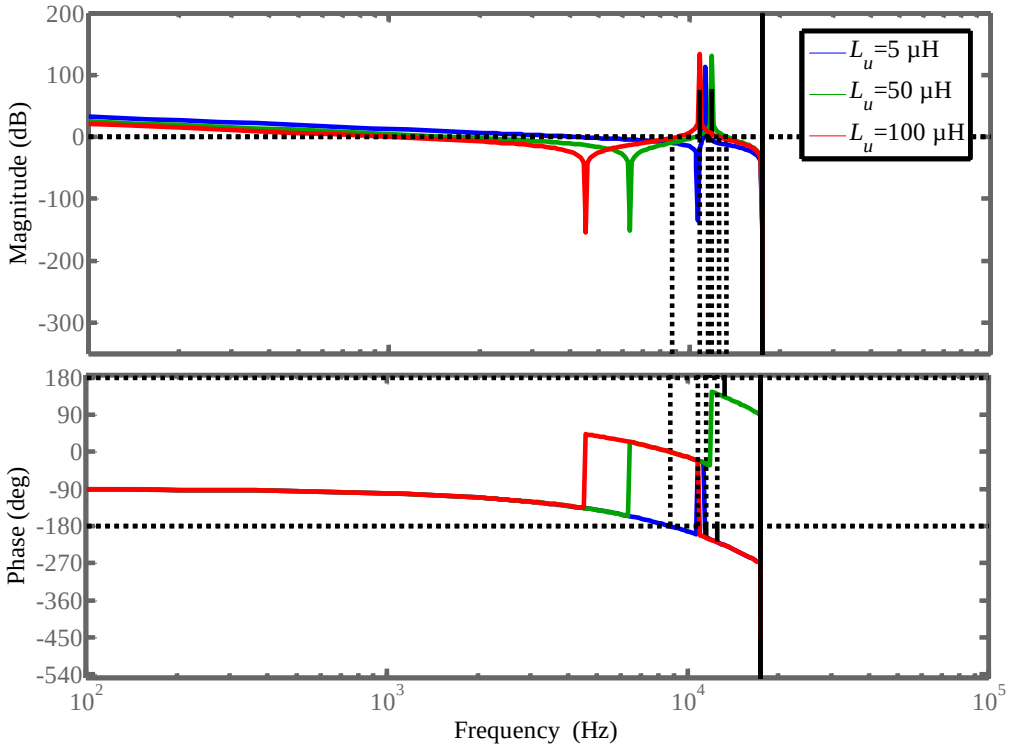


*Fig 5.3: Bode diagram of the system without passive damping*

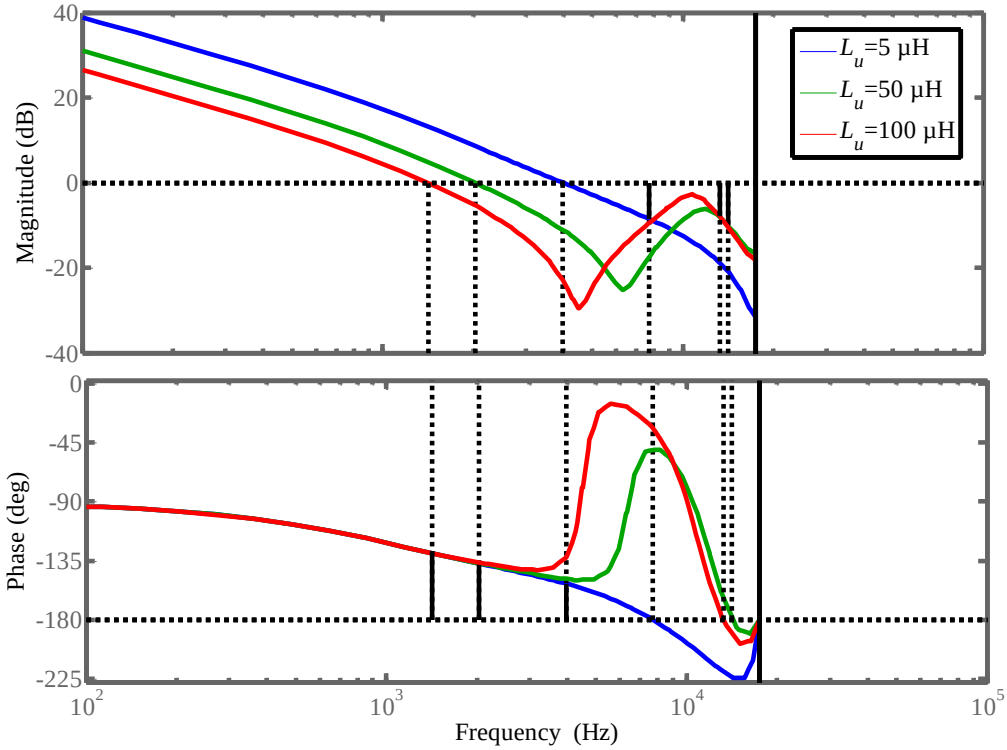


*Fig 5.4: Bode plot of the system with $G_c(z)$ and passive damping*

A limitation of further enhancement in the gain exists. To handle this, the RC is added to the above designed conventional feedback controller and is explained in the next section.

### 5.2.2 Design of the Repetitive Controller (RC):

After having stabilized the system with a conventional feedback controller, a loop of RC is added as shown in Fig. 5.1. The structure of the RC added to the conventional closed loop system is similar to the case of the two-level converter discussed in chapter 4. The most important parameters are: RC gain $K_R$ and low-pass filter $Q(z)$. The repetitive controller gain ($K_R$) is set to be $K_R = 0.1$, which provides enough fast convergence of error. The compensator $G_f(z)$ could be ignored as the system is stable enough and performs well without the compensator. It becomes important when the converter introduces phase lag. The design of the low-pass filter $Q(z)$ is explained. First of all a constant $Q(z) = 1$ is selected for simplification. A Bode diagram with $Q(z) = 1$ is shown in Fig. 5.5 at different values of utility impedance $L_u$.

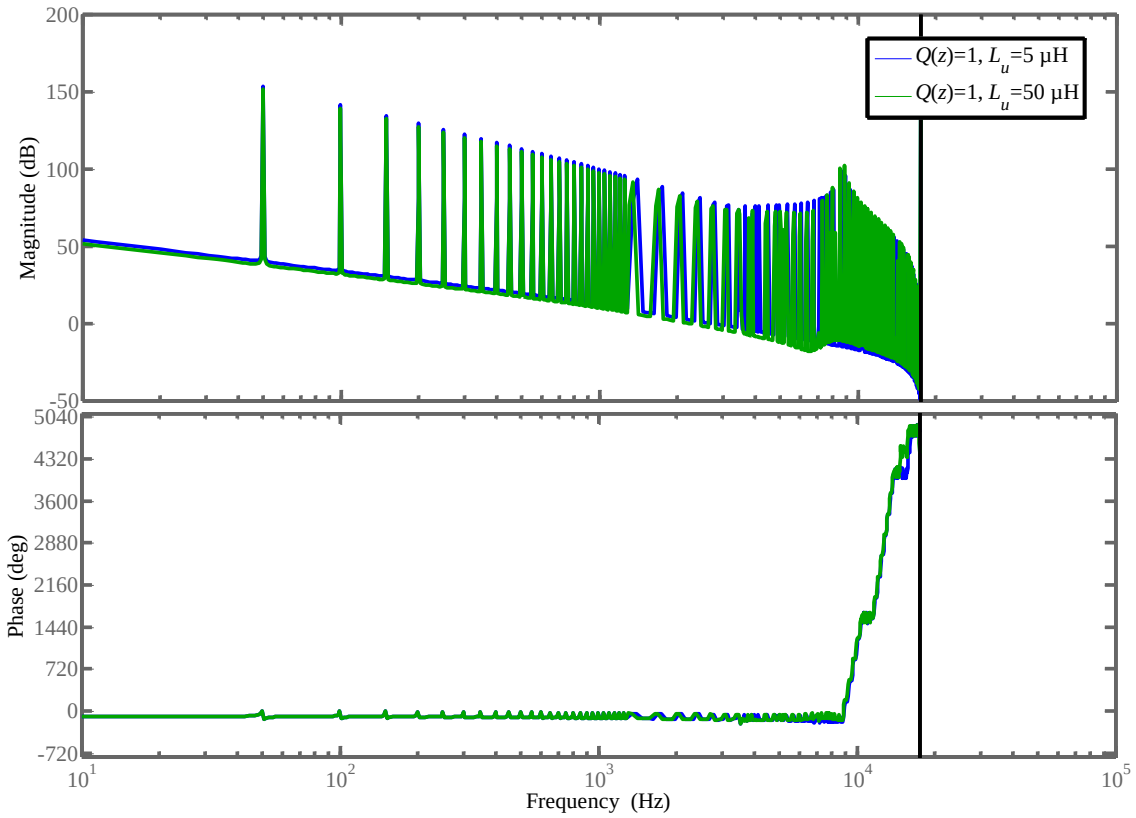


*Fig 5.5: Bode plot of the system with RC ( $Q(z) = 1$)*

At the next stage, a better filter is designed to reject the peaks of gain around the corner frequency which affect stability. From Fig.5.5, it can be seen that $Q(z)=1$ is not a suitable filter. It integrates the error, which affects the controller's stability. A better filter is required to get rid of the peaks at a higher frequency around critical frequency. There exist different types of low pass filters (see section 4.3.2). One of them is to select $Q(z)$ slightly less than unity, such as $0.95 \le Q(z) \le 0.97$. In this case, the magnitude of the gain at higher frequencies can be reduced at the cost of low gains at each harmonics. This results in high current THD. The system does not have higher stability margins and cannot be used in practise. The gain margin is 0.003dB and phase margin is $0.24^{o}$. A Bode diagram is shown in Fig. 5.6.

At the next stage, a simple second order filter is used after the RC block to reject the higher frequencies, by selecting a suitable cut-off frequency. For example $f_c$=900Hz seems suitable in this case. The Bode diagram is shown in Fig. 5.7. It can be observed that the magnitude of gains at higher harmonics around the critical frequency is zero but the phase is also affected which results in an unstable system.

So here, the idea of using a zero phase low-pass filter comes into action and has been discussed already in chapter 4 (section 4.3.2) in case of the two-level converter. Such filter is $Q(z)=0.25z+0.5+0.25z^{-1}$. This filter has better attenuation at higher frequencies and gives a stable system. The magnitude of gain is high enough at low order harmonics to reject them. A Bode diagram of this filter is shown in Fig. 5.8, whereas the Bode diagram of the system with RC including this filter is shown in Fig. 5.9. When the utility impedance $L_u$ is 5μH, the gain margin of the system is 10.4dB and phase margin is $10.6^{o}$. Whereas when utility impedance $L_u$ is 50μH, the gain margin of the system is 12.2dB and phase margin is $9.83^{o}$. The disturbance rejection capability of the system is discussed in the next section with simulation results.

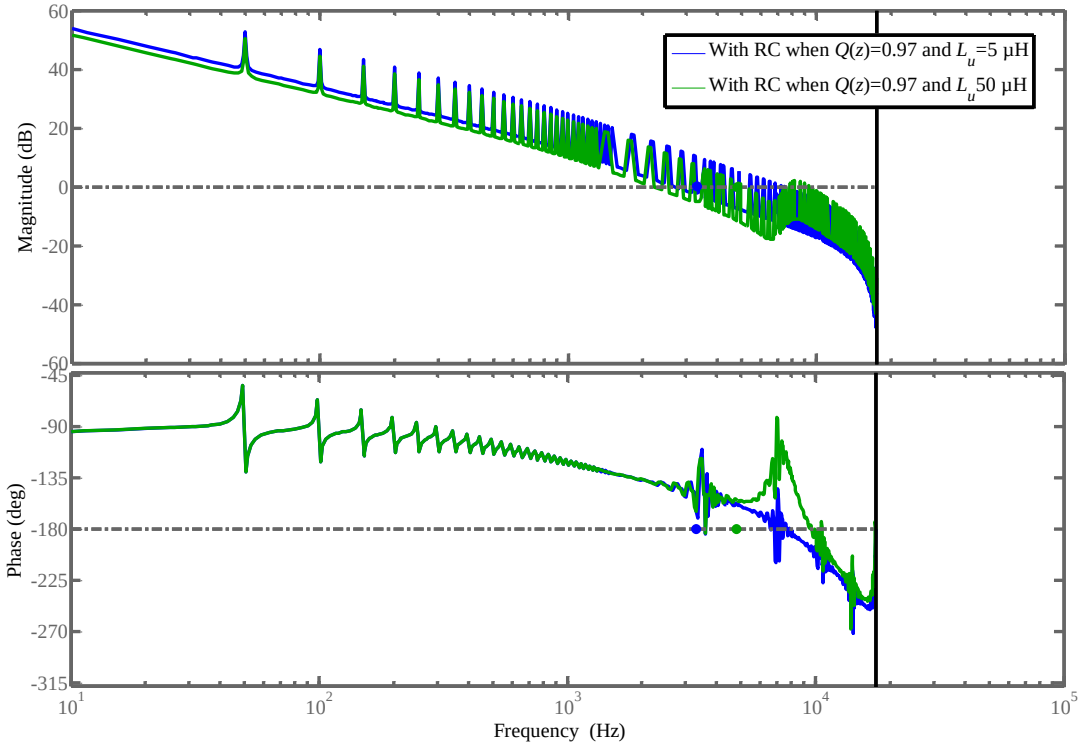


*Fig 5.6: Bode diagram of the system with RC when* $Q(z) = 0.97$

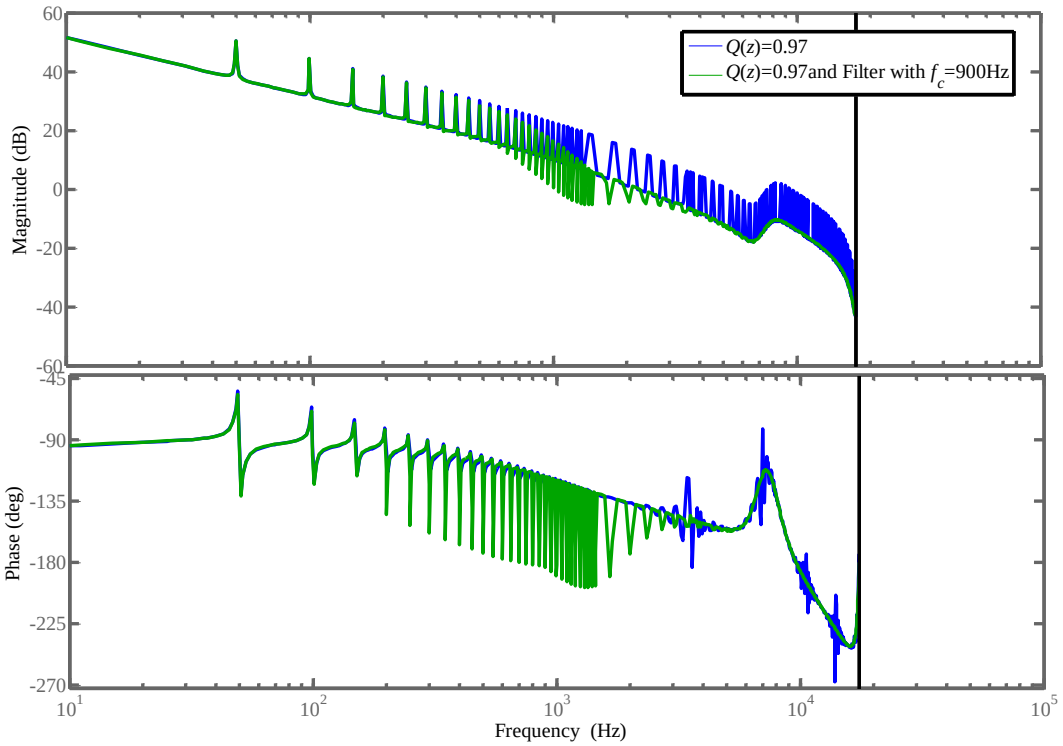


*Fig 5.7: Bode diagram of the system with RC (* $Q(z) = 0.97$ *) and second order filter*

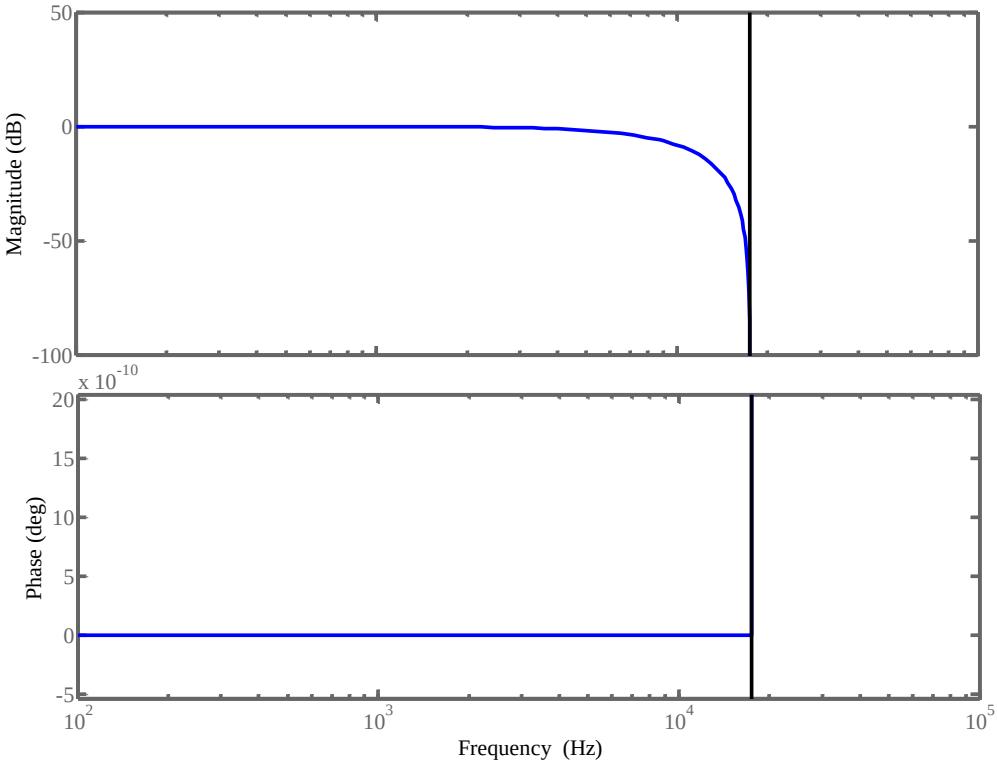


*Fig 5.8: Bode diagram of the filter* $Q(z) = 0.25z + 0.5 + 0.25z^{-1}$

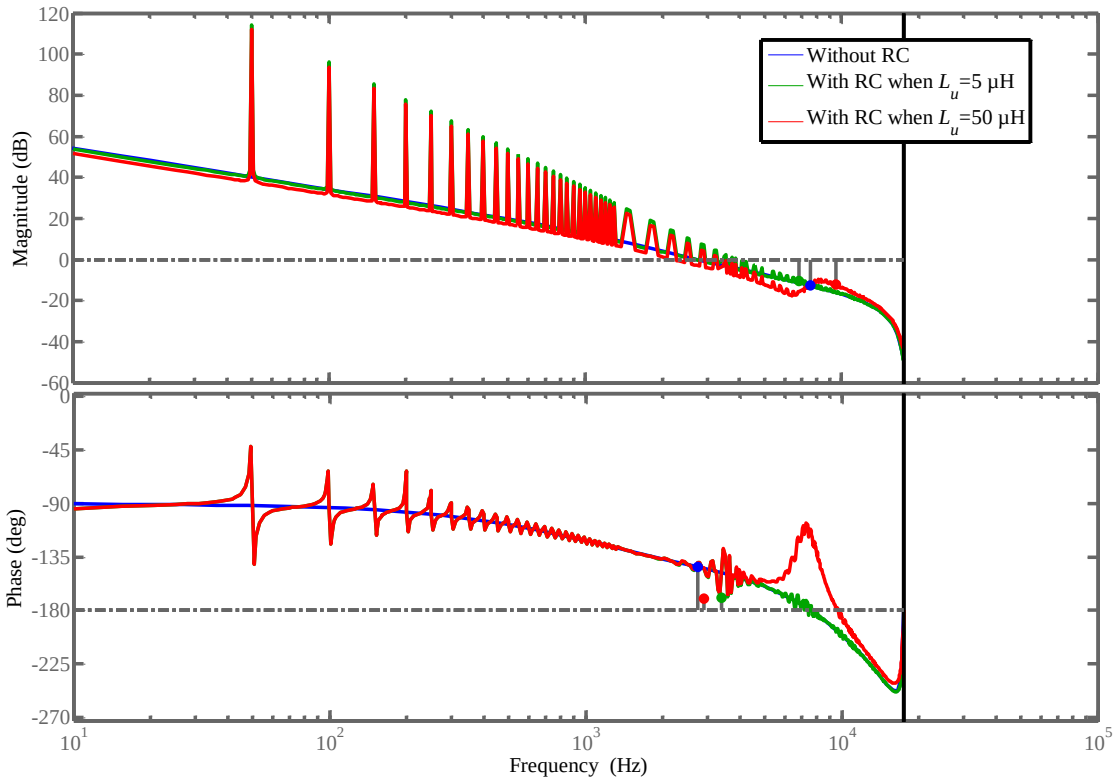


*Fig 5.9: Bode diagram of the system with and without RC- with* $Q(z) = 0.25z + 0.5 + 0.25z^{-1}$

## 5.3 Performance of the RC System

Simulation results and performance of the RC system in terms of disturbance rejection are presented in this section.

### 5.3.1 Simulation Results

Detailed simulation is carried out using the Matlab Simpower Systems Toolbox and the switching model. The performance of the controller is tested against different utility THD levels. To increase utility THD, different levels of harmonics have been added to the utility voltage. Basically, utility voltage is modelled to have only odd harmonics. It has been already discussed that utility THD level depends upon the complexity of the system (load type) and location of installation site. Here we consider practical values measured at the test site of the laboratory at Exeter University. The utility THD is to be 2.74%. The values of individual harmonics can be seen in Table 5.1.

The Matlab/Simulink model is simulated for two seconds to test the effectiveness of the controller in terms of quality of the output current. The system parameters are given in Table 1.4. It has been found that the RC is able to produce an output current without steady state error as shown in Fig. 5.9. The reference current is 10A (rms). Fig. 5.10 and Fig. 5.11 show the steady state output current with RC, and Fig. 5.12 shows the output current without RC. The error convergence with a complete PWM converter model is shown in Fig. 5.13.

Thus, summarising the RC is able to produce the output current as per National/International standards discussed in chapter 1. It provides better disturbance rejection and has higher bandwidth (about 4KHz) compared to the two-level converter. The controller is ready for practical implementation and will be discussed in next section.

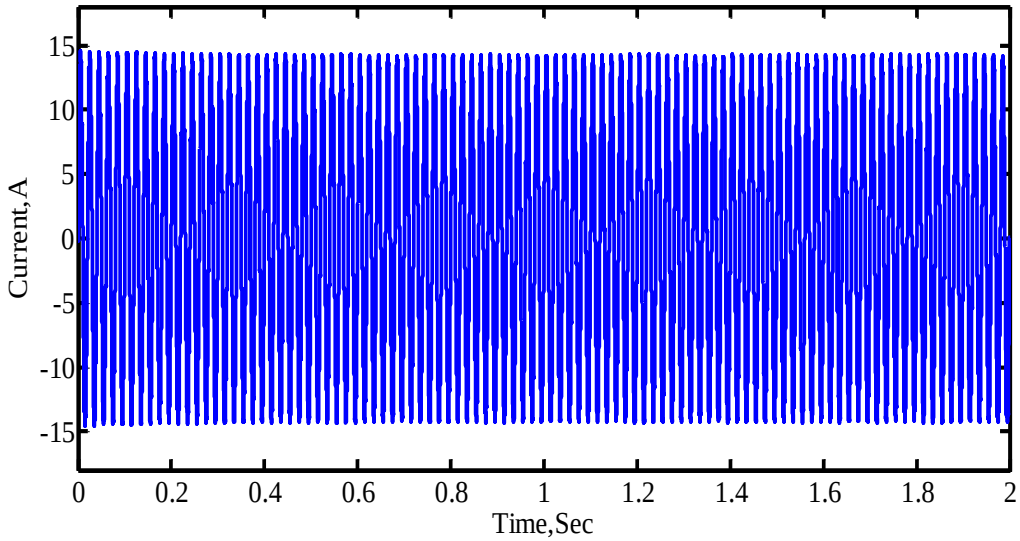


*Fig 5.10: Output current with RC for two seconds*

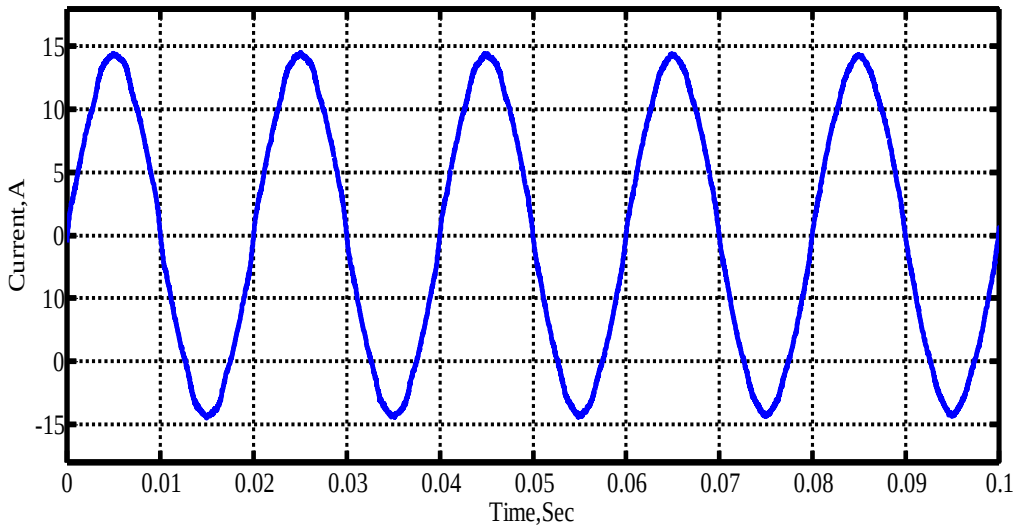


*Fig 5.11: Simulated output current with RC*

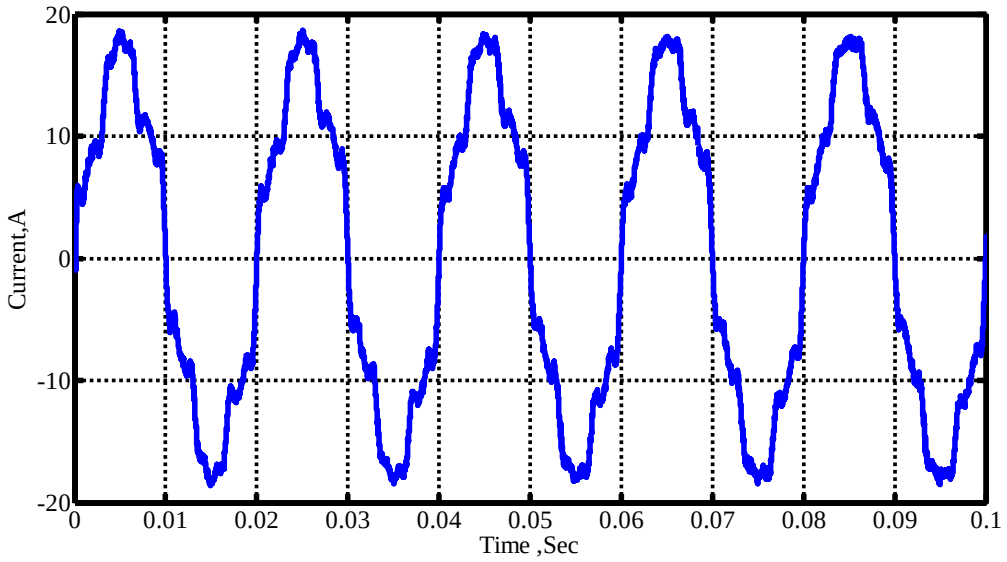


*Fig 5.12: Simulated output current without RC*

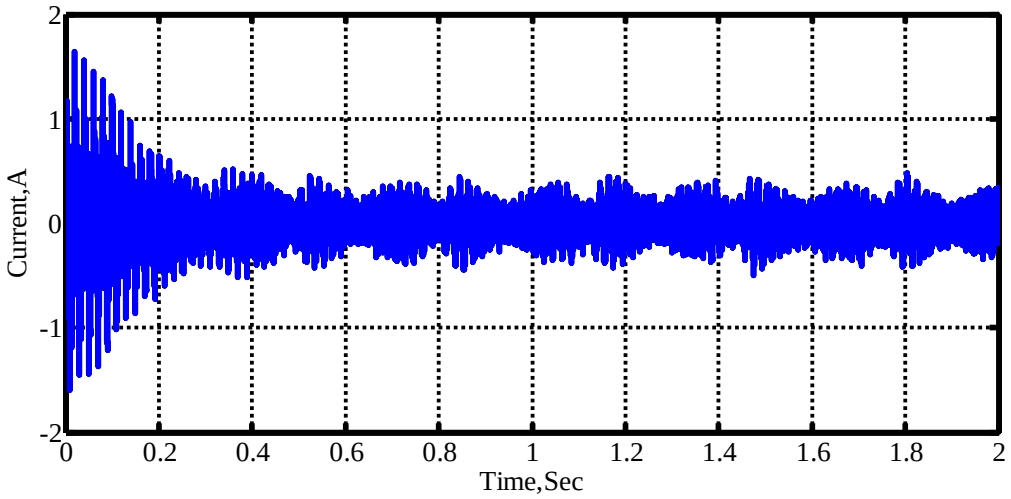


*Fig 5.13: Convergence of error with the PWM converter model*

## 5.3.2 Harmonic Rejection Capability

One of the basic requirements from RC is that it could offer higher gains at fundamental frequency and its harmonics. This gives a reduced output current THD, compared to the conventional feedback controller discussed earlier. In this section, the harmonic rejection capability of individual harmonics is confirmed. For this purpose, the disturbance transfer function of the system derived in chapter 3 (section 3.5) is given by the following equation,

$$G_D(s) = \frac{I_L}{V_u(s)} = \frac{G_p(s)}{1+(1+G_{RC}(s))G_c(s)G_P(s)} \tag{5.6}$$

Where, $G_p(s), G_{RC}(s)$ are transfer functions of the plant and RC and $V_u(s)$ is the disturbance . The disturbance is related to utility harmonics.

By running the actual PWM model for two seconds, the output current THD is 1.91% while the utility THD is 2.74%. The measured values of utility voltage have been used and modelled for simulation. The controller is tested against other high utility THD values and its performance is good in terms of disturbance rejection. Moreover, the magnitude of individual (third, fifth and seventh) harmonics is very low and nearly fully rejected. This could be seen by the frequency response of the disturbance transfer function as shown in Fig. 5.14. Table 5.1 summarises all results obtained with a linear and complete model. This demonstrates how much individual harmonic is attenuated with and without RC, where the RC proves to be effective in terms of disturbance rejection. It should be noted here that a reference current of 10A (rms) is used in the case of the interleaved converter. The reason for having this value as a reference current is due to experimental implementation of this value later on. At low value of a reference current, the difference in THD can be seen clearly with and without RC. It is also obvious that overall output current THD would be less when the reference current is high and vice versa.

| **Harmonic number** (n) | **Utility voltage** V(rms) | **Output current with switching model, A(rms)** | | **Output current with linear model, A (rms)** | |
|---|---|---|---|---|---|
| | | **Without RC** | **With RC** | **Without RC** | **With RC** |
| 3rd | 2.4 | 0.52 | 0.01 | 0.46 | 0.001 |
| 5th | 4.22 | 1.22 | 0.06 | 1.11 | 0.007 |
| 7th | 1.95 | 0.68 | 0.01 | 0.42 | 0.006 |
| 9th | 2.37 | 0.26 | 0.03 | 0.11 | 0.01 |
| 11th | 1.46 | 0.36 | 0.04 | 0.31 | 0.01 |
| 13th | 1.95 | 0.23 | 0.08 | 0.18 | 0.018 |
| 15th | 0.455 | 0.08 | 0.04 | 0.05 | 0.006 |
| 17th | 0.65 | 0.11 | 0.11 | 0.08 | 0.01 |
| 19th | 0.585 | 0.08 | 0.10 | 0.05 | 0.012 |
| **THD (%)** | **2.74** | **15.46** | **1.91** | **13.3** | **0.30** |

*Table 5.1: Harmonic rejection with and without RC for a linear and complete PWM model of the interleaved converter*

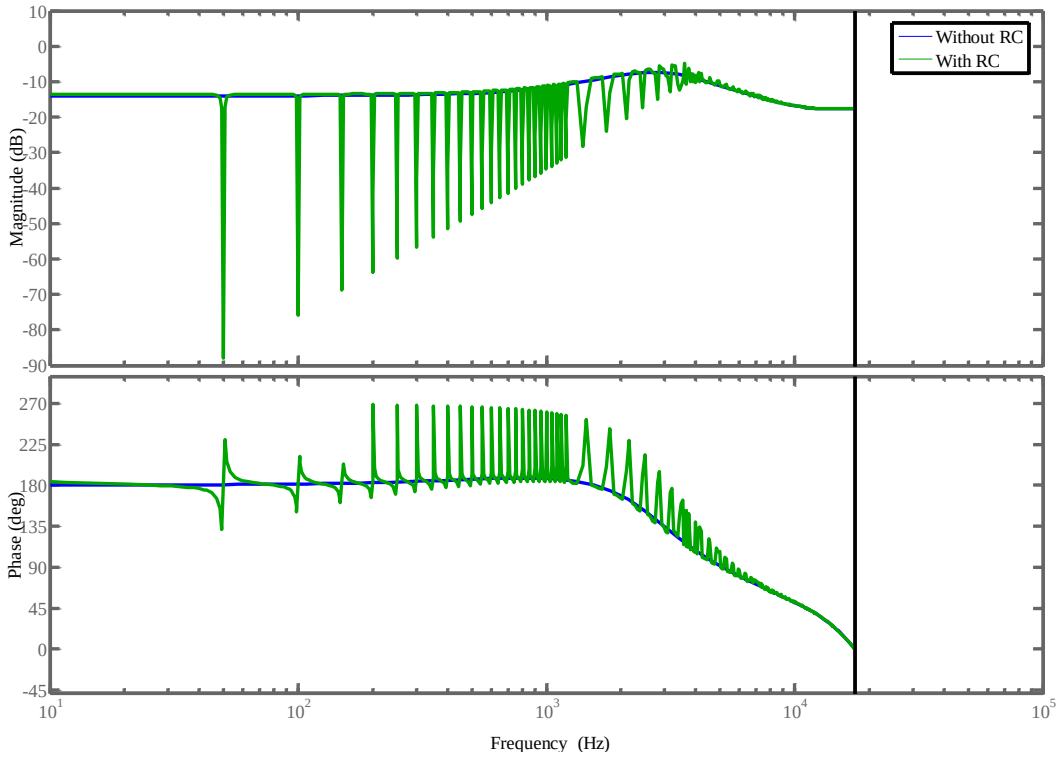


*Fig. 5.14: Frequency response of the disturbance transfer function $G_D(s)$ with and without RC*

## 5.4 Experimental Implementation

The procedure of experimental implementation of the RC based current controller for the interleaved utility connected converter is briefly explained in this section. Fig. 1.3 represents the block diagram of the control system for one channel of one phase. Implementation of the proposed controller is done using the Texas Instrument TMS320LF2808 digital signal processor (DSP), which is a fixed-point 32-bit digital signal processor with 16 analog-to-digital (ADC) channels that can be used for current and voltage sensing. This processor comes with code composer software that comprises a C-complier, an assembler and a debugger. One DSP controller per phase has been used and the low speed communications between the controllers such as start/stop and total current commands has been implemented using the Controller Area Network (CAN) protocol. Synchronization with the utility has been implemented in such a way that each phase controller measures the corresponding utility phase voltage to detect the zero crossing.

It should be noted here that the overall system has six current sensors for measuring the current in each channel in a single-phase and one voltage sensor to measure the voltage at the point of common coupling. Therefore, there are a total of seven control signals in a single-phase in addition to the twelve switching signals. This can be seen in the basic hardware configuration as shown in Fig. 5.15.

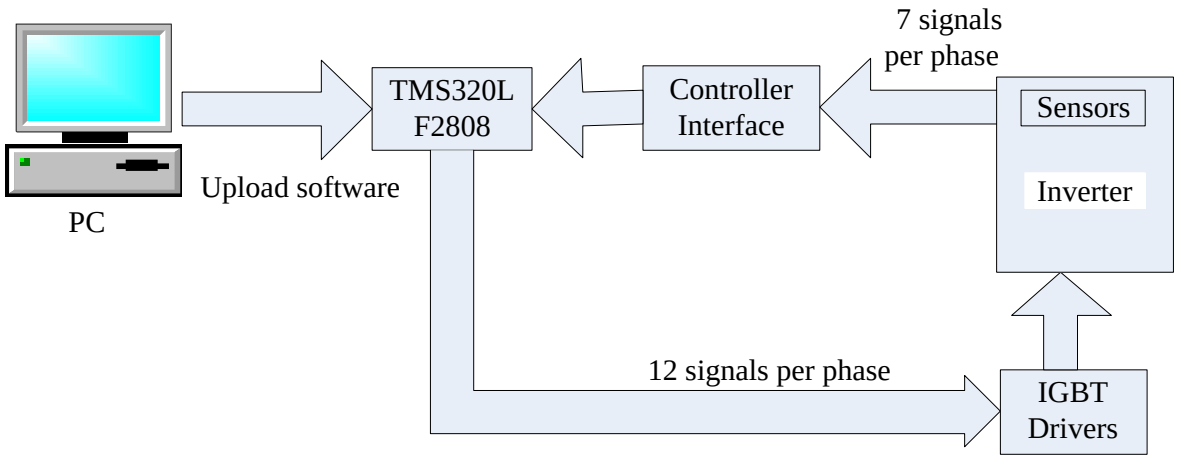


*Fig 5.15: Basic hardware configuration for single-phase*

The most important feature of using the Texas Instrument TMS320LF2808 DSP is to have an enhanced pulse width modulator (ePWM) peripheral, which is a key element in controlling many of the power electronic systems found in both commercial and industrial equipments. The ePWM peripheral performs a digital to analog (DAC) function. Sometimes it is also referred as Power DAC. One can achieve 0% to 100% duty cycles with an ePWM module with minimum processor overhead (Nene, 2006). It consists of six submodules such as time-base, counter-compare, action-qualifier, dead-band generator, PWM chopper, trip-zone and event-trigger. Each submodule contains registers, which can be initialised to configure an ePWM module (Nene, 2006). Further detail of the registers attached with each submodule and ePWM module can be found in the reference guide provide by Texas instrument (Texas Instrument, [online]).

For an interleaved converter, the synchronisation of all PWM signals is necessary and the ePWM peripheral provides effective synchronisation among all PWM signals using

multiple counters (counter-compare submodule). In our case, six interleaved PWM outputs are generated using this processor. The internal counter of the first PWM carrier is set to give the required switching frequency. The second PWM counter is synchronised with the first counter and delayed by $T_s / 6$. The third PWM counter is synchronised with the second counter and delayed by $T_s / 6$ and so on. This generates six interleaved PWM carriers. The DC voltage regulator/controller has not been used in the outer loop to set the amplitude of the reference current. Instead, the current demand is generated by setting a CAN register and the input DC (750 Vdc) is regulated by an external boost circuit. However, using a DC voltage regulator/controller would be the subject of future work.

### 5.4.1 Hardware Description

The schematic diagram of the power circuit of the experimental apparatus is shown in Figure 5.16. The main components include isolation transformer, contractors (C1, C2 and C3), current limiting resistors, miniature circuit breaker (MCB) and a boost card with the interleaved converter (test rig). These components are used for protection of the test rig. The fuses can also be used in conjunction with these protection devices for added protection. The circuit protection scheme is designed for a maximum current of $24A_{rms}$ as the utility three-phase outlet available in the laboratory is rated at this current. The protection devices are normally selected in such a way that the rated current of the protection devices is less than or equal to the maximum circuit current.

A DC supply is obtained by rectifying the utility three-phase AC supply. An isolation transformer is placed to provide galvanic isolation between the utility and the rectified DC supply. It is normally required for the balanced supply (grounding of the system) and safety reasons as well. The leakage inductances of the transformer windings can be beneficial for suppressing the PWM current ripples. However, these leakage inductances can be ignored, as they are small in nature. Instead, additional filter inductances are considered, which are sufficient for small current ripples due to the interleaved topology. The rating of the isolating transformer (1:1) is 25KVA and windings are in wye-delta configuration. The rectified DC voltage is then stepped up to the required DC link voltage of 750V using a boost circuit. The boost circuit also makes sure that this DC link voltage is in the permitted range.

The contactors are installed for connection and isolation of the apparatus to and from the utility. The start-up procedure can be explained as follows. At start-up, all the contactors should be in the open position. As the utility three-phase supply is connected by plugging the three-phase socket to the outlet, the isolating transformer is energised and the DC link capacitors are charged up through the current limiting resistors. The rectifier circuit requires slow pre-charging of the DC link capacitors. For this purpose, contactor C1 is first turned on.

The function of the current limiting resistors is to limit the initial inrush current of the isolating transformer and the charging current of the capacitor to ensure that nuisance tripping of the utility circuit breaker does not occur. In other words, the current limiting resistors are there for soft charging of the DC link capacitors. These resistors can be named as pre-charge resistors and are normally used with contactors for two specific purposes. Firstly, to help protect the equipment and the laboratory from the risk of fire which may be started by a low fault current passing to earth from any one of the phases which may not be detected by the circuit breakers or the fuses. Secondly, their function is to reduce the risk of fatal electric shock to personnel by reducing the length of time that a person is exposed to a current flow through the body (Hussain, 2000). It is worth noting that these resistors do not detect overcurrents or short circuits. Normally they are used in conjunction with the MCB. These resistors are rated at 415Vrms with $30mA_{rms}$ sensitivity. When the isolating transformer is energised and the DC link capacitors are charged up after a few seconds, the contactor C2 automatically turns on. The contactor C2 has a timer for automatic operation.

The MCB provide protection of the circuit against overloads and short circuits. They are rated at $32A_{rms}$ and $415V_{rms}$. Their tripping characteristics provide protection against a continuous overload current of 50A-63A but short circuit current of 400A to avoid any nuisance tripping which may be caused by initial energising of the transformer or charging of capacitors.

The interleaved converter present in the Exeter University laboratory consists of the boost converter controller, the three-phase current controller cards and the Digital Signal

Processor (DSP) system. The DSP chip is built on every card. The schematic diagram of the power electronics control system is shown in Fig. 5.16. The boost card includes a safety interlock circuit for protection against fault conditions caused by a DC link undervoltage or overvoltage. The safety interlock circuit processes the measured DC voltage and inhibits the operation of the boost converter and the three-phase converter if the DC link voltage is outside a permitted range of 16V- 850V.

The Regowski coil has been used for obtaining output current waveforms. These waveforms can be stored using the digital oscilloscope. The Fast Fourier Transform (FFT) analysis can also be done using this scope. The detailed description of the lab setup and components attached with experimental test rig of the three-phase interleaved converter are shown in Fig. 5.17.

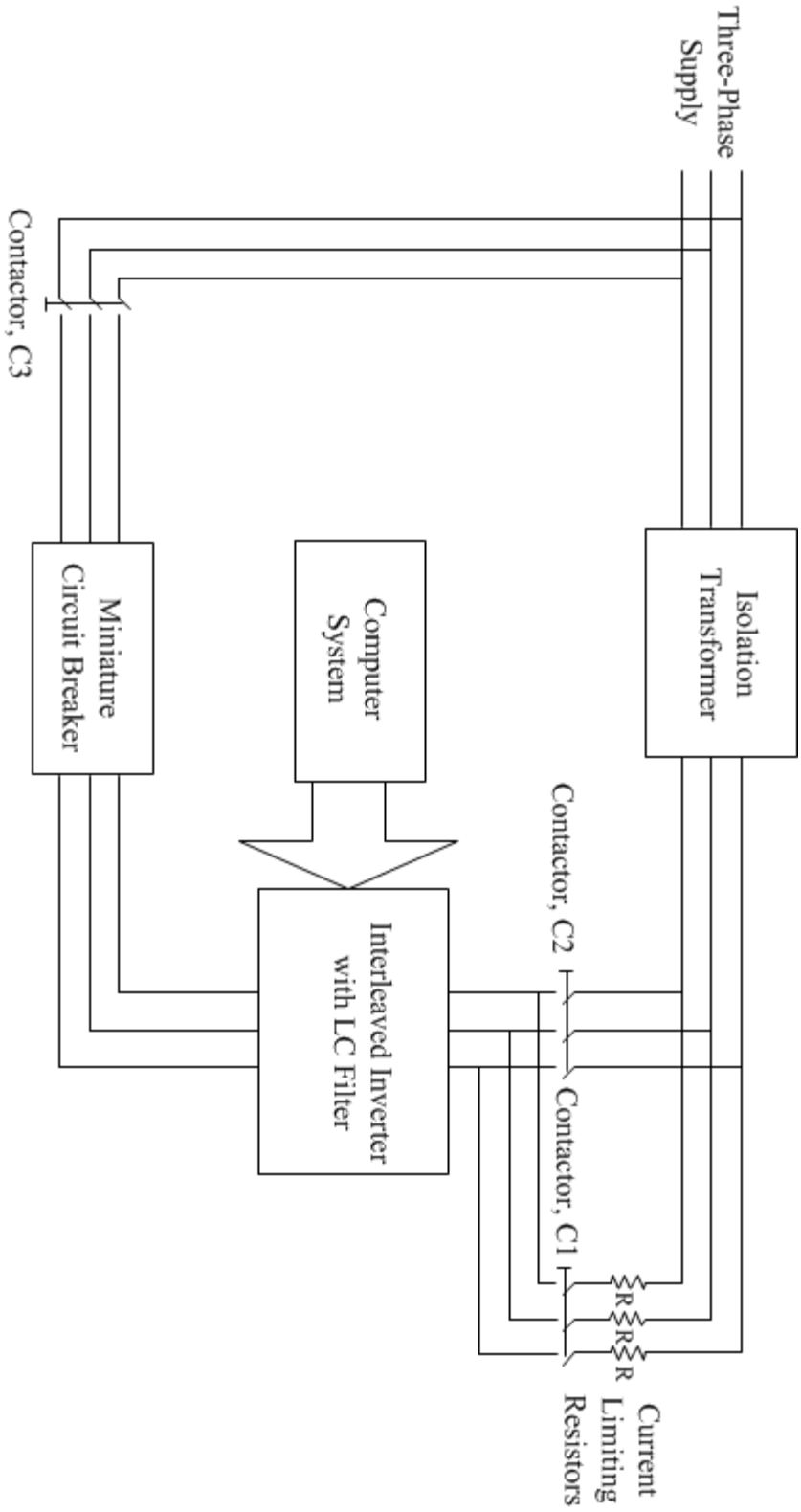


*Fig 5.16: Schematic diagram of the power circuit of the experimental apparatus*

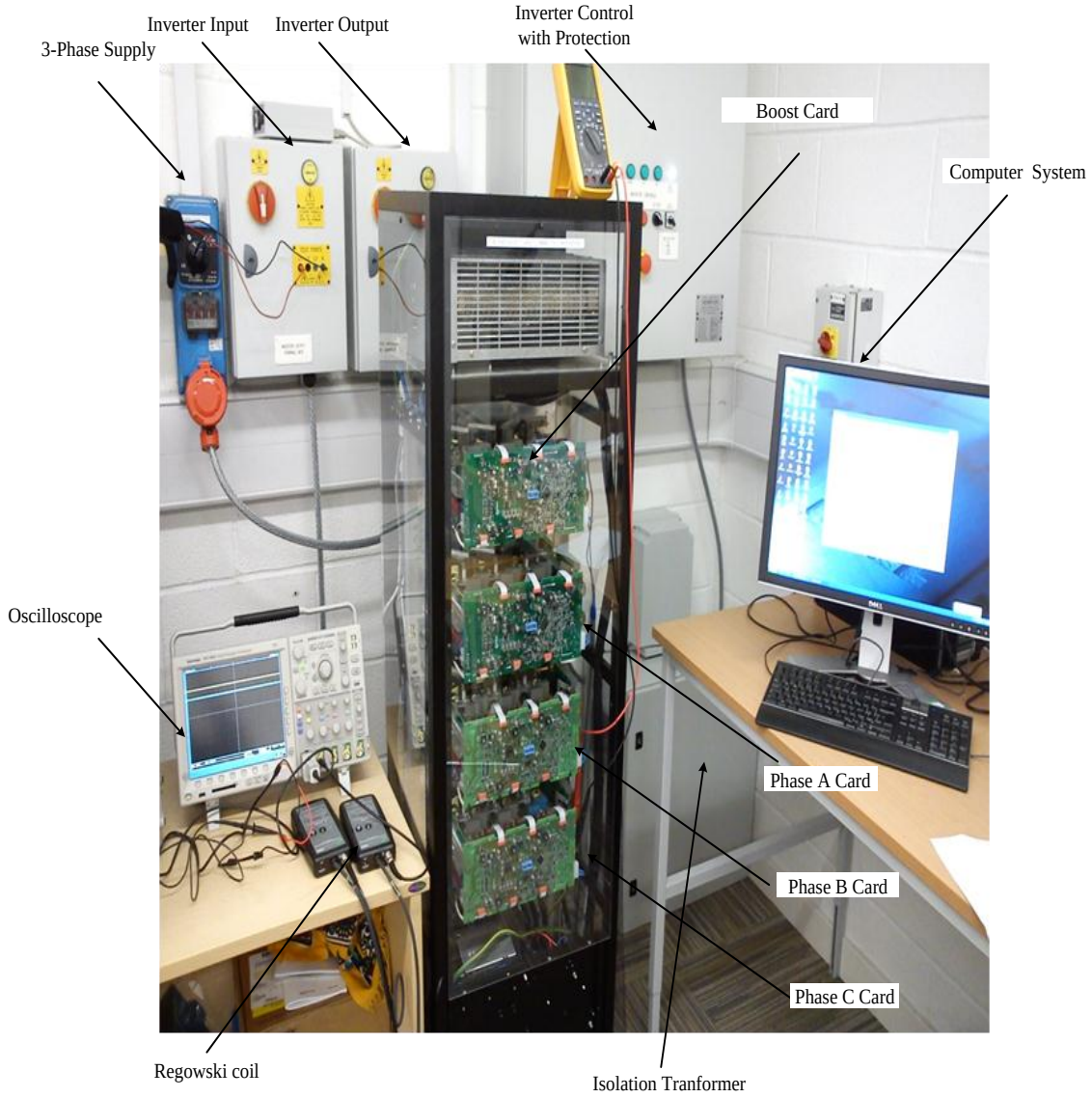


*Fig 5.17: Description of the lab setup and components attached with experimental test rig of the three-phase interleaved converter*

## 5.4.2 Development of the RC Algorithm

After setting up the hardware, developing the algorithm for the RC is then required. The following steps are involved for practical implementation:

1. First of all, a difference equation is obtained from the transfer function of the repetitive controller using Fig. 5.18. This is normally done for every digital implementation case.

2. For the second step, direct form I as shown in Fig. 5.19 and Fig. 5.20 (Newman and Holmes, 2003) is considered. This is achieved using direct implementation of the difference equation of step 1.

3. Finally direct form II as shown in Fig. 5.21and Fig. 5.22 (Newman and Holmes, 2003) is considered due to involvement of less memory compared to direct form I. This will be explained shortly and will make the basis for development of the final algorithm.

Considering the structure of the RC developed in chapter 2, Fig. 5.18 can be drawn. The difference between the reference current and the output current is error $E(z)$, which is input to the RC. The control signal produced by the RC is $U_{RC}(z)$. For the purpose of explanation, if RC gain $K_R$ and compensator $G_f(z)$ are considered to be 1 as shown in Fig. 5.18, then the transfer function of the output control signal $U_{RC}(z)$ produced by the RC with respect to error $E(z)$ can be given by equation (5.7),

$$\frac{U_{RC}(z)}{E(z)} = \frac{0.25z^{-701} + 0.5z^{-700`} + 0.25z^{-699}}{1 - 0.25z^{-701} + 0.5z^{-700`} + 0.25z^{-699}} \tag{5.7}$$

Using the above transfer function, the difference equation can be written as,

$$\begin{aligned} U_{RC}(k) = {} & 0.25U(k-701) + 0.5U_{RC}(k-700) + 0.25U_{RC}(k-699) + 0.25E(k-701) \\ & + 0.5E(k-700) + 0.25E(k-699) \end{aligned} \tag{5.8}$$

The above equation needs to be implemented and programmed for the proposed RC in this section.

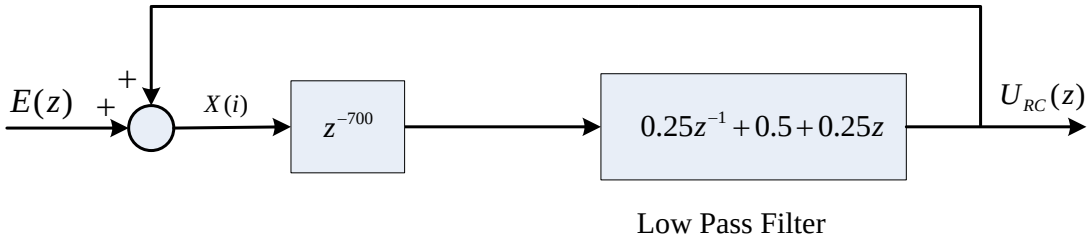


*Fig 5.18: Elements of the RC when* $K_R = 1$ and $G_f(z) = 1$

The implementation of the RC could be realised using a digital filter implementation. The structure of the RC contains zero phase low-pass filter. The selection of a suitable form in terms of the number of operation or storage elements for implementation is normally required. The numerical stability and fewer round-off errors are desirable. The direct form I and direct form II are commonly used for implementation of the difference equation. The direct form I is a straightforward approach and the difference equation is directly evaluated. This is suitable for small filters/systems but may be inefficient and impractical for complex designs. The reason for unsuitability is that it requires 2N delay elements for a system of order N. In other words it involves double memory. Fig. 5.19 shows the implementation of RC in direct form I. The alternative structure of direct form I can be represented by Fig. 5.20. It can be observed that delay elements are used separately for both control signal and error coefficients. On the other hand, direct form II only needs half the memory compared to direct form I. The structure of direct form II is obtained by reversing the order of numerator and denominator as shown in Fig. 5.21. The alternative structure is shown in Fig. 5.22.

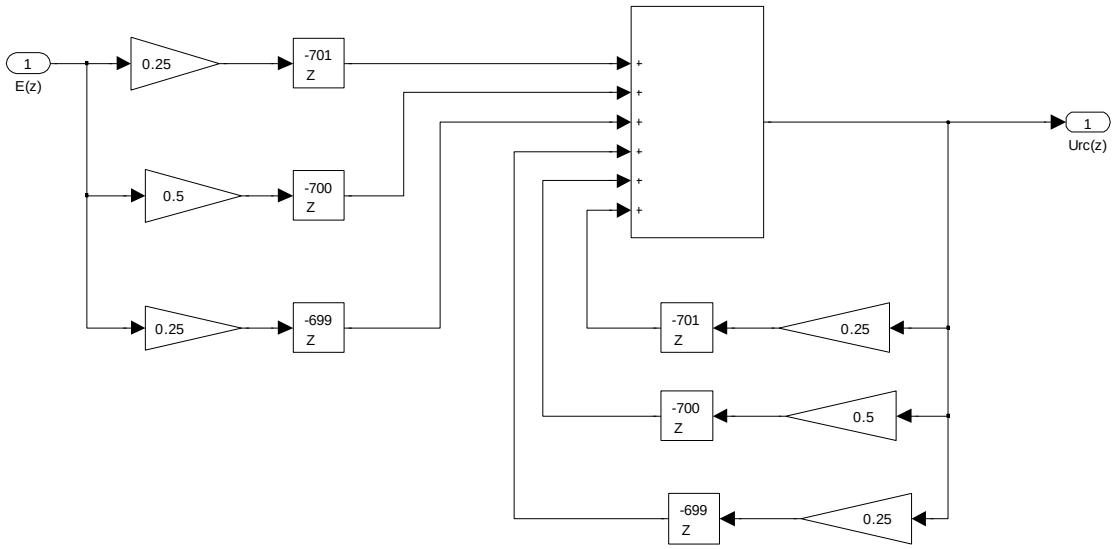


*Fig 5.19: Implementation of the RC in direct form I*

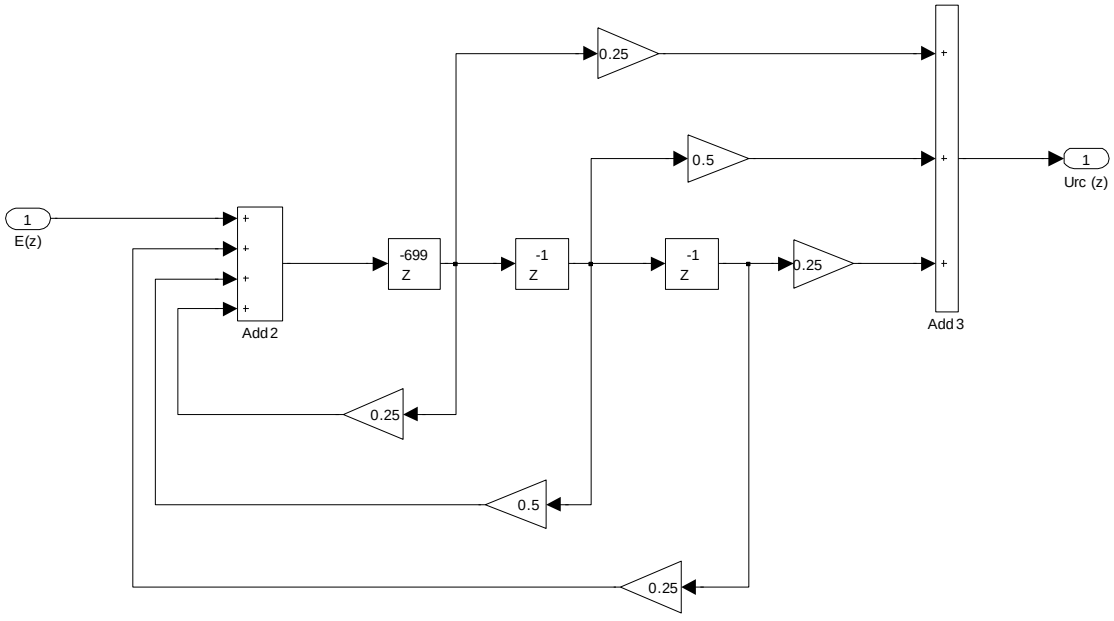


*Fig 5.20: Alternative structure of the RC in direct form I*

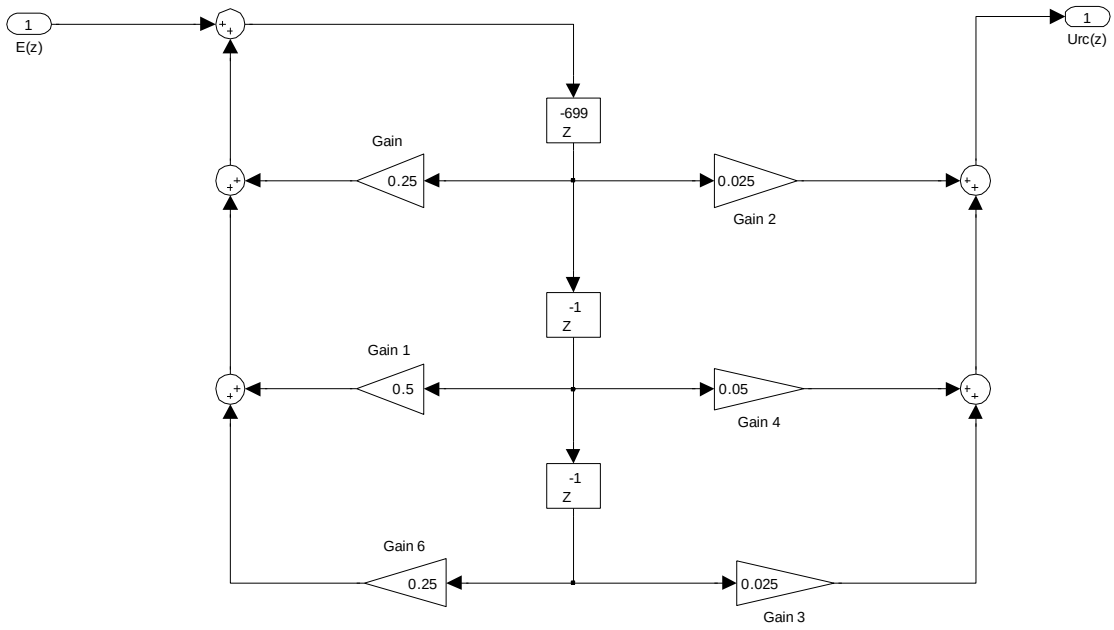


*Fig 5.21: Implementation of the RC in direct form II*

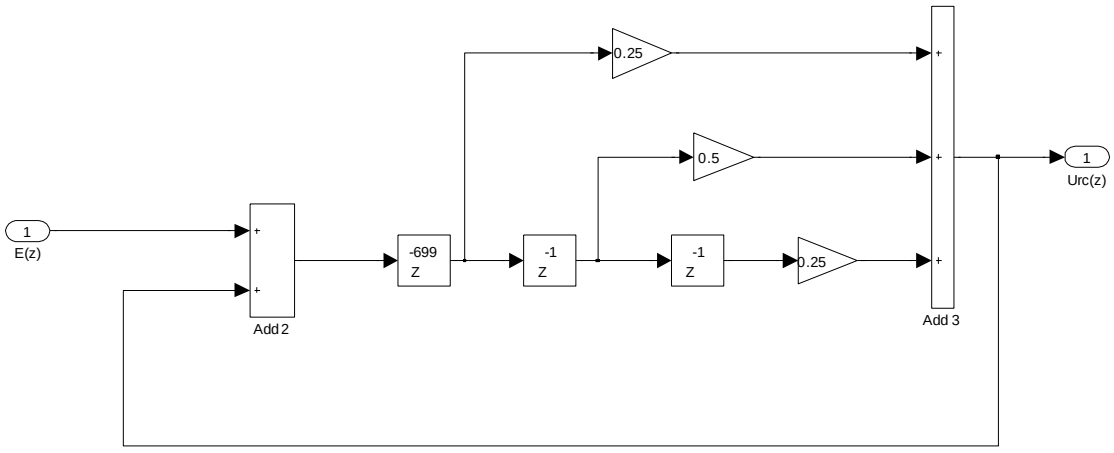


*Fig 5.22: Alternative structure of the RC in direct form II*

However, the possibility of arithmetic overflows can arise for noisy systems. In our case, it is quite effective and provides good results. The algorithm of RC can be developed by considering Fig. 5.18. Basically, an array of 700 elements needs to be assigned which represents the state variables. Instead of having separate arrays for the error and control signal, one array of state variable could be used for both error and control signal i.e.

$X(i) = U_{RC}(z) + E(z)$. Following is the advantage of the direct form II scheme. The flow chart of algorithm for developing the RC is shown in Fig. 5.23.

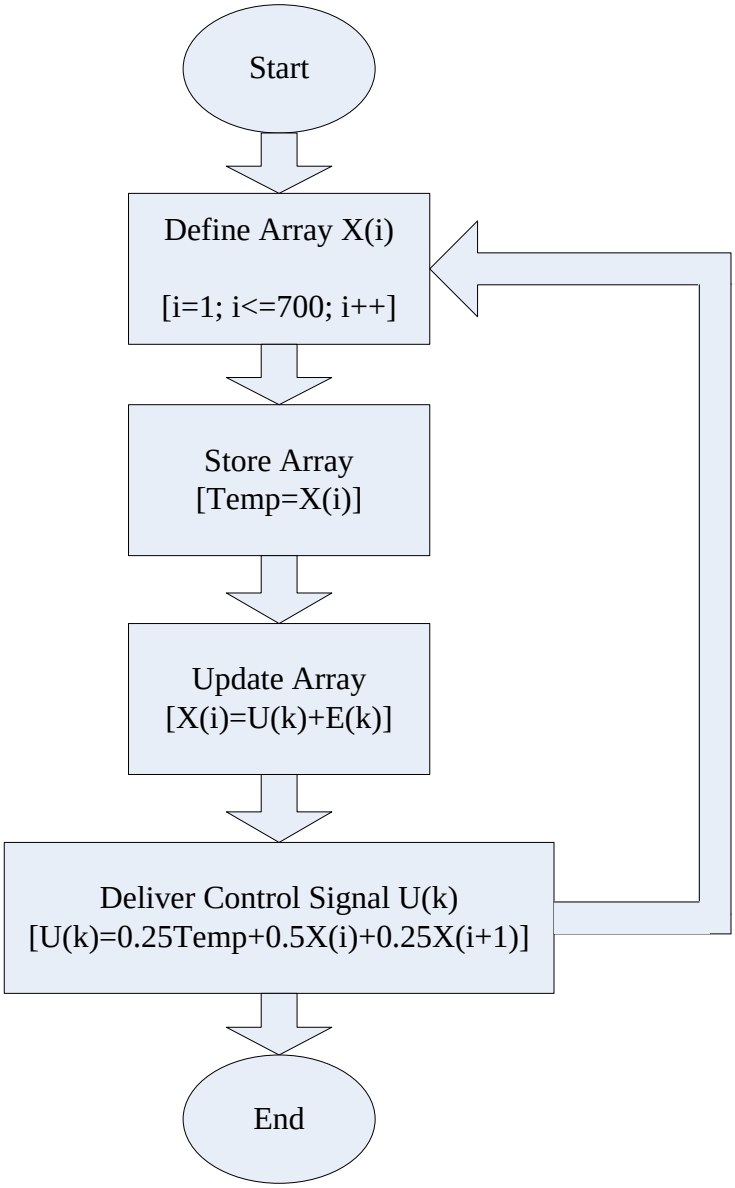


*Fig 5.23: Flowchart of the algorithm for implementation of the RC*

## 5.4.3 Experimental Results

The digital repetitive current controller was tested in a University of Exeter laboratory under the supervision of Dr. Abusara. The experimental waveform of the output current of phase 1 and phase 2 (without RC) for a demand current of 10A (rms) is shown in Fig. 5.24.

Whereas Fig. 5.25 shows the output current when the RC is implemented for phase 1. The current waveforms have been obtained using a high bandwidth Regowski coil, and saved using a digital oscilloscope. The spectrum of the utility voltage is shown in Fig. 5.26 and the spectrum of output current without RC is shown in Fig. 5.26. The dominant harmonics of the utility voltages are measured and included in the Simulink model to compare the simulation results with the experimental ones. The output current THD (without RC) is 16.74% in Fig. 5.24. The experimental spectrum of the output current with RC is shown in Fig. 5.28 and the current THD is 2.05%. This shows the effectiveness of the RC technique as the THD has improved greatly. Now the output current waveforms of one phase and its spectrum, with and without RC, are shown in Fig. 5.29 and Fig. 5.30 respectively. Table 5.2 shows the experimental attenuation of individual harmonics.

Now the simulation and experimental results can be compared. The simulated output current THD in Fig. 5.11 is 1.91% whereas the output current THD in the case of the experiment is 2.05%. The attenuation of individual harmonics can be compared by looking at Table 5.1. and 5.2. There are some differences between the simulation and experimental results especially in the case of attenuation of individual harmonics. The reason for the difference is due to the accuracy of the Regowski coil, which has been used for current measurement. Its accuracy is ±0.25% of a rated current of 200A. This becomes significant when measuring low magnitude harmonics. Moreover it is also interesting to mention that a steady state error exists when the RC is not used which is obvious. By having the RC and comparing the simulation and experimental results, there is almost zero steady state error in the output current.

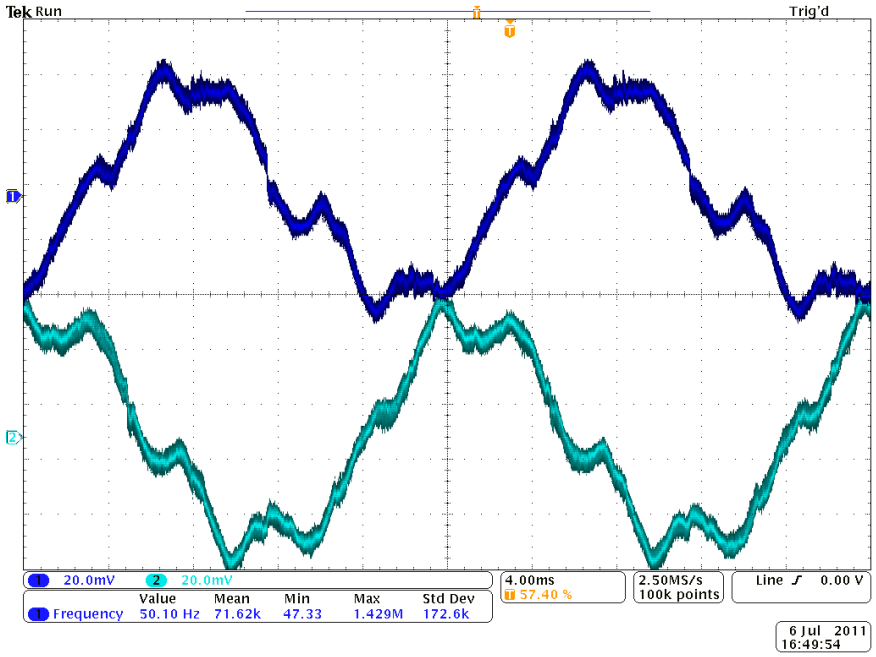


*Fig 5.24: Currents of phase 1 and 2, no repetitive feedback is implemented*

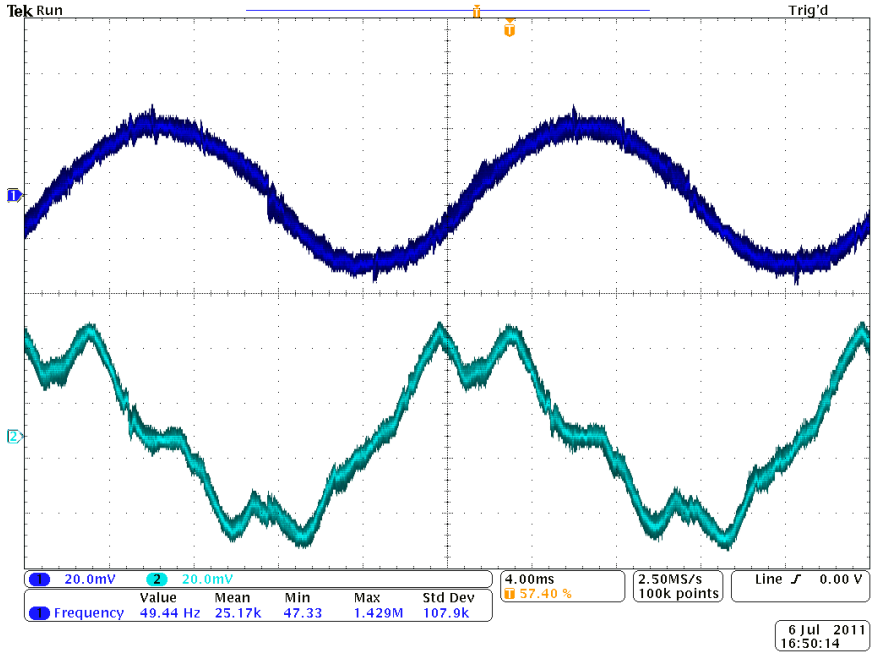


*Fig 5.25: Currents of phase 1 and 2, repetitive feedback is implemented for phase 1*

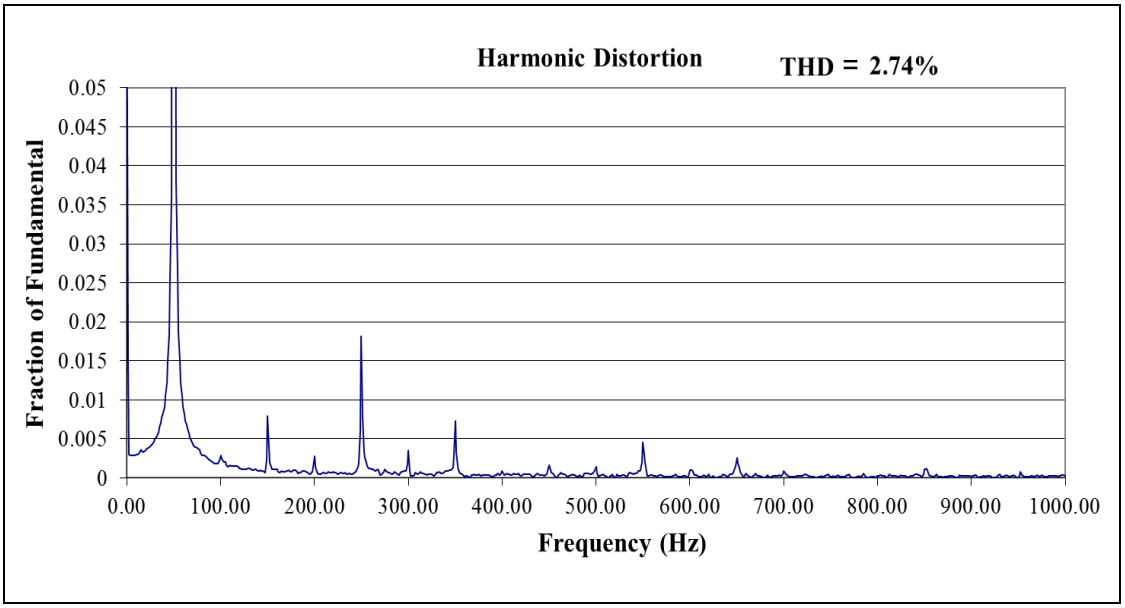


*Fig 5.26: Experimental spectrum of the utility voltage*

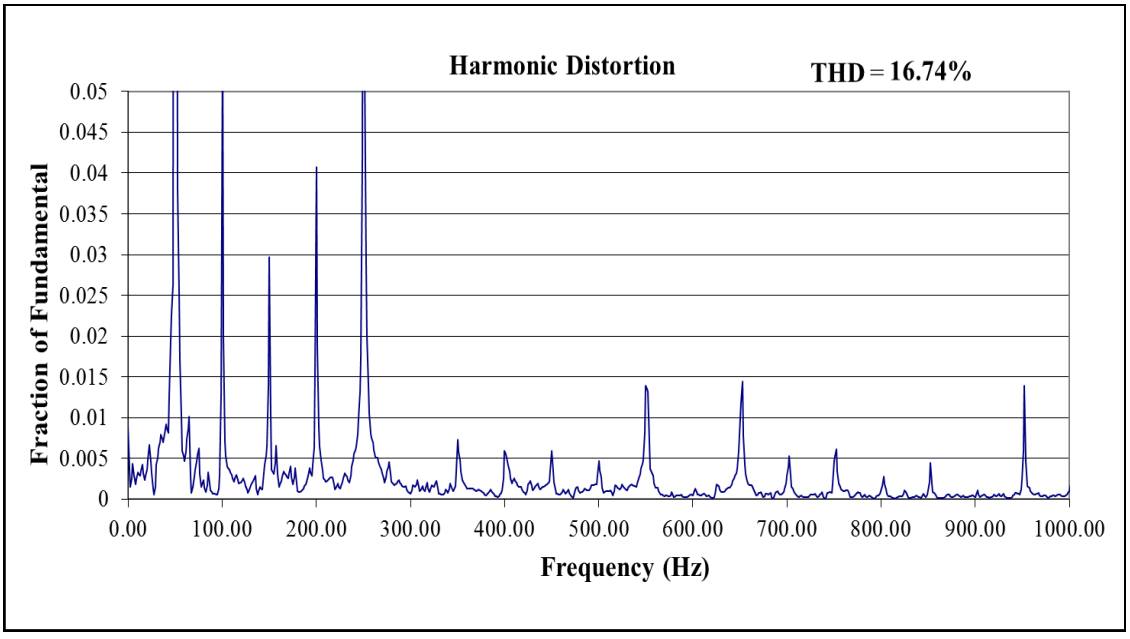


*Fig 5.27: Experimental spectrum of the output current without RC*

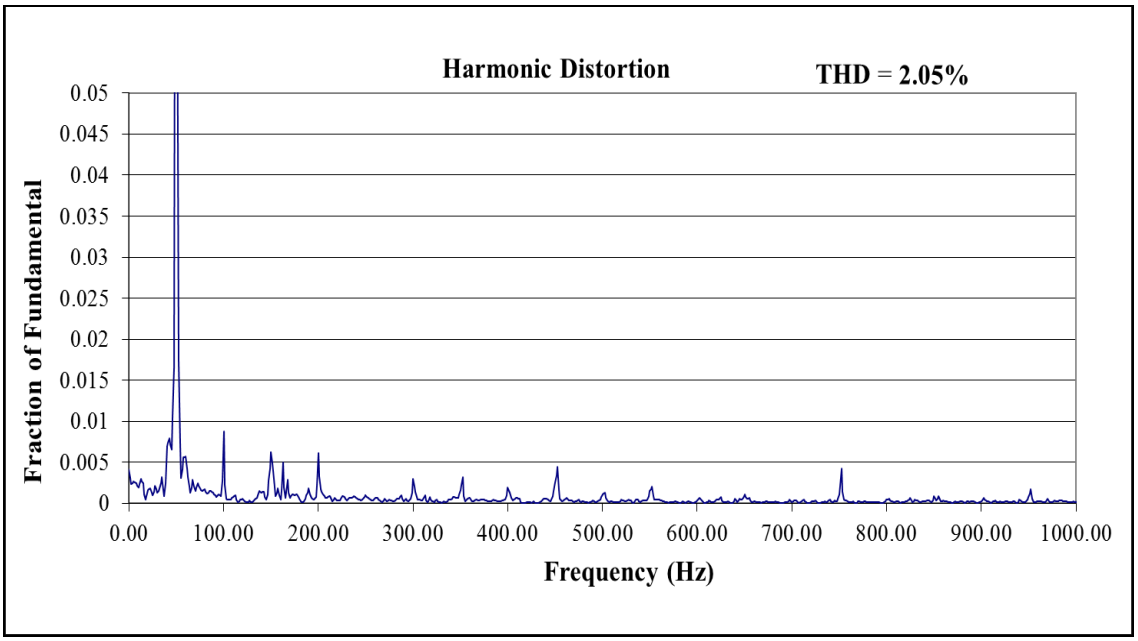


*Fig 5.28: Experimental spectrum of the output current with RC*

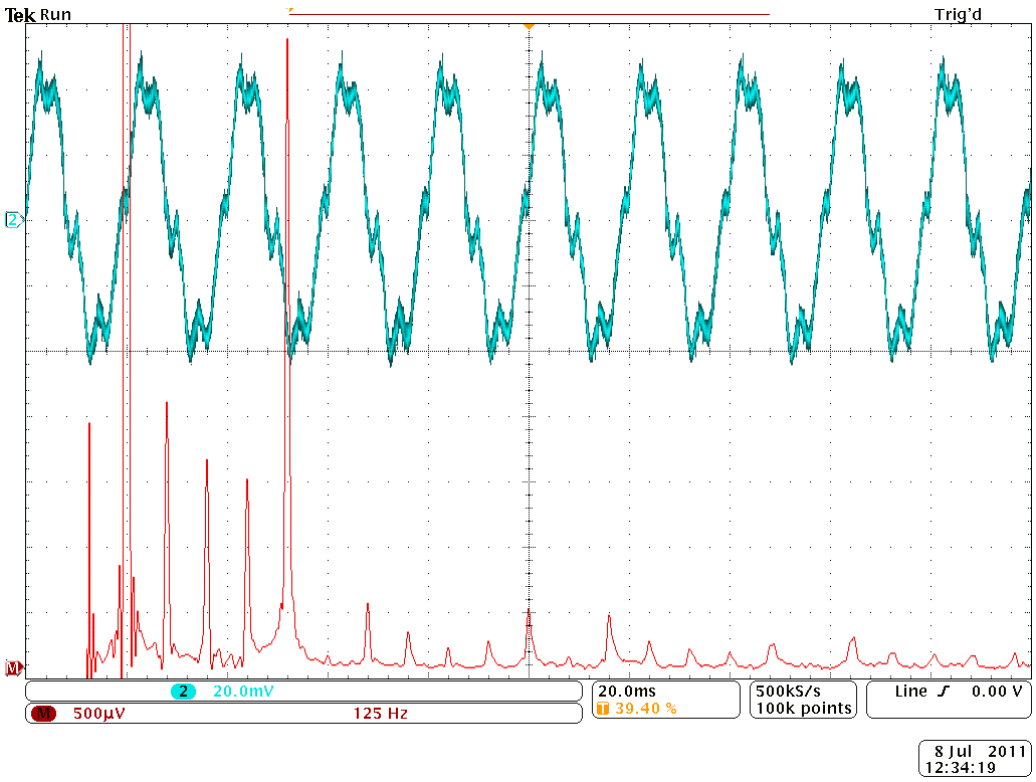


*Fig 5.29: Experimental output current and its spectrum without RC (current 10A/div, spectrum 0.25Arms/div)*

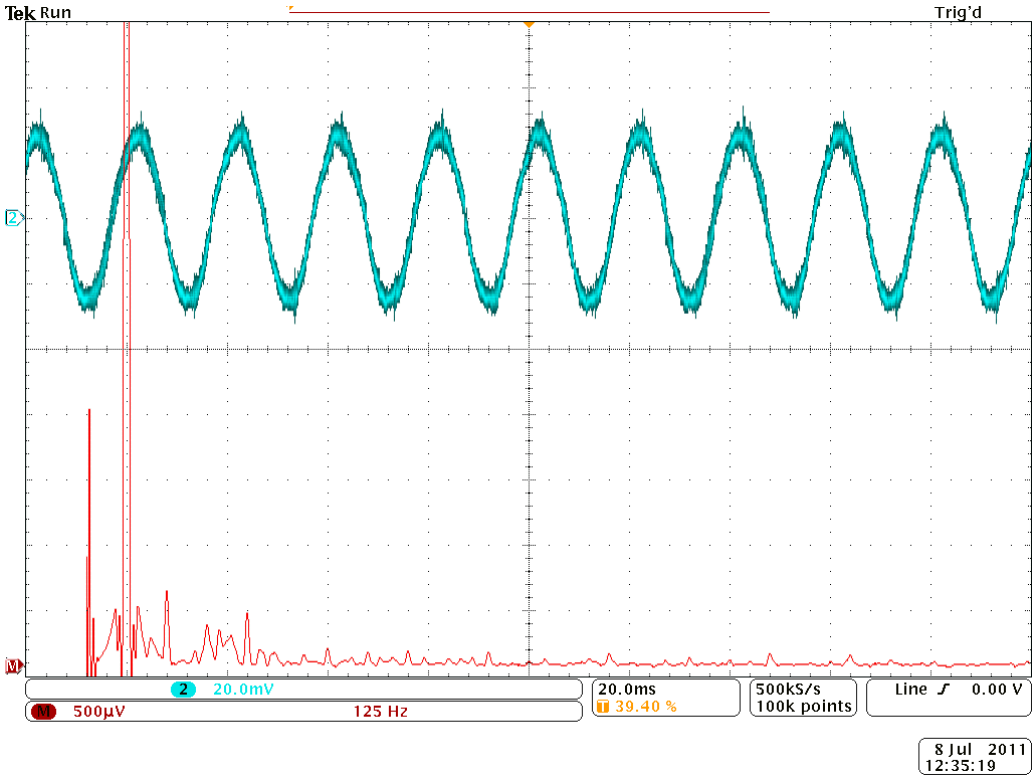


*Fig 5.30: Experimental output current and its spectrum with RC ( current 10A/div, spectrum 0.25Arms/div)*

| Harmonic number (n) | Experimental | |
|---|---|---|
| | Utility phase voltage V(rms) | Output current A(rms) |
| 3rd | 2.4 | 0.11 |
| 5th | 4.22 | 0.1 |
| 7th | 1.95 | 0.05 |
| 9th | 2.37 | 0.07 |
| 11th | 1.46 | 0.055 |
| 13th | 1.95 | 0.08 |
| 15th | 0.455 | 0.09 |
| 17th | 0.65 | 0.01 |
| 19th | 0.585 | 0.01 |
| **THD (%)** | **2.74** | **2.05** |

*Table 5.2: Experimental harmonic attenuation of the output current with RC*

## 5.5 Summary

This chapter has discussed the details of the design and analysis of the RC for the interleaved utility connected converter. A conventional feedback controller with a phase lag has been designed, which can handle the variations in utility impedance very well. In the next step a loop of RC was added to improve the performance in terms of THD rejection and steady state error. The performance of the system was evaluated using simulation results and attenuation of individual harmonics. The harmonics present in the utility were measured and included in the Simulink model. In the last section, the experimental implementation of the proposed technique was discussed. Two forms, such as direct form I and direct form II, were considered for possible implementation. The direct form II is quite useful for saving memory and was thus used for final implementation. The flow chart of the algorithm was described. The experimental results which confirm and validate the design, analysis and simulation results were presented.

# Chapter 6

## CONCLUSIONS AND RECOMMENDATIONS

This chapter summarises and analyses the research related to the application of a repetitive controller (RC) for a two-level LCL filter based converter and interleaved converter, carried out in this thesis. Particular attention has been focused on the contributions made in the field by comparing different methods and approaches. The issues and limitations raised during the research have been addressed by making suggestions for future work.

### 6.1 Summary of the Thesis

The overall aim of this research has been to investigate the digital repetitive current control of utility connected two-level LCL filter based and interleaved converters. The work presented in this thesis consists of two parts, first, an evaluation of the performance of RC for LCL filter based two-level converters (chapter 4), and second, the design and analysis of RC for the interleaved converter (chapter 5). Principally, in terms of the RC, the structure of the controller is similar in both applications.

Chapter 1 discussed the significance of the power electronic converters within microgrids, which can address the limitations of current power systems by promoting distributed generators including renewable energy sources. Among different available topologies of these converters, two-level LCL filter based and interleaved topologies have been adopted by describing their features for the purpose of current control in the utility connected mode. The RC was selected for the presence of periodic errors and problems of poor disturbance rejections due to low loop gains and steady state errors associated with other classical (PI) controllers in this application. The RC was able to offer higher gains at fundamental and its harmonics. This chapter described the main contributions and presented a general outline of the thesis.

Chapter 2 selected the suitable structure of the two-level utility connected converter by looking at the methods of dampening the resonance due to the LCL filters. The problems attached with different controllers (classical P/PI, deadbeat, proportional resonant,

nonlinear and others) were critically reviewed by focusing on limitations of a classical (P/PI) controller. To address these issues, the RC was adopted and different structures were critically reviewed to select the final one to be used in this thesis. The transfer functions were derived based on the selected structure.

Chapter 3 described the linear and nonlinear (switching) models of the two-level LCL filter based and interleaved converters designed using Matlab/Simulink. The assumptions made and different elements attached with these models were provided. The performance criteria for the evaluation and comparison of current control methods were also described. This established the methodology, which was used in this thesis later on.

The effect of filter bandwidth (determined by values of C) on the performance of RC was investigated in chapter 4. Fundamental investigations were carried out into stability constraints, a trade-off between steady state error and system transient response for the design of the RC. A special case of RC known as odd-harmonic repetitive control (ORC) for the two-level converter was also considered. This provided fast error convergence and required half memory compared to the conventional RC. The ORC was able to provide higher gains only at odd harmonic frequencies.

Chapter 5 dealt with investigations into the RC for interleaved utility connected converters. Each phase in the interleaved converter had six half-bridge channels connected in parallel. Due to current ripple cancellation of the interleaving topology, only small capacitors were required which provided high impedance to the utility and larger bandwidth for design of the RC. This resulted in a better quality of current than the LCL filter based two-level converter. The experimental results validated the simulation results and output current had low THD without almost zero steady state error.

## 6.2 Conclusions

The following are the conclusions that can be drawn from this thesis:

- Classical controllers (P/PI) have been simulated to assess their suitability for the application. Simulation results reveal that it is difficult to produce an output current as per national and international recommended standards when utility THD is more

than 5%. The gain at harmonic frequencies of interest is not high enough to reject all harmonics.

- Proportional resonant controllers were reviewed and found to be similar to RC as they also use the internal model principle. However, the main difference is that RC can reject all harmonics simultaneously at the same time.

- A digital RC incorporated within a two loops feedback system has been analysed using analytical and computer simulation tools. The simulation results reveal that the RC helps to lower the THD level in the output current even when utility THD is high.

- Different RC low-pass Q-filters were investigated and findings showed that normal low-pass filters or constant value of Q-filter can make the RC system unstable. To address this issue, the zero-phase low-pass filter used within the RC structure could be useful which gives a stable system and at the same time, the amplitudes of the gains could be increased effectively using RC.

- The RC gain selection was studied and findings showed that the higher gain values make the error convergence faster, but the system becomes less stable.

- The compensator present within the structure of the RC can improve stability. It is desirable to choose the inverse of the system to achieve zero steady state error. However, the utility impedance can vary significantly and the transfer function is not known. Instead, a phase-lead scheme could be used.

- The selection of the capacitance value and the low-pass filter with respect to system bandwidth and its impact on the design of the RC was investigated. This has not been extensively discussed in the literature previously and this work contributes to the field. It was found that the performance of an RC suffers if the system bandwidth is low, which is the case for the two- level converter, if the capacitance is too high.

- The effect of variations in utility impedance for the two-level converter was studied and the proposed RC was found to be able to handle these variations very well. The

system could become unstable if these variations had not been taken into account while designing a controller.

- An odd-harmonic RC for the two-level converter was simulated and was found to provide shorter transients and requires half the memory compared to the conventional RC.

- A digital RC for the interleaved utility connected converter was analysed using analytical and computer simulation tools. This application for RC has not been previously discussed in the literature and thus contributes to the field. The simulation results reveal that the RC helps to lower the THD level considerably without steady state error in the output current even when the utility THD is high.

- While designing the RC, the sampling time and computational time delay taken by the DSP for experimental implementation was considered. It was found that it needs to be properly modelled in the simulation to avoid instability.

- For implementation of RC and digital filters, two forms such as direct form I and direct form II were considered and the direct form II was found to involve less memory and provide a faster response due to less computational burden.

- The designed digital RC was experimentally tested. The experimental results agreed with the simulation results and the quality of the output current complied with ANSI/IEEE standards.

## 6.3 Suggestions for Future Work

Further development is recommended and the following areas for future work are suggested based on the research carried out in this thesis.

**Outer Loop Voltage Control/Regulator**

- The DC link voltage is assumed to be constant in this thesis. In practice, a DC voltage regulator/controller is used in the outer loop, which normally defines the amplitude of the reference current and the converter can support a seamless bidirectional power flow between converter and utility (Sivakumar et al., 2002). The inner loop normally controls the power between DC link and the utility. It

takes the reference current form the outer loop to maintain a constant DC link voltage. For practical implementation in this thesis, a boost card attached to the test rig was used which regulates the DC link voltage. However, an outer loop voltage control loop is recommended to be included in any future simulation model. This will strengthen the simulation.

**Power Flow Control**

- In this thesis, we focused on the current control aspect of the utility connected converter only in one direction i.e. into the utility but other (backward) direction of the current can also be considered. So a bidirectional power flow and its control can be considered in the future. It is also recommended to consider losses (not considered in this thesis), while performing power flow control using utility connected converters (Bifaretti et al., 2011). This normally involves synchronous (d-q) frame transformations and utility phase identification to be carried out using phase-lock-loop (PLL). The PLL identification may not provide accurate information about the phase of the utility and hence needs further investigation.

**Optimization of RC System under Frequency Variations**

- The performance of the RC can vary if the frequency is not constant. This requires updating the number of cycles in a period ($N$) either in an adaptive way or in some off-line methods. There are different references (Hillerstrom, 1994; Steinbuch 2002; Cao and Ledwich, 2002) to handle this issue in other applications. It would be interesting to investigate these methods for the application of utility connected two-level and the interleave converters.

**Scale Factor Based Structures of RC and Ways of Implementation**

- The RC was added to the conventional closed loop system in an add-on fashion. However, it is suggested to look at alternative ways of adding RC to the system such as parallel. Moreover, it would be interesting to look at the performance of an RC system when other structures of RC such as reduced scale by a factor are evaluated. By this way, small memory and low processor such as microcontroller can be used for small-scale prototypes.

**Development of an RC System for other Topologies and Modes**

- The application of RC for other topologies such as multilevel utility connected converters could be another interesting area for further research. Similarly, RC based on voltage control mode could be another area to be looked at using the analysis carried out in this research.

**Combination of an RC System with other Controllers**

- It is known that the RC requires another stable controller such as a classical (P) controller as used in this thesis. It would be interesting to consider other mentioned controllers in this thesis such as proportional resonant, deadbeat and H-infinity with the combination of RC.

**Dual Mode RC**

- Another type of RC known as dual mode RC can be investigated for the application of current control of the two-level and the interleaved converters. In dual mode, two parallel signal generators are used, which work on odd-harmonics and even harmonics separately (Keliang et al., 2009). This could provide faster error convergence than the conventional RC.

## REFERENCES:


Abusara, M. A. (2004). Digital control of utility and parallel connected three-phase PWM inverters. PhD Thesis. University of Southampton U.K.

Abusara, M. A. and Sharkh, S. M. (2010). Design of a robust digital current controller for a utility connected interleaved inverter. *IEEE International Symposium on Industrial Electronics*. Bari Italy.

Baha, B. (1998). Modelling of resonant switched-mode converters using SIMULINK. *IEE Proceedings on Electric Power Applications*. vol. 145 p.159-163.

Basso, T. S. and Deblasio, R. (2004). IEEE 1547 series of standards: interconnection issues. *IEEE Transactions on Power Electronics*. vol.19 p. 1159-1162.

Bifaretti, S., Zanchetta, P., Watson, A., Tarisciotti, L. and Clare, J. C. (2011). Advanced power electronic conversion and control system for universal and flexible power management. *IEEE Transactions on Smart Grids*. vol.2 p. 231-243.

Bouhali, O., Francois, B., Saudemont, C. and Berkouk, E. M. (2006). Practical power control design of a NPC multilevel converter for grid connection of a renewable energy plant based on a FESS and a wind generator. *32nd Annual Conference of IEEE Industrial Electronics Society*. Paris France.

Camargo, D. R. F. and Pinherio, H. (2005). Comparison of six digital current control techniques for three-phase voltage-fed PWM converters connected to the utility grid. *36th IEEE Power Electronics Specialists Conference.* Recife Brazil.

Cao, Z. and Ledwich, G.F. (2002). Adaptive repetitive control to track variable periodic signals with fixed sampling rate. *IEEE/AMSE Transactions on Mechatronics*. vol. 7, p.378-384.

Chen, S.-L. and Hsieh, T.-H. (2007). Repetitive control design and implementation for linear motor machine tool. *International Journal of Machine Tools and Manufacture*. vol.47p.1807-1816.

Chen, S., Lai, Y. M., Tan, S. C. and Tse, C. K. (2008). Analysis and design of repetitive controller for harmonic elimination in PWM voltage source inverter systems. *IET Power Electronics*.vol.1 p. 497-506.

Costa-Castello, R., Grinio, R. and Fossas, E. (2004). Odd-harmonic digital repetitive control of a single-phase current active filter. *IEEE Transactions on Power Electronics*. vol.19 p.1060-1068.

Costa-Castello, R., Grinio, R. and Fossas, E. (2006). Reply to "Concerning 'Odd-harmonic digital repetitive control of a single-phase current active filter". *IEEE Transactions on Power Electronics*. vol.21 p.1159-1160.

Costa-Castello, R., Nebot, J. and Grino, R. (2005). Demonstration of the internal model principle by digital repetitive control of an educational laboratory plant. *IEEE Transactions on Education*. vol.48 p.73-80.

Dannehl, J., Fuchs, F. W. and Togersen, P. B. (2010). PI state space current control of grid-connected PWM inverters with LCL filters. *IEEE Transactions on Power Electronics*. vol.25 p.2320-2330.

Deng, H., Oruganti, R. and Srinivasan, D. PWM methods to handle time delay in digital control of a UPS inverter. *IEEE Power Electronics Letters*. vol.3(1) p.1-6

Dugan, R. C., Key, T. S. and Ball, G. J. (2005). On standards for interconnecting distributed resources. *Rural Electric Power Conference*.San Antonio Texas.

Energy Networks Association (1995). Engineering Technical Report No. 113 Revision 1: Notes of guidance for the protection of embedded generating plant up to 5 MW for operation in parallel with public electricity suppliers' distribution systems.

Electricity Association (Engineering Services) (1991). Engineering Recommendation G59/1, 'Recommendations for the connection of embedded generating plant to the regional electricity companies' distribution systems'.

Espi, J. M., Castello, J., Garcia-Gil, R., Garcera, G. and Figueres, E. (2011). An adaptive robust predictive current control for three-phase grid-connected inverters. *IEEE Transactions on Industrial Electro*nics. vol.58(8) p.3537-3546.

Francis, B.A. and Wonham, W. M. (1976). The internal model principle of control theory. *Automatica*. vol.12 p. 457-465.

Gabe, I. J., Massing, J. R., Montagner, V. F. and Pinheiro, H. (2007). Stability analysis of grid-connected voltage source inverters with LCL-filters using partial state feedback. *European Conference on Power Electronics and Applications.* Aalborg Denamrk.

Gao J., Zheng, Q.T. and Lin, F. (2011). Improved deadbeat current controller with a repetiitve-control-based observer for PWM rectifiers. *Journal of Power Electronics (JPE)*, vol. 11(1) p.64-73.

Garces, A., and Molinas, M. (2012). A study of efficiency in a reduced matrix converter for offshore wind farms. *IEEE Transactions on Industrial Electronics*. vol. 59 (1) p. 184-193.

Grino, R., Cardoner, R., Costa-Castello,R., and Fossas, E. (2007). Digital repetitive control of a three-phase four-wire shunt active filter. *IEEE Transactions on Industrial Electronics*. vol. 54 (3) p. 1495-1503.

Grino, R. and Costa-Castello, R. (2005). Digital repetitive plug-in controller for odd-harmonic periodic references and disturbances. *Automatica*. vol. 41 p.153-157.

Guoqiao, S., Dehong, X., Luping, C. and Xuancai, Z. (2008). An improved control strategy for grid-connected voltage source inverters with an LCL filter. *IEEE Transactions on Power Electronics*. vol. 23 p. 1899-1906.

Guoqiao, S., Xuancai, Z., Jun, Z. and Dehong, X. (2010). A new feedback method for PR current control of LCL-filter based grid-connected inverter. *IEEE Transactions on Industrial Electronics*. vol.57 p. 2033-2041.

Guo, X. Q., and Wu, W. Y. (2009). Improved current regulation of three-phase grid-connected voltage-source inverters for distributed generation systems. *IET Renewable Power Generation*. vol. 4 p.101-115.

Hillerstorm, G. (1994). On repetitive control. PhD Thesis. Lulea University of Technology.

Hornik, T. and Zhong, Q. C. (2011). A current-control strategy for voltage-source inverters in microgrid based on H-infinity and repetitive control. *IEEE Transactions on Power Electronics*. vol. 26 p. 943-952.

Hussein, Z. F. (2000). Current control of three-phase PWM inverter for flywheel energy storage system. PhD Thesis. University of Southampton U.K.

Hwang, J. G., Lehn, P. W. and Winkelnkemper, M. (2010). A generalized class of stationary frame-current controllers for grid-connected AC-DC converters. *IEEE Transactions on Power Delivery*. vol. 25 p. 2742-2751.

IEEE Standard 519-1992 (1993). IEEE recommended practices and requirements for harmonic control in electrical power systems.

IEEE Standard 929-2000 (2000). IEEE recommended practice for utility interface of photovoltaic (PV) systems.

Ito, Y. and Kawauchi, S. (1995). Microprocessor based robust digital control for UPS with three-phase PWM inverter. *IEEE Transactions on Power Electronics*. vol. 10 p.196-204.

Jamil, M., Hussain, B., Abusara, M. A., Boltryk, R. J. and Sharkh, S. M. (2009). Microgrid power electronic converters: State of the art and future challenges. *44th International Universities Power Engineering Conference (UPEC)*. Glasgow U.K.

Jamil, M., Sharkh, S. M., Abusara, M. A. and Boltryk, R. J. (2010). Robust repetitive feedback control of a three-phase grid connected inverter. *5th IET International Conference on Power ElectronicsMachines and Drives (PEMD)*. Brighton U.K.

Kazmierkowski, M. P. and Malesani, L. (1998). Current control techniques for three-phase voltage-source PWM converters: a survey. *IEEE Transactions on Industrial Electronics*. vol. 45 p. 691-703.

Kazmierkowski, M. P., Krishnan, R. and Blaabjerg, F. (2002). Control in power electronics. New York: Academic Prress.

Keliang, Z. and Danwei, W. (2001). Digital repetitive learning controller for three-phase CVCF PWM inverter. *IEEE Transactions on Industrial Electronics*. vol. 48 p. 820-830.

Keliang, Z., Yongaiang, Y. and Wang, D. (2005). Concerning "Odd-harmonic digital repetitive control of a single-phase current active filter". *IEEE Transactions on Power Electronics*. vol. 20 p.511-513.

Keliang, Z., Danwei, W., Bin, Z. and Yigang, W. (2009). Plug-in dual-mode structure repetitive controller for CVCF PWM inverters. *IEEE Transactions on Industrial Eeelctronics*. vol.56 p.784-791

Kim, I.-S. (2006). Sliding mode controller for the single-phase grid-connected photovoltaic system. *Applied Energy*. vol. 83 p. 1101-1115.

Kojabadi, H. M., Gadoura, I. A. and Ghribi, M. (2005). A simple, digital current control design for grid-connected inverters. *2005 European Conference on Power Electronics and Applications (EPE)*. Dresden Germany.

Lee, K.-J., Park, N.-J. and Hyun., D.-S. (2007). Optimal current controller in a three-phase grid connected inverter with an LCL filter. *7th International Conference on Power Electronics*. Daegu Korea.

Lee, S.-H., Song, S.-G., Park, S.-J., Moon, C.-J. and Lee M.-H. (2008). Grid-connected photovoltaic system using current-source inverter. *Solar Energy*. vol. 82, p. 411-419.

Lenwari, W., Summer, M. and Zanchetta, P. (2009). The use of genetic algorithms for the design of resonant compensators for active filters. *IEEE Transactions on Industrial Electronics*. vol. 56 p. 2852-2861.

Liang, Z., Xiong, J., J., Zhang, K. and Shi, P. (2006). Improved dual-loop control plus repetitive control for PWM inverters. *1st IEEE Conference on Industrial Electronics and Applications*. Singapore.

Liserre, M., Teodorescu, R. and Blaabjerg, F. (2006). Multiple harmonics control for three-phase grid converter systems with the use of PI-RES current controller in a rotating frame. *IEEE Transactions on Power Electronics*. vol. 21 p. 836-841.

Longman R. W. (2000). Iterative learning contorl and repetitive control for engineering pratice. *International Journal of Control*. vol. 73 p. 930-954.

Lu, W., Zhou, K. and Yang, Y. (2010). A general internal model principle based control scheme for CVCF PWM converters. *2nd IEEE International Symposium on Power Electronics for Distributed Generation Systems (PEDG)*. Hefei China.

Moore, K.L., Dahlen, M. and Bhattacharyya, S.P. (1992). Iterative learning control:a survey and new results. *Journal of Robotic Systems*. John Wiley and Sons.

Michels, M., Pinheiro, H. and Grundling, H. (2004). Design of plug-in repetitive controllers for single-phase PWM inverters. *39th IAS Annual Meeting:Industry Applications Conference*. Rome Italy.

Miret, J., Castilla, M., Matas, J., Guerrero, J. M. and Vasquez, J. C. (2009). Selective harmonic-compensation control for single-phase active power filter with high harmonic rejection. *IEEE Transactions on Industrial Electronics*. vol. 56 p. 3117-3127.

Mohamed, Y. A. R. and El-Saadany, E. F. (2008). Adaptive discrete-time grid-voltage sensorless interfacing scheme for grid-connected DG-inverters based on neural-network identification and deadbeat current regulation. *IEEE Transactions on Power Electronics*. vol. 23 p. 308-321.

Mohan, N., Undeland T. M. and Robbins, W. P. (2006). *Power electronics: converters, applications and design*. Book published by John Willy and Sons.

Moreno, J. C., Huerta, J. M. E., Gil, R. G. and Gonzalez, S. A. (2009). A robust predictive current control for three-phase utility-connected inverters. *IEEE Transactions on Industrial Electronics*. vol. 56 p. 1993-2004.

Nene, H. (2006). Using the enhanced pulse width modulator (ePWM) module for 0% to 100% duty cycle control. *Texas Instrument-Application Report No. SPRAAl1*. Decmeber 2006.

Newman, M. J. and Holmes, D. G. (2003). Delta operator digital filters for high performance inverter applications. *IEEE Transactions on Power Electronics*. vol. 18 p. 447-454.

Nishida, K., Ahmed, T., Nakaoka, M. and Rukonuzzaman, M. (2003). A robust deadbeat current control method by using adaptive predictor for single-phase voltage source active power filter. *The 29th Annual Conference of the IEEE Industrial Electronics Society*. Roanoke USA.

Nishida, K., Rukonuzzaman, M., Ahmed, T. and Nakaoka, M. (2004). A robust deadbeat current control method by using adaptive line enhancer for single-phase voltage source active power filter. *The 4th International Power Electronics and Motion Control Conference*. Xian China.

Odavic, M., Biagini, V., Zanchetta, P., Sumner, M. and Degano, M. (2011). One-sample-period-ahead predictive current control for high-performance active shunt power filters. *IET Power Electronics*. vol. 4 p. 414-423.

Owens, D. H. and Liu, S. (2011). Iterative learning control: quantifying the effect of output noise. *IET Control Theory and Applications*. vol. 5 p. 379-388.

Peltoniemi, P., Nuutinen, P., Niemela, M. and Pyrhonen, J. (2009). LQG-based voltage control of the single-phase inverter for noisy environment. *2009 European Conference on Power Electronics and Applications (EPE). Barcelona Spain.*

Pengfei, S., Xiong, J., Kai, Z. and Liang, Z. (2006). One cost-effective feedback control scheme for PWM inverters based on repetitive control. *1st IEEE Conference on Industrial Electronics and Applications*. Singapore.

Picardi, C. and Sgro, D. (2009). Grid-connected inverter power flow control based on a new modeling approach of electrical signals. *2009 International Conference on Clean Electrical Power*. Capri Italy.

Pipeleers, G., Demeulenaere, B., De Schutter, J. and Swevers, J. (2008). Generalized repetitive control: Better performance with less memory. *10th IEEE International Workshop on Advanced Motion Control*. Trento Italy.

Pipeleers, G., Demeulenaere, B., De Schutter, J. and Swevers, J. (2009). *Generalised repetitive control: relaxing the period-delay-based structure*. *IET Control Theory and Applications*. vol. 3 p. 1528-1536.

Qiang, Z., Lewei, Q., Chongwei, Z. and Cartes, D. (2006). Study on grid connected inverter used in high power wind generation system. *41st IAS Annual Meeting :Industry Applications Conference*. Tampa Finland.

Qing-Chang, Z., Green, T., Jun, L. and Weiss, G. (2002). Robust repetitive control of utility-connected DC-AC inverters. *41st IEEE Conference on Decision and Control*. Las Vegas USA.

Qingrong, Z. and Liuchen, C. (2005). Study of advanced current control strategies for three-phase utility-connected pwm inverters for distributed generation. *IEEE Conference on Control Applications*. Tronto Canada.

Qu, B., Hong, X. Y., Yao, W. X., Lue, Z. Y., Guerrero, J. M. (2009). An optimized deadbeat control scheme using fuzzy control in three-phase voltage source PWM rectifier. *24th Annual IEEE Applied Power Electronics Conference and Exposition*. Washington USA.

Ramos, G. A., Costa-Castello, R., Olm , J. M. and Cardoner, R. (2010). Robust high-order repetitive control of an active filter using an odd-harmonic internal model. *IEEE International Symposium on Industrial Electronics*. Bari Italy.

Ratclifee, J. D., Lewin, P. L., Rogers, E., Hatonen, J. J. and Owens, D. H. (2006). Norm-optimal iterative learning control applied to gantry robots for automation applications. *IEEE Transactions on Robotics*. vol. 22 p. 1303-1307.

Rech C. and Pinheiro, J. R. (2004). New repetitive control system of PWM inverters with improved dynamic performance under non-periodic disturbances. *35th Annual IEEE Power Electronics Specialists Conference*. Aachen Germany.

Rohouma, W. M., Arevalo, S. L., Zanchetta, P. and Wheeler, P. (2010). Repetitive control for a four leg matrix converter. *5th IET International Conference on Power Electronics, Machines and Drives*. Brighton U.K.

Alepuz, S., Busquets-Monge, S., Bordonau, J., Gago, J., Gonzalez, D. and Balcells, J. (2006). Interfacing renewable energy sources to the utility grid using a three-level inverter. *IEEE Transactions on Industrial Electronics*. vol. 53 p. 1504-1511

Selvaraj, J. and Rahim, N. A. (2009). Multilevel inverter for grid-connected PV system employing digital PI controller. *IEEE Transactions on Industrial Electronics*. vol. 56 p. 149-158.

Selvaraj, J., Rahim, N. A. and Krismadinata, C. (2008). Digital PI current control for grid connected PV inverter. *3rd IEEE Conference on Industrial Electronics and Applications*. Singapore.

Sharkh, S. M. and Abusara M. A. (2004). Current control of utility-connected two-level and three-level PWM inverters. *European Power Electronic Journal*. vol. 14 p.13-18.

Sharkh, S. M., Arnold, R. J., Kohler, J., Li, R., Markvart, T., Ross, J. N., Steemers, K., Wilson, P. and Yao, R. (2006). Can microgrid make a major contribution to UK energy supply? *Renewable and Sustainable Energy Reviews*. vol.10 p.78-127.

Sharkh, S. M., Abusara, M. A. and Hussein., Z. F. (2001). Current control of utility-connected DC-AC three-phase volatge-source inverters using repetitive feedback. *European Power Electronics Conference*. Graz Austria.

Shuitao, Y., Qin, L., Peng, F. Z. and Zhaoming, Q. (2011). A robust control scheme for grid-connected voltage-source inverters. *IEEE Transactions on Industrial Electronics*. vol. 58 p. 202-212.

Silva, G. J., Datta, A. and Bhattacharyya, S. P. (2002). New results on the synthesis of PID controllers. *IEEE Transactions on Automatic Control*. vol. 47 p. 241-252.

Singh, M. and Chandra, A. (2011). Application of adaptive network-based fuzzy inference system for sensorless control of PMSG-based wind turbine with nonlinear-load-compensation capabilities. *IEEE Transactions on Power Electronics*. vol.26 p. 165-175.

Sivakumar, S., Parsons, T. and Sivakumar, S. C. (2002). Modeling , analysis and control of bidirectional power flow in grid connected inverter systems. *Power Conversion Conference.* Osaka Japan.

Steinbuch, M. (2002). Repetitive control for systems with uncertain period-time. *Automatica*. vol.38 p.2103-2109.

Sung-Yeual, P., Chien-Liang, C., Jih-Sheng, L. and Seungryul , M. (2008). Admitance compensation in current loop control for a grid-tie LCL fuel cell inverter. *IEEE Transactions on Power Electronics.* vol. 23 p. 1716-1723.

Svensson, J. and Lindgren, M. (1999). Influence of nonlinearities on the frequency response of a grid-connected vector-controlled VSC. *IEEE Transactions on Industrial Electronics*. vol. 46 p. 319-324.

Texas Instrument. TMS320x280x, 2801x,2804x enhanced pulse width modulator (ePWM) module: reference guide. 2009. Available [online] at : http://www.ti.com/general/docs/lit/getliterature.tsp?baseLiteratureNumber=SPRU791&track=no

Tang, Y., Loh, P. C., Wang, P., Choo, F. H., Gao, F. and Blaabjerg, F. (2012). Generalised design of high performance shunt active power filter with output LCL filter. *IEEE Transactions on Industrial Electronics*. vol. 59 p. 1443-1452.

Teodorescu, R., Blaabjerg , F., Liserre, M. and Loh, P. C. (2006). Proportional-resonant controllers and filters for grid-connected voltage-source converters. *IEE Proceedings on Electric Power Applications*. vol. 153 p. 750-762.

Timbus, A. V., Ciobotaru, M., Teodorescu, R. and Blaabjerg, F. (2006). Adaptive resonant controller for grid-connected converters in distributed power generation systems. *21st Annual IEEE Applied Power Electronics Conference and Exposition*. Dallas USA.

Timbus, A. V., Ciobotaru, M., Teodorescu, R. and Blaabjerg, F. (2009). Evaluation of current controllers for distributed power generation systems. *IEEE Transactions on Power Electronics*. vol. 24 p. 654-664.

Tinone, H. and Aoshima, N. (1996). Parameter identification of robot arm with repetitive control. *International Journal of Control*. vol. 63 p. 225 - 238.

Twining, E. and Holmes, D. G. (2002). Grid current regulation of a three-phase voltage source inverter with an LCL input filter. *33rd IEEE Annual Power Electronics Specialists Conference*. Cairns Australia.

Twining, E. and Holmes, D. G. (2003). Grid current regulation of a three-phase voltage source inverter with an LCL input filter. *IEEE Transactions on Power Electronics*. vol. 18(3) p.888-895.

Wang, W., Panda, S. K. and Jian-Xin, X. (2005). Control of high performance DC-AC converters using frequency domain based repetitive control. *International Conference on Power Electronics and Drives Systems*. Kuala Lumpur Malaysia.

Weiss, G., Qing-Chong, Z., Green, T. C. and Jun L. (2004). H-infinity repetitive control of DC-AC converters in microgrid. *IEEE Transactions on Power Electronics*. vol. 19 p. 219-230.

Won, W., Lee, K. S., Lee, S. and Jung , C. (2010). Repetitive control and online optimization of catofin propane process. *Computers and Chemical Engineering*. vol.34 p. 508-517.

Wu, X. H., Panda, S. K. and Xu, J. X. (2010). Design of a plug-in repetitive control scheme for eliminating supply-side current harmonics of three-phase PWM boost rectifiers under generalized supply voltage conditions. *IEEE Transactions on Power Electronics*. vol. 25 p.1800-1810.

Ying-Yu, T., Rong-Shyang, O., Shih-Liang, J. and Meng-Yueh, C. (1997). High-performance programmable AC power source with low harmonic distortion using DSP-based repetitive control technique. *IEEE Transactions on Power Electronics*. vol. 12 p. 715-725.

Yingjie, H., Jinjun, L., Zhaoan, W. and Yunping, Z. (2009). An Improved repetitive control for active power filters with three-level NPC inverter. *24th Annual IEEE Conference on Applied Power Electronics and Exposition*. Washington USA.

Yongqiang, Y., Keliang, Z., Bin, Z., Wang, D. and Jingcheng, W. (2006). High-performance repetitive control of PWM DC-AC converters with real-time phase-lead FIR filter. *IEEE Transactions on Circuits and Systems*. vol. 53 p. 768-772.

Zhang, B., Zhou, K., Wang, Y. and Wang, D. (2008). Performance improvement of repetitive controlled PWM inverters: A phase-lead compensation solution. *International Journal of Circuit Theory and Applications*. vol. 38 p. 453-469.

Zhou, K., Low, K.-S., Wang, D., Luo, F.-L., Zhang, B. and Wang, Y. (2006). Zero-phase odd-harmonic repetitive controller for a single-phase PWM inverter. *IEEE Transactions on Power Electronics*.vol. 21 p. 193-200.

Zhao, W. and Chen, G. (2009). Comparison of active and passive damping methods for application in high power active power filter with LCL-filter. *International Conference on Sustainable Power Generation and Supply*. Nanajing China.

Zmood, D. N., Holmes, D. G. and Bode, G. (2001). Frequency domain analysis of three-phase linear current regulators. *IEEE Transactions on Industrial Electronics*. vol.37 p.601-610.

Zmood, D. N. and Holmes, D. G. (2003). Stationary frame current regulation of PWM inverters with zero steady-state error. *IEEE Transactions on Power Electronics*. vol.18 p.814-822.

# APPENDIX-PUBLICATIONS

# Microgrid Power Electronic Converters: State of the Art and Future Challenges

M. Jamil[1, 2], B. Hussain[1], M. Abu-Sara[1], R. J. Boltryk[1], S. M. Sharkh[1]
[1]School of Engg. Sciences, University of Southampton U.K., [2] NUST Pakistan.
mj2p07@soton.ac.uk

***Abstract*- This paper presents a review of the state of the art of power electric converters used in microgrids. The paper focuses primarily on grid connected converters. Different topologies and control and modulation strategies for these specific converters are critically reviewed. Moreover, future challenges in respect of these converters are identified along with their potential solutions.**

***Index Terms*—Distributed Generator (DG), Grid connected converters.**

## I. INTRODUCTION

Fossil fuels are running out and current centralised power generation plants are inefficient with a significant amount of energy lost as heat to the environment, in addition to producing harmful emissions and greenhouse gases. Furthermore, current power systems, especially in developing countries, suffer from several limitations such as high cost of expansion and efficiency improvement limits within existing grid infrastructure. Renewable energy sources can help address these issues, but it can be a challenge to get stable power from these sources as they are variable in nature.

Distributed generators (DG), including renewable sources, within microgrids can help overcome power system limitations, improve efficiency, reduce emissions and manage the variability of renewable sources. A microgrid, a relatively new concept, is a zone within the main grid where a cluster of electrical loads and small micro generation systems such as solar cell, fuel cell, wind turbine and small combined heat and power (CHP) systems exist together under an embedded management and control system with the option of storage devices. Other benefits of generating power close to electrical loads include the use of waste heat locally, saving the cost of upgrading the grid to supply more power from central plants, reducing transmission losses and creating opportunities for increasing competition in the sector which can stimulate innovation and reduce consumer prices [1, 2].

Power electronic converters are used in microgrids to control the flow of power and convert it into suitable DC or AC form as required. Different types of converter are needed to perform the many functions within a microgrid, but it is not the aim of this paper to review all of these possible types of converter, many of which are covered in textbooks and other publications [3]. The paper will primarily focus on converters used to connect DG systems including micro CHP and renewable energy sources to an AC grid or to local loads, as illustrated in Fig 1. They convert DC (photovoltaic, batteries, fuel cells) or variable frequency AC (wind and marine turbine) into 50/60 Hz AC power that is injected into the grid and/or used to supply local loads. Of these , they have been extensively used for photovoltaic [4], fuel cell [5] and wind based generation systems [6]. Converters are also used to connect to batteries and flywheel energy storage systems or connect high-speed micro turbine generators to the grid.

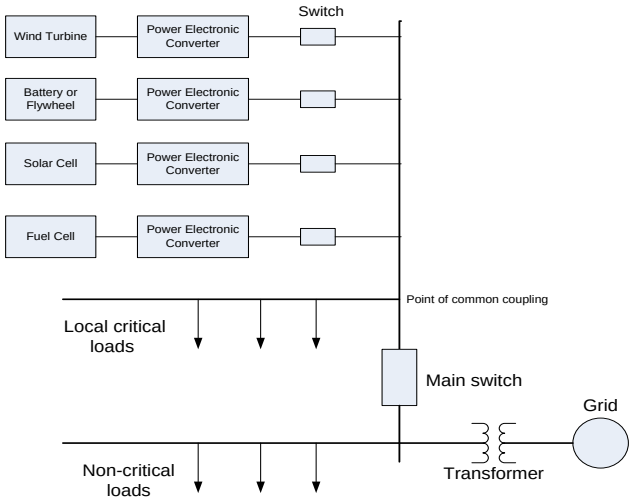


Fig. 1. A Schematic Diagram of a Microgrid

## II. MODES OF OPERATION OF MICROGRID CONVERTERS

Normally, converters are used to connect DG systems in parallel with the grid or other sources, but it may be useful for the converters to continue functioning in stand-alone mode, when the other sources become unavailable to supply critical loads. Converters connected to batteries or other storage devices will also need to be bidirectional to charge and discharge these devices.

### *A. Grid Connection Mode:*

In this mode of operation, the converter connects the power source in parallel with other sources to supply local loads and possibly feed power into the main grid. Parallel connection of embedded generators is governed by national standards [7-9]. The standards require that the embedded generator should not regulate or oppose the voltage at the common point of coupling, and that the current fed into the grid should be of high quality with upper limits on current total harmonic distortion THD levels. There is also a limit on the maximum DC component of the current injected into the grid.

The power injected into the grid can be controlled by either direct control of the current fed into the grid [10], or by controlling the power angle [11]. In the latter case, the voltage is controlled to be sinusoidal. Using power angle

control however, without directly controlling the output current, may not be effective at reducing the output current THD when the grid voltage is highly distorted, but this will be an issue in the case of electric machine generators, which effectively use power angle control. This raises the question of whether it is reasonable to specify current THD limits, regardless of the quality of the utility voltage.

In practice, the converter output current or voltage needs to be synchronized with the grid, which is achieved by using a phase locked loop or grid voltage zero crossing detection [12]. The standards also require that embedded generators, including power electronic converters, should incorporate an anti-islanding feature, so that they are disconnected from the point of common coupling when the grid power is lost. There are many anti-islanding techniques; the most common of these is the rate of change of frequency (RoCoF) technique [13].

*B. Stand-Alone Mode*

It may be desirable for the converter to continue to supply a critical local load when the main grid is disconnected, e.g. by the anti-islanding protection system. In this stand-alone mode the converter needs to maintain constant voltage and frequency regardless of load imbalance or the quality of the current, which can be highly distorted if the load is non-linear.

A situation may arise in a microgrid, disconnected from the main grid, where two or more power electronic converters switch to stand-alone mode to supply a critical load. In this case, these converters need to share the load equally. The equal sharing of load by parallel connected converter operating in stand-alone mode requires additional control. There are several methods for parallel connection, which can be broadly classified into two categories: 1) Frequency and voltage droop method [14], 2) Master-slave method, whereby one of the converters acts as a master setting the frequency and voltage, and communicating to the other converters their share of the power [15].

*C. Battery Charging Mode*

In a microgrid, due to the large time constants of some microsources, storage batteries should be present to handle disturbances and fast load changes [16]. In other words, energy storage is needed to accommodate the variations of available power generation and demand. The power electronic converter could be used as a battery charger thus improving the reliability of the microgrid.

## III. CONVERTERS TOPOLOGIES

Most of the current commercially available power electronic converters used for grid connection are based on the voltage-source 2-level PWM inverter as illustrated in Fig. 2 [10, 17]. An LCL filter is commonly used, although L filters have been also used [18, 19]. An LCL filter is smaller in size compared to a simple L filter, but it requires a more complex control system to manage the filter resonance. Additionally, the impedance of $L_2C$ in Fig.2 tends to be relatively low, and provides an easy path for current harmonics to flow from the grid, which can cause the THD to go beyond permitted limits in cases where the grid voltage THD is relatively high. Ideally, this drawback could be overcome by increasing the feedback controller gain in a current controlled grid connected converter. But this can prove to be difficult to achieve in practice while maintaining good stability [20].

Other filter topologies have also been proposed. For example, Guoqiao et al. [21], proposed an LCCL filter arrangement, feeding back the current measured between the two capacitors. By selecting the values of the capacitors to match the inductor values, the closed loop transfer function of the system becomes non-resonant.

The size and cost of the filter can be very significant. Filter size can be reduced by either increasing the switching frequency of the converter or reducing the converter voltage step changes. However the switching frequency, which is limited by losses in the power electronic devices, tends to reduce as the power ratings of the devices and the converters increase. This means that high power 2-level converters could have disproportionally large filters.

Alterative converter topologies, which can help reduce the size of the filter, have been the subject of recent research. Multi-level converters have been proposed including neutral point clamped shown in Fig. 3a [22] and cascaded converter shown in Fig. 3b [23]. Multi-level converters have the advantage of reducing the voltage step changes, and hence size and the cost of the main filter inductor for given current ripple, at the expense of increased complexity and cost of the power electronics and control components [24]. Additionally, since the switching frequency of commercial power electronic devices tends to reduce and their rated voltage tends to increase as their current ratings increase; practical multi-level converters devices may be underrated. For example, a practical high power multi-level converter may use a relatively low switching frequency device with a voltage rating greater than necessary to meet the current rating requirement.

An alternative to the multi-level converter is to use an interleaved converter topology as illustrated in Fig 4. A grid connected converter based on this topology has already been designed, built and tested by the authors, and further publications on this will follow. Interleaving is a form of paralleling technique where the switching instants are phase shifted over a switching period. By introducing an equal phase shift between parallel power stages, the output filter capacitor ripple is reduced due to the ripple cancellation effect [25, 26]. Additionally, by using smaller low current devices, it is possible to switch at a higher frequency, and therefore the inductors and the overall filters requirement would be smaller. The number of channels in an interleaved converter is a compromise between complexity and filter size.

Other possible converter topologies, which are worth investigating for this application, include current source converters [27] (Fig. 5a), and matrix converters [28] (Fig. 5b). The matrix converter is particularly appealing when the power source is AC, e.g. high frequency turbine generator or variable frequency wind turbine generator. Using a matrix converter, the cost of the AC/DC conversion stage and the

requirement for a DC link capacitor or inductor could be saved. Combinations of the above converters may be also possible, e.g. an interleaved multi-level converter or an interleaved matrix converter, perhaps with soft switching.

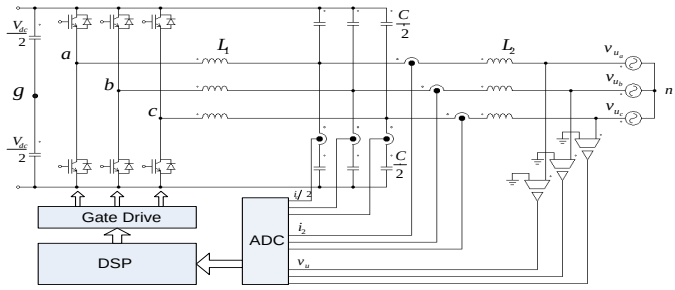


Fig. 2. Two Level Grid Connected Inverter with LCL Filter

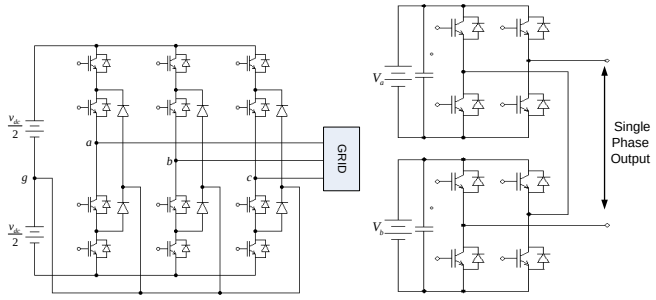


Fig. 3. Multi-level Voltage Source Inverter a) NPC and b) cascaded

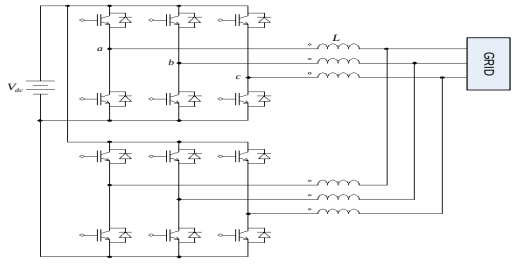


Fig 4: Interleaved Converter with two channels

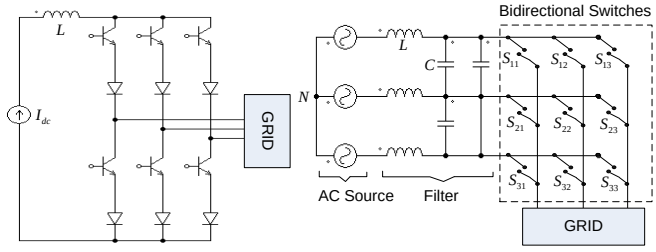


Fig 5 a) Three- Phase Current Source Converter, b) Matrix Converter

## IV. MODULATION STRATEGIES

There are a variety of modulation techniques that can be used in power electronic converters in general, including pulse width modulation (PWM), hysteresis modulation and pulse density modulation (PDM).

Hysteresis modulation is perhaps the simplest to implement in practice, but it has many shortcomings: (i) variable switching frequency in the fundamental cycle and hence spread harmonic spectrum (ii) increased current error if the middle point of dc-link and system neutral are not connected, (iii) due to the non-linear characteristic of this modulation technique, the controller cannot actively control the oscillations of the output filter and hence passive damping becomes essential (iv) poor quality of output current means it has to be used with other techniques such as repetitive feedback to improve the output current quality [17]. Due to these shortcomings, it is not preferred for microgrid inverters where high quality output current and good transient response are essential requirements.

Not surprisingly, most grid connected converters use pulse width modulation (PWM), either carrier based on using space vector modulation (SVM) which has the advantage of ease of implementation using a microprocessor. Third harmonic injection is often used to reduce the required DC link voltage headroom, thus allowing a lower switching frequency to be used. Space vector modulation strategies have also been developed to minimize switching losses or eliminate certain harmonics. In multi-level and interleaved converters, the number of SVM states increases significantly, with many redundant states, which create further opportunities for device switching strategies to reduce or redistribute the losses within the converter and eliminate certain harmonics [29, 30].

Pulse density modulation (PDM) is another possible modulation technique. It is not commonly used in conventional converters, but it has been used in high-frequency (150 kHz) converters used for induction heating [31]. The potential for this modulation strategy is yet to be explored in the context of converters for grid connection applications.

## V. CONTROL AND SYSTEM ISSUES

The control system of a grid connected converter needs to cater for the different possible operating modes that were discussed earlier in section II. In the grid connected mode, either a maximum power tracking system or the user will specify the power and power factor to be injected into the grid. The control system needs then to translate that into a reference demand current, if the output current into the grid is to be controlled. Alternatively, the controller needs to determine the output converter voltage and power angle, if power flow into the grid is based on power angle control. The reference signals need to be synchronized with the grid, as mentioned earlier.

It is common to use the d-q transformation (see Fig .6) to translate the measured AC signals of voltage and current to DC, which simplifies controller design and implementation using a microprocessor based controller [32]. But, such an approach assumes that the measured signals are pure sinusoids and that the grid is balanced, which in practice is often not the case. A slight imbalance as well as harmonic distortions are often present, which act as disturbances that cause a deterioration of the output current THD.

The alternative is to have a separate controller for each phase, with direct control of the sinusoidal output current. But direct feedback of the output grid current of an LCL filter on its own can be inherently unstable, and it is necessary to have another feedback loop of the capacitor current (see Figs 1 and

7) or the current in the main inductor $L_1$ [10, 17, 33]. One of the challenging aspects of this controller structure is that it is not possible to have a high outer loop gain using a simple compensation or PID controller. Resonant controllers [34] and virtual inductance [35] could be used to help increase the outer loop gain, and, hence, improve disturbance rejection. Other types of controllers, including optimal control strategies[36], state-feedback approach [20], and sliding mode controllers [37] have also been proposed.

An alternative is to use feedforward schemes to compensate for grid voltage harmonics [17] or inverter dead time [38] at the expense of extra complexity and cost. Repetitive or cyclic feedback has also been proposed: the output current is compared with the demanded current on a cycle by cycle basis, and accordingly, the effective reference current demanded from the inverter is modified to compensate for the disturbances. However, repetitive feedback was found in practice to lack robustness and to be sensitive to parameter uncertainty [39].

Guoqiao et al. [19] proposed splitting the capacitor into two capacitors in parallel, and adding a minor feedback loop of the current measured after the first capacitor. By carefully selecting the capacitor values, the transfer function of the system can be reduced to first order, which helps to mitigate the resonance problem and enables the outer loop gain to be increased, thus improving disturbance rejection. In practice, it may be difficult to find capacitors with the right values and the uncertainty in the filter values will make the condition for resonance elimination difficult to achieve.

For simplicity and guaranteed stability, many authors [40-42] choose to control the inverter current before the filter rather than the grid current. Such systems can, however, suffer from problems resulting from filter resonance, such as underdamped transient response oscillations, large overshoot and oscillations induced by utility harmonics near the resonance frequency, in addition to poor utility voltage harmonic disturbance rejection. Blasko and Kaura [43] proposed a lead-lag compensating loop in the filter capacitor voltage to actively damp filter resonance. Resistors connected in series with capacitors or inductors are also sometimes used, although this is not an efficient option.

Computational time delay, when a digital controller is used can be significant and could affect system stability. To maintain system stability, a time delay compensation scheme may need to be implemented [15], but with faster DSPs and microcontrollers, this is becoming less of an issue. Care also needs to be taken when generating the reference sinusoidal signal using a look-up table in a microprocessor as using an insufficient number of samples may cause sub-harmonic distortions [44].

The controller also needs to incorporate an anti-islanding protection feature, and needs to seamlessly switch from grid connected mode to stand-alone mode to supply critical loads, in parallel with other converters. This could mean switching from a current control strategy to a voltage control strategy, which can be challenging to implement. An alternative is to adopt a voltage and power angle (i.e. frequency) control strategy for all modes of operation which will make transition between different modes seamless. As mentioned earlier, however, this control method does not directly control the current injected into the grid and meeting the THD standards may be challenging if the grid voltage THD is relatively high.

Often, metering of power is incorporated as a function in commercial controllers, which can be remotely interrogated via Ethernet, CAN bus or wireless connection.

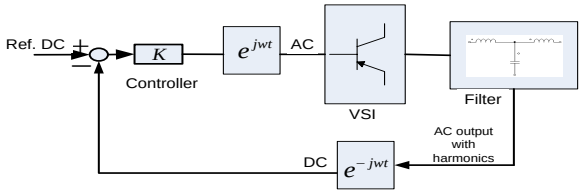


Fig 6: The basic idea of the d-q transformation approach

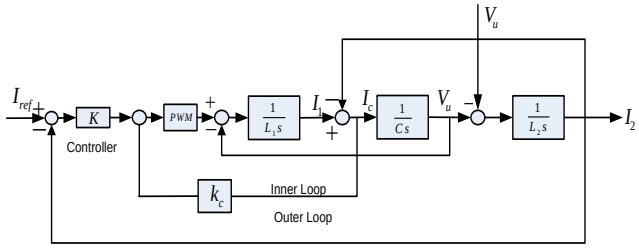


Fig 7: Two Feedback Loop Structure

## VI. FUTURE CHALLENGES AND SOLUTIONS

Cost and size of the converter, particularly the filter components, remain an issue. This, in principle, may be addressed by increasing the frequency and using either muti-level or interleaved topologies as discussed earlier. But further research is needed to establish the optimum tradeoff between power electronic devices and filter components.

It may also be beneficial to take an overall system approach when designing the converter, rather than considering the design of the converter in isolation. For example, a cascaded multilevel converter requires multiple isolated DC links which requires a multi-tap transformer, or complex schemes using flying capacitors. An alternative could be to design the electric machine (of say a wind generator) to have multiple sets of 3 phase coils isolated from each other to connect to independent rectifiers to generate the isolated DC links for the multilevel converter. In a photovoltaic system, the solar cells may be connected to form isolated DC sources.

The proliferation of inverter interfaced DG units is already raising issues related to coordination of protection relays both in grid connected and stand alone modes. This is currently an active area of research [45].

The standards governing these converters are still evolving and practical implementation is continuously giving rise to new issues that need to be thought about and regulated.

## REFERENCES

[1] S. Abu-Sharkh, R. J. Arnold, J. Kohler, R. Li, T. Markvart, J. N. Ross, K. Steemers, P. Wilson, and R. Yao, "Can microgrids make a major contribution to UK energy supply?," Renewable and Sustainable Energy Reviews, vol. 10, pp. 78-127, 2006.

[2] M. Barnes, J. Kondoh, H. Asano, J. Oyarzabal, G. Ventakaramanan, R. Lasseter, N. Hatziargyriou, and T. Green, "Real-World MicroGridsÂ¿An Overview," in System of Systems Engineering, 2007. SoSE '07. IEEE International Conference on, 2007, pp. 1-8.

APPENDIX-PUBLICATIONS


[3] P. Biczel, "Power Electronic Converters in DC Microgrid," in Compatibility in Power Electronics, 2007. CPE '07, 2007, pp. 1-6.

[4] W. Rong-Jong and W. Wen-Hung, "Design of Grid-Connected Photovoltaic Generation System with High Step-Up Converter and Sliding-Mode Inverter Control," in Control Applications, 2007. CCA 2007. IEEE International Conference on, 2007, pp. 1179-1184.

[5] M. Gaiceanu, "Inverter Control for Three-Phase Grid Connected Fuel Cell Power System," in Compatibility in Power Electronics, 2007. CPE '07, 2007, pp. 1-6.

[6] Q. Zhiling and C. Guozhu, "Study and Design of Grid Connected Inverter for 2 MW Wind Turbine," in Industry Applications Conference, 2007. IEEE 42nd IAS Annual Meeting, 2007, pp. 165-170.

[7] "Engineering Recommendation G59/1, 'Recommendations for the Connection of Embedded Generating Plant to the Regional Electricity Companies' Distribution Systems," Electricity Association (Engineering Services), 1991.

[8] "IEEE Recommended Practice for Utility Interface of Photovoltaic (PV) Systems," IEEE Std 929-2000, 2000.

[9] T. S. Basso and R. DeBlasio, "IEEE 1547 series of standards: interconnection issues," IEEE Transactions on Power Electronics, vol. 19, pp. 1159-1162, 2004.

[10] S. M. Sharkh and M.Abu-Sara, "Digital current control of utility connected two-level and three-level PWM voltage source inverters," European Power Electronic Journal 2004, vol. 14 No. 4, 2004.

[11] Mohan Ned, Tore M. Undeland, and W. P. Robbins, Power Electronics Converters, Applications, and Design, 3rd ed.: John Willy and Sons 2006.

[12] L. N. Arruda, S. M. Silva, and B. J. C. Filho, "PLL structures for utility connected systems," in Industry Applications Conference, 2001. IEEE 36th IAS Annual Meeting. Conference Record of the 2001, vol.4, pp. 2655-2660.

[13] P. Mahat, C. Zhe, and B. Bak-Jensen, "Review of islanding detection methods for distributed generation," in Electric Utility Deregulation and Restructuring and Power Technologies, 2008. DRPT 2008. Third International Conference on, 2008, pp. 2743-2748.

[14] K. De Brabandere, B. Bolsens, J. Van den Keybus, A. Woyte, J. Driesen, and R. Belmans, "A Voltage and Frequency Droop Control Method for Parallel Inverters," IEEE Transactions on Power Electronics, vol. 22, pp. 1107-1115, 2007.

[15] M. Abu-Sara, "Digital Control of Utility and Parallel Connected Three-Phase PWM Inverters," in PhD Thesis, University of Southampton, 2004.

[16] J. A. P. Lopes, C. L. Moreira, and A. G. Madureira, "Defining control strategies for MicroGrids islanded operation," Power Systems, IEEE Transactions on, vol. 21, pp. 916-924, 2006.

[17] S. M. Sharkh, M.Abu-Sara, and Z. F. Hussein., "Current control of utility -connected DC-AC three-phase volatge-source inverters using repetitive feedback," in European Power Electronic Conference EPE 2001,Graz, p. 6 pages.

[18] W. Eric and P. W. Lehn, "Digital Current Control of a Voltage Source Converter With Active Damping of LCL Resonance," IEEE Transactions on Power Electronics, vol. 21, pp. 1364-1373, 2006.

[19] S. Guoqiao, X. Dehong, C. Luping, and Z. Xuancai, "An Improved Control Strategy for Grid-Connected Voltage Source Inverters With an LCL Filter," IEEE Transactions on Power Electronics, vol. 23, pp. 1899-1906, 2008.

[20] I. J. Gabe, J. R. Massing, V. F. Montagner, and H. Pinheiro, "Stability analysis of grid-connected voltage source inverters with LCL-filters using partial state feedback," in Power Electronics and Applications, 2007 European Conference on, 2007, pp. 1-10.

[21] S. Guoqiao, X. Dehong, X. Danji, and Y. Xiaoming, "An improved control strategy for grid-connected voltage source inverters with a LCL filter," in IEEE 21st Annual Applied Power Electronics Conference and Exposition, 2006. APEC '06, 2006, p. 7.

[22] O. Bouhali, B. Francois, C. Saudemont, and E. M. Berkouk, "Practical power control design of a NPC multilevel inverter for grid connection of a renewable energy plant based on a FESS and a Wind generator," in 32nd Annual Conference on IEEE Industrial Electronics, IECON 2006 , 2006, pp. 4291-4296.

[23] J. Selvaraj and N. A. Rahim, "Multilevel Inverter For Grid-Connected PV System Employing Digital PI Controller,", IEEE Transactions on Industrial Electronics, vol. 56, pp. 149-158, 2009.

[24] M. Ikonen, O. Laakkonen, and M. Kettunen, "Two-level and three-level converter comparison in wind power application," Avaiable online: www.elkraft.ntnu.no/smola2005/Topics/15.pdf ,Finalnd, 2005.

[25] F. Xunbo, E. Chunliang, L. Jianlin, and X. Honghua, "Modeling and simulation of parallel-operation grid-connected inverter," in IEEE International Conference on Industrial Technology, 2008, pp. 1-6.

[26] M. T. Zhang, M. M. Jovanovic, and F. C. Y. Lee, "Analysis and evaluation of interleaving techniques in forward converters," IEEE Transactions on Power Electronics, vol. 13, pp. 690-698, 1998.

[27] S.-H. Lee, S.-G. Song, S.-J. Park, C.-J. Moon, and M.-H. Lee, "Grid-connected photovoltaic system using current-source inverter," Solar Energy, vol. 82, pp. 411-419, 2008.

[28] S. M. Barakati, M. Kazerani, and X. Chen, "A new wind turbine generation system based on matrix converter," in Power Engineering Society General Meeting, 2005. IEEE, 2005, pp. 2083-2089 Vol. 3.

[29] M. P. Kazmierkowski and L. Malesani, "Current control techniques for three-phase voltage-source PWM converters: a survey," IEEE Transactions on Industrial Electronics, vol. 45, pp. 691-703, 1998.

[30] H. M. Kojabadi, Y. Bin, I. A. Gadoura, C. Liuchen, and M. Ghribi, "A novel DSP-based current-controlled PWM strategy for single phase grid connected inverters," IEEE Transactions on Power Electronics, vol. 21, pp. 985-993, 2006.

[31] N. Nguyen-Quang, D. A. Stone, C. Bingham, and M. P. Foster, "Comparison of single-phase matrix converter and H-bridge converter for radio frequency induction heating," in European Conference on Power Electronics and Applications, 2007, pp. 1-9.

[32] T. Erika and D. G. Holmes, "Grid current regulation of a three-phase voltage source inverter with an LCL input filter," IEEE Transactions on Power Electronics, vol. 18, pp. 888-895, 2003.

[33] E. Twining and D. G. Holmes, "Grid current regulation of a three-phase voltage source inverter with an LCL input filter," IEEE 33rd Annual, Power Electronics Specialists Conference, 2002, pp. 1189-1194.

[34] A. V. Timbus, M. Ciobotaru, R. Teodorescu, and F. Blaabjerg, "Adaptive resonant controller for grid-connected converters in distributed power generation systems," Annual IEEE Applied Power Electronics Conference and Exposition, 2006, p. 6

[35] H. L. Jou, W. J. Chiang, and J. C. Wu, "Virtual inductor-based islanding detection method for grid-connected power inverter of distributed power generation system," IET Renewable Power Generation Conference, vol. 1, pp. 175-181, 2007.

[36] Kui-Jun Lee, Nam-Ju Park, and D.-S. Hyun., "Optimal current controller in a three-phase grid connected inverter with an LCL filter," in Hong Kong conference on control, 2007.

[37] I.-S. Kim, "Sliding mode controller for the single-phase grid-connected photovoltaic system," Applied Energy, vol. 83, pp. 1101-1115, 2006.

[38] Z. Qingrong and C. Liuchen, "Improved Current Controller Based on SVPWM for Three-phase Grid-connected Voltage Source Inverters," IEEE 36th Power Electronics Specialists Conference, 2005, pp. 2912-2917.

[39] G. Weiss, Z. Qing-Chang, T. C. Green, and L. Jun, "H∞ repetitive control of DC-AC converters in microgrids," IEEE Transactions on Power Electronics, vol. 19, pp. 219-230, 2004.

[40] M. Lindgren and J. Svensson, "Control of a voltage-source converter connected to the grid through an LCL-filter-application to active filtering," in IEEE Power Electronics Specialists Conference, 1998, pp. 229-235.

[41] M. Liserre, F. Blaabjerg, and S. Hansen, "Design and control of an LCL-filter-based three-phase active rectifier," IEEE Transactions on Industry Applications, vol. 41, pp. 1281-1291, 2005.

[42] M. Prodanovic and T. C. Green, "Control and filter design of three-phase inverters for high power quality grid connection," IEEE Transactions on Power Electronics, vol. 18, pp. 373-380, 2003.

[43] V. Blasko and V. Kaura, "A novel control to actively damp resonance in input LC filter of a three-phase voltage source converter," IEEE Transactions on Industry Applications, vol. 33, pp. 542-550, 1997.

[44] T. Abeyasekera, C. M. Johnson, D. J. Atkinson, and M. Armstrong, "Elimination of subharmonics in direct look-up table (DLT) sine wave reference generators for low-cost microprocessor-controlled inverters,", IEEE Transactions on Power Electronics, vol. 18, pp. 1315-1321, 2003.

[45] W. E. Feero, D. C. Dawson, and J. Stevens, "White paper on Protection Issues of The MicroGrid Concept", Consortium for Electric Reliability Technology Solutions, March 2002.

# ROBUST REPETITIVE FEEDBACK CONTROL OF A THREE-PHASE GRID CONNECTED INVERTER

***M. Jamil, S. M. Sharkh, M. Abusara, R. J. Boltryk***

School of Engineering Sciences,University of Southampton,
Highfield,Southampton SO17 1BJ,United Kingdom.
Tel +44 2380 594641,Fax +44 2380 593053
Email: mj2p07@soton.ac.uk

**Keywords:** Distributed Generator (DG), Grid Connected Converters, Current Control, Repetitive Controller (RC)

## Abstract

This paper discusses the design of a repetitive feedback controller for a grid-connected two-level three-phase voltage-source inverter connected between a DC source and the grid through an LCL filter. The controller incorporates a classical two loop feedback of the output current and the capacitor current in addition to a repetitive feedback loop. The results show that the proposed technique improves the steady state error and the total harmonic distortion of output current in presence of utility harmonics.

## 1 Introduction

Pulse width modulation (PWM) voltage source inverters (VSI) similar to that shown in Fig.1 are commonly used to connect distributed generator (DG) systems such as micro combined heat and power (CHP) and renewable energy sources to an AC grid or local loads. They convert DC from photovoltaic generators, batteries, fuel cells or variable frequency AC from wind and marine turbine into 50/60 Hz AC power. The output current of the converter should meet the total harmonic distortion (THD) standards in the presence of grid harmonics [1, 2]. This is commonly achieved using active feedback control of the current injected into the grid.

Alternative control strategies and structures have been used for grid-connected inverters such as deadbeat control [3], optimal control [4], state-feedback [5], sliding mode [6] and resonant controllers [7], in addition to PID and classical compensators. It is also common to use the d-q transformation [8]. The objective of these controllers is to increase the outer loop gain, and, hence improve disturbance rejection. But most of these controllers tend to suffer from relatively low loop gain at the fundamental frequency and its harmonics and hence tend to have poor disturbance rejection which results in poor output current THD if the grid voltage THD is relatively high. A better controller is required with high gain at the harmonic frequencies of interest.

Repetitive feedback based control techniques have the potential to improve the THD quality of the converter output by effectively increasing the loop gain at the fundamental frequency and its harmonics [9]. The effectiveness of repetitive control in terms of eliminating harmonic distortion in a voltage source inverter operating has been demonstrated in several publications [9-15].

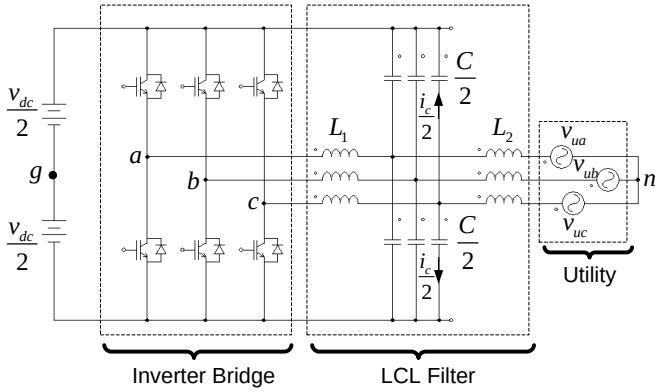


Fig. 1: Three Phase Grid Connected Inverter with LCL Filter

| Parameter | Value |
|---|---|
| Utility Phase voltage | 230 V (rms) |
| DC Link Voltage | 800 V dc |
| Inductor $L_1$ | 350 µH |
| Inductor $L_2$ | 50 µH |
| Capacitance $C$ | 22.5 µF |
| Switching Frequency | 10 KHz |

Table 1: Electrical Parameters

This paper discusses the design of an alternative control system based on repetitive feedback for the 3-phase grid connected inverter shown in Fig.1. Stability constraints and trade-off between steady state error and system transient response are analysed. Table 1 shows the electrical parameters of the system.

## 2 System Modelling

The analysis and design of the control system for the voltage source grid connected inverter in Fig.1 is based upon the

single phase equivalent circuit shown in Fig.2. The small resistances of inductors and the equivalent series resistance (ESR) of the capacitors are neglected.

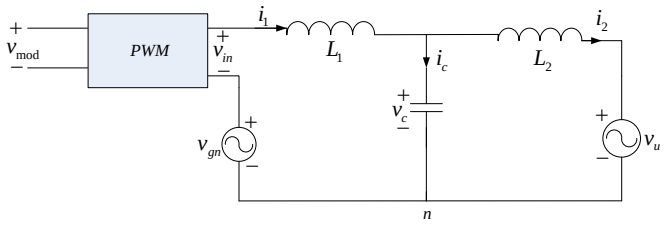


Fig. 2: Single Phase Equivalent Circuit

In Fig. 2, $v_{gn}$ is the voltage difference between the neutral point and middle of the dc link. In control terms this may be viewed as a source of disturbance caused by phase interaction. The disturbance $v_{gn}$ can be expressed by the following equation:

$$v_{gn} = \frac{v_{ag} + v_{bg} + v_{cg}}{3} \quad (1)$$

where $v_{ag}$, $v_{bg}$ and $v_{cg}$ are phase voltages of the phase with respect to the ground. Equation (1) shows that the phase interaction voltage $v_{gn}$ depends on the switching states of all three phases. It can be shown that, when filter capacitors are connected to dc link as shown in Fig.1, the voltage $v_{gn} \approx 0$, showing only a very small switching frequency ripple component [16].

To derive the transfer function of the grid connected inverter we could write the following equations using Kirchhoff's Voltage Law (KVL) and Kirchhoff's Current Law (KCL) based upon Fig. 2.

$$v_{in} - v_c = L_1 \frac{di_1}{dt} \quad (2)$$

$$i_c = i_1 - i_2 \quad (3)$$

$$i_c = C \frac{dv_c}{dt} \quad (4)$$

$$v_c - v_u = L_2 \frac{di_2}{dt} \quad (5)$$

Based on these equations, we can represent the system using the following block diagram.

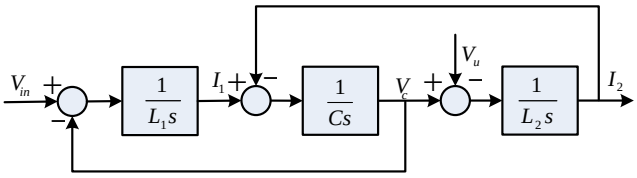


Fig. 3: Block Diagram of the Single-Phase Circuit

## 3 Proposed Control Scheme

The proposed digital controller comprises a conventional two loop feedback system and a repetitive controller, as shown in Fig. 4. The repetitive feedback controller (RC) requires the basic plant (i.e. the two loop system $G_p(s)$ ) to be stable. Since direct feedback of the output grid current of an LCL filter on its own is inherently unstable, it is necessary to have another feedback loop of the capacitor current or the current in the main inductor $L_1$ [16] to stabilize the system. The transfer function relating the output current $I_2$ to the reference current $I_{ref}$ (assuming the PWM block is a unity gain block) can be shown to be,

$$I_2 = \frac{G_c(s)G_s(s)}{1+G_c(s)G_s(s)} I_{ref} - \frac{G_s(s)}{1+G_c(s)G_s(s)} D(s) \quad (6)$$

where, $G_s(s)$ is the transfer function of the two loop plant given by,

$$G_s(s) = \frac{I_2}{V_{in}*} = \frac{1}{(L_1L_2C)s^3 + (K_cL_2C)s^2 + (L_1+L_2)s} \quad (7)$$

and $D(s)$ is the transfer function of input disturbance, which is given by,

$$D(s) = V_u(L_1Cs^2 + K_cCs + 1) \quad (8)$$

The system in Fig. 4 can be reduced to that in Fig. 5, with $G_P(z)$ given by,

$$G_p(z) = \frac{G_c(z)G_s(z)}{1+G_c(z)G_s(z)} \quad (9)$$

The simplified general form of the overall control scheme by replacing $R = I_{ref}{}^*$, $D = V_u$ and $Y = I_2$ represented by Fig. 5 which will be used for analysis later on.

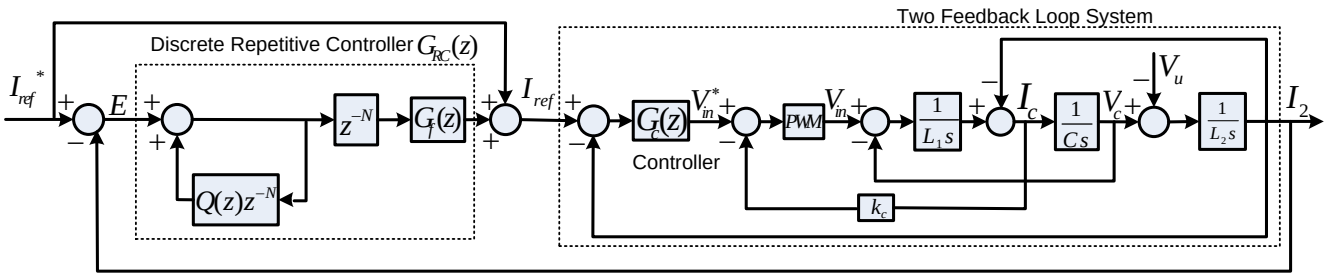


Fig 4: Overall Block Diagram of Proposed Control Scheme

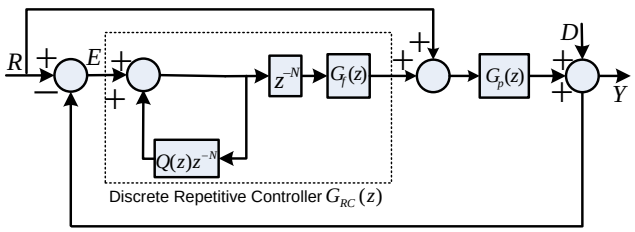


Fig 5: Simplified Block Diagram of Proposed Controller

### 3.1 The Conventional Two Loop Feedback System

We choose the controller to be a simple proportional controller, such that $G_c(z) = K_P$, since alternative classical controllers such as PID or one of its derivatives, were found to provide marginal improvements (if any) in comparison, at the expense of additional complexity. The values of $K_p = 6$ and $K_c = 13$ were selected to provide a compromise between stability, speed of response and disturbance rejection as discussed in [16]. The bode diagram of the two loop system is shown in Fig. 6; the system has a phase margin of 52.6° and a gain margin of 7.88 dB. The loop gain at 50 Hz is 18 db and reduces further at higher frequencies. Hence the disturbance rejection at 50 Hz and its harmonics will be relatively poor. However, it is not possible to increase the loop gain any further as without compromising stability.

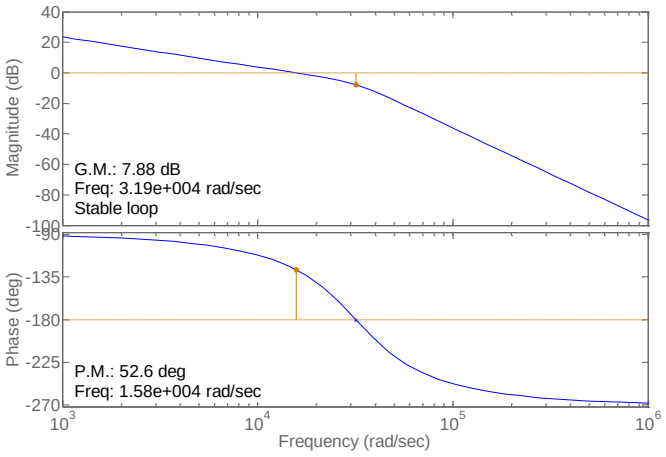


Fig. 6: Bode Plot of Conventional Two Loop Feedback System

### 3.2 The Digital Repetitive Controller

The theory of repetitive control (RC) is based on the internal model principal [17-19], whereby a model of the repetitive reference and disturbance signals is included in the controller. The RC tracks the error on a cycle by cycle basis and corrects the control effort on a periodic basis to compensate for the error.

In the discrete time domain, a periodic signal with a known period $T$ can be generated by a time delay block $z^{-N}$ with a positive feedback loop. Here, $N$ is the number of samples in one period given by,

$$N = \frac{T}{T_s} \tag{10}$$

where, $T$ is the time period of the any periodic input and $T_s$ corresponds to sampling time. Normally $N$ is a large number and hence a basic RC requires a large memory buffers which is one of its drawbacks [20]. The transfer function $G_{RB}(z)$ of a basic RC comprises a gain $K_R$ multiplied by the transfer function of a periodic signal generator,

$$G_{RB}(z) = K_R \frac{z^{-N}}{1 - z^{-N}} = \frac{K_R}{z^N - 1} \tag{11}$$

The control objective is to find an appropriate optimal value of the repetitive controller gain $K_R$ such that the tracking error converges to zero as the number of iterations approaches to infinity.

$$\lim_{k \to \infty} \|e(k)\| = 0 \tag{12}$$

The basic repetitive feedback control in (10) is most suitable for those applications where the period $T$ is constant or accurately measureable [20]. This basic repetitive feedback does not ensure stability and error convergence criteria and is normally modified to overcome these problems.

To avoid pure integration, a filter *Q(z)* is introduced in the basic repetitive control structure, followed by a compensator $G_f(z)$ such that

$$G_{RC}(z) = G_R(z) G_f(z) \tag{13}$$

where, $$G_R(z) = K_R \frac{z^{-N}}{1 - Q(z) z^{-N}} \tag{14}$$

The filter $Q(z)$ ensures the stability and robustness of the system. It can be either a low-pass filter or a constant less than 1.

The compensator $G_f(z)$ should ideally be designed to be a zero magnitude and phase compensator for the closed loop transfer function of the plant [9]. This however results in a complex compensator, which is computationally costly to implement. A reasonable approximation is achieved by selecting $G_f(z)$ to be equal to a gain $K_R$ multiplied by the time advance unit $z^k$ [15].

$$G_f(z) = z^k K_R \tag{15}$$

The time advance $z^k$ compensates for the phase lag of the inverter to improve stability.
Using equations (13) and (15), we can rewrite the transfer function of RC as follows:

$$G_{RC}(z) = \frac{K_R z^{-N+k}}{1 - Q(z) z^{-N}} \quad (16)$$

There are various schemes to design the *Q*-filter and the compensator $G_f(z)$ to improve the robustness of RC [21] . In this paper we select *Q* filter as a constant less than 1 and *k*=3 for the leading unit of the compensator. The value of $K_R$ is adjusted after selecting the value of *Q*. The values of $K_R$ and *Q* are tuned to ensure stability while achieving a good speed of response and steady state error.

From Fig. 5, the error *E(z)* in terms of the reference *R(z)* and the disturbance *D(z)* can be derived as:

$$E(z) = \frac{[1 - G_p(z)][z^N - Q(z)]}{z^N - [(Q(z) - G_f(z) G_p(z)]} R(z) + \frac{[Q(z) - z^N]}{z^N - [(Q(z) - G_f(z) G_p(z)]} D(z) \quad (17)$$

*Theorem:* Assume two systems $G_1$ and $G_2$ are connected in a feedback loop, then the closed loop system is input-output stable if $\|G_1\| . \|G_2\| < 1$

According to the above gain theorem the overall stability conditions can be devised as:

a) The roots of characteristic equation, $1 + G_c(z) G_s(z) = 0$ of conventional two loop feedback system without RC should be inside the unit circle.

b) From equation (17),

$$\left| H(e^{j\omega T}) \right| < 1$$

where,

$$H(e^{j\omega T}) = Q(e^{j\omega T}) - e^{j\omega T} K_R G_P(e^{j\omega T}) \quad (18)$$

and,

$\omega \in [0, \frac{\Pi}{T}]$, and *T* = Sample Time.

## 4 Selection of Controller Parameters for Robustness

The two parameters, $K_R$ and $Q$, are closely related to the system stability. The critical value $Q_{critical}$ of $Q$ at which the system becomes unstable, for a given value of $K_R$, was calculated using equation (18) and readjusted by simulation. The results are plotted in Fig. 7. Fig. 8 illustrates the relationship between the speed of response of the controller and the parameters *Q* and $K_R$. Basically, for a given value $K_R$ the speed of response improves by increasing *Q*, at the expense of reducing stability. Increasing $K_R$ improves the steady state error (SSE) for a given value of *Q*. Using Figs. 7 and 8, the values of *Q* and $K_R$ can be selected to ensure stability and achieve a fast speed of response and small steady state error. *Q* = 0.9, and $K_R$ = 0.4 were found to give a satisfactory performance.

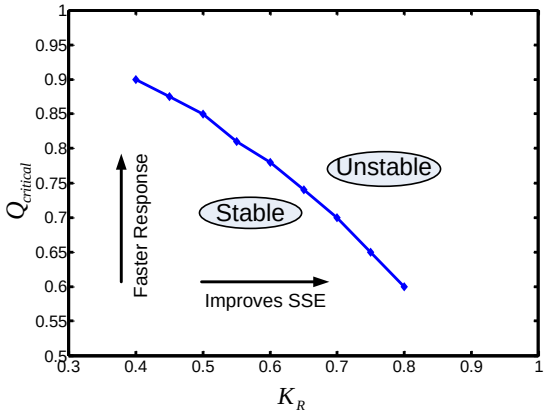


Fig. 7: Relationship between $Q_{critical}$ and $K_R$

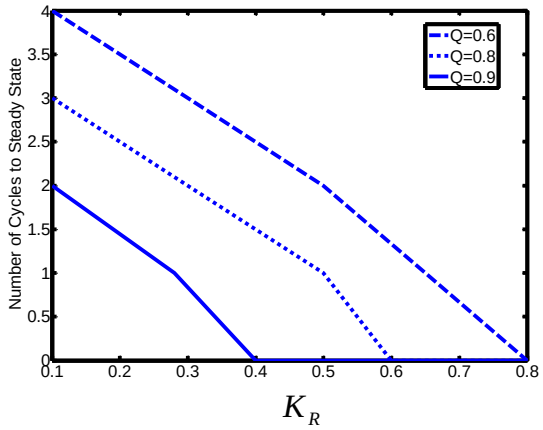


Fig 8: Graph between Number of Cycles to SSE and $K_R$

The value of the inductor $L_2$ , which is determined by the grid impedance, can vary significantly depending on the site where the inverter is installed. This uncertainty needs to be taken into account to ensure that the system can tackle these uncertainties under the worst condition. To assess the robustness of the system to the uncertainty in the value of $L_2$ was added up to ±50% and it was observed that there is no big change in system behaviour.

## 5 Simulation Results

Detailed simulation has been carried out using the MATLAB Simpower Systems Toolbox. The system parameters are shown in Tables 1 and 2. Four cases with different utility THD values have been considered; the grid harmonic content when the THD was 14% is shown in Table 3. The reference current was 100 A (peak).

| Parameter | Value |
|---|---|
| Outer Loop Controller Gain $K_P$ | 6 |
| Inner Loop Capacitor Gain $K_C$ | 13 |
| Repetitive Controller Gain $K_R$ | 0.4 |
| Value of $Q$ | 0.9 |
| $N$ for delay term $z^{-N}$ | 400 |

Table 2: Controller Parameters

| **Harmonic Number** | 3rd | 5th | 7th | 9th | 11th | 13th |
|---|---|---|---|---|---|---|
| **Fundamental Component** | 35 | 25 | 15 | 5 | 2 | 1 |

Table 3: Grid voltage harmonics when the THD is 14%

Fig. 9 shows the output current without the use of repetitive controller, while Fig.10 shows simulation results with the repetitive controller. The THD of the output current improves significantly in any case when the RC is used as shown in Fig. 11.. For example, in the 2nd case when the utility THD is 14 %, the output current THD with the repetitive controller improves from 9.5% to 4.4 %.

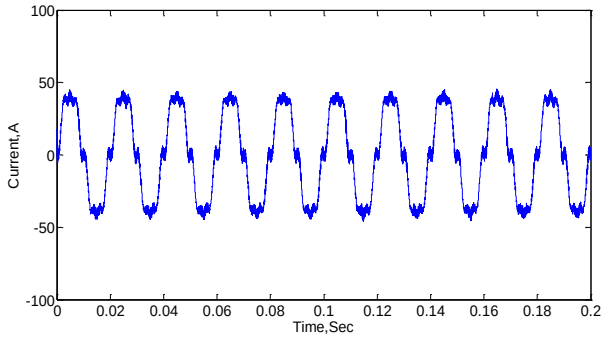


Fig 9: Output Current without RC

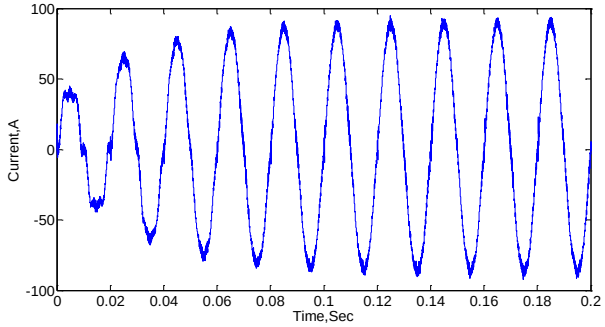


Fig 10: Output Current with RC When Utility THD=14 % and $Q = 0.9, K_R = 0.4$

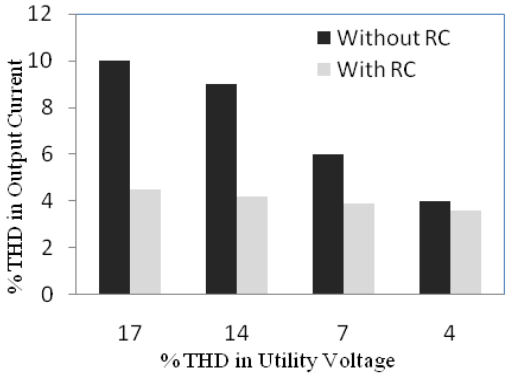


Fig 11: Comparison of % THD in Output Currents at Different Utility THD levels with and without RC

## Conclusion

Simulations results show repetitive control can significantly improve the THD quality of the output current. The RC parameters need to be selected carefully to ensure stability despite uncertainty in grid impedance, while achieving a fast response and a small steady state error. The proposed controller was demonstrated to be robust to changes in parameters. Further work is needed to improve the steady state error.

## Acknowledgements

Mr. M. Jamil is thankful to National University of Science and Technology (NUST), Pakistan for giving scholarship for his PhD studies. Also thanks to Dr. Wali Mohammed Trust for partial support.

## References

[1] T. S. Basso and R. DeBlasio, "IEEE 1547 series of standards: interconnection issues", *IEEE Transactions on Power Electronics*, **vol. 19**, pp. 1159-1162, (2004).

[2] "Engineering Recommendation G59/1, 'Recommendations for the Connection of Embedded Generating Plant to the Regional Electricity Companies' Distribution Systems", *Electricity Association (Engineering Services)*, (1991).

[3] B. Qu, X.-y. Hong, W.-x. Yao, Z.-y. Lu, and J. M. Guerrero, "An Optimized Deadbeat Control Scheme Using Fuzzy Control in Three-Phase Voltage Source PWM Rectifier", *Twenty-Fourth Annual IEEE Conference on Applied Power Electronics Conference and Exposition (APEC)*, pp. 1215-1219, (2009).

[4] Kui-Jun Lee, Nam-Ju Park, and D.-S. Hyun., "Optimal current controller in a three-phase grid connected inverter with an LCL filter", *Hong Kong Conference on Control*, (2007).

[5] I. J. Gabe, J. R. Massing, V. F. Montagner, and H. Pinheiro, "Stability analysis of grid-connected voltage source inverters with LCL-filters using partial state feedback", *12th European Conference*

*on Power Electronics and Applications*, pp. 1-10, (2007).

[6] I.-S. Kim, "Sliding mode controller for the single-phase grid-connected photovoltaic system", *Applied Energy*, **vol. 83**, pp. 1101-1115, (2006).

[7] A. V. Timbus, M. Ciobotaru, R. Teodorescu, and F. Blaabjerg, "Adaptive resonant controller for grid-connected converters in distributed power generation systems", *Twenty-First Annual IEEE Conference on Applied Power Electronics and Exposition(APEC)*, p. 6 ,(2006).

[8] T. Erika and D. G. Holmes, "Grid current regulation of a three-phase voltage source inverter with an LCL input filter", *IEEE Transactions on Power Electronics*, **vol. 18,** pp. 888-895, (2003).

[9] S. Chen, Y. M. Lai, S. C. Tan, and C. K. Tse, "Analysis and design of repetitive controller for harmonic elimination in PWM voltage source inverter systems", *IET Journal of Power Electronics*, **vol. 1**, pp. 497-506, (2008).

[10] G. Weiss, Z. Qing-Chang, T. C. Green, and L. Jun, "H infinity repetitive control of DC-AC converters in microgrids", *IEEE Transactions on Power Electronics*, **vol. 19,** pp. 219-230, (2004).

[11] W. Wang, S. K. Panda, and X. Jian-Xin, "Control of high performance DC-AC inverters using frequency domain based repetitive control", *International Conference on Power Electronics and Drives System ( PEDS)*,pp. 442-447,(2005).

[12] S. M. Sharkh, M.Abu-Sara, and Z. F. Hussein., "Current control of utility -connected DC-AC three-phase voltage-source inverters using repetitive feedback", *European Conference on Power Electronics and Applications, (EPE)*, p. 6, (2001).

[13] Z. Qing-Chang, T. Green, L. Jun, and G. Weiss, "Robust repetitive control of grid-connected DC-AC converters", *41st IEEE Conference on Decision and Control*, **vol.3**, pp. 2468-2473,(2001).

[14] S. PengFei, J. Xiong, Z. Kai, and Z. Liang, "One cost-effective feedback control scheme for PWM inverters based on repetitive control", 1st *IEEE Conference on Industrial Electronics and Applications (ICIEA)*, pp. 1-5,(2006).

[15] L. Fei, D. Shanxu, X. Pengwei, C. Guoqiang, and L. Fangrui, "Design and control of three-phase PV grid connected converter with LCL filter", *33rd Annual Conference of the IEEE Industrial Electronics Society, (IECON)*, pp. 1656-1661,(2007).

[16] S. M. Sharkh and M.Abu-Sara, "Digital current control of utility connected two-level and three-level PWM voltage source inverters", *European Journal of Power Electronic*, **vol. 14-4**, (2004).

[17] Yigang Wang, Danwei Wang, and X. Wang, "A three-step deisgn method for performance improvement of robust repetitive Control", *American Control Conference*, (2005).

[18] Z. Keliang and W. Danwei, "Digital repetitive learning controller for three-phase CVCF PWM inverter", *IEEE Transactions on Industrial Electronics*, **vol. 48**, pp. 820-830, (2001).

[19] Z. F. Hussein, "Current Control of Three-Phase PWM Inverter for Flywheel Energy Storage System", *PhD Thesis , University of Southampton*, (2000).

[20] G. Pipeleers, B. Demeulenaere, J. De Schutter, and J. Swevers, "Generalised repetitive control: relaxing the period-delay-based structure", *IET Journal of Control Theory and Applications*, **vol. 3,** pp. 1528-1536, (2009).

[21] Y. Wang, F. Gao, and F. J. Doyle Iii, "Survey on iterative learning control, repetitive control, and run-to-run control", *Journal of Process Control*, **vol. 19**, pp. 1589-1600, (2009).

*International Review of Automatic Control (IREACO) Vol. 4, N.2*
*March 2011*

# Current Regulation of Three-Phase Grid Connected Voltage Source Inverter Using Robust Digital Repetitive Control

M.Jamil[1], S.M.Sharkh[2], M.A.Abusara[3]

**Abstract** – *Most of renewable and conventional energy sources generate DC/AC power at inconvenient frequency. An inverter is typically used to integrate such distributed generation systems into the grid. There is a growing interest in developing appropriate control strategies to ensure that the current fed into the grid has a low total harmonic distortion. In this paper, a control scheme for a three-phase grid connected inverter is proposed. The scheme contains a traditional conventional tracking controller with a dual loop feedback system, and a plug-in repetitive controller. The working principle of the controller, stability constraints and trade-off between the steady state error and the dynamics response of the system are analyzed. The results indicate that the proposed repetitive feedback control scheme improves the steady state error and total harmonic distortion of the output current by compensating for the distortion caused by grid voltage harmonics.*

***Keywords****: Current Control, Distributed Generation (DG), Grid Connected Converters, Repetitive Control (RC)*

## Nomenclature

| | |
|---|---|
| $C$ | Capacitance within LCL filter |
| $D(z)$ | Disturbance i.e. utility harmonics |
| $E(z)$ | Error signal i.e. $E(z) = R(z) - Y(z)$ |
| $F$ | Grid frequency |
| $F_s$ | Sampling frequency |
| $G(z)$ | Overall system with repetitive and conventional controller. |
| $G_c(z)$ | Conventional tracking controller |
| $G_E(z)$ | Error transfer function |
| $G_f(z)$ | Phase compensator within repetitive controller |
| $G_o(z)$ | Closed loop transfer function without repetitive control |
| $G_p(z)$ | Discrete transfer function of open loop plant |
| $G_{RC}(z)$ | Repetitive control transfer function |
| $I_2$ | Output Current |
| $K_c$ | Inner loop capacitor gain of open loop plant |
| $K_p$ | Proportional controller gain |
| $K_R$ | Repetitive controller gain |
| $L_1$ | 1st inductor of LCL filter |
| $L_2$ | 2nd inductor of LCL filter |
| $m$ | Lead step in phase lead compensator |
| $N$ | Number of samples per period i.e. [ $N$ = Time period ( $T_P$ ) / Sample time ( $T_S$ )] |
| $Q(z)$ | Null-phase low pass filter of repetitive controller |
| $R(z)$ | Controller demand |
| $V_{dc}$ | DC link voltage |
| $V_u$ | Utility phase voltage |
| $Y(z)$ | Controller output |

## I. Introduction

Voltage source inverters (VSI) with inductor-capacitor-inductor (LCL) output filter as shown in Fig. 1 are increasingly used to interface small DC/AC renewable and conventional energy sources to the AC utility. They convert DC from photovoltaic generators, batteries, fuel cells or variable frequency AC from wind and marine turbine into 50/60 Hz AC power. The quality of the output electric current of the inverter must conform to standards and regulations that define the total harmonic distortion (THD) limits in presence of grid harmonics [1]-[2].

This is normally achieved by combination of well designed pulse width modulated (PWM) inverter, output

filter and active feedback control of the current injected into the grid [3].

Alternative control strategies and structures have been used for grid-connected inverters such as deadbeat control [4], optimal control [5], state-feedback [6], non-linear control [7] and resonant controllers [8], in addition to PID and classical compensators. The objective of these controllers is to increase the outer loop gain, and, hence improve disturbance rejection. But most of these controllers tend to suffer from relatively low loop gain at the fundamental frequency and its harmonics. Further they tend to have poor disturbance rejection which results in poor output current THD if the grid voltage THD is relatively high. A better controller is required with high gain at the harmonic frequencies of interest.

Repetitive feedback based control techniques have the potential to improve the THD quality of the converter output by effectively increasing the loop gain at the fundamental frequency and its harmonics [9]. The repetitive control concept and technique has been widely used for different applications such as robotics [10], disk drives [11], machines [12] steel casting processes [13] and vibration suppression [14]. The effectiveness of repetitive control for low THD voltage regulation in a VSI has been demonstrated in several publications as well [15]-[19]. However most design methods have been applied to VSI in voltage control mode. To date effectiveness of RC in PWM VSI for current control mode has been partially explored [20]-[22] in detailed and systemic way. In [20], a hybrid controller consisted of state feedback pole placement and repetitive control was designed. Performance of the controller under strong grid harmonics was not investigated. In [22], the RC requires resetting after few cycles to avoid instability.

This paper investigates the synthesis of a current control scheme based on repetitive feedback for the 3-phase grid connected inverter shown in Fig.1 to improve the current tracking accuracy, both during transients and steady state. A method for analyzing the RC system from the frequency point of view is presented. A systematic way of optimizing the system is proposed by incorporating a phase lead compensator and a low pass filter. Stability constraints and trade-off between steady state error and system transient response are analyzed. Table 1 shows the electrical parameters of the system.

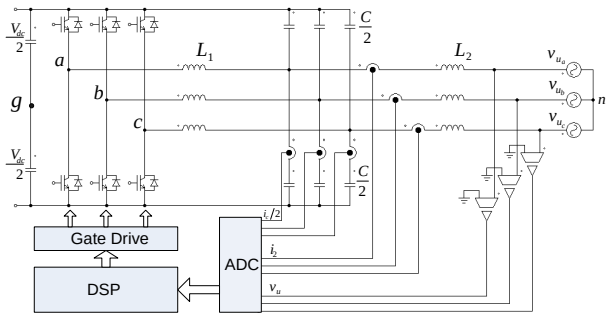


Fig. 1. Two level three-phase grid connected inverter with LCL filter

TABLE I
SYSTEM PARAMETERS

| Components | Description | Rating values |
|---|---|---|
| $V_u$ | Utility phase voltage | 230 V (rms) |
| $V_{dc}$ | DC link voltage | 800 V dc |
| $L_1$ | 1st Inductor of filter | 350 µH |
| $L_2$ | 2nd Inductor of filter | 50 µH |
| $C$ | Capacitance | 22.5 µF |
| $F_s$ | Switching frequency | 10 KHz |
| $F$ | Grid frequency | 50 Hz |

## II. System Description and Control Scheme

The analysis and design of the control system for the voltage source grid connected inverter in Fig.1 is based upon the single phase equivalent circuit shown in Fig.2. This circuit was derived for star (or delta) connected filter capacitors by Ito and Kawauchi [23].The small resistances of inductors and the equivalent series resistance (ESR) of the capacitors are neglected.

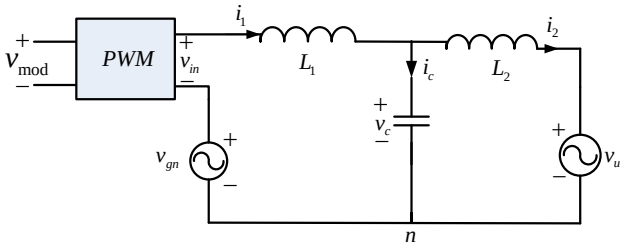


Fig. 2. Single-phase equivalent circuit

In Fig. 2, $v_{gn}$ is the voltage difference between the neutral point and middle of the DC link. In control terms this may be viewed as a source of disturbance caused by phase interaction. The disturbance $v_{gn}$ can be expressed by the following equation:

$$v_{gn} = \frac{v_{ag} + v_{bg} + v_{cg}}{3} \qquad (1)$$

Where $v_{ag}$, $v_{bg}$ and $v_{cg}$ are phase voltages of the phase with respect to the ground. Equation (1) shows that the phase interaction voltage $v_{gn}$ depends on the switching states of all three phases. It can be shown that, when filter capacitors are connected to dc link as shown in Fig.1, the voltage $v_{gn} \approx 0$, showing only a very small switching frequency ripple component [24].

To derive the transfer function of the grid connected inverter we could write the following equations using Kirchhoff's Voltage Law (KVL) and Kirchhoff's Current Law (KCL) based upon Fig. 2.

$$v_{in} - v_c = L_1 \frac{di_1}{dt} \quad (2)$$

$$i_c = i_1 - i_2 \quad (3)$$

$$i_c = C \frac{dv_c}{dt} \quad (4)$$

$$v_c - v_u = L_2 \frac{di_2}{dt} \quad (5)$$

Based on these equations, we can represent the linear model of system with tracking conventional controller $G_c(s)$ as shown in Fig. 3.

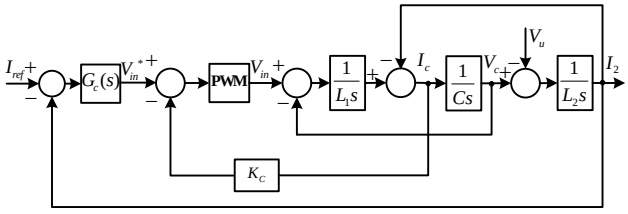


Fig. 3. Linear model of grid connected inverter system with conventional tracking controller

The linear model of system in Fig.3 can be simplified as shown in Fig.4.

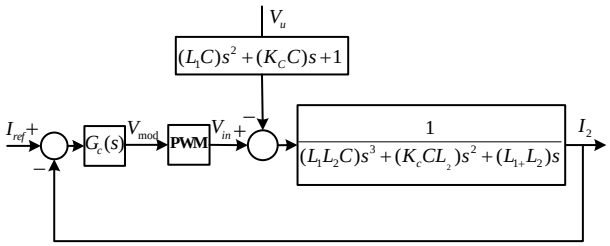


Fig. 4. Simplified linear model of system with tracking conventional controller

Since direct feedback of the output grid current of an LCL filter on its own is inherently unstable, it is necessary to have another feedback loop of the capacitor current or the current in the main inductor $L_1$ [24] to stabilize the system. The transfer function relating the output current $I_2$ to the reference current $I_{ref}$ (assuming the PWM block is a unity gain block) can be shown to be,

$$I_2 = \frac{G_c(s)G_p(s)}{1 + G_c(s)G_p(s)} I_{ref} - \frac{G_p(s)}{1 + G_c(s)G_p(s)} U(s) \quad (6)$$

Where, $G_p(s)$ is the transfer function of the two loop plant given by,

$$G_p(s) = \frac{I_2}{V_{in}*} = \frac{1}{(L_1L_2C)s^3 + (K_c L_2 C)s^2 + (L_1 + L_2)s} \quad (7)$$

and $U(s)$ is the transfer function of input disturbance, which is given by,

$$U(s) = V_u(L_1Cs^2 + K_c Cs + 1) \quad (8)$$

The two loop feedback system with the repetitive controller $G_o(z)$ in Fig. 5 is given by,

$$G_o(z) = \frac{G_c(z)G_p(z)}{1 + G_c(z)G_p(z)} \quad (9)$$

Where,

$$G(z) = Z\left(\frac{1-e}{s} G(s)\right) \quad (10)$$

The proposed digital controller comprises a conventional two loop feedback system and a repetitive controller, as shown in Fig. 3 and Fig. 5. The repetitive feedback controller (RC) requires the basic plant $G_p(s)$ to be stable.

The simplified general form of the overall control scheme by replacing $R = I_{ref}^*$ and $Y = I_2$ represented by Fig. 5 which will be used for analysis later on. The disturbance $D(z)$ is related to $V_u$.

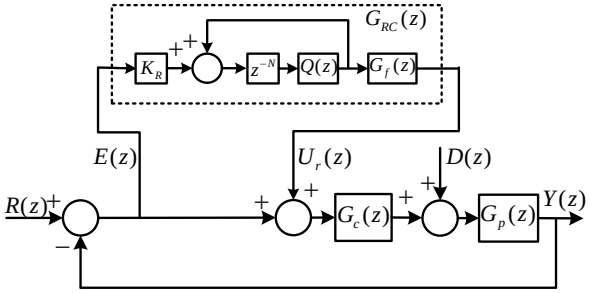


Fig. 5. Overall control scheme

## III. Conventional Tracking Controller

We choose the controller to be a simple proportional controller, such that $G_c(z) = K_P$, since alternative classical controllers such as PID or one of its derivatives, were found to provide marginal improvements (if any) in comparison, at the expense of additional complexity. The values of $K_p = 3.2$ and $K_c = 13.41$ were selected to provide a compromise between stability, speed of response and disturbance rejection as discussed in [24]. The bode diagram of the two loop system is shown in Fig. 6; the system has a phase margin of $71.8^o$ and a gain

margin of 13.6 dB. The loop gain at 50 Hz is 24 with reduction in loop gain. However, it is not possible to increase the loop gain further without compromising stability.

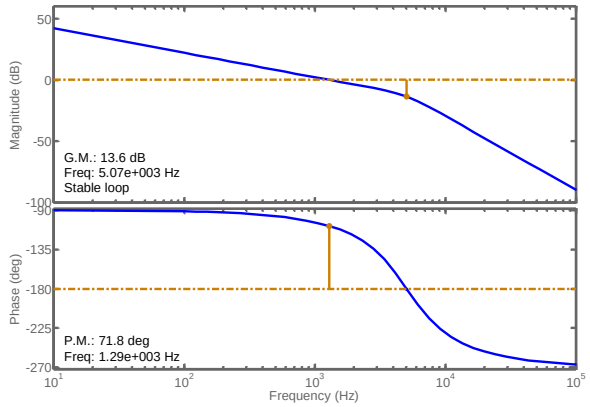


Fig. 6. Bode plot of dual loop feedback system

## IV. Synthesis of the Repetitive Controller

The concept of repetitive control was originally developed for SISO plants in continuous time for tracking a periodic reference signal with known period $T_p$ [24]. The basic concept of RC comes from the internal model principle (IMP) proposed by Francis and Wonham [26]. According to this principle, controlled outputs track a set of reference inputs without steady state error if the model that generates these references is included in the stable closed loop system [18]. For example, there is no steady state error for step reference commands if we include generator of step function i.e. integrator $1/s$ in the stable closed loop. Based on the IMP, a periodic signal generator ($e^{-T_p s}/1-e^{-T_p s}$) could be included in the RC feedback loop as the internal model. From frequency point of view, the repetitive control generates as infinitely large feedback gain at the periodic signal's fundamental frequency and its harmonics as shown in Fig. 7.

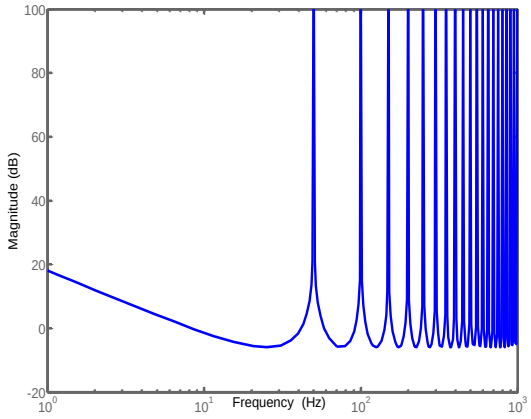


Fig. 7. Magnitude frequency response of a periodic signal generator

Therefore the periodic signals can be tracked or rejected asymptotically provided that the closed loop system is stable. The repetitive controller utilizes the knowledge of previous cycle error and control effort for each frequency component to eliminate periodic error in the current cycle. The transfer function of a periodic signal generator can be represented as:

$$G_{rc}(s)=\frac{e^{-sT_p}}{1-e^{-sT_p}}=\frac{1}{e^{sT_p}-1} \tag{11}$$

$$G_{rc}(s)=\left[-\frac{1}{2}+\frac{1}{2}\left(\frac{1+e^{-sT_p}}{1-e^{-sT_p}}\right)\right] \tag{12}$$

$$\pi\frac{e^{\pi x}+e^{-\pi x}}{e^{\pi x}-e^{-\pi x}}=x\sum_{k=-\infty}^{\infty}\frac{1}{x^2+k^2}=\frac{1}{x}+\sum_{k=1}^{\infty}\frac{2x}{x^2+k^2} \tag{13}$$

$$G_{rc}(s)=K_R\left\{-\frac{1}{2}+\frac{1}{T_p}\left[\frac{1}{s}+\frac{2s}{s^2+\omega_p{}^2}+\frac{2s}{s^2+(2\omega_p)^2}+\frac{2s}{s^2+(3\omega_p)^2}+....\right]\right\} \tag{14}$$

According to above equation the RC is mathematically equivalent to a parallel combination of an integral controller, many resonant controllers and a proportional controller [27]. It is interesting to compare Fig. 7 with equation (14) where we have the frequency response of an integral controller initially and then many resonant controllers with infinite gain and different frequency bands.

When RC is applied in the discrete time domain with a sampling period $T_s$, the transfer function of the periodic signal generator that needs to be included in the loop is:

$$G_R{}'(z)=\frac{z^{-N}}{1-z^{-N}}=\frac{1}{z^N-1} \tag{15}$$

Where, $$N=\frac{T_p}{T_s} \qquad \forall N\in\mathbb{Z} \tag{16}$$

In addition to above relation it should be noted that according to Nyquist theorem, the discrete implementation of RC can cancel those harmonics whose frequencies are less than half of sampling frequency $\left(\frac{\omega_s}{2}=\frac{\pi}{T_p}\right)$.

### *IV.1. Structure of RC and Stability Analysis*

Repetitive controllers are normally implemented in a plug-in fashion [28] i.e. they are used to supplement the existing conventional controller $G_c(z)$ as shown in Fig. 5. This conventional controller has been discussed in section 3. The product of the repetitive controller gain

$K_R$ and equation (15) produce the transfer function of a basic repetitive control

$$G_R''(z) = K_R \frac{z^{-N}}{1-z^{-N}} = \frac{K_R}{z^N - 1} \quad (17)$$

The control objective is to find an appropriate optimal value of the repetitive controller gain $K_R$ such that the tracking error converges to zero as the number of iterations approaches infinity.

$$\lim_{k\to\infty} \|e(k)\| = 0 \quad (18)$$

The basic repetitive feedback control represented by equation (17) is most suitable for those applications where the period $T_p$ is constant or accurately measureable [29]. This basic repetitive feedback does not ensure stability and error convergence and is normally modified to overcome these problems.

It is a nontrivial problem to stabilize the system due to the positive feedback loop present in RC. Moreover the open loop poles of the repetitive controller are on the stability boundary; the stability of overall system is sensitive to unmodeled dynamics. To overcome this limitation and to enhance robustness of system, a low pass filter $Q(z)$ is introduced to filter out the high frequency components. Robustness is achieved at the expense of performance at high frequency. However, the frequencies of interest in this application are the low order harmonics. The design of the low pass filter is very important and it reflects the tradeoff between closed loop system performance and stability robustness.

A compensator $G_f(z)$ for close loop stability is also normally added to the design. The transfer function of repetitive controller is then modified as follows:

$$G_{RC}(z) = G_R(z)G_f(z) \quad (19)$$

$$G_{RC}(z) = \frac{K_R Q(z) z^{-N}}{1-Q(z)z^{-N}} G_f(z) \quad (20)$$

From Fig. 5, we could drive the transfer function of overall closed-loop system with respect to reference $R(z)$ as follows:

$$\frac{Y(z)}{R(z)} = \frac{\left(1+G_{RC}(z)\right)G_c(z)G_P(z)}{1+\left(1+G_{RC}(z)\right)G_c(z)G_P(z)} \quad (21)$$

By substituting equation (20) into (21) and using equation (9), we could derive the following relation:

$$\frac{Y(z)}{R(z)} = \frac{\left(1-Q(z)z^{-N} + K_R Q(z) z^{-N} G_f(z)\right)G_o(z)}{1-Q(z)z^{-N}\left(1-K_R G_f(z)G_o(z)\right)} \quad (22)$$

Similarly we get overall closed-loop system with respect to disturbance $D(z)$ as:

$$\frac{Y(z)}{D(z)} = \frac{1}{1+(1+G_{RC}(z))G_c(z)G_P(z)} \quad (23)$$

Using equation (9) and (20) we have

$$\frac{Y(z)}{D(z)} = \frac{1-Q(z)z^{-N}}{\left(1+G_c(z)G_p(s)\right)\left(1-Q(z)z^{-N}(1-K_R G_f(z)G_o(z))\right)} \quad (24)$$

The error transfer function for overall system is

$$E(z) = \frac{1}{1+\left(1+G_{RC}(z)\right)G_c(z)G_P(z)} R(z) - \frac{1}{1+\left(1+G_{RC}(z)\right)G_c(z)G_P(z)} D(z) \quad (25)$$

$$G_E(z) = \frac{E(z)}{R(z)-D(z)} = \frac{1}{1+\left(1+G_{RC}(z)\right)G_c(z)G_P(z)} \quad (26)$$

$$G_E(z) = \left(\frac{1-Q(z)z^{-N}}{\left(1+G_c(z)G_p(s)\right)}\right)\left(\frac{1}{1-Q(z)z^{-N}\left(1-K_R G_f(z)G_o(z)\right)}\right) \quad (27)$$

Using equation (9), (22), (24) and (27) we can deduce the stability conditions for overall closed loop system as follows:

*Theorem:* Assume two systems $G_1$ and $G_2$ are connected in a feedback loop, then the closed loop system is input-output stable if $\|G_1\|.\|G_2\| < 1$

According to the above gain theorem the overall stability conditions can be devised as:

Condition 1: The roots of characteristic equation, $1+G_c(z)G_p(z) = 0$ of conventional two loop feedback system without RC should be inside the unit circle.

Condition 2: From equation (27),

$$\left\|Q(z)\left(1-K_R G_f(z)G_o(z)\right)\right\| \quad (28)$$

Where, $$\forall z = e^{j\omega},\ 0 < \omega < \frac{\Pi}{T_p} \quad (29)$$

Using equation (28), we can easily design suitable values of all parameters by ensuring the poles of the system are within unit circle.

## V. Choice of Parameters for Robustness

### *V.1. Low Pass Filter $Q(z)$*

The filter $Q(z)$ can be a constant or a zero phase low pass filter. It is worth comparing both cases. There are two methods presented to find zero-phase low pass filter. In practice normally zero phase low-pass filter has the following structure;

$$Q(z) = \frac{\alpha_1 z + \alpha_o + \alpha_1 z^{-1}}{\alpha_o + 2\alpha_1} \; ; \quad \alpha_o, \alpha_1 > 1 \qquad (30)$$

By some deduction, the normalized frequency response ($T_s = 1$) of equation (30) is $Q(e^{j\omega}) = \alpha_o + 2\alpha_1 \cos(\omega)$ and $\omega \in (0, \pi)$ .By considering $\alpha_o + 2\alpha_1 = 1$ for unit gain response we can write the magnitude of $Q(j\omega)$ as

$$|Q(j\omega)| = \begin{cases} \alpha_o + 2\alpha_1 = 1 & \omega = 0 \\ \alpha_o + 2\alpha_1 \cos(\omega) & \omega(0, \pi) \\ \alpha_o - 2\alpha_1 & \omega = \pi \end{cases} \qquad (31)$$

By selecting $\alpha_o = 0.25$ and $\alpha_1 = 0.5$ , then

$$|Q(j\omega)| = \begin{cases} 1 & \omega = 0 \\ 0 < 0.5(1 + \cos\omega) < 1 & \omega \in (0, \pi) \\ 0 & \omega = \pi \end{cases} \qquad (32)$$

Equation (32) concludes that $|Q(j\omega)|$ is 1 at low frequencies and zero at high frequencies. We can achieve different low pass filters by using different $\alpha_o$ and $\alpha_1$ . Typically a first order filter is sufficient and is given by,

$$Q(z) = 0.25z + 0.5 + 0.25z^{-1} \qquad (33)$$

No causality problem exists because the filter is cascaded with the transfer function of the repetitive control having *N* period delay as shown in Fig.5. Another type of low pass finite impulse response (FIR) filter can be obtained using Matlab window method. We can define the order of filter and cut off frequency to obtain the coefficients of filter. For example, the 2nd order filter having cutoff frequency of 100 Hz is $Q(z) = 0.0689 + 0.8623z^{-1} + 0.0689z^{-2}$ .

The advantage of this filter is that it is causal and can be analyzed in Simulink without the need of combining the transfer function of repetitive controller with the filter transfer function. An alternative way is to select constant $Q(z)$ slightly less than one [30]. However in practice a constant $Q(z)$ is less robust than a low pass filter. We investigated the performance of all three filters i.e. non causal low pass filter, causal low pass FIR filter and a constant. The Bode diagram of RC including filters (assuming $K_R = 1$) is shown in Fig. 8.

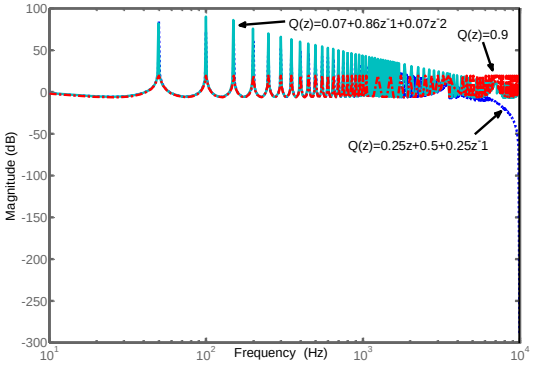


Fig. 8. Bode diagram of [ $Q(z)z^{-N}/1-Q(z)z^{-N}$ ] with different Filter $Q(z)$

It has been observed the filter $Q(z)$ given by equation (33) has better attenuation at higher frequency than the FIR filter and the constant filter $Q(z)$ .

In many applications $Q(z)$ given by equation (33) results in a sufficient stability margin. It also enhances the robustness of RC system.

### *V.2. The Compensator $G_f(z)$*

Since $G_0(z)$ is a minimum phase function (no zero outside unit circle), it is desirable to choose $G_f(z)$ to be the inverse of system model to achieve zero-phase error tracking. However in practice the grid impedance vary significantly and the transfer function is therefore not known [17]. Instead phase-lead compensation scheme is used such that,

$$G_f(z) = z^m \qquad (34)$$

This phase-lead compensator compensates the phase lag introduced by the transfer function of the inverter and hence improves the stability of the system. In addition, it can also compensate the unknown time delay, which is not modeled. The suitable value $m = 3$ is selected using equation (28) to have enough stability and robustness.

### *V.3. Repetitive Controller Gain $K_R$*

Its selection is related to stability and transient response of the RC system. It must fulfill the stability

condition given by equation (28). Increasing $K_R$ improves the steady state error (SSE) for a given value of $Q(z)$ and vice versa. We select $K_R$ value to be 0.3. It gives enough fast transient (2 cycles to reach steady state) response and stability.

After suitable selection of all above three parameters we can get the bode diagram of system with and without repetitive controller selecting. This is shown by Fig. 9.

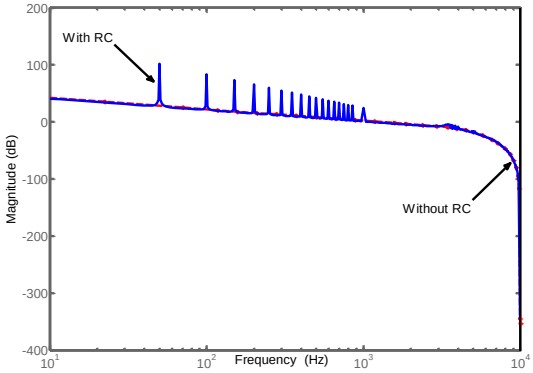


Fig. 9. Bode diagram of system with and without repetitive controller

### *V.4. Effect of Grid Impedance*

The value of the inductor $L_2$ , which is determined by the grid impedance, can vary significantly depending on the site where the inverter is installed. This uncertainty needs to be taken into account to ensure that the system can tackle these uncertainties under the worst condition. To assess the robustness of the system, the uncertainty in the value of $L_2$ was varied by ±50% and it was observed that RC system can handle these uncertainties very well. This could be seen in Fig. 10.

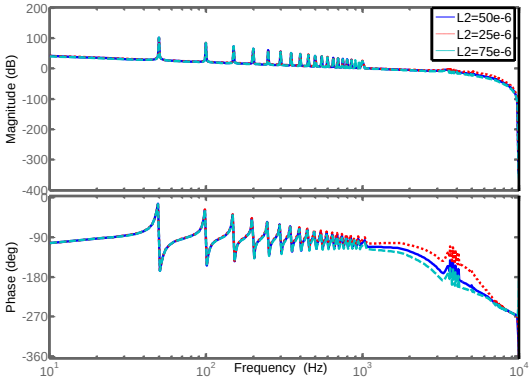


Fig. 10. Effect of variations in $L_2$ on overall RC system

## VI. Simulation Results

Detailed simulation has been carried out using the MATLAB Simpower Systems Toolbox. The system and controller parameters are shown in Table 1 and 2. A high grid THD value has been considered; the grid harmonic content when the THD was 10.44%. To get this THD value, the 3rd, 5th, 7th, 9th, 11th and 13th harmonics were introduced. The value of fundament component against each harmonic number was 26, 16, 13, 6.5, 0.16 and 0.08 respectively. In practice grid THD is lower than this value. The reason for selecting the higher value is to test controller in a worst case scenario. The reference current was 100 A (peak).

TABLE II
CONTROLLER PARAMETERS

| Components | Part name/ Manufacturer | Rating values |
|---|---|---|
| $K_P$ | Outer loop controller gain | 3.2 |
| $K_C$ | Inner loop capacitor gain | 13.41 |
| $K_R$ | Repetitive controller gain | 0.3 |
| $N$ | Delay term | 400 |
| $m$ | Lead step for compensator | 3 |

Fig. 11 shows the output current without RC system. Whereas Fig. 12 shows the steady state output current with RC system. The Fig. 13 shows the transient response of output current with RC system. The THD of the output current improves significantly when the RC is used. The output current THD with the repetitive controller improves from 10.4 % to 2.5 % without steady state error. Moreover it is noticeable in Fig. 13 that enough faster transient response is achieved and steady state response comes after three cycles.

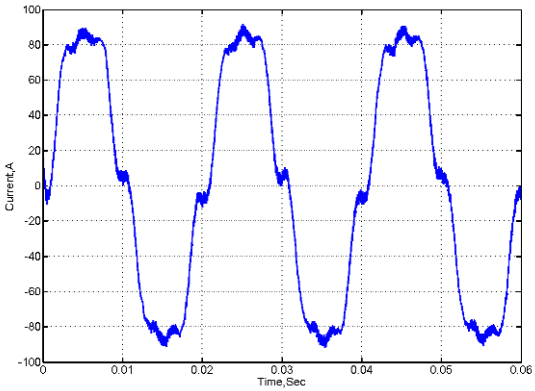


Fig. 11. Output current without RC system

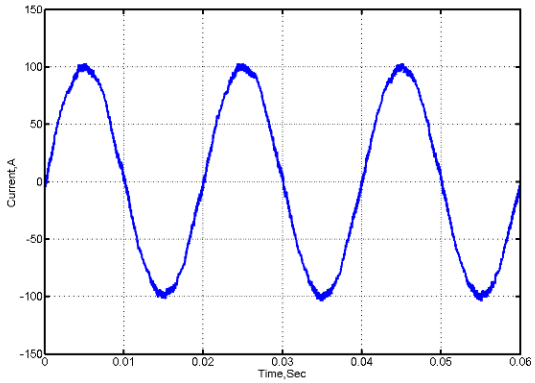


Fig. 12. Steady state output current with RC system

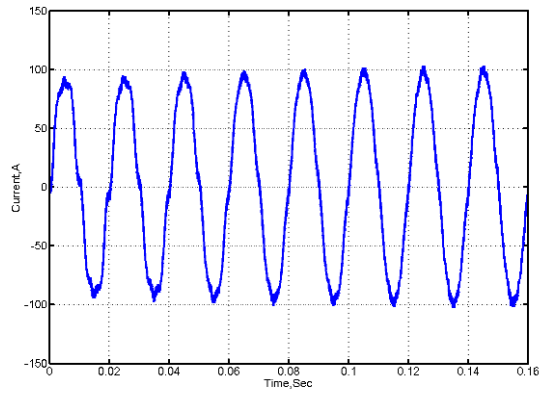


Fig. 13. Transient response of output current with RC system

## VII. Conclusion

A discrete time plug-in RC was designed for a three-phase grid connected inverter to achieve high quality sinusoidal current. Simulations results indicate that the RC can significantly improve the steady state error and the THD of the output current. The RC parameters need to be selected carefully to ensure stability despite uncertainty in grid impedance, while achieving a fast response and a zero steady state error. The proposed controller has better disturbance rejection as compared to classical control (P/PI/PID) techniques. Moreover it was demonstrated to be robust against parameters uncertainties.

## Acknowledgement

Mr. M. Jamil is thankful to National University of Sciences and Technology (NUST) and Higher Education Commission of Pakistan for providing financial assistance to do research at University of Southampton, United Kingdom.

## References

[1] T.S. Basso, R. DeBlasio, IEEE 1547 Series of Standards: Interconnection Issues, *IEEE Transaction on Power Electronics* , *vol. 19*, 2004, pp. 1159-62

[2] Electricity Association (Engineering Services), Engineering Recommendation G59/1, Recommendations for the Connection of Embedded Generating Plant to the Regional Electricity Companies Distribution Systems, 1991.

[3] M.Jamil, B.Hussain, M. Abu-Sara, R.J.Boltryk, S.M.Sharkh, Microgrid Power Electronic Converters: State of Art and Future Challenges, *The 44th International Universities Power Engineering Conference ~UPEC 2009~*, September 1-4, 2009, Glasgow, U.K.

[4] O.Kukrer, Deadbeat Control of a Three-Phase Inverter with an Output LC Filter, *IEEE Transactions on Power Electronics*, *vol.11*, 2004, pp. 16-23.

[5] K.J. Lee, N.J. Park, D.S. Hyun, Optimal Current Controller in a Three-Phase Grid Connected Inverter with an LCL Filter,*The 7th International Conference on Power Electronics~ICPE 2007~*,October 22-26, 2007, Daegu, South Korea, p.568-71

[6] I.J. Gabe, J.R. Massing, V.F. Montagner, H. Pinheiro, Stability Analysis of Grid-Connected Voltage Source Inverters with LCL-Filters Using Partial State Feedback, The 12th *European Conference on Power Electronic and Applications~EPE 2007~*,September 2-5, 2007, Aalborg, Denmark.

[7] M. Nazari, M. Abedi, G. B. Gharehpetian, H. Toodeji, Fuel Cell and Electrolyzer Connection to Grid by Direct Non-Linear Controlled H-Bridge Multilevel Inverter, *International Review on Automatic Control (IREACO) ,vol.3-6, November 2010*,pp. 633-40.

[8] S. Guoqiao, Z. Xuancai, Z. Jun, X. Dehong, A New Feedback Method for PR Current Control of LCL-filter-based Grid-Connected Inverter, *IEEE Transactions on Industrial Electronics*, *vol. 57*, 2010, pp. 2033-41.

[9] S. Chen, Y. M. Lai, S. C. Tan, C. K. Tse, Analysis and Design of Repetitive Controller for Harmonic Elimination in PWM Voltage Source Inverter Systems, *IET Power Electronics*, *vol. 1*, 2008, pp. 497-506.

[10] S. Mingxuan, S. S. Ge, I. M. Y. Mareels, Adaptive Repetitive Learning Control of Robotic Manipulators without the Requirement for initial Repositioning, *IEEE Transactions on Robotics*, *vol. 22*,2006, pp. 563-68.

[11] V. Alexandrov, G. van Albada, P. Sloot, J. Dongarra, K. Chang, G. Park, A Novel Method of Adaptive Repetitive Control for Optical Disk Drivers, *The 6th International Conference on Computational Science ~ICCS 2006~*, May 28-31, 2006, Reading, U.K.

[12] S.-L. Chen, T.-H. Hsieh, Repetitive Control Design and Implementation for Linear Motor Machine Tool, *International Journal of Machine Tools and Manufacture*, *vol. 47*, 2007, pp. 1807-16.

[13] T. J. Manayathara, T. Tsu-Chin, J. Bentsman, Rejection of Unknown Periodic Load Disturbances in Continuous Steel Casting Process Using Learning Repetitive Control Approach, *IEEE Transactions on Control Systems Technology*, *vol. 4*, 1996, pp. 259-65.

[14] G. Hillerstrom, Adaptive Suppression of Vibrations - a Repetitive Control Approach, *IEEE Transactions on Control Systems Technology*, *vol. 4*, 1996, pp. 72-78.

[15] G. Weiss, Z. Qing-Chang, T. C. Green, L. Jun, H infinity Repetitive Control of DC-AC Converters in Microgrids, *IEEE Transactions on Power Electronics*, *vol. 19*, 2004, pp. 219-230.

[16] K. Zhou, D. Wang, K. S. Low, Periodic Errors Elimination in CVCF PWM DC/AC Converter Systems: Repetitive Control Approach, *IEE Proceedings on Control Theory and Applications*, *vol. 147*, 2000, pp. 694-700.

[17] B. Zhang, K. Zhou, Y. Wang, D. Wang, Performance Improvement of Repetitive Controlled PWM Inverters: A phase-Lead Compensation Solution, *International Journal of Circuit Theory and Applications*, *vol. 38*, 2008, pp. 453-69.

[18] T. Ying-Yu, O. Rong-Shyang, J. Shih-Liang, C. Meng-Yueh, High-Performance Programmable AC Power Source with Low Harmonic Distortion Using DSP-Based Repetitive Control Technique, *IEEE Transactions on Power Electronics*, *vol. 12*, 1997, pp. 715-25.

[19] T. Ying-Yu, J. Shih-Liang, Y. Hsin-Chung, Adaptive Repetitive Control of PWM Inverters for very Low THD, *IEEE Transactions on Power Electronics*, *vol. 14*, 1999, pp. 973-81.

[20] S. Engel, K. Rigbers, R. W. De Doncker, Digital Repetitive Control of a Three-Phase Flat-Top-Modulated Grid Tie Solar , *The* 13th *European Conference on Power Electronic and Applications ~EPE 2009~*,September 8-10, 2009, Barcelona, Spain.

[21] L. Fei, D. Shanxu, X. Pengwei, C. Guoqiang, L. Fangrui, Design and control of three-phase PV grid connected converter with LCL filter, *The* 33rd *Annual Conference of IEEE Industrial Electronics~IECON 2007~*,November 5-8,2007, Taipei, Taiwan.

[22] S. M. Sharkh, M. Abu-Sara, Z. F. Hussein, Current Control of Utility Connected DC-AC Three-Phase Voltage-Source Inverters Using Repetitive Feedback, *The* 9th *European Conference on Power Electronic and Applications ~EPE 2001~* August 27-29 , 2001, Graz, Austria.

[23] Y. Ito , S. Kawauchi, Microprocessor Based Robust Digital Control for UPS with Three-Phase PWM Inverter, *IEEE Transactions on Power Electronics, vol. 10*, 1995, pp. 196-204.

[24] S. M. Sharkh, M. Abu-Sara, Digital current control of utility connected two-level and three-level PWM voltage source inverters, *European Journal of Power Electronic, vol. 14 n.4*, 2004,

[25] T. Inoue, M. Nankano, S. Iwai, High Accuracy Control of a Proton Synchrotron Magnet Power Supply, *The 8th World Congress of IFAC*, 1981, Kyoto, Japan.

[26] B. A. Francis and W. M. Wonham, The Internal Model Principal of Control Theory, *Automatica, Vol.12*, 1976, pp. 457-65.

[27] W. Lu, K. Zhou, and Y. Yang, A General Internal Model Principle Based Control Scheme for CVCF PWM Converters, *The 2nd International Symposium on Power Electronics for Distributed Generation Systems, ~PEDG 2010~,* June 16-18, 2010, Hefei, China.

[28] R. Costa-Castello, J. Nebot, and R. Grino, Demonstration of the Internal Model Principle by Digital Repetitive Control of an Educational Laboratory Plant, *IEEE Transactions on Education, vol. 48*, 2005,pp. 73-80.

[29] G. Pipeleers, B. Demeulenaere, J. De Schutter, J. Swevers, Generalised Repetitive Control: Relaxing the Period-Delay-Based Structure, *IET Control Theory & Applications, vol. 3*, 2009, pp. 1528-36.

[30] M. Jamil, S. M. Sharkh, M. Abusara, R. J. Boltryk, Robust Repetitive Feedback Control of a Three-Phase Grid Connected Inverter, *The 5th IET International Conference on Power Electronics, Machines and Drives ~PEMD 2010~,*April 19-21,2006, Brighton, U.K.

## Authors' information

[1,2] University of Southampton, SO17 1BJ Southampton, U.K.
[1]National University of Science and Technology (NUST), Pakistan.
[1,3]University of Exeter, TR10 9EZ Penryn Cornwall, U.K.

**M. Jamil** received his BEng Industrial Electronics degree from NED University, Pakistan, in 2004. He is MSc Electrical Engineering degree holder from Dalarna University Sweden and National University of Singapore in controls and automation. Since February 2008, he has been working towards his PhD degree at University of Southampton, UK. His research interests include digital control design for grid connected inverters and system identification of dynamic systems. He is an author of a book chapter and several IEEE publications.

**S. M. Sharkh** obtained his BEng and PhD degrees in Electrical Engineering from the University of Southampton in 1990 and 1994, respectively. He current works as a senior lecturer in the School of Engineering Sciences at the University of Southampton. He is also a director of HiT Systems Ltd. He has published over 100 papers in academic journals and conferences. His main research interests are in the area of electrical machines and drives. Dr Sharkh is a member of the IEE and a Chartered Engineer.

**M.A. Abusara** received his BEng degree from Birzeit University, Palestine, in 2000 and his PhD degree from the University of Southampton, UK, in 2004, both in electrical engineering.
Dr. Abusara joined the College of Engineering, Mathematics, and Physical sciences, University of Exeter, UK, in 2010 as a lecturer in Renewable Energy. He has over ten years of industrial experience with Bowman Power Group, Southampton, UK, in the field of research and development of digital control of power electronics for distributed energy sources, hybrid vehicles, and machines and drives. During his years in the industry he designed and prototyped a number of commercial products that include grid and parallel connected inverters, MicroGrid, DC/DC converters for hybrid vehicles, and sensorless drives for high speed permanent magnet machines. His main research interests include grid integration of marine renewable energy systems, distributed energy systems, Microgrid, and power electronics for hybrid vehicles.